Biotin protein ligase inhibitors as new antibacterial agents to target *Staphylococcus aureus.*

Studies of efficacy, mechanism of action and resistance.

By
Andrew James Hayes
B.Sc. (Advanced)

THE UNIVERSITY of ADELAIDE

A thesis submitted to the University of Adelaide, South Australia in fulfilment of the requirements for the degree of Master of Philosophy

Department of Molecular and Cellular Biology
School of Biological Sciences
University of Adelaide
South Australia
August 2017

Table of Contents

Abstract

There is a desperate need for new antibacterials to combat the growing threat of antimicrobial resistant infections. One of the most common causes of such infections is the Gram-positive pathogen *Staphylococcus aureus*. *S. aureus* is responsible for the majority of hospital based infective deaths, with strains resistant to even last resort antibacterial agents. To combat these infections novel antibiotic agents are required. However, few novel antibacterial agents have been approved in the past 4 decades, with most products being derivatives of previously used chemical classes. As a result, resistance mechanisms are often already present in bacteria, or develop rapidly after introduction. Antibacterial agents with novel mechanism of action against *S. aureus* are needed to address this crisis.

One potential target for the development of novel antibacterials is the essential enzyme biotin protein ligase (BPL). The BPL of *S. aureus* serves two major functions. Firstly, BPL catalyses attachment of the vitamin biotin onto biotin-dependent enzymes, such as acetyl-CoA (ACC) and pyruvate carboxylase (PC). Secondly BPL is a transcriptional repressor that regulates expression of proteins required for biotin biosynthesis and biotin transport. Previous work in our laboratory and others has sought to generate inhibitors that target BPL catalytic activity, however little is known about their effect on transcriptional repression. As a result, several BPL inhibitors with a variety of chemical scaffolds are described in the literature focusing on creating mimics of the reaction intermediate biotinyl-5′-AMP. Despite success in creating antibacterial inhibitors, a selective compound that completely inhibits bacterial growth has proved elusive. The most potent and selective anti-staphyloccocal compound, biotin-triazole, shows promising inhibitory activity (K_i = 90 nM) but is unable to completely inhibit bacterial growth.

The first aim of this thesis is to characterise three distinct chemical classes of BPL inhibitors designed to improve whole cell antibacterial activity. Each series of inhibitors was tested to

determine *in vitro* potency and whole cell efficacy through enzyme and antibacterial susceptibility assays. The first and second compound series are modifications of the previously described biotin-triazole pharmacophore. Series 1 describes the shortening of the triazole pharmacophore with a view to producing a refined pharmacophore with greater drug like properties. For a similar purpose series 2 was created by halogenation of the C5 position on the triazole ring. Improvements in whole cell activity were achieved in series 2, yielding our first biotin-triazole inhibitor to completely inhibit bacterial growth (MIC = 8μg/ml). The third series tested a separate sulfonyl based compound series and provided the most potent BPL inhibitor and antibacterial to date. This compound, BPL 199, exhibited a sub-nanomolar K_i (0.7 nM) and an MIC of < 0.5 μg/ml against a panel of *S. aureus* isolates. Importantly, BPL199 also showed no cytotoxicity against two human cell lines, HepG2 and HEK293, and was well tolerated in mouse models.

The second aim of this thesis was to validate the mechanism of antibacterial action of BPL inhibitors and investigate potential mechanisms of resistance in *S. aureus*. To validate the mechanism of action, a BPL overexpression strain was constructed in *S. aureus* strain RN4220 and used to test the effect of increased BPL on compound efficacy. This system was used against the most potent compounds from all three series. The assay confirmed that BPL inhibitors exerted antibacterial effects through inhibition of the BPL enzyme for the most potent antibacterial compounds. To determine resistance mechanisms to BPL inhibitors in *S. aureus* several individual isolates of *S. aureus* NCTC 8325 were exposed to sub-optimal concentrations of BPL199 to evolve resistance. Whole genome sequencing of the strains resistant to BPL199 was then undertaken to identify potential resistance mechanisms. The mutations present occurred in a diverse range of genes including BPL and the biotin dependent enzyme pyruvate carboxylase. The one missense mutation in BPL (D200E) was further explored with both *in vitro* and *in vivo* testing. This amino acid substitution was found to not greatly affect catalytic activity, reducing the affinity for biotin by 2-fold (K_m wt = 1.8 ±

0.3 μM , D200E = 3.8 ± 0.4 μM) and did not affect repression by the inhibitor (K_i wt = 4.8 ± 2.1 nM , D200E =10.9 ± 3.5 nM). However native mass spectrometry was able to show that the substitution abolished dimerization of the BPL *in vitro* and EMSA showed that this resulted in reduced DNA binding activity. Further *in vivo* testing, with a chromosomally integrated lacZ reporter assay in *E. coli*, demonstrated that the mutation was sufficient for dysregulation of the biotin transport and synthesis genes with a greater than 50 – fold increased biotin concentration required to facilitate repression of biotin transport. Several of the other mutations identified, such as the one in PC, were likely to induce loss of function. The individual effect of a loss of function in these genes was further explored using transposon mutagenesis knock-out strains. The effect of individual loss of function mutations in pyruvate carboxylase in *S. aureus* JE2 determined that this mutation alone was sufficient for a four-fold decrease in susceptibility to BPL199.

In summary this thesis has looked at the development of BPL inhibitors for the purpose of antibacterial drug discovery. Using the most potent compounds the mechanism of action and resistance to BPL inhibitors was also characterised. This work will help in the future design of BPL inhibitors with the resistance mechanisms suggesting potential pathways that are important for BPL inhibitor resistance.

Thesis layout:

The thesis will be presented as a series of manuscripts either published, submitted or to be submitted for publication. Each manuscript will be a chapter with its own references. Supplementary material for published manuscripts is available online with citation information. A general introduction and discussion will also be included to link together all the research conducted during candidature. A publishing agreement with all co-authors involved with the work is also included.

Declaration for thesis containing published work and/or work prepared for publication

I certify that this work contains no material which has been accepted for the award of any other degree or diploma in any university or other tertiary institution and, to the best of my knowledge and belief, contains no material previously published or written by another person, except where due reference has been made in the text, In addition, I certify that no part of this work will, in the future, be used in a submission for any other degree or diploma in any university or other tertiary institution without the prior approval of the University of Adelaide and where applicable, any partner institution responsible for the joint-award of this degree.

I give consent to this copy of my thesis when deposited in the University library, being made available for loan and photocopying, subject to the provisions of the Copyright Act 1968. I acknowledge that copyright of published works contained within this thesis resides with the copyright holder(s) of those works.

I also give permission for the digital version of my thesis to be made available on the web, via the University's digital research repository, the Library catalogue and also through web search engines, unless permission has been granted by the University to restrict access for a period of time.

I acknowledge the support I have received for my research through the provision of an Australian Government Research Training Program Scholarship

…… …… 21/11/17……..

Andrew James Hayes Date

I acknowledge the copyright of published works contained within this thesis including:

Chapter 3:

Jiage Feng, Ashleigh S. Paparella, William Tieu, David Heim, Sarah Clark, **Andrew Hayes**, Grant W. Booker, Steven W. Polyak, Andrew D. Abell (2016) A new series of BPL inhibitors to probe the ribose-binding pocket of *Staphylococcus aureus* biotin protein ligase. Accepted for publication in *ACS Medicinal Chemistry Letters,* Manuscript ID: ml-2016-00248v.R1.

Chapter 4:

Ashleigh S. Paparella, Kwang Jun Lee, **Andrew J. Hayes**, Jiage Feng, David Heim, Zikai Feng, Danielle Cini, Grant W. Booker, Matthew C. J. Wilce, Steven W. Polyak, and Andrew D. Abell, Halogenation of biotin protein ligase inhibitors improves whole cell activity against *Staphylococcus aureus*, Manuscript in preparation

Chapter 5:

Hayes, A.J., Satiaputra, J., Paparella, A.S., Sternicki, L.M., Rodriguez, B.B., Feng, J., Tieu, W., Cini, D., Heim, Feng, Z, Bell, J.M., Pukala, T.L, Turnidge, J.D., Wilce, M.C.J., Abell, A. D., Booker, G.W., Polyak, S.W. Probing the mechanism of action of BPL inhibitors in *Staphylococcus aureus* using an antibacterial sulfonyl based mimic of biotinyl-5′-AMP., Manuscript in preparation

Chapter 6:

Andrew J. Hayes, Grant W. Booker, Steven W. Polyak, Loss of functional pyruvate carboxylase is a major contributor for resistance to antibacterial biotin protein ligase inhibitors in *Staphylococcus aureus,* Manuscript in preparation

Authorization to publish each paper has been given and provided in print for each chapter containing copyright and co-authored work, including acknowledgement of contribution to the work from each author All supplementary material can be found online using the citation information as described above for each published article.

Communications and Presentations

Andrew Hayes, Jiulia Satiaputra, Ashleigh Paparella, Zikai Feng, Louise Sternicki, Beatriz Bianco Rodriguez, Andrew Abell, Grant Booker, Steven Polyak. "Characterisation of resistance mechanisms to biotin protein ligase inhibitors, a novel antibacterial class targeting *Staphylococcus aureus*." *EMBL Australia Postgraduate Symposium* 2016, Oral Presentation. **Winner** Highly commended **o**ral presentation prize, awarded $250 from University of Sydney

Andrew Hayes, Jiulia Satiaputra, Ashleigh Paparella, Beatriz Bianco Rodriguez, Stephen Pederson, Andrew Abell, Grant Booker, Steven Polyak "Characterising the mutations involved in resistance to biotin protein ligase inhibitors, a novel class of antibacterial agent to combat *Staphylococcus aureus*." *Adelaide Protein Group, Adelaide Australia*, 2016 Poster

Andrew Hayes "Advanced resistance studies define the mechanism of action for a new antibiotic inhibitor of biotin protein ligase from *Staphylococcus aureus*." *School of Biological Sciences Research Symposia, University of Adelaide, Adelaide, Australia.*2016 Poster

Andrew Hayes, Jiulia Satiaputra, Ashleigh Paparella, Beatriz Bianco Rodriguez, Stephen Pederson, Andrew Abell, Grant Booker, Steven Polyak Characterising resistance mechanisms to BPL inhibitors, a promising new class of antibacterial agents, through use of whole genome sequencing. *Australian Society for Medical Research (ASMR) South Australian Conference, Adelaide Australia* 2016, Oral presentation

Andrew Hayes, Beatriz Rodriguez, Ashleigh Paparella, Jacko Feng, Danielle Cini, David Heim, Jan Bell, John Turnidge, Matthew Wilce, Andrew Abell, Grant Booker, Steven Polyak "Characterisation of a novel inhibitor of biotin protein ligase from *Staphylococcus aureus*." *41st Lorne Conference on Protein Structure and Function, Lorne, Victoria, Australia* 2016. Poster

Acknowledgements

Firstly I would like to thank and acknowledge my supervisors, Professor Grant Booker and Dr Steven Polyak for their support and advice throughout the course of my candidature.

Grant, thank you for allowing me to design and undertake a slightly less biochemistry based project giving me the chance to explore the genetics behind resistance mechanisms. Your advice throughout my degree, especially when it came to making decisions about potential career paths has been really valuable. Steven, thank you for providing help and guidance in all aspects of my project, from teaching me new experimental techniques, to offering guidance and many hours in the preparation of the manuscripts that comprise this thesis.

I would also like to acknowledge all the members of the BPL team in the department of Chemistry that I have had the pleasure of working with, namely Professor Andrew Abell, Jacko, Jun and Bea, for their help with all the chemistry aspects of the project. Andrew, thank you for your advice and help with the preparation of manuscripts and your insightful comments on the other aspects of my project. As well thank you to Jacko, Jun and Bea for the hours that went into making the compounds for each experiment and drafting the chemical methods for all the manuscripts in this thesis.

Thank you to all past members of the Booker lab, Jiulia, Ashleigh, Zikai, David and Okki. In particular thank you to Jiulia and Ashleigh for all the advice and help over the past two years and for the lunchtime conversations. Thank you to all the current members of the lab, Andrew T, Louise, Kate, Stephanie and Jordan, as well as the members of the Bruning and Shearwin labs across the hall, Andrew M, Bec and Jia, who are always up for a chat. You have all made the last 2 years a fun time and were always happy to share in both the many successes and failures.

Thank you to our collaborators, Professor Matthew Wilce and Danielle Cini at Monash University for providing us with X-ray crystal structures, and John Turnidge and Jan Bell for the microbiological testing. As well, thank you to Professor John Wallace for sharing your knowledge on all aspects of the BPL project.

Thank you to Dr Stephen Kidd for the use of your lab and the advice on the genetic manipulation of *S. aureus*, Dr Alistair Standish for your help in sourcing the strain RN4220, Stephen Pederson for your help and advice on the bioinformatics aspects of my project, and Bart as well as the members of the McDevitt lab for their help and advice.

Thank you to Dr. Keith Shearwin, Dr Michelle Coulson and Dr John Conran for giving me the opportunity to be involved in undergraduate teaching in the past year, I really appreciate it. As well, thank you to all the CSU and professional staff in the School of Biological sciences for all their support.

Lastly the continued support of my family and friends has been instrumental in the completion of this thesis. Mum and Dad, thank you for your support and motivation over the course of my studies, all 18 years of it so far. Sai, thank you for your support over the last five years, always offering a sympathetic ear when things haven't gone to plan, all whilst studying yourself. As well, thank you to all of my friends that have been there to either grab a beer after a hard week, go watch a movie on a Monday at the Palace Nova, or have a chat.

Abbreviations

ACC	Acetyl-CoA carboxylase
AMP	Adenosine monophosphate
Apo	Unliganded enzyme
ATP	Adenosine triphosphate
BC	Biotin carboxylase
BCCP	Biotin carboxyl carrier protein
BirA	Biotin inducible repressor
BME	β-mercaptethanol
bp	Base pair
BPL	Biotin protein ligase
BSA	Bovine serum albumin
CAMHB	BBL™ Mueller Hinton II broth, cation-adjusted
CFU	Colony-forming units
Da	Dalton
DELFIA®	Dissociation-enhanced lanthanide fluorescence immunoassay
DMSO	Dimethyl sulfoxide
DNA	Deoxyribonucleic acid
DTT	Dithiothreitol
*Ec*BPL	*Escherchia coli* biotin protein ligase
EDTA	Ethylenediaminetetraacetic acid
Eu-streptavidin	Europium-labelled streptavidin
FIC	Fractional inhibition constant
FDA	Food and Drug Administration
GST	Glutathione S-Transferase
Holo	Ligand bound enzyme
*Hs*BPL	*Homo sapiens* BPL
IC_{50}	Inhibition concentration at 50% enzyme activity

kd	Dissociation rate constant
*K*D	Dissociation constant
kDa	kilo Dalton
*K*m	Michaelis-Menten constant
Ki	Inhibition constant
LB	luria broth
M	Molar
m	milli-
MW	Molecular weight
min	Minute
MIC	Minimal inhibitory concentration
MRSA	Methicillin resistant *Staphyloccous aureus*
MSSA	Methicillin sensitive *Staphylococcus aureus*
n	nano-
ODx	optical density at x nm wavelength
PAGE	Polyacrylamide gel electrophoresis
PC	Pyruvate carboxylase
PCR	Polymerase chain reaction
PDB	Protein data bank
PBS	Phosphate buffered saline
PMSF	phenylmethylsulfonylfluoride
rpm	Revolutions per minute
RNA	Ribonucleic acid
RU	Resonance units
s	Seconds
*Sa*BPL	*Staphylococcus aureus* biotin protein ligase
*Sa*PC	*Staphylococcus aureus* pyruvate carboxylase
SAR	Structure-activity relationship

SDS	Sodium dodecyl sulphate
SEM	standard error of the mean
SPR	Surface plasmon resonance
SNV	Single nucleotide variant
TBS	Tris buffered saline
TCA	Tricarboxylic acid
Tris	2-amino-2-hydroxymethylpropane-1,3-diol
μ	micro-
V	Voltage
WT	Wild-type

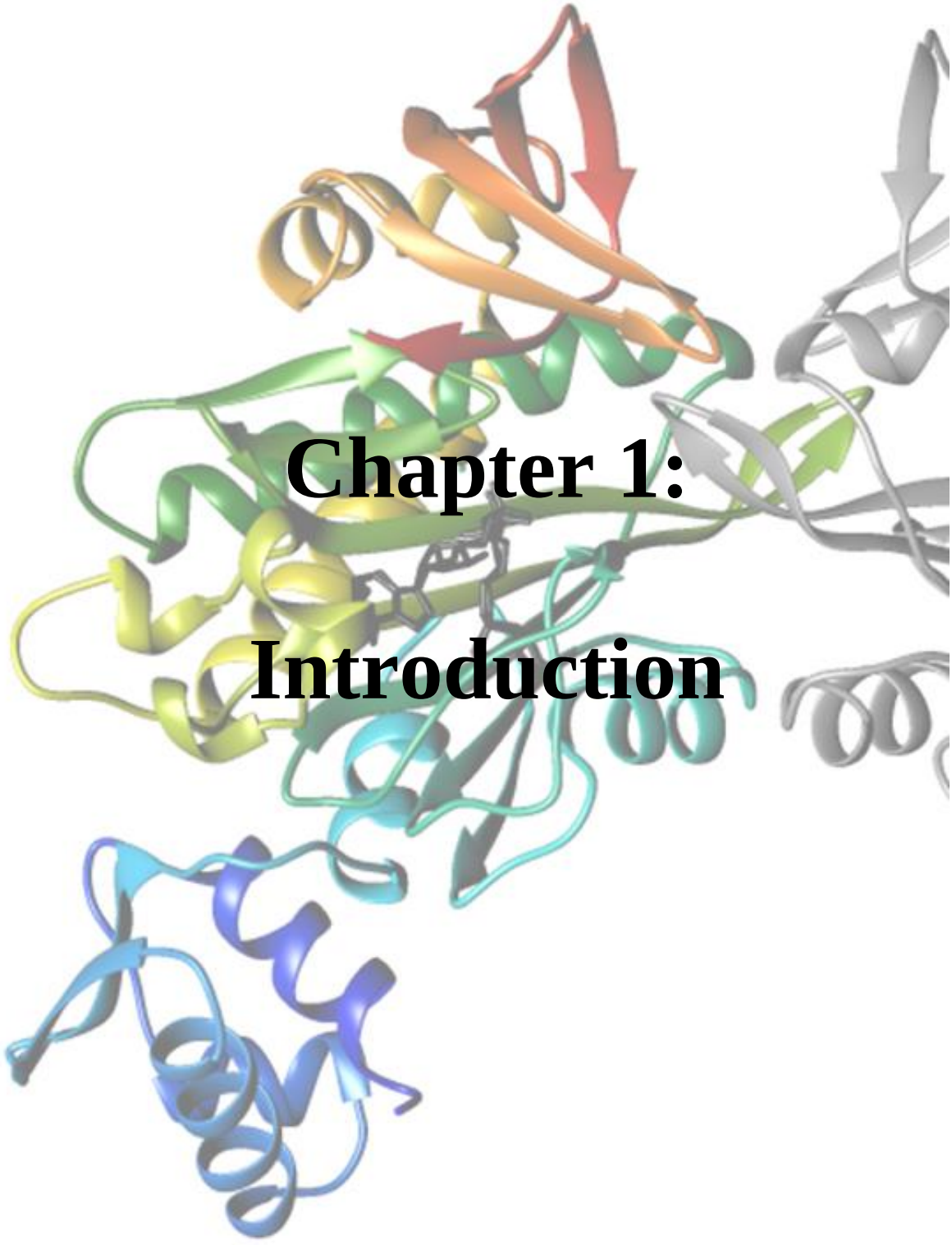

Chapter 1:

Introduction

CONTENTS

1.1 Need for new antibiotic agents

There is a dire need for new agents to target antimicrobial resistance in hospital, community and agricultural settings. With deaths due to drug resistant pathogens expected to exceed 10 million per year by 2050, and trillions of dollars in associated loss of GDP through lost productivity [1], there is a desperate need for action to combat the rise in resistance. Of these drug resistant bacteria some of the most concerning are the so called 'ESKAPE' pathogens (*Enterococcus faecium, Staphylococcus aureus, Klebsiella pneumoniae, Acinetobacter baumanii, Pseudomonas aeruginosa,* and *Enterobacter* species) [2] which exhibit extensive drug resistance (XDR). Multidrug resistance presents infections that are unresponsive to even antibiotics of last resort [3] leading to treatment failure and in many cases mortality. Despite the need for treatments to combat these XDR strains there has been a decrease in successful new antimicrobials being discovered. In the past 40 years only four novel antibacterial classes have received FDA approval [4, 5] with few candidates in the development pipeline [6]. This is largely attributed to the high risk, low financial rewards and punishing regulations that has led many large pharmaceutical companies to downsize their antibiotic drug discovery programs or leave the space entirely, opting to pursue more lucrative options [7, 8]. As the threat of antimicrobial resistance (AMR) increases, further research must be pursued to develop new chemotherapies. The winding back of large scale and, as discussed later on in this review, largely unsuccessful early stage research and development by industry has made publically funded university level research an important part of this development.

1.2 *Staphylococcus aureus* is a pathogen of concern

The bacterial pathogen *S. aureus* is a Gram-positive bacterial species that is one of the most common nosocomial infections and a leading cause of hospital based mortality [7]. Typically colonising the anterior nares, upper respiratory tract or urinary tract [9], *S. aureus* is

implicated in several serious disease states including skin infections, bacteraemia and meningitis [10]. AMR in *S. aureus* is a major concern with many strains resistant to β-lactam antibiotics, such as methicillin [11]. According to a recent survey 20% of all cases of *S. aureus* bacteraemia worldwide are due to MRSA, with certain countries having rates exceeding 40% [4]. As patients with MRSA have a 64% higher risk of infection based mortality than those with susceptible strains [4], this increased resistance is highly concerning. Clinicians are forced to use treatments previously considered as 'last resort' such as vancomycin, daptomycin, linezolid and colistin. These treatments often have significant dose limiting toxicity, and for the case of colistin little information is available for dosing regimens [4, 7, 12, 13]. However resistance to these agents is emerging, with some strains now resistant to all frontline antibacterial classes [14, 15].

1.3 Project aims

One strategy to combat increasing AMR is to develop new antibacterial classes with novel mechanisms of action and that function through new targets. To take an antibacterial agent from discovery to preclinical studies requires overcoming many hurdles. Some of the key steps in early stage antibiotic discovery include: **identifying compounds with whole cell antibacterial activity, devoid of cytotoxic effects** and favourable pharmacology**, confirming the mechanism of action, and determining both the rate and potential mechanisms of resistance.** Failure at any of these milestones can be a serious roadblock for a new antibiotic. The bolded sections above highlights my role in our laboratory's antibiotic project targeting the inhibition of biotin protein ligase (BPL) [16-19]. Below I discuss the literature surrounding the decision to target BPL, the previous antibacterial discovery that has been pursued, the importance of discovering resistance mechanisms early in development and the new technologies that enable such an approach. In particular I will introduce 3 chemical series which are the focus of this thesis. Series 1 and 2 **(figure 6, compounds 8, 9)**, in chapters 3

and 4 respectively, detail the chemical optimisation of the previously described biotin-triazoles chemical scaffold [16] with a focus on improvement of whole cell antibacterial activity. Series 3 **(figure 6, compound 10),** in chapter 5, details a sulphonamide chemical scaffold [20]. One compound using this scaffold was particularly potent leading to further investigation of its mechanism of action and resistance. Chapter 6 addresses these mechanisms of resistance further, with whole genome sequencing used to discover resistance causing mutations.

1.4 Biotin

Biotin, also known as vitamin H or B7, is a micronutrient essential for all life. Biotin serves as a co-factor for biotin-dependent enzymes, which catalyse key carboxylation, decarboxylation or trans-carboxylation reactions [21]. Despite its ubiquitous biological role, biotin is only produced by plants, bacteria and some fungi. Other organisms scavenge biotin from exogenous sources [22]. Mammals primarily obtain biotin from either dietary sources or from gut microflora that produce the vitamin. Recycling of protein bound biotin is also possible through the activity of biotinidase [23]. No equivalent biotinidase activity has been identified in bacteria [24]. In *S. aureus* there are two biotin dependent enzymes acetyl-CoA carboxylase (ACC) and pyruvate carboxylase (PC). The biological roles of these important bacterial biotin-dependent enzymes is described below, as is their activation by the covalent attachment of biotin.

Acetyl-CoA carboxylase function in *S. aureus*

ACC catalyses the first step in fatty acid synthesis (FAS), converting acetyl-CoA to malonyl-CoA, and is required for cell wall maintenance and replication [25]. This reaction occurs by carboxylation of acetyl-CoA and is facilitated by biotin attached to a key lysine residue on ACC. Cell membrane biogenesis is essential for the continued growth and proliferation of cells. Thus, inhibition of the ACC enzyme through prevention of biotinylation

should both impede growth of the organism and prevent its proliferation. This is true of all Gram-negative organisms where the FAS pathway is essential (reviewed [26, 27]). However, there is debate as to whether FAS inhibition is a viable target for Gram-positive pathogens. Unlike Gram-negative organisms which have a specific lipid A core that cannot be synthesised from host derived fatty acids [26], exogenous fatty acids can be used to circumvent the inhibition of the FAS pathway in certain Gram-positive organisms [28, 29]. This is not the case in *S. aureus* as exogenous fatty acids cannot fully ameliorate the knockdown of the *FabI* enzyme in the FASII pathway [26, 27, 29]. This is due to the different levels that exogenous fatty acids can be incorporated in the *S. aureus* membrane. Only 50% of phospholipids in the *S. aureus* membrane can be incorporated from exogenous sources compared to 100% in the Gram positive *S. pneumoniae* [30]. This, and the fact that ACC inhibitors have shown efficacy *in vitro* as well as in mouse models of *S. aureus* bacteraemia [25, 31, 32], supports that antibiotics targeting fatty acid synthesis are viable for *S. aureus* .

Pyruvate Carboxylase is important for several biosynthetic pathways

The effect of inhibiting pyruvate carboxylase (PC) activity through reduced protein biotinylation is less well understood in comparison to the inhibition of ACC. PC catalyses the conversion of pyruvate to oxaloacetate, a molecule that plays a vital role in the tri-citric acid (TCA) cycle and hence, cellular energy production. Oxaloacetate is also a precursor molecule to the synthesis of several amino acids (aspartate, lysine, threonine and methionine), and pyrimidine nucleotides [33]. As a result inhibiting PC activity should impact upon bacterial growth and protein synthesis. This is supported by studies showing that addition of exogenous biotin improves growth rates [34, 35] and protein synthesis in *S. aureus* (reviewed [36]). Of particular interest is lysine biosynthesis. In *S. aureus* lysine is utilised in both peptidoglycan cell wall synthesis and in modifying lipids in the cell membrane [37]. Bacterial adaptation to defend against cationic lipopeptides, such as daptomycin and innate immune response

peptides, require these membrane incorporated lysines. Therefore the inability to synthesise sufficient lysine has the potential to increase bacterial susceptibility to these antibiotics [38].

Roles of TCA cycle metabolism on virulence in *S. aureus*

Despite its important role PC is not essential for bacterial growth in the laboratory. PC does not appear in genome wide screens for essential genes [39, 40]. However, genetic knockout studies showed that PC is required for virulence in a murine model of infection [41]. Knockouts of several TCA cycle enzymes have also been shown to decrease virulence in a nematode killing model [42]. Conversely, one study showed increased virulence as a result of reduced TCA cycle activity in a biofilm model of infection [43]. These conflicting results highlight that the mechanism for regulation of virulence by PC and the TCA cycle is poorly understood, making it difficult to predict the effect of PC inhibition. Understanding the effects of PC inhibition on virulence is important for determining appropriate usage of BPL inhibitors. Metabolic pathways, such as TCA cycle activity, in staphylococci have previously been shown to regulate virulence factor expression in response to environmental conditions (reviewed [44]). One such regulation is increased synthesis of polysaccharide intracellular adhesins (PIA), involved in biofilm formation, that results from repression of TCA cycle activity [44]. Recently a transcriptional regulator, catabolite control protein E (CCPE), was identified that is positively regulated by the TCA cycle intermediate citrate, offering one mechanism for some of the roles of the TCA cycle intermediate enzymes in virulence [45-48]. Deletion of the CCPE gene in *S. aureus* strain Newman caused a $\geq$ 2-fold change in mRNA for 126 target genes, including several gene products required for virulence and pathogenesis [45]. The upregulated genes included those involved in synthesising capsular polysaccharides, consistent with the observation that decreased TCA cycle activity increased this metabolic pathway [44]. Downregulated factors however were also involved in virulence, though largely encompassing super antigen like proteins and inflammatory excreted factors. This indicates

that cells adapt in response to their environment, through production of various virulence factors and this adaptation is mediated by signals such as changes in the TCA cycle [45, 46]. Disrupting the cycle by inhibiting PC will therefore disrupt the ability of the pathogen to adapt to better suit its environment. As a result, understanding how PC inhibition effects the bacteria in the niche habitats it colonises may be important for clinical use of BPL inhibitors.

Biotin protein ligase

Biotin protein ligase reaction

Biotin protein ligase is the enzyme which catalyses the attachment of biotin onto biotin dependent enzymes [49]. BPL is present in all organisms alongside at least one biotin dependent enzyme. The biotinylated enzymes in *S. aureus* are ACC and PC [50]. Biotinylation of these enzymes occurs through two partial reactions. In the first partial reaction, biotin and ATP bind to the enzyme in adjacent ligand binding pockets and react to produce an adenylated reaction intermediate, biotinyl-5′-AMP **(figure 1, compound 2)** and pyrophosphate. This reaction intermediate adopts a V-shaped geometry which is required to occupy both biotin and ATP binding sites (**see figure 4)**. The second partial reaction involves the hydrolysis of this reaction intermediate, resulting in attachment of biotin to a specific lysine residue on the biotin-accepting domain of the biotin-dependent enzymes [49] and release of adenosine monophosphate (AMP) **(figure 1)**. Protein bound biotin then serves as a cofactor to transfer carbon dioxide to small molecules such as acetyl-CoA (for ACC) or pyruvate (for PC). Without protein biotinylation neither ACC nor PC is capable of fulfilling their metabolic functions, making inhibition of BPL a promising target for antibacterial drug discovery.

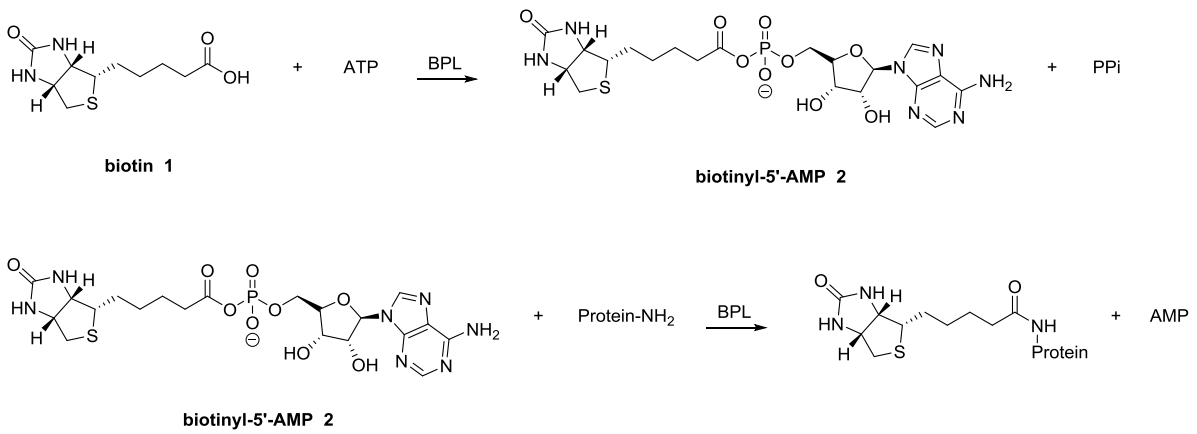

Figure 1. Reaction mechanism of biotin protein ligase. Equation 1, biotin interacts with ATP in the binding pockets of BPL to produce and adenylated reaction intermediate, biotinyl-5′-AMP. Equation 2, biotinyl-5′-AMP interacts with the specific lysine on the biotin domain of biotin dependent enzymes to biotinylate the protein. Adapted from trisubstituted triazole paper

Structural classes of BPL

Three distinct structural classes of BPL exist, with each containing a highly conserved catalytic domain and C-terminal cap **(figure 2)** [36]. *S. aureus* and *E. coli* belong to the Class II BPLs which contain an additional N-terminal DNA binding domain. This allows the BPL to serve as a transcriptional repressor when they form a homodimer (reviewed [51, 52]). The class I BPLs, with notable member *Mycobacterium tuberculosis*, lack this domain. Class III BPLs, including human and fungi, contain a distinct N-terminal extension. Though a high resolution X-ray structure remains elusive, this N-terminal extension has been shown to be important for aiding recognition of the target domain of biotin dependent enzymes, but does not exhibit any DNA binding motifs [53, 54].

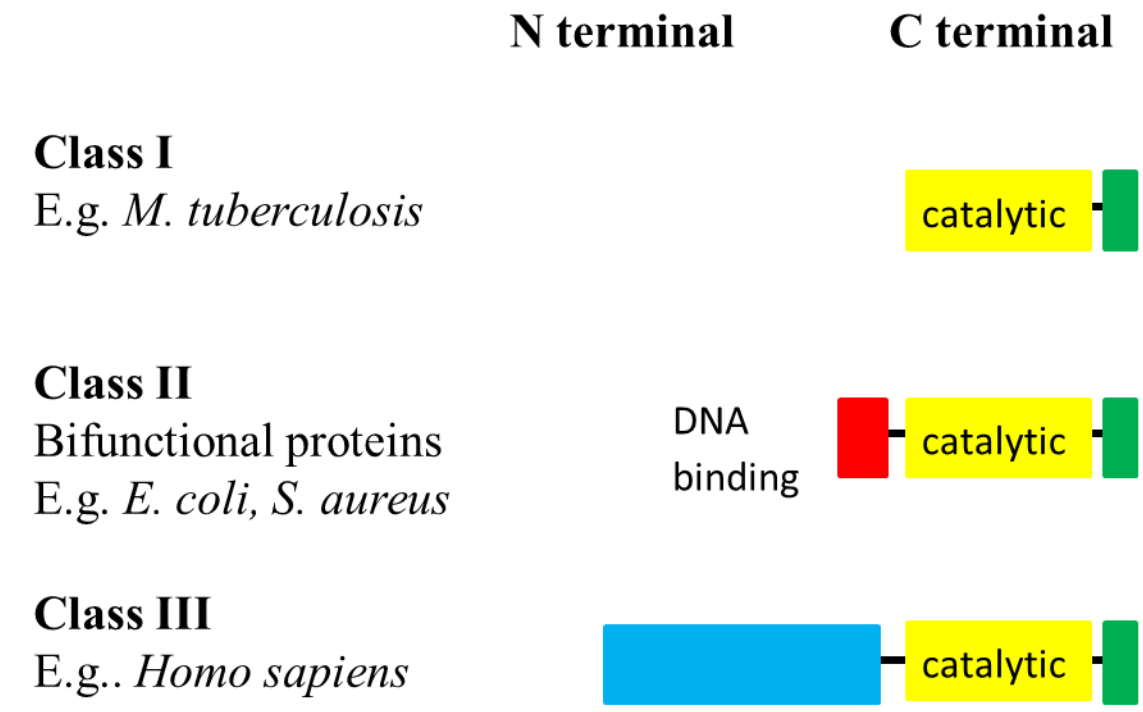

Figure 2: Structural classes of BPL. Three distinct structural classes of BPL exist with a conserved catalytic function. All classes contain a conserved catalytic domain with Class II BPLs additionally contain an N-terminal DNA binding domain and class III BPLs a large N-terminal domain with unknown function. (adapted from Paparella et al.)

BPL transcriptional repression

The transcriptional repressor capability of class II BPLs has the potential to play a role in antibacterial activity. The BPL of *S. aureus* acts to transcriptionally repress expression of transcripts for both the biotin synthesis enzymes and biotin import protein, BioY, in response to biotin levels in the cell. This transcriptional repressor function of the class II BPLs relies on the homo-dimerisation of the enzyme and binding to two independent half-site recognition sequences. The dimerisation is stabilised through interactions of side chains R122 and F123 with D200 of the opposing monomer **(figure 4)** on *S. aureus* BPL (*Sa*BPL) [50, 55, 56] and equivalent residues R118, R119 and D197 on *E. coli* BPL [57]. However, the exact

requirements for DNA-binding to occur are still unclear with recent evidence that *S. aureus* BPL may bind recognition sequences as a monomer [55] and recruit a second BPL subunit (Jiulia Satiaputra, Thesis 2017). This is in contrast with the *E. coli* BPL where dimerization proceeds prior to DNA binding (reviewed [51, 52]). For both enzymes dimerisation is induced by the presence of the reaction intermediate, biotinyl-5′-AMP, **(figure 1, compound 2).** Many successful BPL inhibitors described in the literature are chemical analogues of **2,** making it likely that BPL inhibitors could similarly induce dimerisation. This has been shown with two separate reaction intermediate mimics with *E. coli* BPL [58]. As BPL inhibitors can act as a co-repressor the DNA binding function may play a role in the antibacterial effect of BPL inhibitors, making understanding this process important for the future design of BPL inhibitors. Recent studies investigating the DNA binding of *Sa*BPL show *Sa*BPL represses expression of the biotin biosynthesis operon (*bioO*), transporter (*bioY*) [59] and putative long chain fatty acid ligases (*yhfT/ yhfS*) (Jiulia Satiaputra, Thesis 2017) [60] in response to increasing biotin levels. The respective half sites for these binding sites differ slightly, establishing a hierarchy of the three targets in response to biotin stress (Jiulia Satiaputra, Thesis 2017). This results in more rapid and complete repression of biotin synthesis enzymes than biotin import protein BioY at the same (10 nM) biotin concentrations (Jiulia Satiaputra, Thesis 2017). This is thought to be a result of the prioritisation of the less metabolically expensive transport system to prevent excess energy usage, as each biotin molecule synthesised requires the energetic equivalent of 20 ATP molecules (Jiulia Satiaputra, Thesis 2017). [61]. The presence of an inhibitor that induces dimerization could, therefore, feasibly maintain constitutive repression of either biotin synthesis or both biotin synthesis and transport genes. This would be expected to either reduce biotin competing for binding sites or lead to biotin starvation. This function was explored in depth by Jiulia Satiaputra, a PhD student in the lab and will be discussed further in chapter 5.

Essential nature of BPL

Several lines of evidence support targeting BPL for the creation of a new antibiotic class. BPL and ACC have been identified as an essential enzyme in *S. aureus* [39, 40] and other organisms [20, 62, 63]. Additionally chemical inhibition of protein biotinylation has also been demonstrated, with two mechanisms described in the literature. One, a natural biotin mimic with antibacterial activity acts by incorporating into and crippling biotin dependent enzymes [64]. The other, which is the focus of this thesis, are synthetic mimics of the reaction intermediate which have been produced to block BPL activity with antibacterial effect [16, 17, 19, 20, 36, 65, 66]. This antibacterial activity occurs through indirectly inhibiting the activity of biotin-dependent enzymes which in *S. aureus* are important for the cellular processes of both fatty acid synthesis (FAS), and the tri-citric acid (TCA) cycle **(figure 3)** [67]. The drug design approaches used to inhibit BPL and their antibacterial effect against *S. aureus* are discussed further below.

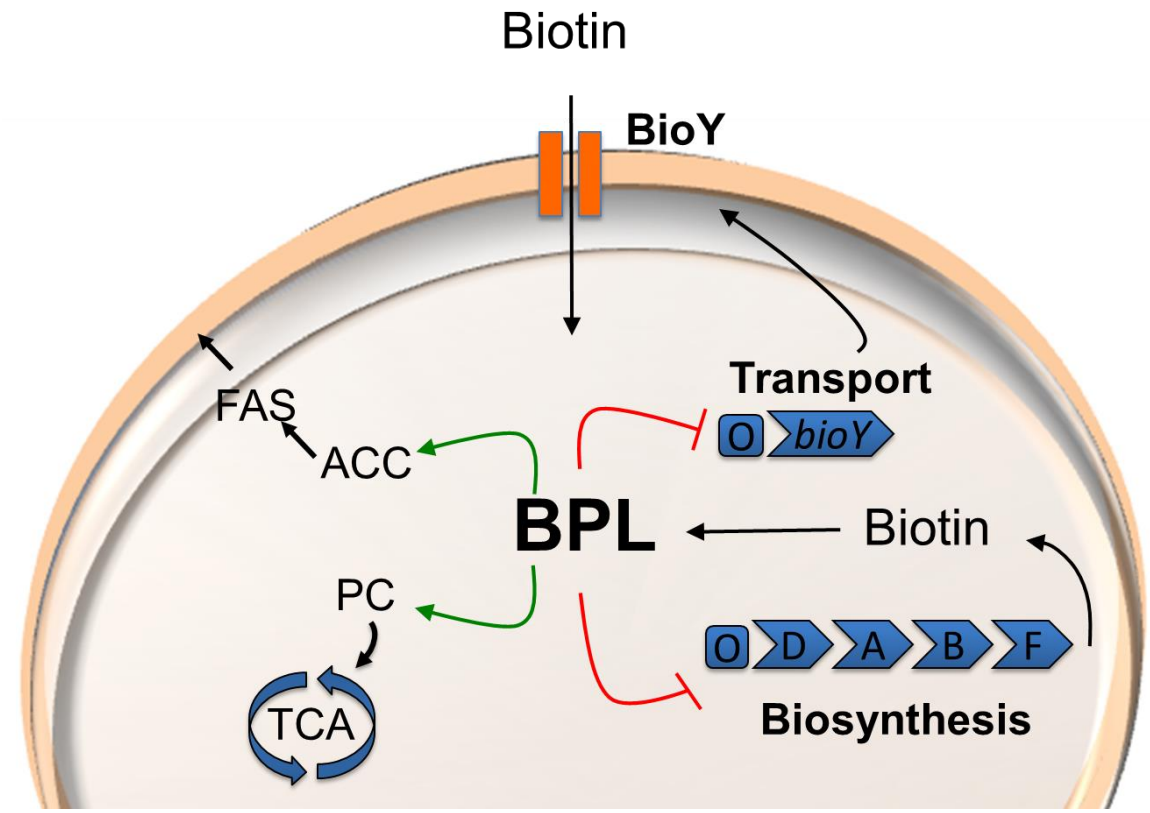

Figure 3: Roles of BPL in *S. aureus*. BPL catalyses the attachment of biotin and activation of biotin dependent enzymes acetyl-CoA carboxylase (ACC) and pyruvate carboxylase (PC) which are involved in fatty acid synthesis (FAS) and replenishment of the tri-citric acid (TCA) cycle respectively (green arrows). As a homodimer BPL also represses expression of genes involved in biotin transport and synthesis in response to increasing biotin (red lines). (adapted from slide provided by S. Polyak)

1.5 Drug design approach

Structure based approaches can succeed where HTS has failed

Despite the genetic evidence to suggest that the inhibition of BPL provides a route to new antibacterials, GSK failed to identify inhibitors in a high throughput screen with a library of 260,000-530,000 compounds [68]. This lack of success highlights a major difficulty in antibacterial drug discovery, namely poor sampling of chemical space even in large compound libraries. As it is impossible to sample all of chemical space with these 'shotgun' approaches, structural data is vital to direct compound discovery. Poor entry of compounds into bacteria also contributes to failure. Using the same library of 260,000-530,000 compounds only three anti-staphylococcal compounds were identified [68]. This highlights why whole cell testing is important for compound development. Additional to these general concerns, the desire for a broad spectrum antibiotic that lacks toxicity is particularly challenging in the case of BPL, due to the presence of a human BPL homologue. The failures discussed above indicate the problems with high-throughput screening approaches. Hence, our group and others have attempted structure based drug design. The success of BPL inhibition attempts recently, using structure guided drug design, suggest the approach is more likely to produce a successful antibiotic.

Targeting BPL by probing the active site/ compound progression

Using X-ray crystal structures of BPL, structure guided drug design of BPL inhibitors has been performed by our laboratory [16-19], and others [20, 66, 69]. The BPL of *S. aureus* undergoes an ordered reaction mechanisms to catalyse protein biotinylation **(figure 2)**. In the first step biotin binds to the enzyme and induces a disordered to ordered transition for residues 118 to 129 known as the biotin binding loop. This conformational change results in the positioning of W127 in the active site such that it can accommodate a π-π stacking interaction with ATP **(figure 4)** [16]. Subsequent binding of ATP permits conjugation with

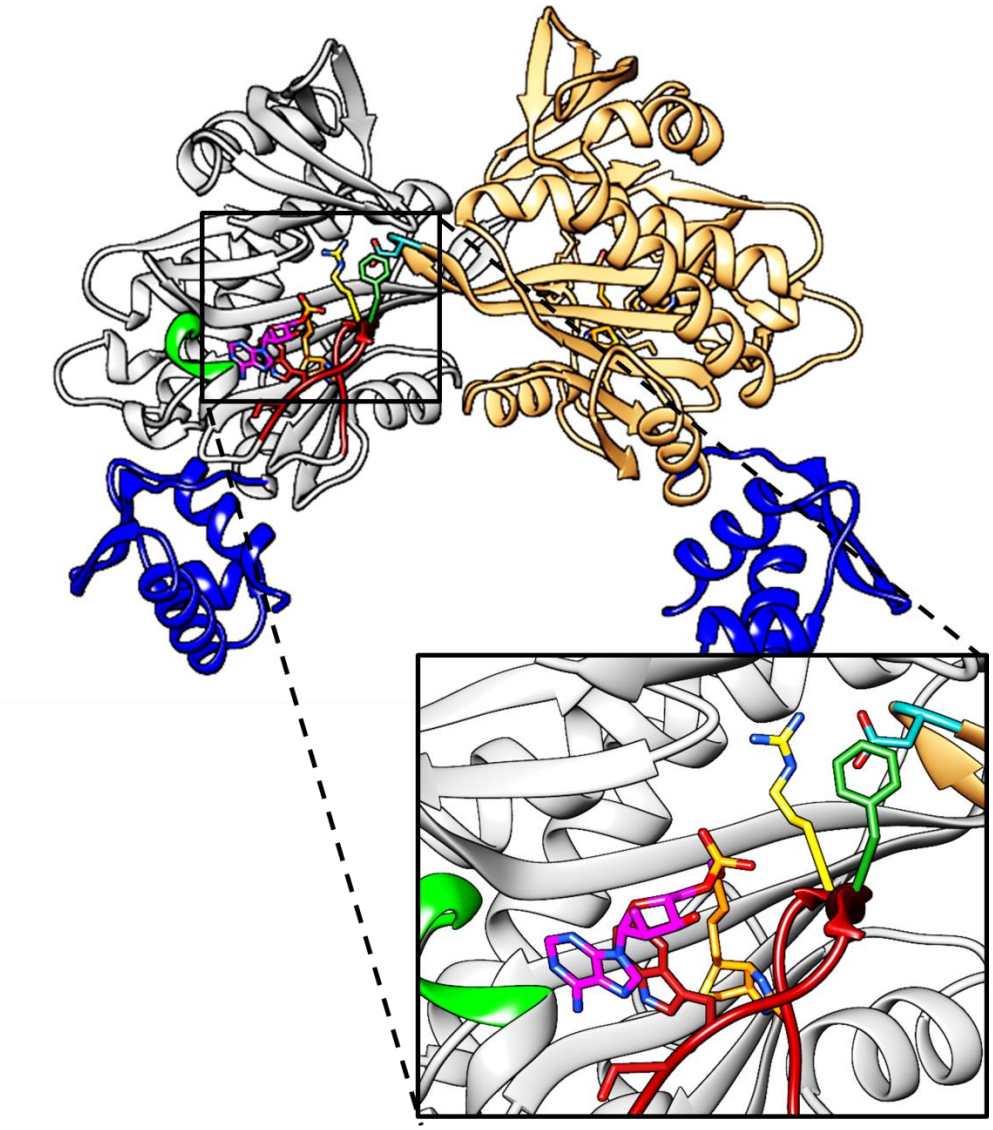

Figure 4: *S. aureus* BPL dimer with biotinol-5′-AMP bound (PDB 3RIR). The biotin binding loop 118-129 (red) is present initially allowing the biotin moiety (orange) to bind. This causes a conformational change ordering the nucleotides involved in nucleotide binding I224, A228 (light green) as well as positioning the tryptophan W127 involved in π-π stacking with the ATP. This allows the binding of ATP or adenine moeity (purple). Binding of ATP and biotin in adjacent pockets leads to the formation of the reaction intermediate which binds with a V-shaped geometry. The DNA binding domains of *Sa*BPL are also highlighted at the N-terminal end (blue). **Inset** the residues involved in dimerisation of the BPL are highlighted: F123 (dark green), R122 (yellow) and D200 of the opposing monomer (light blue).

biotin to form an adenylated reaction intermediate, **2** [70]. Consequently, the enzyme must bind biotin first, then ATP. Initial attempts to inhibit BPL with analogues of biotin, such as biotin acetylene **(figure 5, compound 3)**, were pursued. However, highly conserved amino acids in the biotin-binding pocket made selectivity difficult [17]. On the other hand, the nucleotide binding pockets of human and *S. aureus* enzymes show greater diversity in amino acid sequence [16, 71]. As a result of this, the knowledge of the reaction mechanism has impacted inhibitor design. Inhibitors that target the active site must contain a biotin moiety, as biotin is required for the formation of the nucleotide-binding pocket. The biotinyl pharmacophore can then be elaborated with groups that can occupy the ATP site. This allows selectivity to be engineered into the compound.

Phosphodiester linker and creation of the pan inhibitor biotinol-5′-AMP

Replacing the labile phosphoanhydride linker of the reaction intermediate **2** with more stable bioisosteres yields competitive inhibitors that target the active site. Several modifications to the linker have improved selectivity and potency **(figure 5)**. First, replacing the phosphoanhydride group from the reaction intermediate with a non-hydrolysable phosphodiester bioisostere, produced a potent inhibitor biotinol-5′-AMP (MIC 1-4μg/ml) with no observed cell toxicity against HepG2 cells (CC_{50} < 200 μg/mL) **(figure 5, compound 4)** [19, 57]. Unfortunately, **4** still exhibited poor selectivity, inhibiting the human enzyme (K_i = 182 nM) as well as that of *S. aureus* (K_i = 18 nM, MIC 1-4μg/ml) and *M. tuberculosis* (K_i = 52 nM, MIC 0.5-2.5μg/ml). Subsequent attempts to produce a selective inhibitor have focused on replacing the phosphoanhydride linker with a triazole bioisostere in *S. aureus* (**figure 5, compounds 4-6)** and a sulfonyl linker for *M. tuberculosis*. These are described in further detail below.

3) Biotin acetylene

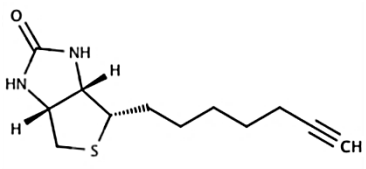

4) Biotinol-5′-AMP

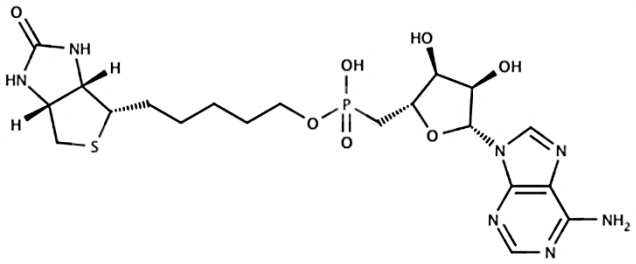

5) Biotin adenosine triazole

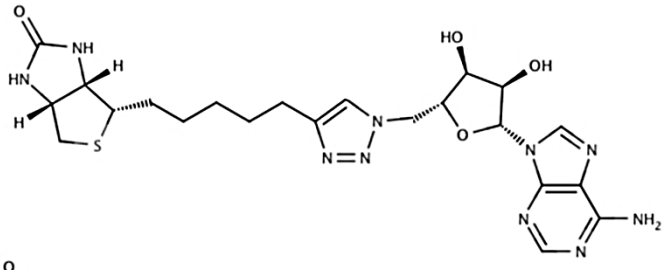

6) Biotin adenine triazole

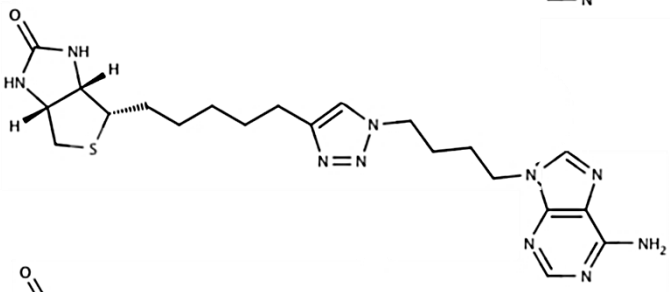

7) Biotin benzoxazolone triazole

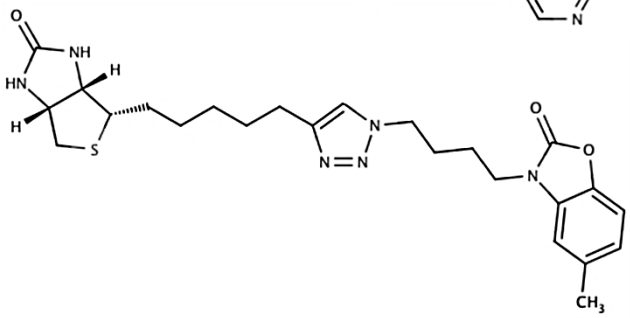

Figure 5: Previously described compounds used to inhibit BPL. **3)** biotin acetylene, **4)** biotinol-5′-AMP, **5)** biotin triazole without modifications to the adenosine moiety, **6)** removal of the ribosyl moiety and **7)** replacement of adenine with a benzoxalone of **5** improved potency and selectivity

Series 1
10) Benzyl triazoles

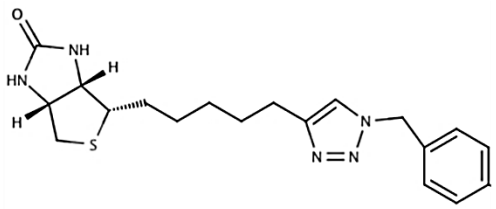

Series 2
11) Halogenated triazoles

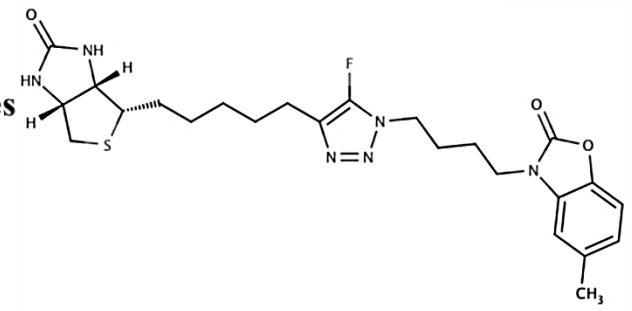

Series 3
12) sulfonamides

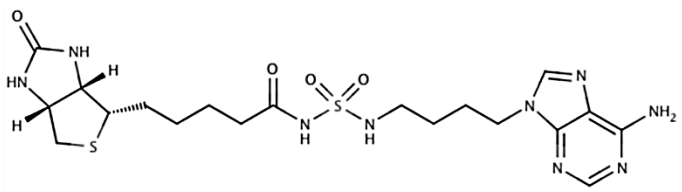

Figure 6: Representative compounds of the 3 series addressed in this thesis. **Series 1,** Benzyl biotin-triazoles, were attempts to shorten the triazole pharmacophore and probe the ribose binding pocket to improve activity. **Series 2,** halogenation at the 5C position on the triazole ring of both biotin-triazole **6** and series 1 was attempted to improve whole cell activity. **Series 3,** removal of the ribose and other modifications to the biotin sulfonamide Bio-AMS produced by Duckworth et al. was attempted to improve selectivity and whole cell anti-staphylococcal activity.

Biotin triazoles- Series 1 and 2

Our group has focused on designing selective BPL inhibitors using a triazole based linker. The triazole heterocycle has several desirable features for drug discovery of BPL inhibitors: 1. The linker is stable to enzymatic degradation, including biotinidase [72], 2. hydrogen bonding interactions are available through the nitrogens of the triazole heterocycle, and 3. the linker can impart the same V-shaped geometry observed in the natural substrate **2** [16]. Using the 1,2,3-triazole **5 (figure 5)** yielded activity against the *Sa*BPL (K_i 1.17 μM) but not the human homologue. Development of this compound series to improve potency was undertaken with removal of the ribosyl moiety **6 (figure 5)**. Further replacement of the adenine with a benzoxalone, as in **7 (figure 5)** produced the most potent (K_i 0.09 μM) and selective compound with >1100 fold selectivity over the human homologue. However, the compound failed to completely inhibit bacterial growth, with only 80% inhibition observed at 8 μg/ml [16]. Chapters 3 and 4 will focus on our attempts to improve the whole cell antibacterial activity of the biotin-triazole inhibitors. **Series 1 (figure 6, compound 8)**, in chapter 3, focuses on shortening the biotin-triazole pharmacophore, by appending a benzyl moiety to probe binding in the ribose pocket of BPL. **Series 2 (figure 6, compound 9)**, in chapter 4, explores halogenation on the C5 position of the triazole ring as an alternative route to improve whole cell activity.

Sulfonamide linker-series 3

Another chemical scaffold that has been described in the literature are the biotin sulphonamides. Replacement of the phosphoanhydride linker of **2** with a sulfonyl bioisostere was first used to produce a series of inhibitors targeting the BPL of *M. tuberculosis* [20]. The most potent of this series, Bio-AMS demonstrated efficacy against *M. tuberculosis* BPL *in vitro* and possessed whole cell antibacterial activity (MIC= 0.31–0.78 μM) [20]. Despite the whole cell activity against *M. tuberculosis* the compound lacked antibacterial activity against

S. aureus and had cytotoxicity against one of two cell lines, with 50% inhibition of a Vero liver cell line at 58 μM [20]. As the ribose on biotin-triazole was shown to be dispensable for anti-staphylococcal activity [16], **Series 3 (figure 6, compound 10)** in chapter 5, focuses on compounds based around the Bio-AMS sulfonyl linker with no ribose moiety to create new selective *Sa*BPL inhibitors. The Bio-AMS compound is also the only BPL inhibitor described in literature that has a confirmed mechanism of antibacterial action through inhibition of biotinylation activity [20]. A similar approach to that adopted for this compound is used in this thesis to characterise promising compounds from Series 1, 2 and 3.

1.6 Resistance mechanisms and detection

Trying to understand the evolution and dispersal of drug resistant pathogens is an important part of modern healthcare. Although AMR can occur through many independent mechanisms, they broadly fall into 4 categories: 1) The antibiotic is prevented from entering the cell through modification of the cell membrane, 2) is actively removed from the cell by efflux pumps, 3) the antibiotic is degraded enzymatically, or 4) the antibiotic target is modified through mutation to prevent activity [73]. Understanding these resistance mechanisms can help guide further drug development by determining if new analogues avoid obvious mechanisms or if new approaches are needed. Additionally, discovery of pre-existing resistance mechanisms, or rapid spontaneous resistance rates during development, can prevent costly failures in clinical trials [74, 75]. Cross-resistance to existing antibacterial agents should also be investigated as often patients treated with last line treatments will have previously been subjected to other antibacterial agents [76, 77]. Understanding what cross-resistance may be present for BPL inhibitors is therefore important information for eventual clinical use.

AMR has been reported for every antibiotic released to clinic [7, 78]. The advent of vastly improved and cheaper sequencing technologies, capable of probing entire bacterial

genomes, has greatly enhanced the quantity of biological data surrounding these resistant strains. This has allowed for faster and easier identification of resistance conveying mutations in the lab through parallel evolution studies [79-83] and determining how resistance may develop and disseminate in the clinic [84-86]. Parallel evolution studies expose bacteria to sub-inhibitory concentrations of an antibiotic for extended periods of time, allowing resistance to evolve. The resistant strains can then be compared through whole genome sequencing. Several studies in *S. aureus* and other organisms reported only 1-6 mutations are required for a strain to become resistant to certain antibiotics [79-81, 87]. These studies have also shown that in parallel isolates, most mutations occur in the same regions of the genome and, for some antibiotics, with a defined order. In combination with the use of sequencing in diagnosis of infections, such studies could be used to predict a strains resistance potential in clinical settings as is already the case for some resistance determinants [88-90]. The clinical relevance of such studies has also been explored with comparison of resistance evolution in clinical and laboratory settings. To address how the evolution of resistance differs *in vitro* vs in the clinic, one study looked at *M. tuberculosis* strains [86]. Using whole genome sequencing (WGS) conserved resistance mechanisms were observed in both cohorts. However, the clinical strains also contained additional compensatory mutations not selected for in the controlled evolution experiment [86]. This highlights that whilst such *in vitro* studies are valuable for understanding mutational hotspots and resistance mechanisms they may not necessarily fully explore all possible mechanisms. As fitness deficits associated with resistance can be detrimental in a competitive environment, resistance often is slower and requires additional mutations to flourish *in vivo*. Similarly, adaptive resistance that requires particular environmental conditions will not be discovered, as described for one *Pseudomonas aeruginosa* resistance mechanism [75]. In chapter 6 of this thesis parallel evolution studies of the mutational hotspots involved in *S. aureus* resistance to BPL inhibitors were undertaken allowing understanding of the mechanisms involved.

1.7 Research described in this thesis.

This thesis focuses on characterising the next generation of BPL inhibitors for antibacterial drug discovery. Three different pharmacophores are presented the benzyl triazoles, C5-halogenated triazoles and sulfonyl-linked compounds. Their potency, whole cell antibacterial activity and mechanism of action are studied, providing valuable information for future compound development. Each series undergoes the same compound progression plan, summarised in **figure 7**. This encompasses initial screening undertaken against the target enzyme, subsequent analysis of active compounds in cell based systems, both for efficacy against bacteria and lack of toxic side effects against human cell lines, and finally investigation of the mechanisms of action and resistance for the most promising compounds.

The first paper in this thesis "A new series of BPL inhibitors to probe the ribose-binding pocket of *Staphylococcus aureus* biotin protein ligase" addresses attempts to improve the activity of triazole based BPL inhibitors as well as create a smaller pharmacophore for further development and optimisation. My contribution to this paper was cytotoxicity testing of the most potent compounds as well as generation of a BPL overexpression system in *S. aureus* RN4220 which I subsequently used to test the mechanism of action of compounds. The second manuscript in progress "Halogenation of biotin protein ligase inhibitors improves whole cell activity against *Staphylococcus aureus*" addresses the hypothesis that halogenation at the C5 position on triazole inhibitors would improve whole cell antibacterial activity. My contribution to this paper was assisting in antibacterial susceptibility testing of the second halogenated series and undertaking mechanism of action studies against the most potent compound in the first series. The third manuscript in preparation "Sulfonyl based mimic of biotinyl-5′-AMP as antibacterial agents against *Staphylococcus aureus*" addresses modification of a sulfonyl based linked BPL inhibitor described in literature to improve selectivity and anti-staphylococcal activity. Due to the potent antibacterial activity observed,

further investigation into the mechanism of action and resistance was undertaken with a particular focus on the transcriptional co-repressor function of the compound. My contribution to this work was to perform: antibacterial susceptibility against ATCC49775 and RN4220, cytotoxicity assays, mechanism of action and advanced resistance studies, and expression, purification and characterisation of the D200E mutant BPL. The final manuscript in preparation in this thesis "Mutations associated with reduced susceptibility to a novel antibacterial class, Biotin Protein Ligase inhibitors, in *Staphylococcus aureus"* addresses the mutations associated with resistance to BPL inhibitors in strains generated in the previous manuscript. All of the experiments described in the manuscript were performed by myself with the exception of the whole genome sequencing run. The aim of this thesis is to help guide the development of BPL inhibitors as antibacterial agents, in particular highlighting the role of the co-repressor function of BPL inhibitors in antibacterial activity. The studies into resistance mechanisms further address concerns of rapid resistance, as well as providing indicative mutations that lead to resistance, helping understand what pathways are required to combat BPL inhibition.

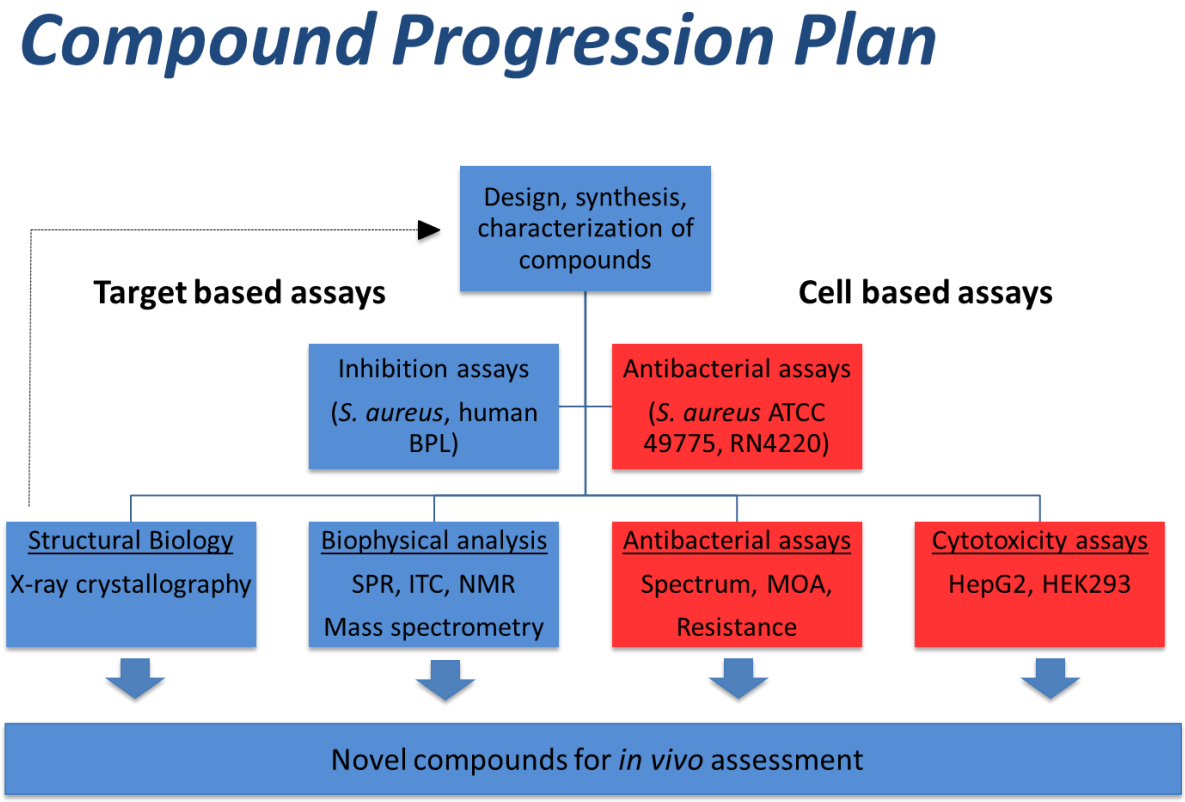

Figure 7: General progression of compounds used for series 1-3 in this thesis, red boxes represent work that was directly undertaken by me as part of this thesis (adapted from slide provided by S. Polyak)

1.8 References

1. *Review on Antimicrobial Resistance. Antimicrobial Resistance: Tackling a Crisis for the Health and Wealth of Nations*. 2014.
2. Rice, L.B., *Federal funding for the study of antimicrobial resistance in nosocomial pathogens: no ESKAPE.* J Infect Dis, 2008. **197**(8): p. 1079-81.
3. Pendleton, J.N., S.P. Gorman, and B.F. Gilmore, *Clinical relevance of the ESKAPE pathogens.* Expert Rev Anti Infect Ther, 2013. **11**(3): p. 297-308.
4. World Health Organisation, *Antimicrobial resistance: Global report on resistance.* 2014.
5. Cooper, M.A. and D. Shlaes, *Fix the antibiotics pipeline.* Nature, 2011. **472**(7341): p. 32-32.
6. Butler, M.S., M.A. Blaskovich, and M.A. Cooper, *Antibiotics in the clinical pipeline at the end of 2015.* J Antibiot, 2016.
7. Boucher, H.W., et al., *Bad bugs, no drugs: no ESKAPE! An update from the Infectious Diseases Society of America.* Clin Infect Dis, 2009. **48**(1): p. 1-12.
8. Tommasi, R., et al., *ESKAPEing the labyrinth of antibacterial discovery.* Nat Rev Drug Discov, 2015. **14**(8): p. 529-42.
9. Archer, G.L., *Staphylococcus aureus: a well-armed pathogen.* Clin Infect Dis, 1998. **26**(5): p. 1179-81.
10. Lowy, F.D., *Staphylococcus aureus infections.* N Engl J Med, 1998. **339**(8): p. 520-32.
11. Chambers, H.F., *Methicillin-resistant staphylococci.* Clin Microbiol Rev, 1988. **1**(2): p. 173-86.
12. Butler, M.S., et al., *Glycopeptide antibiotics: back to the future.* J Antibiot (Tokyo), 2014. **67**(9): p. 631-44.

13. Bishop, E., et al., *Good clinical outcomes but high rates of adverse reactions during linezolid therapy for serious infections: a proposed protocol for monitoring therapy in complex patients.* Antimicrob Agents Chemother, 2006. **50**(4): p. 1599-1602.

14. Gardete, S. and A. Tomasz, *Mechanisms of vancomycin resistance in Staphylococcus aureus.* J Clin Invest, 2014. **124**(7): p. 2836-40.

15. Tsiodras, S., et al., *Linezolid resistance in a clinical isolate of Staphylococcus aureus.* The Lancet, 2001. **358**(9277): p. 207-208.

16. Soares da Costa, T.P., et al., *Selective inhibition of Biotin Protein Ligase from Staphylococcus aureus.* J Biol Chem, 2012. **287**(21): p. 17823-17832.

17. Soares da Costa, T.P., et al., *Biotin analogues with antibacterial activity are potent inhibitors of biotin protein ligase.* ACS Med Chem Lett, 2012. **3**(6): p. 509-14.

18. Tieu, W., et al., *Heterocyclic acyl-phosphate bioisostere-based inhibitors of Staphylococcus aureus biotin protein ligase.* Bioorg Med Chem Lett, 2014. **24**(19): p. 4689-93.

19. Tieu, W., et al., *Improved Synthesis of Biotinol-5'-AMP: Implications for Antibacterial Discovery.* ACS Med Chem Lett, 2015. **6**(2): p. 216-20.

20. Duckworth, B.P., et al., *Bisubstrate adenylation inhibitors of biotin protein ligase from Mycobacterium tuberculosis.* Chem Biol, 2011. **18**(11): p. 1432-41.

21. Knowles, J.R., *The mechanism of biotin-dependent enzymes.* Annu Rev Biochem, 1989. **58**(1): p. 195-221.

22. Polyak, S. and A. Chapman-Smith, *Biotin*. 2004, Elsevier.

23. Hymes, J. and B. Wolf, *Biotinidase and its roles in biotin metabolism.* Clinica Chimica Acta, 1996. **255**(1): p. 1-11.

24. Chapman-Smith, A. and J.E. Cronan, Jr., *Molecular biology of biotin attachment to proteins.* J Nutr, 1999. **129**(2S Suppl): p. 477S-484S.

25. Freiberg, C., et al., *Identification and Characterization of the First Class of Potent Bacterial Acetyl-CoA Carboxylase Inhibitors with Antibacterial Activity.* J Biol Chem, 2004. **279**(25): p. 26066-26073.

26. Parsons, J.B. and C.O. Rock, *Is bacterial fatty acid synthesis a valid target for antibacterial drug discovery?* Curr Opin Microbiol, 2011. **14**(5): p. 544-9.

27. Yao, J. and C.O. Rock, *Bacterial fatty acid metabolism in modern antibiotic discovery.* Biochim Biophys Acta, 2017. **1862**(11): p. 1300-1309.

28. Brinster, S., et al., *Type II fatty acid synthesis is not a suitable antibiotic target for Gram-positive pathogens.* Nature, 2009. **458**(7234): p. 83-6.

29. Balemans, W., et al., *Essentiality of FASII pathway for Staphylococcus aureus.* Nature, 2010. **463**(7279): p. E3; discussion E4.

30. Parsons, J.B., et al., *Metabolic basis for the differential susceptibility of Gram-positive pathogens to fatty acid synthesis inhibitors.* Proc Natl Acad Sci U S A, 2011. **108**(37): p. 15378-15383.

31. Payne, D.J., et al., *Discovery of a novel and potent class of FabI-directed antibacterial agents.* Antimicrob Agents Chemother, 2002. **46**(10): p. 3118-24.

32. Freiberg, C., et al., *Novel bacterial acetyl coenzyme A carboxylase inhibitors with antibiotic efficacy in vivo.* Antimicrob Agents Chemother, 2006. **50**(8): p. 2707-12.

33. Jitrapakdee, S. and J.C. Wallace, *Structure, function and regulation of pyruvate carboxylase.* Biochem J, 1999. **340 (Pt 1)**(1): p. 1-16.

34. Gretler, A.C., et al., *Vitamin nutrition of the staphylococci with special reference to their biotin requirements.* J Bacteriol, 1955. **70**(1): p. 44.

35. Porter, J. and M.J. Pelczar Jr, *The Nutrition of Staphylococcus aureus: The Influence of Biotin, Bios IIB and Vitamin H on the Growth of Several Strains.* J Bacteriol, 1941. **41**(2): p. 173.

36. Paparella, A.S., et al., *Structure guided design of biotin protein ligase inhibitors for antibiotic discovery.* Curr Top Med Chem, 2014. **14**(1): p. 4-20.

37. Hutton, C.A., M.A. Perugini, and J.A. Gerrard, *Inhibition of lysine biosynthesis: an evolving antibiotic strategy.* Mol Biosyst, 2007. **3**(7): p. 458-65.

38. Baltz, R.H., *Daptomycin: mechanisms of action and resistance, and biosynthetic engineering.* Curr Opin Chem Biol, 2009. **13**(2): p. 144-51.

39. Chaudhuri, R.R., et al., *Comprehensive identification of essential Staphylococcus aureus genes using Transposon-Mediated Differential Hybridisation (TMDH).* BMC Genomics, 2009. **10**: p. 291.

40. Forsyth, R.A., et al., *A genome-wide strategy for the identification of essential genes in Staphylococcus aureus.* Mol Microbiol, 2002. **43**(6): p. 1387-400.

41. Benton, B.M., et al., *Large-scale identification of genes required for full virulence of Staphylococcus aureus.* J Bacteriol, 2004. **186**(24): p. 8478-89.

42. Bae, T., et al., *Staphylococcus aureus virulence genes identified by bursa aurealis mutagenesis and nematode killing.* Proc Natl Acad Sci U S A, 2004. **101**(33): p. 12312-12317.

43. Zhu, Y., et al., *Tricarboxylic acid cycle-dependent attenuation of Staphylococcus aureus in vivo virulence by selective inhibition of amino acid transport.* Infect Immun, 2009. **77**(10): p. 4256-64.

44. Somerville, G.A. and R.A. Proctor, *At the crossroads of bacterial metabolism and virulence factor synthesis in Staphylococci.* Microbiol Mol Biol Rev, 2009. **73**(2): p. 233-48.

45. Ding, Y., et al., *Metabolic sensor governing bacterial virulence in Staphylococcus aureus.* Proc Natl Acad Sci U S A, 2014. **111**(46): p. E4981-90.

46. Hartmann, T., et al., *The catabolite control protein E (CcpE) affects virulence determinant production and pathogenesis of Staphylococcus aureus.* J Biol Chem, 2014.

47. Hartmann, T., et al., *Catabolite Control Protein E (CcpE) Is a LysR-type Transcriptional Regulator of Tricarboxylic Acid Cycle Activity in Staphylococcus aureus.* J Biol Chem, 2013. **288**(50).

48. Lan, L., et al., *Golden pigment production and virulence gene expression are affected by metabolisms in Staphylococcus aureus.* J Bacteriol, 2010. **192**(12): p. 3068-3077.

49. Chapman-Smith, A. and J.E. Cronan, Jr., *The enzymatic biotinylation of proteins: a post-translational modification of exceptional specificity.* Trends Biochem Sci, 1999. **24**(9): p. 359-63.

50. Pendini, N.R., et al., *Purification, crystallization and preliminary crystallographic analysis of biotin protein ligase from Staphylococcus aureus.* Acta Crystallogr Sect F Struct Biol Cryst Commun, 2008. **64**(Pt 6): p. 520-3.

51. Beckett, D., *Biotin sensing: universal influence of biotin status on transcription.* Annu Rev Genet, 2007. **41**: p. 443-64.

52. Satiaputra, J., et al., *Mechanisms of biotin-regulated gene expression in microbes.* Synth Syst Biotechnol, 2016. **1**(1): p. 17-24.

53. Sternicki, L.M., et al., *Mechanisms Governing Precise Protein Biotinylation.* Trends Biochem Sci, 2017. **42**(5): p. 383-394.

54. Polyak, S.W., et al., *Biotin Protein Ligase from Saccharomyces cerevisiae THE N-TERMINAL DOMAIN IS REQUIRED FOR COMPLETE ACTIVITY.* J Biol Chem, 1999. **274**(46): p. 32847-32854.

55. Soares da Costa, T.P., et al., *Dual roles of F123 in protein homodimerization and inhibitor binding to biotin protein ligase from Staphylococcus aureus.* Mol Microbiol, 2014. **91**(1): p. 110-20.

56. Pendini, N.R., et al., *Structural characterization of Staphylococcus aureus biotin protein ligase and interaction partners: an antibiotic target.* Protein Sci, 2013. **22**(6): p. 762-73.

57. Wood, Z.A., et al., *Co-repressor induced order and biotin repressor dimerization: a case for divergent followed by convergent evolution.* J Mol Biol, 2006. **357**(2): p. 509-523.

58. Brown, P.H., et al., *The biotin repressor: modulation of allostery by corepressor analogs.* J Mol Biol, 2004. **337**(4): p. 857-869.

59. Hebbeln, P., et al., *Biotin uptake in prokaryotes by solute transporters with an optional ATP-binding cassette-containing module.* Proc Natl Acad Sci U S A, 2007. **104**(8): p. 2909-14.

60. Rodionov, D.A., A.A. Mironov, and M.S. Gelfand, *Conservation of the biotin regulon and the BirA regulatory signal in Eubacteria and Archaea.* Genome research, 2002. **12**(10): p. 1507-1516.

61. Feng, Y., et al., *A Francisella virulence factor catalyses an essential reaction of biotin synthesis.* Mol Microbiol, 2014. **91**(2): p. 300-14.

62. Thanassi, J.A., et al., *Identification of 113 conserved essential genes using a high-throughput gene disruption system in Streptococcus pneumoniae.* Nucleic Acids Res, 2002. **30**(14): p. 3152-3162.

63. Gerdes, S.Y., et al., *Experimental determination and system level analysis of essential genes in Escherichia coli MG1655.* J Bacteriol, 2003. **185**(19): p. 5673-84.

64. Hanka, L., M. Bergey, and R. Kelly, *Naturally occurring antimetabolite antibiotic related to biotin.* Science, 1966. **154**(3757): p. 1667-1668.

65. Bockman, M.R., et al., *Targeting Mycobacterium tuberculosis Biotin Protein Ligase (MtBPL) with Nucleoside-Based Bisubstrate Adenylation Inhibitors.* J Med Chem, 2015. **58**(18): p. 7349-7369.

66. Park, S.W., et al., *Target-based identification of whole-cell active inhibitors of biotin biosynthesis in Mycobacterium tuberculosis.* Chem Biol, 2015. **22**(1): p. 76-86.

67. Jitrapakdee, S., et al., *Structure, mechanism and regulation of pyruvate carboxylase.* Biochem J, 2008. **413**(3): p. 369-87.

68. Payne, D.J., et al., *Drugs for bad bugs: confronting the challenges of antibacterial discovery.* Nat Rev Drug Discov, 2007. **6**(1): p. 29-40.

69. Shi, C., et al., *Bisubstrate Inhibitors of Biotin Protein Ligase in Mycobacterium tuberculosis Resistant to Cyclonucleoside Formation.* ACS Med Chem Lett, 2013. **4**(12): p. 12131217.

70. Bagautdinov, B., et al., *Crystal Structures of Biotin Protein Ligase from Pyrococcus horikoshii OT3 and its Complexes: Structural Basis of Biotin Activation.* J Mol Biol, 2005. **353**(2): p. 322-333.

71. Pendini, N.R., et al., *Microbial biotin protein ligases aid in understanding holocarboxylase synthetase deficiency.* Biochim Biophys Acta, 2008. **1784**(7-8): p. 973-82.

72. Germeroth, A.I., et al., *Triazole biotin: a tight-binding biotinidase-resistant conjugate.* Org Biomol Chem, 2013. **11**(44): p. 7700-4.

73. Tenover, F.C., *Mechanisms of antimicrobial resistance in bacteria.* The American journal of medicine, 2006. **119**(6): p. S3-S10.

74. Gupta, A., et al., *A Polymorphism in leuS Confers Reduced Susceptibility to GSK2251052 in a Clinical Isolate of Staphylococcus aureus.* Antimicrob Agents Chemother, 2016. **60**(5): p. 3219-3221.

75. Tomaras, A.P., et al., *Adaptation-based resistance to siderophore-conjugated antibacterial agents by Pseudomonas aeruginosa.* Antimicrob Agents Chemother, 2013. **57**(9): p. 4197-207.

76. Cui, L., et al., *An RpoB mutation confers dual heteroresistance to daptomycin and vancomycin in Staphylococcus aureus.* Antimicrob Agents Chemother, 2010. **54**(12): p. 5222-5233.

77. Lázár, V., et al., *Genome-wide analysis captures the determinants of the antibiotic cross-resistance interaction network.* Nat Commun, 2014. **5**.

78. Lewis, K., *Platforms for antibiotic discovery.* Nat Rev Drug Discov, 2013. **12**(5): p. 371-87.

79. Friedman, L., J.D. Alder, and J.A. Silverman, *Genetic changes that correlate with reduced susceptibility to daptomycin in Staphylococcus aureus.* Antimicrob Agents Chemother, 2006. **50**(6): p. 2137-45.

80. Johnston, P.R., A.J. Dobson, and J. Rolff, *Genomic signatures of experimental adaptation to antimicrobial peptides in Staphylococcus aureus.* bioRxiv, 2015: p. 023549.

81. Blake, K.L., C.P. Randall, and A.J. O'Neill, *In vitro studies indicate a high resistance potential for the lantibiotic nisin in Staphylococcus aureus and define a genetic basis for nisin resistance.* Antimicrob Agents Chemother, 2011. **55**(5): p. 2362-8.

82. Renzoni, A., et al., *Whole genome sequencing and complete genetic analysis reveals novel pathways to glycopeptide resistance in Staphylococcus aureus.* PLoS One, 2011. **6**(6): p. e21577.

83. Toprak, E., et al., *Evolutionary paths to antibiotic resistance under dynamically sustained drug selection.* Nat Genet, 2011. **44**(1): p. 101-5.

84. Harris, S.R., et al., *Evolution of MRSA during hospital transmission and intercontinental spread.* Science (New York, N.Y.), 2010. **327**(5964): p. 469-474.

85. Mwangi, M.M., et al., *Tracking the in vivo evolution of multidrug resistance in Staphylococcus aureus by whole-genome sequencing.* Proc Natl Acad Sci U S A, 2007. **104**(22): p. 9451-6.

86. Comas, I., et al., *Whole-genome sequencing of rifampicin-resistant Mycobacterium tuberculosis strains identifies compensatory mutations in RNA polymerase genes.* Nat Genet, 2011. **44**(1): p. 106-10.

87. Toprak, E., et al., *Evolutionary paths to antibiotic resistance under dynamically sustained drug selection.* Nat Genet, 2012. **44**(1): p. 101-5.

88. Dutka-Malen, S., S. Evers, and P. Courvalin, *Detection of glycopeptide resistance genotypes and identification to the species level of clinically relevant enterococci by PCR.* J Clin Microbiol, 1995. **33**(1): p. 24-27.

89. Sutcliffe, J., et al., *Detection of erythromycin-resistant determinants by PCR.* Antimicrob Agents Chemother, 1996. **40**(11): p. 2562-6.

90. Strommenger, B., et al., *Multiplex PCR assay for simultaneous detection of nine clinically relevant antibiotic resistance genes in Staphylococcus aureus.* J Clin Microbiol, 2003. **41**(9): p. 4089-4094.

Chapter 2:

Materials & Methods

2.1 Materials

2.1.1 General materials

Materials	Suppliers
CoStar 96 well flat bottom clear plate	Corning Life Sciences, USA
CoStar 96 well round bottom clear plate	Corning Life Sciences, USA
96 well LUMITRAC 600 white plate	Greiner Bio One, Germany
Thermo Scientific™ centrifuge tubes (10 mL)	Thermofisher Scientific
BD Falcon™ conical centrifuge tubes (50 mL)	
epT.I.P.S.® Standard 50-1250µL	Eppendorf, Hamburg, Germany
epT.I.P.S.® Standard 20-300µL	Eppendorf, Hamburg, Germany
Eclipse Pipette Tip refill System	Labcon, North America
Thermo Scientific™ QSP filtered pipette tips (0.1 - 10 µL)	Thermofisher Scientific
ART® self-sealing barrier pipette tips (20,200,1000 µL)	
SealPlate® Plate seals	Excel Scientific Inc., Victorville, USA
T25/T75/T175 Corning Flask	Corning Life Science, USA
Eppendorf® UVette® disposable cuvettes	
Parafilm M® laboratory film	
PVDF membrane (HybondTM-C extra)	Ammersham Pharmacia Biotech, CA, USA
Gel blotting paper	Schleicher & Schuell Bioscience GmbH, Germany
Whatman® qualitative filter paper	
Amicon® centrifugal devices	Millipore, MA, USA
Satorius VIVASPIN20, 10000 MWCO	Sartorius, Goettingen, Germany
Cellu.SepT2 MWCO 6000-8000 dialysis tubing	Membrane Filtration Products Inc., Seguin, TX, USA
BD precise syringes (5 mL, 50 mL)	
Ministart syringe filter 0.2µM, 0.45µM and 0.8µM	Sartorius, Goettingen, Germany
5 mL Profinia® IMAC cartridge	Bio-Rad Laboratories Inc., CA, USA
NuPage® 4-12% Bis-Tris polyacrylamide gels	Invitrogen, CA, USA
Electroporation cuvette 2 mm	Bio-Rad, California, U.S.A.

2.1.2 Chemical reagents

function	Reagents	Supplier
antibiotics	Ampicillin	Sigma-Aldrich, MO, USA
	Chloramphenicol	Sigma-Aldrich, MO, USA
	Erythromycin	Sigma-Aldrich, MO, USA
	Streptomycin sulfate salt	Sigma-Aldrich, MO, USA
	Chloramphenicol	Amresco Inc., OH, USA
	Daptomycin	Sigma-Aldrich Inc., MO, USA
	Methicillin Sodium Salt	Sigma-Aldrich Inc., MO, USA
	Tetracycline	University of Adelaide, SA, Australia
	Vancomycin Hydrochloride from Streptomyces orientalis	Sigma-Aldrich Inc., MO, USA
assay reagents	Biotin	Sigma-Aldrich inc., CA, USA
	Dithiothreitol (DTT)	Sigma-Aldrich, MO, USA
	Dissociation-Enhanced Lanthanide Fluorescence Immunoassay (DELFIA®) Enhancement Solution	Perkin Elmer, Boston, MA, USA
	Eu-Streptavidin	Perkin Elmer, Boston, MA, USA
	Anti-Glutathione-S-transferase Antibody (Anti-GST Ab) Produced in Rabbit	Sigma-Aldrich Inc., MO, USA
	ATP	Sigma-Aldrich Inc., MO, USA
bacterial reagents	Bacto™ Agar	Becton, Dickinson and Company, MD, USA
	BBL™ Mueller Hinton II Broth, Cation-Adjusted (CAMHB)	Becton, Dickinson and Company, MD, USA
	Defibrillated Sheep's Blood	Institute of Medical and Veterinary Science, SA, Australia
	Lysostaphin	Sigma- Aldrich Inc, MO, USA
cell culture reagents	Foetal Calf Serum	Sigma- Aldrich Inc, MO, USA
	Trypan blue	
	Sodium pyruvate (100mM)	
	Glutamine	
	WST-1 cell proliferation reagent	Roche Diagnostics, IN, USA
DNA analysis	2-log DNA ladder	New England Biolabs, MA, USA
	Agarose, DNA grade	Probiogen Biochemicals, Australia
	GelRED™ Nucleic acid gel stain	Biotium Inc., CA, USA
	BigDye (version 3) reaction mix	Perkin Elmer, CA, USA
RNA analysis	DNAsaI (RNAse free)	Life technology, Carlsbad, USA
	RNAse free water	Life technology, Carlsbad, USA
	RNAprotect Bacteria reagent	Qiagen, GmbH, Germany
protein work	Bradford protein reagent concentrate	Bio-Rad Laboratories Inc., CA, USA
	Phenylmethanesulfonyl fluoride (PMSF)	Sigma-Aldrich, MO, USA
	Isopropyl β-D-1-thiogalactopyranoside (IPTG)	BioVectra, PE, USA

	MOPS/MES SDS running buffer	Invitrogen Life Technologies Inc., NY, USA
	Precision Plus Protein Kaleidoscope standards	Bio-Rad Laboratories Inc., CA, USA
	Bovine Serum Albumin	Roche Diagnostics, IN, USA
	Streptavidin sepharose™ High performance beads	GE healthcare, Uppsala, Sweden
general	Dimethyl Sulfoxide (DMSO)	Sigma-Aldrich Inc., MO, USA
	Ethylenediaminetetraacetic Acid (EDTA)	University of Adelaide, SA, Australia
	Magnesium Chloride ($MgCl_2$)	University of Adelaide, SA, Australia
	Milli-Q® Water (MQ-H2O)	University of Adelaide, SA, Australia
	Polyoxyethylene Sorbitan Monolaurate (Tween® 20)	Sigma-Aldrich Inc., MO, USA
	Potassium Chloride (KCl)	University of Adelaide, SA, Australia
	Trisaminomethane (Tris)	University of Adelaide, SA, Australia
	Tris-Buffered Saline (TBS)	University of Adelaide, SA, Australia

2.1.3 DNA modifying enzymes

All enzymes were all obtained from New England Biolabs, MA, USA unless otherwise stated

Enzymes Used	
Restriction endonucleases	*Eco*RI
	*Sph*I
	*Nco*I
	*Pst*I
	*Pci*I
	*Dpn*I
Polymerases	Phusion DNA polymerase
	Taq DNA polymerase
Ligases	T4 DNA ligase
Phosphatases	Antarctic DNA phosphatase

2.1.4 Commercial Kits

Kit	**Suppliers**
QIAprep miniprep kit	QIAGEN, GmbH, Germany
QIAquick gel extraction kit	QIAGEN, GmbH, Germany
Qiaquick PCR purification kit	QIAGEN, GmbH, Germany
RNeasy mini Kit	QIAGEN, GmbH, Germany
Wizard genomic DNA purification kit	Promega, Wisconsin, USA
Superscript II platinum sybr RT-PCR kit	Life technology, NY, USA

2.1.5 Buffers and Media

Reagents	**recipe**
CAMHB	3 % (w/v) Beef Extract, 17.5 % (w/v) Acid Hydrolysate of Casein, 1.5 % (w/v) Starch, supplemented to contain 20-25 mg/L calcium and 10-12.5 mg/L magnesium.
CAMHB Agar	CAMHB supplemented with 1.25 % (w/v) Bacto™ agar
CAMHB Blood Agar	CAMHB supplemented with 1.25 % (w/v) Bacto™ agar and 5 % Defibrillated Sheep's Blood
Luria Broth (LB):	1% (w/v) tryptone, 0.5% (w/v) yeast extract, 1% (w/v) NaCl, adjusted to pH 7.0 with NaOH
LB agar:	LB supplemented with 1.5% (w/v) bacto-agar
SOC Broth	2% w/v tryptone, 0.5% w/v Yeast extract, 10mM NaCl, 2.5mM KCl, 10mM MgCl2 and 10mM MgSO4
DMEM	
Trypsin EDTA	
Blocking Buffer (For Western analysis):	1% (w/v) BSA in PBS
Cell Lysis Buffer:	10% (v/v) β-mercaptoethanol, 2% (w/v) SDS
Cleaning solution 1 (2x):	100 mM NaCl, 100 mM Tris, at pH 8.0
Cleaning solution 2 (4x):	2M NaCl, 0.4 M sodium acetate, at pH 4.5
DNA loading buffer (6X):	0.5x Tris-borate-EDTA (TBE) buffer, 40% (v/v) glycerol, 1mg/ml bromophenol blue
Native IMAC lysis buffer/wash buffer 1:	300 mM KCl, 50 mM Tris at pH 8.0, 5 mM imidazole
Native IMAC wash buffer 2 :	300 mM KCl, 50 mM Tris at pH 8.0, 10 mM imidazole
Native elution buffer :	300 mM KCl, 50 mM Tris at pH 8.0, 250 mM imidazole
SDS-PAGE loading buffer:	0.1 M Tris (pH 7), 4% (w/v) SDS, 0.2% (w/v) bromophenol blue
SDS-PAGE Coomassie Blue staining solution:	0.2% (w/v) Coomassie brilliant blue, 10% (v/v) Methanol, 10% (v/v) Acetic acid
SDS-PAGE de-staining solution:	10% (v/v) Methanol, 10% (v/v) Acetic acid
PBS:	0.136 M NaCl, 2.7 mM KCl, 1.46 mM KH2PO4 at pH 7.4
PBS-Tween:	PBS, 0.1% (v/v) Tween 20
TAE:	40mM tris pH 8.2, 20 mM sodium acetate, 1 mM EDTA
TBS:	25 mM Tris pH 7.5, 150 mM NaCl
TE:	10 mM Tris pH 7.5, 1 mM EDTA
Transfer Buffer:	39 mM glycine, 48 mM Tris, 0.037% (w/v) SDS, 20% (v/v) methanol
Transformation buffer 1:	30 mM potassium acetate, 100 mM RbCl, 10 mM $CaCl_2$, 50 mM $MnCl_2$, 15% glycerol
Transformation buffer 2:	10 mM MOPS, 10 mM RbCl, 75 mM $CaCl_2$, 15% glycerol
BPL storage buffer:	50 mM Tris pH 8.0, 100 mM KCI, 5% glycerol, 0.1 mM EDTA pH 8.0, 1mM DTT

2.1.6 General bacterial strains

***E. coli* DH5α (*sup*EΔ*lac*169 (p80*lacZ*ΔM15) *hsdR17 rec*A1 *end* AA1 *gyr*A96 *thi*-1 *rel*A1):** For routine molecular cloning (New England Biolabs, MA, USA)

***E. coli* BL21-CodonPlus(DE3)-RIPL strain (B F- ompT hsdS(rB- mB-) dcm+ Tetr gal λ(DE3) endA The [argU proL Camr] [argU ileY leuW Sterp/Specr]:** *E. coli* BL21 carrying (λDE3) insertion and contains plasmids encoding extra copies of genes for rare tRNAs in *E. coli*. This strain was used for recombinant expression of pET expression vector encoding the gene for *Staphylococcus aureus* wild type and D200E mutant biotin protein ligases (Aglient Technologies, CA, USA).

Methicillin Sensitive *Staphylococcus aureus* ATCC 49775: Purchased from the American Tissue Culture Collection. This strain was used for antimicrobial susceptibility assays.

***Staphylococcus aureus* NCTC8325:** Purchased from the American Tissue Culture Collection. This strain was used for antimicrobial susceptibility assays and resistance studies.

***Staphylococcus aureus* RN4220:** Obtained from Dr Alistair Standish, University of Adelaide. This strain was used for transformation, mechanism of action and antimicrobial susceptibility assays.

2.1.7 Plasmids

Plasmid	Description	Source
pGEMT-*Sa*BPL(6xHis)	pGEMT plasmid containing *saBPL* with 6x his-tag	[1]
pGEMT-*Sa*BPL-D200E-(6xHis)	pGEMT plasmid containing *saBPL* D200E with 6x his-tag	This study
pIT4_TL_152002	Chromosomal integration plasmid (λ-attP, Tc^R, R6Kγ ori, *ccdB*, pUC ori)	[2]
pIT4_TL_SaBPL (D200E)	plac-UV5 fused with SaBPL (D200E) sequence cloned into pIT4_TL_152002	This study
pCN51	Shuttle vector for *E. coli* to *S. aureus* transformation with cadmium inducible promoter	[3]
pCN51-*Nco*I	Negative control vector with *Nco*I site for cloning	This study
pCN51-*Sa*BPL	Vector with over-expressable *Sa*BPL	This study

2.1.8 Oligonucleotides

All custom oligonucleotides were ordered from Geneworks, Adelaide, SA, Australia

Primer	Sequence	Function	Reference
B138	5′-ACATGTCAAAATATAGTCAAG ATGTACTTCAATTACTC-3′	amplification and sequencing genomic SaBPL	[1]
B139	5′-GGATCCAAGCTTAAAAATCTAT ATCTGCACTAATAAAACG-3′	amplification and sequencing genomic SaBPL	[1]
B200	5′-GGTATAGAAGCAATAATATGT GG-3′	Internal BPL sequencing primer	
B481	5′-GGTTGCTAATAATGAAGGTAT AGAAGCAATAATATGTGG-3′	QuikChange mutagenesis D200E	This Study
B482	5′-CCACATATTATTGCTTCTATAC CTTCATTATTAGCAACC-3′	QuikChange mutagenesis D200E	This Study
B493	5′ -TAGGTGATGAACATATCAGGC-3′	pCN51 MCS sequencing primer	This Study
594	5′-TGCGATGCATGCGCACTTATTC AAGTGTATTT-3′	pCN51 Cd cassette forward primer	[3]
B459	5′-ATTATTATTCTGCAGCCATGGA CCTTCACTTCTTTCTTATGT-3′	pCN51 Cd cassette reverse primer with *Nco*I site and *Pst*I site for cloning	This Study
Lambda P1	5′-GGCATCACGGCAATATAC-3′	attp-λ PCR screening primer	[2]
Lambda P2	5′ -ACTTAACGGCTGACATGG-3′	attp-λ PCR screening primer	[2]
Lambda P3	5′-GGGAATTAATTCTTGAAGACG-3′	attp-λ PCR screening primer	[2]
Lambda P4	5′-TCTGGTCTGGTAGCAATG-3′	attp-λ PCR screening primer	[2]

2.1.9 General Software:

software	function
graphpad prism 7	data analysis
UCSF Chimera 1.10.2	protein structure analysis
APE A plasmid editor	plasmid viewing and primer design
SnapGene Viewer	plasmid viewing and diagram creation
Ugene	biological data viewer
Applied biosystems SeqScanner 2	analysis of sanger sequencing data
IGV	Next generation sequencing alignment viewer
Mauve Progressive aligner	genome alignment
Bio-Rad ImageLab 5.2.1	Gel imaging and analysis

2.1.10 Web based services

service	address	function
NCBI	(http://www.ncbi.nlm.nih.gov/)	Used to access protein, nucleotide, and PubMed databases. Including BLAST search and Gene Expression Omnibus
Clustal omega	(www.ebi.ac.uk/Tools/msa/clustalo/)	multiple sequence alignment (protein and nucleotide)
Emboss Needle	(www.ebi.ac.uk/Tools/psa/emboss_needle/)	dual sequence alignment (protein and nucleotide)
bioCyc	(biocyc.org/)	genomic annotation viewer
Prodoric	(www.prodoric.de/)	Promoter region prediction software
Kegg	(www.genome.jp/kegg/)	enzymatic reaction database

2.2 Methods:

2.2.1 Microbiological methods

2.2.1.1 Antibiotic selection

Unless stated otherwise the following concentrations were used to select for plasmids or chromosomal integration events. Tetracycline (4 μg/ml), Chloramphenicol (34 μg/ml), Ampicillin (100 μg/ml), Erythromycin (10 μg/ml plasmid, 5 μg/ml chromosomal), Streptomycin (75 μg/ml).

2.2.1.2 Antibacterial susceptibility evaluation

Antibacterial activity was determined by the microdilution broth method as recommended by the CLSI (Clinical and Laboratory Standards Institute, Document M07-A8, 2009, Wayne, Pa.) using cation-adjusted Mueller-Hinton broth (CAMHB) (Trek Diagnostics Systems, U.K.). Overnight cultures of bacteria were subcultured 1:1000 and grown to mid log phase (OD600 of approximately 1.2 = 10^9CFU/ml). Cultures were further diluted 1:1000 into CAMHB and used to inoculate 96 well plates containing diluted compound. Compound dilution plates were prepared by serial two-fold dilution of DMSO dissolved compounds into CAMHB such that the concentration of DMSO was consistently 50%. This master stock was further diluted, 6.4 μl into 43.5 μl of CAMHB, into a 96 well flat bottom plates. An equal volume, 50 μL, of the diluted cell suspension was added to each well. After addition of the cell inoculum each well contained ≈ 5 x 10^4 CFU with a concentration range of 64 to 0.06 μg/ml in 3.2% DMSO. Plates were incubated at 37°C for 20-22 hours with shaking. Growth of the culture was quantified after this time by measuring the absorbance at 620 nm using a Thermo Multiskan Ascent plate reader after shaking for 15 seconds to disrupt any sedimentation.

2.2.1.3 Mechanism of action studies

Antibacterial activity was determined on *S. aureus* RN4220 containing either pCN51-*Nco*I (parent vector) or pCN51-BPL (BPL over-expression). Compounds, dissolved in DMSO, were serially diluted from 64 to 0.0625 µg/ml in Mueller Hinton broth (3.2% (v/v) DMSO) supplemented with 10 µg/ml erythromycin for plasmid selection and 25 nM $CdCl_2$ to induce BPL expression. Log phase cultures of transformed *S. aureus* RN4220 strains, grown in the absence of compound, were diluted 1:1000 into media containing compound. Growth of the cultures at 37°C with shaking was then monitored with absorbance at 630 nm every 30 mins for 16 hours using an EL808™ Absorbance Microplate Reader (BioTek Instruments Inc, Winooski, VT, USA). *S. aureus* harbouring pCN51-BPL grown in the absence of compound served as a negative control. The mechanism of action assays were performed in triplicate.

2.2.1.4 Bacterial Cell enumeration

Cell density of a growing culture was estimated by using optical density (OD600 1.2 = 10^9 CFU/ml) to determine an appropriate dilution series. The culture was then serially diluted 1 in 10 and aliquots of the dilution (20 µL) applied to pre-warmed LB Agar plates in duplicate. The plates were incubated at 37°C overnight and colonies enumerated from the first countable dilution to determine initial cell density.

2.2.2 Tissue culture methods

2.2.2.1 Culturing of HepG2 and HEK293 cells

Mammalian cell lines were propagated and incubated at 37°C with constant 5% CO_2. Cells were seeded at approximately 10^5 cells/ml and grown to 80% confluence in DMEM (+ 10%FCS, 1 mM sodium pyruvate and 2 mM glutamine), in a T75 flask before media was removed and cells washed twice with 10 ml of PBS. Cells were subsequently treated for 5 minutes with 1mL of trypsin EDTA at 37^{o}C. Following this 9mL of DMEM was added, cells were centrifuged, supernatant removed and cells resuspended in 4mL of DMEM. An aliquot of the cell suspension was viewed under the microscope at this stage to ensure proper cell dispersion, and the cell density determined using a haemocytometer following trypan blue staining. Cells were centrifuged 2 minutes and resuspended in DMEM such that the concentration of cells was 10^5 cells/ml for seeding either 96 well plates or a second flask.

2.2.2.2 Cytotoxicity Assay

HepG2 or HEK293 cells were seeded in 96-well tissue culture plates at 10^4 cells per well (**protocol 2.2.2.1**). After 24 hours growth, cells were treated with varying concentrations of test compound. Dilutions of compound were prepared by two fold serial dilution of compound in DMEM, maintaining a constant DMSO concentration, 2% (v/v) for HepG2 or 0.5% (v/v) for HEK293. After treatment for 48 hours, 10 µl WST-1 cell proliferation reagent (Roche) was added to each well and incubated for 30 minutes at 37°C. The WST-1 assay quantitatively monitors the metabolic activity of cells by measuring the hydrolysis of the WST-1 reagent, the products of which are detectable at absorbance 450 nm on Perkin Elmer plate reader.

2.2.3 Protein methods

2.2.3.1 Protein expression

Histidine tagged proteins were expressed using the following protocol, antibiotics were used as required by plasmid selection. *E. coli* BL21 (DE3) colonies containing the desired expression plasmid were streaked out onto LB Agar. A single colony was used to inoculate a 50 ml overnight culture and grown overnight at 37°C. This culture was diluted 1:50 into 2 L (4× 500 mL) and grown until an OD of approximately 0.6-0.8. Recombinant protein expression was then induced by addition of IPTG to a concentration of 0.5 mM. Cells were induced for 2-3 hours before being harvested by centrifugation at 5000 × g for 5 minutes at 4°C. The cell pellets were washed with 100 mL of 1× PBS and then further pelleted at 5000 × g for 5 minutes with the resulting pellets either used immediately or stored at -80°C until required.

2.2.3.2 Purification of recombinantly expressed *Sa*BPL

Cell pellets were resuspended in 30 mL ice cold native IMAC lysis buffer containing 1 mM PMSF. Cells were disrupted by at least 5 passages through a M110L homogenizer (Microfluidics, USA) until the solution became clear and homogenous. Cellular debris was removed by two centrifugation steps each at 20 000 x g for 10 minutes at 4 ºC and then the solution was passed through 0.8 μm and 0.45 μm filters. His-tagged BPL proteins were purified by immobilized nickel affinity chromatography (IMAC). The filtered lysate was applied at 5 mL/min onto a 5 mL Profinia IMAC cartridge that was pre-equilibrated with 10 column volumes of milliQ water then 10 column volumes of native IMAC lysis buffer. The column was washed with 6 column volumes of native IMAC lysis buffer (300 mM KCl, 50 mM Tris pH 8.0, 5 mM imidazole) followed by 6 column volumes of native IMAC wash buffer 2 (300 mM, 50 mM Tris pH 8.0, 10 mM imidazole). His-tagged BPL was eluted with native elution buffer (300 mM KCl, 50 mM Tris pH 8.0, 250 mM imidazole). Material eluting from the column was detected by UV absorbance at 280 nm and pooled and subsequently exchanged into storage buffer (50 mM tris pH 8.0, 100 mM KCl, 5% glycerol, 1 mM EDTA, 1mM DTT) using overnight dialysis at 4 °C. For SPR experiments *Sa*BPL was dialysed into storage buffer containing 1× PBS, 100 mM KCl, 5 % glycerol, 1 mM EDTA and 1 mM DTT. Protein concentrations were determined using a Bradford protein assay (BioRad) using bovine serum albumin (Sigma Aldrich®) as a standard (section **2.2.3.5**). The fractions containing BPL were confirmed using SDS-PAGE gel electrophoresis and the *in vitro* biotin incorporation assay. The purified enzyme was aliquoted and stored at -80 °C.

2.2.3.3 Preparation of bacterial cell lysates

For cell lysates 1ml of OD600 = 1 culture was resuspended in 40 µl of lysis buffer (2% SDS, 10% BME) and vortexed to resuspend cells before boiling for 5 minutes. Samples were then centrifuged and boiled as per SDS PAGE analysis procedure (**2.2.3.4**). *S. aureus* cell lysates were prepared by first incubating cells in TE buffer containing 1 mg/mL lysozyme and 0.5 mg/ml lysostaphin for 30 minutes at 37°C before addition of 2% SDS and 10% βME. Concentration was quantified prior to SDS and βME addition by Bradford assay (**2.2.3.5**).

2.2.3.4 SDS PAGE analysis

Protein, 10µL (approximately 5µg), was added to an equal volume of 2× SDS loading buffer containing 5% βME. The samples were then boiled at 100°C for 5 min and centrifuged briefly before being loaded and fractioned on a NuPage® 4-12% Bis-Tris polyacrylamide precast gel (Invitrogen) using 1X NuPAGE® MES running buffer (Invitrogen) at 200 V for approximately 40 min or until the dye front reached the bottom of the gel. The gel was stained with Coomassie blue for 1 hour and destained overnight or transferred onto a PVDF membrane (HybondTM-LFP) using a semi dry transfer unit (Hoefer Semiphor, Amersham Pharmacia Biotech, CA, USA) for Streptavidin blot analysis (**2.2.3.7**).

2.2.3.5 Determination of protein concentration

Protein concentration was assayed using the Bradford Reagent (Bio-Rad Laboratories Inc., CA, USA). A standard curve of bovine serum albumin (BSA) was generated from 0 to 1 mg/mL and a linear regression was used to calculate protein concentration. For the Bradford assay 10 μL of sample was mixed with 200 μL of 1x Bradford Reagent in a 96 well plate (Corning Life Sciences, USA). Absorbance at 620 nm wavelength was measured on a microplate reader (Molecular Devices, CA, USA).

2.2.3.6 Concentration of proteins

Concentration of protein solutions was performed using Amicon® centrifugal filter devices (10000 MWCO) (Millipore, MA, USA) following manufacturer's instruction manual. The columns were rinsed with MilliQ water and then equilibrated in the appropriate buffer by centrifugation at 5000 x g at 4 °C for 20 minutes or until reaching a required retentate volume. The buffer was discarded prior to adding protein sample into the spin column. Likewise, protein was concentrated by centrifugation at 5000 x g at 4 °C until reaching a required retentate volume. For retentate recovery, the concentrate was collected using a pipette with 200 microliter tip to new pre-cold microcentrifuge tube. The protein was kept at -80 ºC until needed. For storage of using Amicon® centrifugal filter devices, the centrifuge tube was washed with distilled water to remove residual buffer components and kept in MilliQ water at 4 ºC.

2.2.3.7 Streptavidin blot analysis of biotinylated protein

For detection of biotinylated protein from either an *in vitro* biotinylation reaction or bacterial cell lysates the following protocol was performed. After biotinylation reaction (**2.2.3.8**) or cell lysate preparation (**2.2.3.3**) an appropriate volume of 2X SDS loading dye was added to each preparation. The samples were then boiled at 100 °C for 5 min and centrifuged briefly before being loaded and fractioned on a NuPage® 4-12% Bis-Tris polyacrylamide precast gel (Invitrogen) using 1X NuPAGE® MES running buffer (Invitrogen) at 200 V for approximately 40 min or until the dye front reached the bottom of the gel. The proteins fractionated by SDS-PAGE were transferred onto a PVDF membrane (HybondTM-LFP) using a semi dry transfer unit (Hoefer Semiphor, Amersham Pharmacia Biotech, CA, USA). The PVDF membrane was pre-soaked briefly in methanol, then milliQ water, followed by transfer buffer. The transfer was run for 1 hour at 80 mA per gel. The membrane was then soaked with blocking buffer (1% (w/v) BSA in PBS) for at least 1 hour at room temperature and washed 3 times with PBS-Tween before being probed with streptavidin conjugated - Alexa-488 (Life Technologies, 1:1000 dilution, PBS-Tween) for another hour at room temperature. The membrane was washed another 3 times with PBS-Tween then analysed using the ChemiDoc XRS imaging system (Bio-Rad, California, U.S.A.) .

2.2.3.8 *In vitro* protein biotinylation assay

Enzymatic biotinylation of an acceptor subtrate protein (GST-SaPC90) was performed with 2 µl of a BPL stock (6 nM in storage buffer: 50 mM Tris (pH 8.0), 100 mM KCL, 1 mM EDTA, 1 mM DTT *added fresh each time, 5% (w/v) glycerol) added to 14 µl of pre-warmed reaction mix (50 mM Tris pH 8.0, 5.5 mM $MgCl_2$, 100 mM KCl, 5 µM biotin, 3 mM ATP, 0.1 µM DTT, 25 µM Apo substrate [GST-SaPC90]), with 4 µL of either compound or vehicle control and incubated for 20 minutes. The reaction was terminated by the addition of 80 µL stopping buffer (110 mM EDTA, 50 mM Tris (pH 8.0)). The biotinylated GST-fusion proteins were then captured using anti-glutathione-S-transferase antibody (Sigma-Aldrich Inc., MO, USA). 96 well white plates (Greiner Bio One, Germany) that had been pre-treated overnight at 4°C with 50 µL of anti-glutathione-S-transferase antibody (Sigma-Aldrich Inc., MO, USA) diluted 1:40,000 in TBS were blocked for 2 hours at 37°C with 1% (w/v) BSA in TBS. Before the reaction, plates were prewarmed at 37°C for 30 minutes. Twenty microliters of the completed biotinylation reaction was added to the antibody capture plates in triplicate wells. The plate was sealed with parafilm to prevent evaporation and incubated for 1 hour at 37° to allow antibody capture of the GST fusion proteins. The reaction mix was then discarded and the plates washed 5× in Wash buffer (TBS + 0.1% Tween-20). Fifty microlitres of Eu-Streptavidin , diluted 1:1000 into Wash buffer was then added to each well and the plate covered by parafilm before incubation for 30 minutes at 37°C. (Each step following the addition of Eu-streptavidin was protected from light by covering with aluminium foil.) The unbound Eu-streptavidin was then removed and wells again washed 5× with wash buffer before addition of 50µL of DELFIA enhancement solution to facilitate dissociation of the Europium ion. Dissociated Europium was measured using time resolved fluorescence at 340 nm for excitation and 615 nm emission using the Victor X5 plate reader (Perkin Elmer).

2.2.4 Molecular Biology Techniques

2.2.4.1 Preparation of chemically competent *E. coli* cells

Overnight cultures of cells in LB media were prepared and subcultured the next day into LB medium (330 µL of overnight culture into 10 mL of LB). The cell cultures were grown at 37 ºC for 1.5 – 2 hours until they reached an OD600 measurement of 0.6. The growing culture was then subcultured 5 mL into 100 mL of pre-warmed LB media in a 1 L flask and was grown at 37 ºC for 1.5 hours. The cells were then pelleted by centrifugation at 5000 x g for 5 minutes at 4 ºC and resuspended in 10 mL/pellet of transformation buffer 1 (30 mM potassium acetate, 100 mM RbCl, 10 mM $CaCl_2$, 50 mM $MnCl_2$ (4.H20), 15% glycerol) and incubated on ice for 5 minutes. The cells were then pelleted by centrifugation at 4000 x g for 5 minutes at 4 ºC and resuspended in 1 mL/ pellet of transformation buffer 2 (10 mM MOPS, 10 mM RbCl, 75 mM $CaCl_2$, 15% glycerol) and incubated on ice for 5 minutes. The cells were then aliquoted and stored in pre-chilled 1.5 mL microcentrifuge tubes at -80 ºC.

2.2.4.2 Transformation of chemically competent *E. coli* cells

Competent cells were thawed on ice and 1-5 µL of plasmid DNA added to a 50 µL ml aliquot before being incubated on ice for at least 30 minutes. This was followed by heat shock treatment at 42°C for 90 seconds followed by further 5 minutes incubation on ice. Pre-warmed SOC media, 900 µL, was added to each transformation and the cells were incubated for 1 hour at 37 ºC with shaking. Cells were then pelleted by centrifugation at 2600 x g for 1 min and the pellet was resuspended in 100 – 200 µL of supernatant. Cells were immediately plated onto pre-warmed LB plates containing relevant antibiotics for selection.

2.2.4.3 Agarose Gel Electrophoresis

Analysis of DNA and separation of DNA fragments was performed using Agarose gel electrophoresis. Gels were prepared with 1-2% (w/v) Agarose in TAE buffer. 6x DNA loading buffer was added to DNA samples before loading and samples were electrophoresed 100V in TAE buffer. Gels were stained in 1x GelRed, 0.1 M NaCl solution for at least 10 minutes. DNA was visualised on a blue light transluminator for gel extraction or imaged using the Chemidoc XRS (Bio-Rad, California, U.S.A.)

2.2.4.4 Plasmid preparation

A 5 mL overnight culture of the desired bacterial strain was prepared at 37°C, or relevant permissive temperature for replication. Plasmid DNA was extracted as per manufacturer's instructions using the QIAGEN plasmid Mini Kit. When extracting from *S. aureus* a pre-lysis incubation in the presence of 250 μL buffer P1 containing 10 μg lysostaphin was undertaken for 10 minutes at 37 degrees. Plasmid concentration was quantified using the nanodrop 2000 and quality determined by A260/280 ratio of 1.8-2.

2.2.4.5 Plasmid purification

Plasmid DNA was purified using the QIAGEN QIAprep Miniprep Kit according to manufacturer's instructions.

2.2.4.6 Gel extraction

Gel extraction was performed using the QIAGEN gel extraction kit as per manufacturer's instructions.

2.2.4.1 Sanger sequencing

Sanger sequencing was undertaken by preparation of a 12 µl reaction containing plasmid or PCR product DNA in milliQ H_2O with 10 pmol of sequencing primer to AGRF for their Purified DNA service and sequenced as per AGRF guidelines (Sanger Sequencing Sample Submission Guide (GSEQDOC00166) v1.8). Sequencing was performed using Applied Biosystems 3730 and 3730xl capillary sequencers with Big Dye Terminator (BDT) chemistry version 3.1 (Applied Biosystems) under standardised cycling PCR conditions.

.

References

1. Pendini, N.R., et al., *Purification, crystallization and preliminary crystallographic analysis of biotin protein ligase from Staphylococcus aureus.* Acta Crystallogr Sect F Struct Biol Cryst Commun, 2008. **64**(Pt 6): p. 520-3.

2. St-Pierre, F.o., et al., *One-step cloning and chromosomal integration of DNA.* ACS synthetic biology, 2013. **2**(9): p. 537-541.

3. Charpentier, E., et al., *Novel cassette-based shuttle vector system for gram-positive bacteria.* Applied and environmental microbiology, 2004. **70**(10): p. 6076-6085.

Chapter 3:

Statement of Authorship

Title of Paper	A new series of BPL inhibitors to probe the ribose-binding pocket of *Staphylococcus aureus* biotin protein ligase.
Publication Status	☑ Published ☐ Accepted for Publication ☐ Submitted for Publication ☐ Unpublished and Unsubmitted w ork w ritten in manuscript style
Publication Details	Jiage Feng, Ashleigh S. Paparella, William Tieu, David Heirn, Sarah Clark, Andrew Hayes, Grant W. Booker, Steven W. Polyak, Andrew D. Abell. *ACS Medicinal Chemistry Letters*, accepted October 2016

Principal Author

Name of Principal Author (Candidate)	Andrew Hayes		
Contribution to the Paper	Performed all cytotoxicity assays Constructed pCN51-SaBPL expression system Performed mechanism of action assays		
Overall percentage (%)	5%		
Certification:	This paper reports on original research I conducted during the period of my Higher Degree by Research candidature and is not subject to any obligations or contractual agreements with a third party that would constrain its inclusion in this thesis. I am a co-author on this paper		
Signature		Date	1/08/17

Co-Author Contributions

By signing the Statement of Authorship, each author certifies that:

i. the candidate's stated contribution to the publication is accurate (as detailed above);

ii. permission is granted for the candidate in include the publication in the thesis; and

iii. the sum of all co-author contributions is equal to 100% less the candidate's stated contribution.

Name of Co-Author	Jiage Feng		
Contribution to the Paper	Performed synthesis and characterisation of analogues, docking studies, analysis of data, provided advanced draft of manuscript and subsequent revisions. Co-author of the manuscript		
Signature		Date	6/7/2017

Name of Co-Author	Ashleigh Paparella		
Contribution to the Paper	Expression and purification of *Sa*BPL and *Hs*BPL Performed all *in vitro* biotinylation assays, and analysis of assay results. Co-author of the manuscript		
Signature		Date	3/7/2017

Name of Co-Author	William Tieu
Contribution to the Paper	Performed synthesis and characterisation of compounds 12a-c and 12g-i Revised manuscript
Signature	Date 10/7/17

Name of Co-Author	David Heim
Contribution to the Paper	Performed all antimicrobial susceptibility assays
Signature	Date 24/07/2017

Name of Co-Author	Sarah Clark
Contribution to the Paper	Performed synthesis and characterisation of 12j and 12k
Signature	Date 21/5/2017

Name of Co-Author	Grant Booker
Contribution to the Paper	Supervised the biological aspects of the project, revised manuscript
Signature	Date 25/5/2017

Name of Co-Author	Steven Polyak
Contribution to the Paper	Worked closely with the co-authors to write the manuscript Supervised biological testing
Signature	Date 25/5/2017

Name of Co-Author	Andrew Abell
Contribution to the Paper	Supervised all aspects of medicinal chemistry, revised manuscript and is corresponding author
Signature	Date 25/5/2017

ACS Medicinal Chemistry Letters

Letter

pubs.acs.org/acsmedchemlett

New Series of BPL Inhibitors To Probe the Ribose-Binding Pocket of *Staphylococcus aureus* Biotin Protein Ligase

Jiage Feng,[†,‡] Ashleigh S. Paparella,[§] William Tieu,[†,∥] David Heim,[§] Sarah Clark,[†] Andrew Hayes,[§] Grant W. Booker,[§] Steven W. Polyak,[§] and Andrew D. Abell*[,†,‡]

[†]Department of Chemistry, [§]Department of Molecular and Cellular Biology, and [‡]Centre for Nanoscale BioPhotonics (CNBP), University of Adelaide, Adelaide, South Australia 5005, Australia

Supporting Information

ABSTRACT: Replacing the labile adenosinyl-substituted phosphoanhydride of biotinyl-5′-AMP with a N1-benzyl substituted 1,2,3-triazole gave a new truncated series of inhibitors of *Staphylococcus aureus* biotin protein ligase (*Sa*BPL). The benzyl group presents to the ribose-binding pocket of *Sa*BPL based on *in silico* docking. Halogenated benzyl derivatives (**12t**, **12u**, **12w**, and **12x**) proved to be the most potent inhibitors of *Sa*BPL. These derivatives inhibited the growth of *S. aureus* ATCC49775 and displayed low cytotoxicity against HepG2 cells.

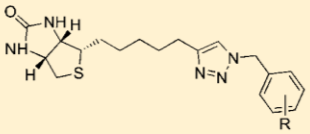

	R	K_i *Sa*BPL (μM)	K_i *Hs*BPL (μM)
12t	3F	0.28 ± 0.02	>10
12u	4F	0.60 ± 0.10	>10
12w	3Cl	0.39 ± 0.04	>10
12x	4Cl	1.10 ± 0.07	>10

KEYWORDS: *Enzyme inhibitors, antibiotics, biotin protein ligase, Staphylococcus aureus*

Biotin protein ligase (BPL) catalyzes the reaction of biotin **1** and ATP **2** to give biotinyl-5′-AMP **3**, which then biotinylates and activates essential metabolic enzymes required for fatty acid biosynthesis and gluconeogenesis, specifically acetyl CoA carboxylase and pyruvate carboxylase (Figure 1).[1−5]

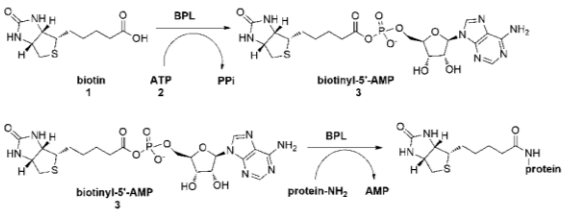

Figure 1. General mechanism of BPL catalyzed biotinylation.

A number of analogues of biotinyl-5′-AMP have recently been reported as inhibitors of BPL as shown in Figure 2. Some of these compounds have potential as antibacterial agents by inhibiting BPL from clinically important pathogens such as *Staphylococcus aureus*,[6] *Escherichia coli*,[7,8] and *Mycobacterium tuberculosis*.[9,10] A range of bioisosteres have been investigated as replacements for the labile phosphoanhydride of biotinyl-5′-AMP **3**, including phosphodiester **4**,[11,12] hydroxyphosphonate **5**,[13] ketophosphonate **6**,[13] acylsulfamate **7**,[11] and sulphonmyl amide **8**[10] (Figure 2). We have also reported biotin triazoles (e.g., **9**−**11**) as a novel class of BPL inhibitor that selectively targets BPL from the clinically important bacterial pathogen *Staphylococcus aureus* over the human homologue.[3,14,15]

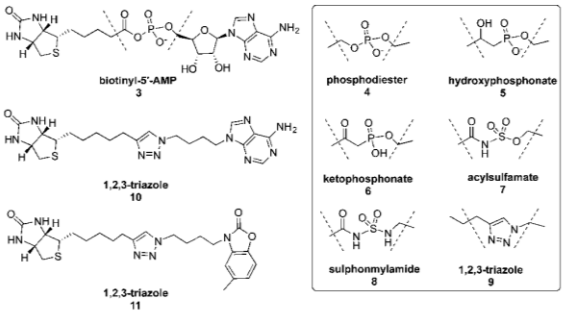

Figure 2. Reported BPL inhibitors, with isosteric replacements for the phosphoanhydride of biotinyl-5′-AMP **3** shown in the box.

Without exception, all isostere-based BPL inhibitors reported to date contain a biotin and an adenine group, or analogue thereof, as discussed above and as shown in Figure 2. These two groups occupy well-defined binding pockets in the enzyme as per biotinyl-5′-AMP **3**, as supported by X-ray crystallographic and mutagenesis studies.[3,16] The ribose group of the triazole series can be removed as in **10**, and the adenine can be modified as in **11**, which has improved stability and >1000-fold specificity for the BPL from *S. aureus* over the human homologue.[3] We now report the first examples of truncated 1,2,3-triazole-based BPL inhibitors with a 1-benzyl substituent

Received: June 26, 2016
Accepted: October 10, 2016
Published: October 10, 2016

DOI: 10.1021/acsmedchemlett.6b00248
ACS Med. Chem. Lett. 2016, 7, 1068−1072

designed to interact with the ribose binding pocket of *S. aureus* BPL (*Sa*BPL), see **12a−y**, Figure 3. These derivatives are the

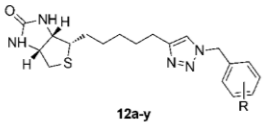

R = a 2-OH, b 3-OH, c 4-OH, d 2-OMe, e 3-OMe, f 4-OMe, g 2-NH_2, h 3-NH_2, i 4-NH_2, j 3-Me, k 4-Me, l 3-CF_3, m 4-CF_3, n 4-*t*-butyl, o 4-COOH, p 2-Br, q 3-I, r 4-I, s 2-F, t 3-F, u 4-F, v 2-Cl, w 3-Cl, x 4-Cl, y 3,4-diF

Figure 3. Benzyl-substituted 1,2,3-triazole analogues.

first examples of isostere-based BPL inhibitors lacking an appended adenine or analogue thereof and the associated tether as discussed above. The ribose-binding pocket is composed of amino acids that provide potential hydrogen bonding sites, specifically through the side chains of K187, R122, R125, and R227 as well as the backbone peptide atoms from H126 and S128 (Figure 4a). This series of inhibitors provides an important starting point for further optimization and antibiotic development.

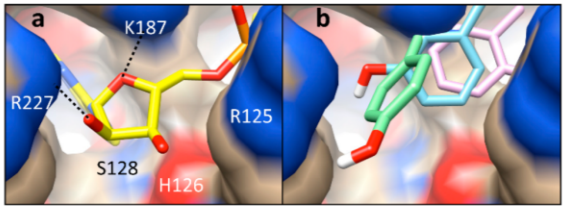

Figure 4. (a) X-ray structure of the *Sa*BPL active site with biotinyl-5′-AMP 3 (yellow) bound PDB ID 3RIR.[10] Amino acids that encompass the ribose-binding pocket are shown. Dashed lines represent hydrogen bonds. (b) *In silico* docking poses for biotin triazole analogues **12a**, **12b**, and **12c** containing a hydroxyl group at C2- (pink), C3- (blue), and C4- (green), respectively.

In silico docking experiments were carried out in order to explore possible binding modes by which this series of benzyl analogues might occupy the active site of *Sa*BPL. Flexible ligand docking was carried out using AutoDockTools (version 1.5.6). The docking protocol was first validated by removing compound **11** from its cocrystal structure with *S. aureus* BPL (PDB 3V7S) and then redocking. This occurred with a high degree of commonality as revealed by superimposition of the docked and crystallized ligands in the active site. We next docked benzylated triazoles **12a−c** (Figure 3) into *Sa*BPL. Each of these structures contains a single hydroxyl substituent on the benzyl ring capable of forming a hydrogen bond as per the diol in the ribose of biotinyl-5′-AMP **3**. Gratifyingly, the top ranking poses of all three analogues placed the hydroxyl group in the site occupied by the ribose diol of **3** (Figure 4a). Rotation around the alkyl linker connecting the triazole and benzyl moieties produced subtly different poses with regards to the ribose-binding site (Figure 4b). These binding modes minimized steric clashes with the protein and facilitated hydrogen bonding between the alcohol group and R122 for **12a** and R227 for **12b** and **12c**. This data reflects an apparent openness of the solvent exposed pocket and suggests that this site can accommodate a variety of functional groups as exemplified in the extended series depicted in Figure 3. Synthesis and biological testing of this series provides an opportunity to probe potential interaction with the ribose pocket.

The synthesis of the 1,2,3-triazoles **12a−y** was carried out as summarized in Scheme 1. The key benzyl azides **14a−y** were

Scheme 1[a]

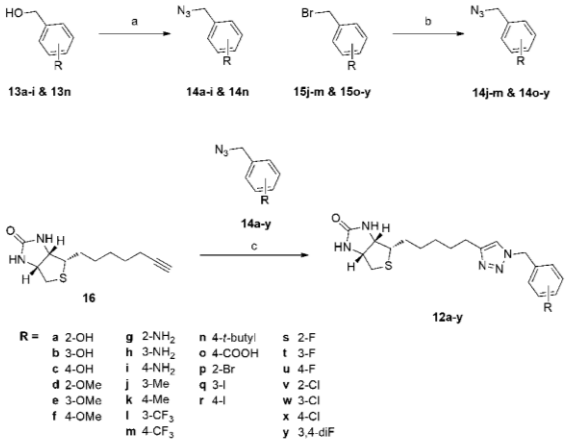

R = a 2-OH, b 3-OH, c 4-OH, d 2-OMe, e 3-OMe, f 4-OMe, g 2-NH_2, h 3-NH_2, i 4-NH_2, j 3-Me, k 4-Me, l 3-CF_3, m 4-CF_3, n 4-*t*-butyl, o 4-COOH, p 2-Br, q 3-I, r 4-I, s 2-F, t 3-F, u 4-F, v 2-Cl, w 3-Cl, x 4-Cl, y 3,4-diF

[a]Conditions and reagents: (a) (i) PPh_3, CCl_4, DMF; (ii) NaN_3, DMF, rt; (b) NaN_3, DMF, rt; (c) Cu_2SO_4 ascorbate, DMSO/H_2O, rt, 12 h (give **12a−y** (18%−55%)).

prepared from commercially available benzyl alcohols (**13a−i** and **13n**) and bromides (**15j−m** and **15o−y**). Specifically, commercially available benzyl alcohols **13a−i** and **13n** were converted directly[17] into the corresponding azides **14a−i** and **14n** on reaction with triphenylphosphine, in the presence of carbon tetrachloride and sodium azide at ambient temperature. The second series of benzyl azides (**14j−m** and **14o-y**) was prepared from commercially available benzyl bromides **15j−m** and **15o−y** on reaction with sodium azide in DMF as shown. Huisgen cycloaddition of biotin alkyne **16**[18] with each of the benzyl azides **14a−y**, in the presence of copper sulfate and sodium ascorbate,[3] then gave the desired 1,2,3-triazole **12a−y** as shown.

The activity profiles of 1,2,3-triazoles **12a−y** were determined using established biochemical and microbiological assay protocols.[3,19] Compounds displaying inhibitory activity against *Sa*BPL and cytotoxic activity against bacteria, but not mammalian cells, are considered important candidates for further antibiotic development. The *in vitro* potency and selectivity profiles of the 1,2,3-triazoles **12a−y** were measured using recombinant BPLs from *S. aureus* and *Homo sapiens*. Here the enzymatic incorporation of radiolabeled biotin onto an acceptor protein was measured in the presence of varying concentrations of each compound with the results shown in Tables 1 and 2. Previous enzymology and X-ray crystallography studies have demonstrated that the biotin triazoles are competitive inhibitors against biotin,[3,15,16] and as such, inhibitory constants (K_i) were calculated from IC_{50} values using the known K_M for biotin as previously described.[20] The antibacterial activity of the compounds was also determined using *S. aureus* strain ATCC 49775.[18] Growth of the bacteria 20 h post-treatment was measured spectrophotometrically at 600

DOI: 10.1021/acsmedchemlett.6b00248
ACS Med. Chem. Lett. 2016, 7, 1068−1072

Table 1. *In Vitro* Biotinylation and Antibacterial Assay Results for Benzyl Triazole Series 1

ID	R	K_i *Sa*BPL (μM)	K_i human BPL (μM)	anti-*S. aureus* activity[a]
12a	2-OH	>10	>16	–
12b	3-OH	>10	>16	–
12c	4-OH	1.59 ± 0.08	>16	–
12d	2-OMe	0.53 ± 0.05	>16	–
12e	3-OMe	1.17 ± 0.1	>16	–
12f	4-OMe	>10	>16	–
12g	2-NH_2	1.48 ± 0.14	>16	+
12h	3-NH_2	>10	>16	–
12i	4-NH_2	>10	>16	–
12j	3-Me	0.71 ± 0.04	>16	+
12k	4-Me	>10	>16	–
12l	3-CF_3	>10	>16	–
12m	4-CF_3	>10	>16	–
12n	4-*t*Bu	1.22 ± 0.07	>16	+
12o	4-COOH	0.67 ± 0.06	>16	–
12p	2-Br	0.96 ± 0.13	>16	+
12q	3-I	>10	>16	–
12r	4-I	0.56 ± 0.06	>16	+

[a]+, Optical density of the culture reduced by >40% of nontreated controls. –, compound did not inhibit bacterial growth.

Table 2. *In Vitro* Biotinylation and Antibacterial Assay Results for Benzyl Triazole Series 2

ID	R	K_i *Sa*BPL (μM)	K_i Human BPL (μM)	anti-*S. aureus* activity[a]	cytotox HepG2[b]
12s	2-F	>10	>16	–	N/D
12t	3-F	0.28 ± 0.02	>16	+	>40
12u	4-F	0.6 ± 0.1	>16	+	>40
12v	2-Cl	>10	>16	–	N/D
12w	3-Cl	0.39 ± 0.04	>16	+	>40
12x	4-Cl	1.1 ± 0.07	>16	+	>40
12y	3,4-diF	>10	>16	–	N/D

[a]+, optical density of the culture reduced by >40% of nontreated controls. –, compound did not inhibit bacterial growth. [b]Compounds were assayed at 40 μg/mL.

nm. Finally, selected compounds were assessed for potential toxicity using a cytotoxicity assay with cultured mammalian HepG2 cells (ATCC HB-8065).[3]

The initial series of alcohol analogues **12a–c** docked against *Sa*BPL were first assayed against the enzyme (Table 1) with the compound containing a C4 hydroxyl group (**12c**) showing modest activity (K_i = 1.59 μM). Interestingly, the C2 and C3 hydroxylated derivatives (**12a** and **12b**, respectively) were devoid of activity. It thus appears that the ribose pocket is sensitive to the position of the hydroxyl group and more so than predicted by the modeling. This observation is supported on analysis of the results for compounds containing other substituents, although there is little consistency regarding which position is most favored. Specifically, derivatives with a methoxyl group at C2 and C3 were both active (**12d**, K_i = 0.53 μM; **12e**, K_i = 1.1 μM), while the C4 analogue (**12f**) was inactive. For an amino substituent, C2 is active (**12g**, K_i = 1.49 μM), while both C3 (**12h**) and C4 (**12i**) were inactive. Of the other derivatives initially tested, C3 methyl (**12j**, K_i = 0.71 μM), C4 carboxyl and tertiary butyl (**12o**, K_i = 0.67 μM; **12n**, K_i = 1.1 μM) were active. The 2-bromo and 4-iodo derivatives **12p** and **12r** showed good activity against *S. aureus* BPL (K_i = 0.96 and 0.56 μM, respectively), and these compounds provided impetus for the expanded series of halogenated compounds shown in Table 2 and as discussed in detail below. A strongly electron withdrawing trifluoromethyl group at C3 and C4, resulted in compounds (**12l** and **12m**) that were devoid of activity against *Sa*BPL. All of the biotin triazoles tested were inactive against human BPL when 100 μM of compound was included in the assay medium. This is an important finding as it demonstrates that benzyl truncated triazoles retain the selectivity profile (i.e., active against *S. aureus* but not human BPL) of the earlier and more complex triazoles.[3,15]

The compounds shown in Table 1 were also assayed for antibacterial activity against *S. aureus* ATCC 49775. Compounds were designated as antibacterial if they reduced the optical density of the culture by >40% relative to the nontreated controls (Figure 5). Of the 18 compounds assessed,

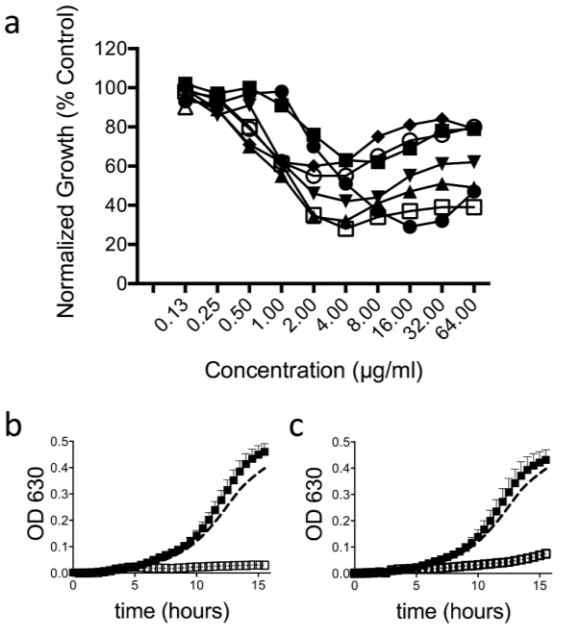

Figure 5. Inhibition of *S. aureus* growth *in vitro*. (a) Compounds **12g** (□), **12j** (♦), **12p** (○), **12r** (△), **12t** (■), **12u** (●), **12w** (▼), and **12x** (▲) were tested against *S. aureus* strain ATCC 49775. (b,c) Mechanism of action studies for **12g** (b) and **12t** (c). Growth curves for *S. aureus* RN4220 harboring the plasmid pCN51 (open boxes, negative control) or pCN51-BPL (solid boxes, for recombinant BPL overexpression) are shown. Growth media contained 16 μg/mL of compound, except, for no treatment controls (dashed line).

only five (those bearing amine, methyl, tertiary butyl, bromo, and iodo substituents, see **12g**, **12j**, **12n**, **12p**, and **12r**, respectively) were active in the whole cell assays. The fact that these compounds also inhibited *Sa*BPL is consistent with a mechanism of antibacterial action being through the BPL target. It is possible that those BPL inhibitors devoid of whole cell activity, namely, **12c–e**, **12g**, **12j**, and **12p**, are unable to penetrate the bacterial membrane, a problem often encountered in antibacterial discovery.[21]

Of the extended halogenated series (**12s–x** in Table 2) four compounds displayed good activity against *Sa*BPL, see **12t**, **12u**, **12w**, and **12x** that had K_i values of 0.28, 0.6, 0.39, and 1.1 μM, respectively. A 3-halo substituent was most favored for

DOI: 10.1021/acsmedchemlett.6b00248
ACS Med. Chem. Lett. 2016, 7, 1068–1072

activity as in **12t** and **12w**. In these cases, the inhibition constants were approximately 2- and 3-fold lower for the 3- vs 4- halogenated analogues, cf. **12t**/**12u** and **12w**/**12x**. A 3-fluoro substituent (**12t**) provided the most potent compound in this series with a K_i = 0.28 μM. The incorporation of a halogen at C2 removed all activity (see **12s** and **12v**) as did the introduction of a second fluoro substituent as in **12y**. Again all active compounds in this series showed excellent selectivity for *Sa*BPL over the human homologue. In addition, **12t**, **12u**, **12w**, and **12x** did not show cytotoxicity toward mammalian HepG2 cells at a single concentration of 40 μg/mL.

Finally, to demonstrate that compounds inhibited protein biotinylation *in vivo*, antibacterial susceptibility assays were performed using a *S. aureus* strain engineered to overexpress the BPL target. Similar approaches to establish the mechanism of action have been employed on *M. tuberculosis*,[10] but not previously for *S. aureus*. Bacteria were grown in media containing 16 μg/mL of either **12g** (series 1) or **12t** (series 2) for 16 h, with the optical density of the culture measured every 30 min. Overexpression of the BPL target abolished the antibacterial activity of both compounds, as *S. aureus* grew at the same rate as nontreated controls (Figure 5b,c). Bacteria harboring the parent cloning vector pCN51[22] that did not express additional BPL, remained highly sensitive to both inhibitors and failed to grow in their presence. Together these data show that the mechanism of action of **12g** (from series 1) and **12t** (series 2) is clearly via the inhibition of BPL.

The 1-benzyl substituted 1,2,3-triazoles reported here represent a new class of BPL inhibitors that lack the adenine group, or analogue thereof, found in all other isostere-based BPL inhibitors. These compounds have much reduced molecular weight and are relatively easy to prepare. Importantly, the biochemical and microbiological data provide a clear relationship between *in vitro* inhibition of BPL and anti-*S. aureus* activity, with our most potent enzyme inhibitors generally providing our most promising antibacterials (see **12j**, **12p**, **12r**, **12t**, **12u**, and **12w**). In antibiotic drug discovery, this is not always the case as a number of external factors contribute to bioactivity, such as cell permeability and susceptibility to efflux mechanisms and metabolic degradation.

The best lead compound in this new series (**12t**) with a 3-fluoro substituted benzyl group, has a K_i of 280 nM against *Sa*BPL and demonstrated mechanism of antibacterial activity consistent with the inhibition of protein biotinylation. It is essentially nontoxic to mammalian HepG2 cells and is devoid of activity against human BPL. This compares to the extended 1,2,3-triazole **11** that has K_i of 90 nM against *Sa*BPL. This compound provides clear interactions with both the biotin and adenine pockets of *Sa*BPL and, like the new benzyl series, is essentially inactive against human BPL.[3] Our initial SAR data on the new benzyl series provides confidence that further optimization of *in vitro* inhibition will lead to improved antibacterial activity. *In silico* docking supports a binding mechanism in which the benzyl group interacts with the ribose pocket of *Sa*BPL. The compounds reported here provide important new scaffolds for further chemical modification and activity optimization, specifically to interact with the adjacent adenyl-binding site in the enzyme. Such studies are currently underway, particularly the inclusion of extended substituents on the benzyl group and also substitution at C5 of the triazole.

■ ASSOCIATED CONTENT

Supporting Information

The Supporting Information is available free of charge on the ACS Publications website at DOI: 10.1021/acsmedchemlett.6b00248.

Biological assays, synthetic procedures, and data for selected compounds (PDF)

■ AUTHOR INFORMATION

Corresponding Author

*Tel: +61 88 3135652. E-mail: andrew.abell@adelaide.edu.au.

Present Address

[‖]School of Medical Sciences (Pharmacology) and Bosch Institute, The University of Sydney, Sydney, New South Wales 2006, Australia.

Author Contributions

The manuscript was written through contributions of all authors. Medicinal chemistry was performed by J.F., W.T., S.C., and A.D.A., biochemical assays were performed by A.S.P. and S.W.P., antibacterial susceptibility assays were performed by D.H. and A.H. under the guidance of S.W.P. and G.W.B., and cell culture assays were performed by A.H. and S.W.P.

Funding

This work was supported by the National Health and Medical Research Council of Australia (application APP1068885), the Centre for Molecular Pathology, University of Adelaide, and Adelaide Research and Innovation's Commercial Accelerator Scheme. We are grateful to the Wallace and Carthew families for their financial support of this work.

Notes

The authors declare no competing financial interest.

■ ACKNOWLEDGMENTS

We are grateful to the Institute for Photonics and Advanced Sensing (IPAS) for providing access to analytical HPLC and the National Health and Medical Research Council (NHMRC) and Australian Research Council (ARC) for funding. We also thank Dr. Beatriz Blanco Rodriguez for her critical comments on the manuscript.

■ REFERENCES

(1) Feng, J.; Paparella, A. S.; Booker, G. W.; Polyak, S. W.; Abell, A. D. Biotin Protein Ligase Is a Target for New Antibacterials. *Antibiotics* **2016**, *5* (3), 26.

(2) Duckworth, B. P.; Nelson, K. M.; Aldrich, C. C. Adenylating enzymes in *Mycobacterium tuberculosis* as drug targets. *Curr. Top. Med. Chem.* **2012**, *12* (7), 766.

(3) Soares da Costa, T. P.; Tieu, W.; Yap, M. Y.; Pendini, N. R.; Polyak, S. W.; Sejer Pedersen, D.; Morona, R.; Turnidge, J. D.; Wallace, J. C.; Wilce, M. C.; Booker, G. W.; Abell, A. D. Selective inhibition of biotin protein ligase from *Staphylococcus aureus*. *J. Biol. Chem.* **2012**, *287* (21), 17823−32.

(4) Pendini, N. R.; Bailey, L. M.; Booker, G. W.; Wilce, M. C.; Wallace, J. C.; Polyak, S. W. Microbial biotin protein ligases aid in understanding holocarboxylase synthetase deficiency. *Biochim. Biophys. Acta, Proteins Proteomics* **2008**, *1784* (7−8), 973−82.

(5) Polyak, S.; Abell, A.; Wilce, M.; Zhang, L.; Booker, G. Structure, function and selective inhibition of bacterial acetyl-coa carboxylase. *Appl. Microbiol. Biotechnol.* **2012**, *93* (3), 983−992.

(6) Paparella, A. S.; Soares da Costa, T. P.; Yap, M. Y.; Tieu, W.; Wilce, M. C.; Booker, G. W.; Abell, A. D.; Polyak, S. W. Structure guided design of biotin protein ligase inhibitors for antibiotic discovery. *Curr. Top. Med. Chem.* **2014**, *14* (1), 4−20.

DOI: 10.1021/acsmedchemlett.6b00248
ACS Med. Chem. Lett. 2016, 7, 1068−1072

(7) Xu, Y.; Beckett, D. Kinetics of biotinyl-5′-adenylate synthesis catalyzed by the Escherichia coli repressor of biotin biosynthesis and the stability of the enzyme-product complex. *Biochemistry* **1994**, *33* (23), 7354−7360.
(8) Brown, P. H.; Beckett, D. Use of binding enthalpy to drive an allosteric transition. *Biochemistry* **2005**, *44* (8), 3112−3121.
(9) Bockman, M. R.; Kalinda, A. S.; Petrelli, R.; De la Mora-Rey, T.; Tiwari, D.; Liu, F.; Dawadi, S.; Nandakumar, M.; Rhee, K. Y.; Schnappinger, D. Targeting *Mycobacterium tuberculosis* Biotin Protein Ligase (MtBPL) with Nucleoside-Based Bisubstrate Adenylation Inhibitors. *J. Med. Chem.* **2015**, *58* (18), 7349−7369.
(10) Duckworth, B. P.; Geders, T. W.; Tiwari, D.; Boshoff, H. I.; Sibbald, P. A.; Barry, C. E., 3rd; Schnappinger, D.; Finzel, B. C.; Aldrich, C. C. Bisubstrate adenylation inhibitors of biotin protein ligase from *Mycobacterium tuberculosis*. *Chem. Biol.* **2011**, *18* (11), 1432−41.
(11) Brown, P. H.; Cronan, J. E.; Grøtli, M.; Beckett, D. The biotin repressor: modulation of allostery by corepressor analogs. *J. Mol. Biol.* **2004**, *337* (4), 857−869.
(12) Tieu, W.; Polyak, S. W.; Paparella, A. S.; Yap, M. Y.; Soares da Costa, T. P.; Ng, B.; Wang, G.; Lumb, R.; Bell, J. M.; Turnidge, J. D.; Wilce, M. C.; Booker, G. W.; Abell, A. D. Improved Synthesis of Biotinol-5′-AMP: Implications for Antibacterial Discovery. *ACS Med. Chem. Lett.* **2015**, *6* (2), 216−20.
(13) Sittiwong, W.; Cordonier, E. L.; Zempleni, J.; Dussault, P. H. beta-Keto and beta-hydroxyphosphonate analogs of biotin-5′-AMP are inhibitors of holocarboxylase synthetase. *Bioorg. Med. Chem. Lett.* **2014**, *24* (24), 5568−71.
(14) Tieu, W.; Jarrad, A. M.; Paparella, A. S.; Keeling, K. A.; Soares da Costa, T. P.; Wallace, J. C.; Booker, G. W.; Polyak, S. W.; Abell, A. D. Heterocyclic acyl-phosphate bioisostere-based inhibitors of *Staphylococcus aureus* biotin protein ligase. *Bioorg. Med. Chem. Lett.* **2014**, *24* (19), 4689−93.
(15) Tieu, W.; Soares da Costa, T. P.; Yap, M. Y.; Keeling, K. L.; Wilce, M. C. J.; Wallace, J. C.; Booker, G. W.; Polyak, S. W.; Abell, A. D. Optimising *in situ* click chemistry: the screening and identification of biotin protein ligase inhibitors. *Chem. Sci.* **2013**, *4*, 3533−3537.
(16) Pendini, N. R.; Yap, M. Y.; Polyak, S. W.; Cowieson, N. P.; Abell, A.; Booker, G. W.; Wallace, J. C.; Wilce, J. A.; Wilce, M. C. Structural characterization of *Staphylococcus aureus* biotin protein ligase and interaction partners: An antibiotic target. *Protein Sci.* **2013**, *22* (6), 762−73.
(17) Koziara, A. A Facile, One-Pot Conversion of Primary Alcohols into Amines. *J. Chem. Res. (S)* **1989**, No. 9, 296−297.
(18) Soares da Costa, T. P.; Tieu, W.; Yap, M. Y.; Zvarec, O.; Bell, J. M.; Turnidge, J. D.; Wallace, J. C.; Booker, G. W.; Wilce, M. C.; Abell, A. D.; Polyak, S. W. Biotin analogues with antibacterial activity are potent inhibitors of biotin protein ligase. *ACS Med. Chem. Lett.* **2012**, *3* (6), 509−14.
(19) Polyak, S. W.; Chapman-Smith, A.; Brautigan, P. J.; Wallace, J. C. Biotin Protein Ligase from *Saccharomyces cerevisiae*: The N-terminal domain is required for complete activity. *J. Biol. Chem.* **1999**, *274* (46), 32847−32854.
(20) Cheng, Y.; Prusoff, W. H. Relationship between the inhibition constant (K_I) and the concentration of inhibitor which causes 50% inhibition (IC50) of an enzymatic reaction. *Biochem. Pharmacol.* **1973**, *22* (23), 3099−108.
(21) Tommasi, R.; Brown, D. G.; Walkup, G. K.; Manchester, J. I.; Miller, A. A. ESKAPEing the labyrinth of antibacterial discovery. *Nat. Rev. Drug Discovery* **2015**, *14* (8), 529−42.
(22) Charpentier, E.; Anton, A. I.; Barry, P.; Alfonso, B.; Fang, Y.; Novick, R. P. Novel cassette-based shuttle vector system for gram-positive bacteria. *Appl. Environ. Microbiol.* **2004**, *70* (10), 6076−6085.

DOI: 10.1021/acsmedchemlett.6b00248
ACS Med. Chem. Lett. 2016, 7, 1068−1072

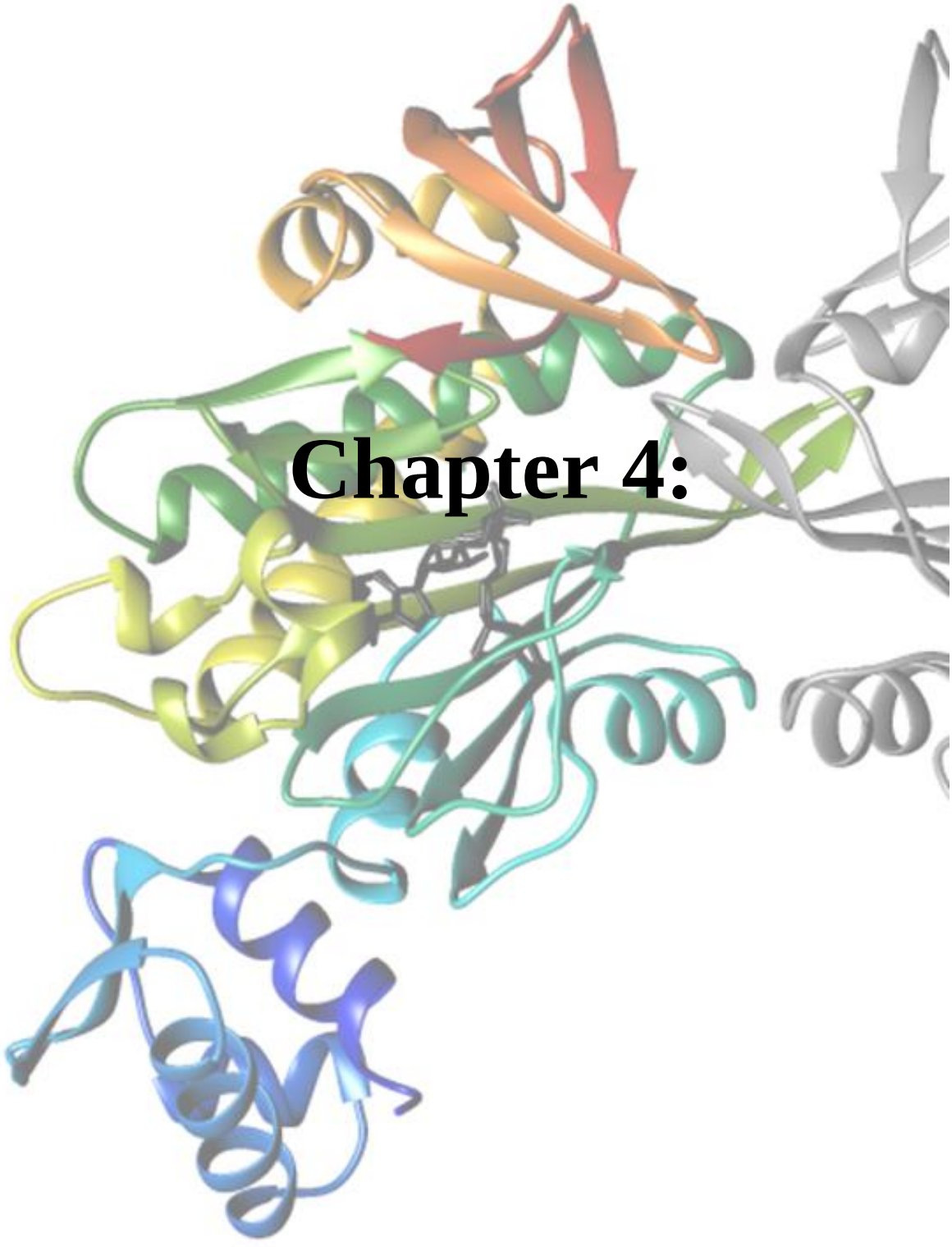

Chapter 4:

Statement of Authorship

Title of Paper	5-Halogenation effect of 1,2,3-triazole biotin protein ligase inhibitors on antibacterial activity against Staphylococcus aureus
Publication Status	☐ Published ☐ Accepted for Publication ☐ Submitted for Publication ☑ Unpublished and Unsubmitted work written in manuscript style
Publication Details	Andrew Hayes, Kwang Jun Lee, Ashleigh S. Paparella, Jiage Feng, David Heim, Zikai Feng, Danielle Cini, Grant W. Booker, Matthew Wilce, Steven W. Polyak, and Andrew D. Abell

Principal Author

Name of Principal Author (Candidate)	Andrew Hayes		
Contribution to the Paper	Performed mechanism of action studies on all compounds Performed antibacterial susceptibility testing on compound series 2 Analysed structure activity relationship of series 2 Primary role in manuscript preparation (biological results and discussion)		
Overall percentage (%)	15 %		
Certification:	This paper reports on original research I conducted during the period of my Higher Degree by Research candidature and is not subject to any obligations or contractual agreements with a third party that would constrain its inclusion in this thesis.		
Signature		Date	1/08/17

Co-Author Contributions

By signing the Statement of Authorship, each author certifies that:

i. the candidate's stated contribution to the publication is accurate (as detailed above);

ii. permission is granted for the candidate in include the publication in the thesis; and

iii. the sum of all co-author contributions is equal to 100% less the candidate's stated contribution.

Name of Co-Author	Kwang Jun Lee		
Contribution to the Paper	Synthesised and characterised compounds in series 2, Docking studies with compounds series 1 and 2. Primary role in manuscript preparation (chemical methods, results and discussion) Co-author		
Signature		Date	25/5/17

Name of Co-Author	Ashleigh S Paparella		
Contribution to the Paper	Expression and purification of *Sa*BPL and *Hs*BPL Performed *in vitro* biotinylation assays against *Sa*BPL and *Hs*BPL for series 1. SPR analysis of compounds from series 1. Provided advanced manuscript of series 1 data. Co-author		
Signature		Date	3/7/2017

Name of Co-Author	Jiage Feng		
Contribution to the Paper	Synthesised and characterised compounds for series 1		
Signature		Date	6/7/2017

Name of Co-Author	David Heim		
Contribution to the Paper	Performed cytotoxicity on compounds from series 1		
Signature		Date	24/07/2017

Name of Co-Author	Zikai Feng		
Contribution to the Paper	Performed antibacterial susceptibility testing on compound series 2 Performed *in vitro* biotinylation assays against *Sa*BPL for series 2.		
Signature		Date	11/7/2017

Name of Co-Author	Danielle Cini		
Contribution to the Paper	Performed crystallography of compound 4b		
Signature		Date	10/7/17

Name of Co-Author	Matthew Wilce		
Contribution to the Paper	Supervised the crystallography aspects of the project, revised manuscript		
Signature		Date	10/7/2017

Name of Co-Author	Grant Booker		
Contribution to the Paper	Supervised the biological aspects of the project, revised manuscript		
Signature		Date	25/5/2017

Name of Co-Author	Steven Polyak		
Contribution to the Paper	Worked closely with the co-authors to write the manuscript Supervised biological testing		
Signature		Date	25/5/2017.

Name of Co-Author	Andrew Abell		
Contribution to the Paper	Supervised all aspects of medicinal chemistry, revised manuscript and is corresponding author		
Signature		Date	25/5/2017

Halogenation of biotin protein ligase inhibitors improves whole cell activity against *Staphylococcus aureus*

Ashleigh S. Paparella, [†‡] *Kwang Jun Lee,* [‡ ‡] *Andrew J. Hayes,* [†‡] *Jiage Feng,* [‡] *David Heim,* [†] *Zikai Feng,* [†] *Danielle Cini,* [§] *Grant W. Booker,* [†] *Matthew C. J. Wilce,* [§] *Steven W. Polyak,* [†] *and Andrew D. Abell* [‡ #]

[‡]Department of Chemistry, University of Adelaide, Adelaide, South Australia 5005, Australia

[†] Department of Molecular and Cellular Biology, University of Adelaide, South Australia 5005, Australia

[§]School of Biomedical Science, Monash University, Victoria 3800, Australia

[#]Centre for Nanoscale BioPhotonics (CNBP), University of Adelaide, Adelaide, South Australia 5005, Australia

ABSTRACT

We report the synthesis and evaluation of 5-halogenated-1,2,3-triazoles as inhibitors of biotin protein ligase from *Staphylococcus aureus*. Whilst the inhibitory activity of the compounds against *Sa*BPL was comparable to previous 1,4-disubstituted-1,2,3-triazoles, the halogenated compounds exhibited significantly improved antibacterial activity over their non-halogenated counterparts. Importantly the 5-fluoro-1,2,3-triazole compound **4c** had antibacterial activity against *S. aureus* ATCC49775 with a minimum inhibitory concentration (MIC) of 8 μg/mL.

INTRODUCTION:

There is an urgent need to discover new therapeutics to combat antibiotic resistant bacteria.[1] Target based approaches to antibiotic discovery have been somewhat limited by poor translation of compounds with potent *in vitro* activity into bio-actives with whole cell antibacterial activity.[2,3,4] This is often due to the formidable bacterial cell wall and/or membranes that present as barriers, preventing compounds from permeating into the cell and accessing intracellular drug targets. Bacteria also employ efficient efflux pumps to eliminate cytotoxic compounds from the cell. One approach to improve whole cell activity is through halogenation of compounds that are otherwise cell impermeable.[5] This has been successfully demonstrated with the fluoroquinolones, where replacement of the hydrogen on C6 of the quinolone moiety improved whole cell potency ~100-fold.[6,7] Similar approaches using halogenation have also been reported to improve anti-biofilm activity of phenazines and quinolones.[8-9] Due to its small size and high electronegativity, the fluorine atom is an attractive modification that can improve the binding affinity, membrane permeability and metabolic stability.[10] As such, 20% of available drugs are fluorinated.[11]

Biotin protein ligase (BPL) is a promising drug target that has been the subject of antibiotic drug discovery programs by several groups.[2, 12-21] BPL serves as the sole enzyme responsible for the biotinylation, and subsequent activation, of biotin-dependent enzymes. The clinically important bacterial pathogen *Staphylococcus aureus* possesses two such biotin-dependent enzymes, namely acetyl-CoA carboxylase and pyruvate carboxylase, which catalyze key reactions in the important metabolic pathways of fatty acid biosynthesis and gluconeogenesis respectively.[14] BPL catalyzes protein biotinylation through ligation of biotin **1** and ATP to form biotinyl-5′-AMP, **2** (see **Figure 1**).[14] Replacement of the labile phosphoanhydride linker in **2** with more stable bioisosteres has produced inhibitors that target BPL from bacterial pathogens such as *S. aureus,*[18,19] *Escherichia coli,*[22,23,24] and *Mycobacterium tuberculosis*.[21,20]

These pieces of work have recently been reviewed.[13] However, there are precious few examples of BPL inhibitors with whole cell anti-staphylococcal activity. One example of a bioactive BPL inhibitor is biotinol-5′-AMP **3** (**Figure 2**) that reduces the growth of *S. aureus* and *M. tuberculosis* with minimal inhibitory concentrations (MIC) of 2 and 2.5 μg/mL respectively,[19] thereby providing *in vitro* proof of concept that pharmacological inhibition of BPL is a strategy for new antibacterials. Recently we reported 1,4-disubstituted-1,2,3-triazoles as a novel class of BPL inhibitor that selectively targets the BPL from *S. aureus* over the human homologue.[12,13, 17] This biotin triazole class is exemplified by **4a** (**Figure 3**) that has the *in vitro* potency and selectivity over the human homologue necessary for a pre-clinical candidate, but poor whole cell activity.[12] For example, 8 μg/mL of **4a** only reduced the growth of *S. aureus* ATCC 49775 by 60% of non-treated controls. [12, 18] Inhibition of cell growth by > 90% is a minimum requirement for a lead compound. Attempts to improve antibacterial potency by shortening and simplifying the 1,4-disubstituted-1,2,3-triazole pharmacophore (see **5a-k, 5m, 5o, Figure 3**)[13] have had modest success. Here we present halogenated derivatives of two pharmacophores **4a** and **5a-o** as the first examples of 1,4,5-trisubstituted triazole BPL inhibitors. Specifically, the hydrogen on C5 of the triazole heterocycle is replaced with iodine, fluorine or chlorine as in compounds **4b, 4c** and **4d**, respectively. Whole cell activity of these compounds was determined using antimicrobial susceptibility assays, with further microbiological testing and biochemical assays performed to confirm the mechanism of action was consistent with the inhibition of BPL. We show that halogenation of the triazole linker improved whole cell antibacterial activity whilst maintaining selectivity for *Sa*BPL, providing a new approach to the development of chemotherapeutics to combat *S. aureus*.

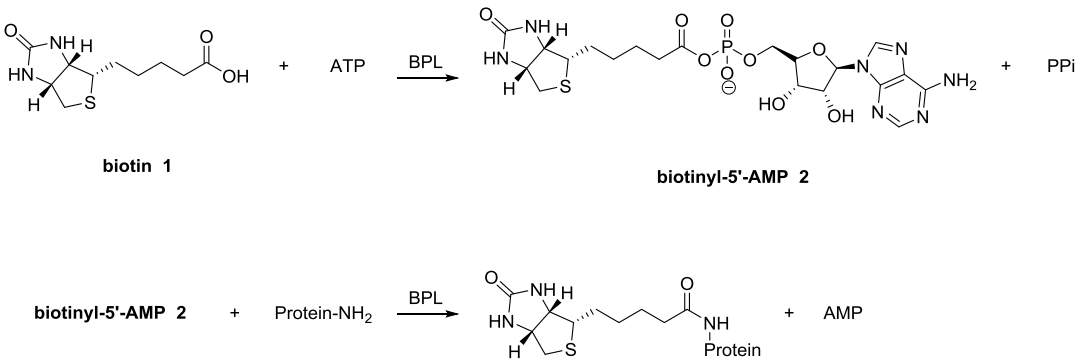

Figure 1. Reaction mechanism of biotin protein ligase.

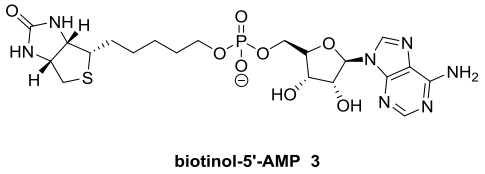

Figure 2. Chemical structure of biotinol-5′-AMP.

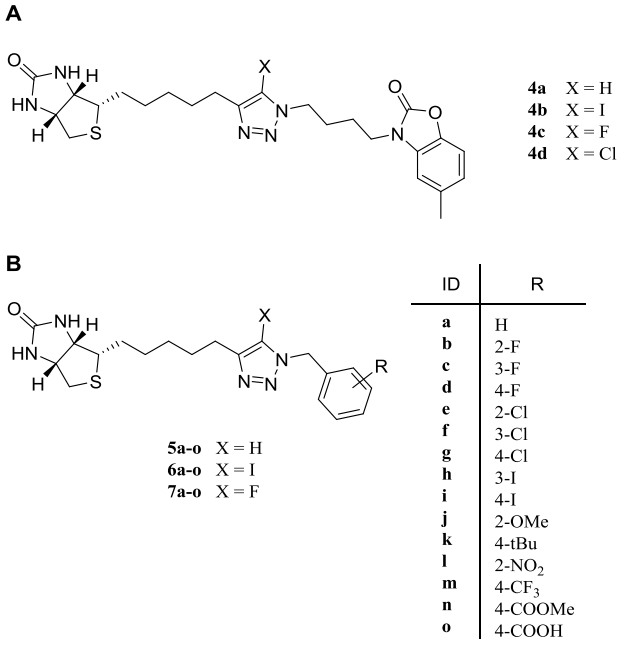

Figure 3. Chemical structure of BPL inhibitors. (B) Benzoxazolone triazole series. (C) Benzyl triazole series.

Series 1: compounds 4a-d (Figure 3A)

The synthesis of the 1,4-disubstituted-1,2,3-triazole **4a**[12] and the 1,4,5-trisubstituted-1,2,3-triazoles **4b-d** was carried out as summarized in **Scheme 1**. 5-iodo-1,2,3-triazole **4b** was synthesized from biotin acetylene **8**[12], which was firstly elaborated to biotin 1-iodoacetylene **10** under CuI and N-iodomorpholine. Biotin 1-iodo acetylene **10** was reacted with azide **9**[12] in the presence of CuI as a catalyst and TEA as an amine ligand to afford 5-iodo-1,2,3-triazole **4b** with 36% yield.[25] Iodinated **4b** was subsequently converted to fluorinated **4c** and chlorinated **4d** by halogen exchange reaction based on the optimised conditions reported by Worrell *et al*.[26] In particular iodide **4b** was treated with 5 equivalents of either potassium fluoride or potassium chloride in MeCN/H_2O (1:1) mixture and reacted in the microwave reactor at 180ºC for 10 minutes to give 5-fluoro-1,2,3-triazole **4c** and 5-chloro-1,2,3-triazole **4d** in 89% and 80% yields respectively.

Scheme 1. Synthesis of benzoxazolone triazole series

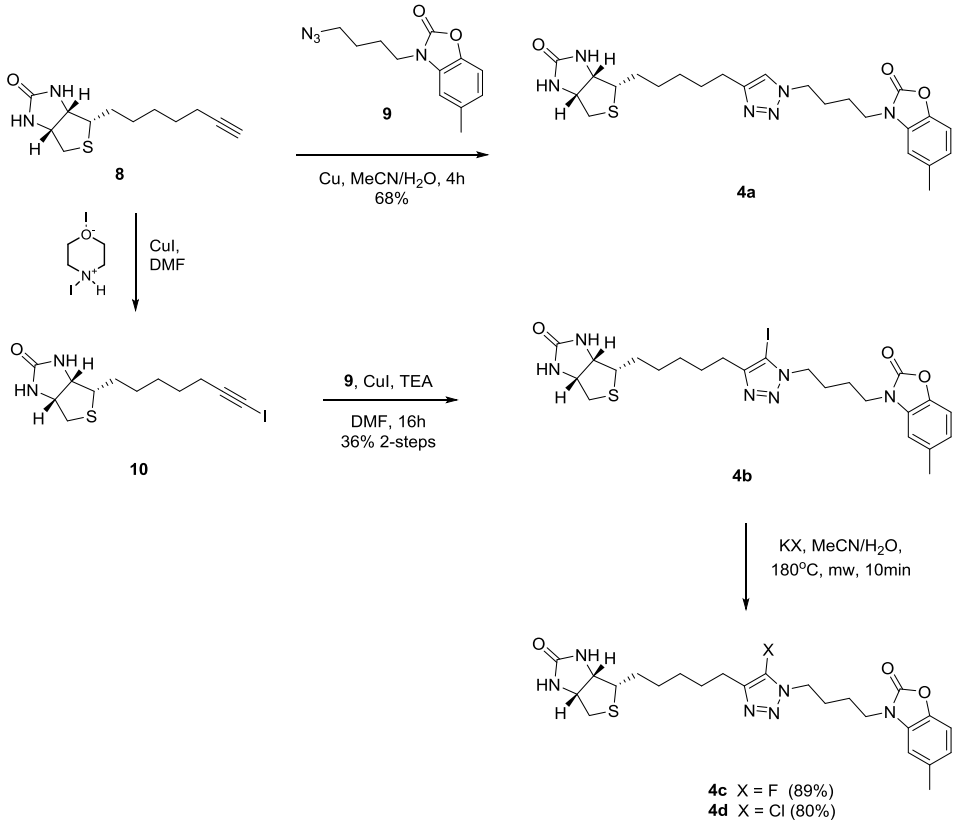

Fluorination of compound 4a improved whole cell activity without cytotoxic effects.

Antimicrobial sensitivity assays were performed upon *S. aureus* clinical isolate ATCC 49775 to quantitate the antibacterial potency of **4a-d** (**Figure 4A**).[16] Whole cell activity was determined by measuring the optical density of the bacterial cultures spectrophotometrically at 620 nm after 24 hours of treatment with **4a-d**. As previously reported,[27] parent compound **4a** only reduced the optical density of the culture by ~40%. This low level of activity was insufficient to determine an MIC. In contrast, fluorinated analogue **4c** was bioactive against *S. aureus* and inhibited measurable growth of the bacteria with an MIC of 8 μg/mL (16 μM). This was the first example of a biotin triazole with potent antibacterial activity. This data provides the first proof of concept data to support halogenation of BPL inhibitors as a route towards improved whole cell bioactivity against *S. aureus*. Interestingly, the effect was specific for fluorination as the 5-iodo (**4b**) and the 5-chloro (**4d**) analogues did not improve antibacterial activity against *S. aureus.* To verify that the mechanism of antibacterial action of **4c** was due to the inhibition of BPL, antibacterial susceptibility assays were performed upon *S. aureus* RN4220 engineered to recombinantly over-produce the BPL target (**Figure 4B**) .[13] A concomitant decrease in whole cell activity is expected upon over-expression of a drug target, should a compound's mechanism of action be directly through that target.[13, 21] In support of this, an 8-fold increase in the MIC was observed for the BPL inhibitor biotinol-5′-AMP **3** as a result of BPL overexpression (Supporting information **Figure S4).** Consistent with **4c** binding directly to the BPL target, over-expression of BPL also significantly reduced antibacterial potency of the inhibitor, with an MIC increase of greater than 16-fold and only ~60% growth reduction observed at the highest concentration tested (approx. 100μM). Finally, cytotoxicity assays were performed with HepG2 liver cells on inhibitors **4b-d**. No cytotoxicity was measured at the highest concentration tested (approx. 80μM) (**Table 1**). Together these results suggested that halogenation of BPL inhibitors may provide one avenue towards improved whole cell bioactivity against *S. aureus*.

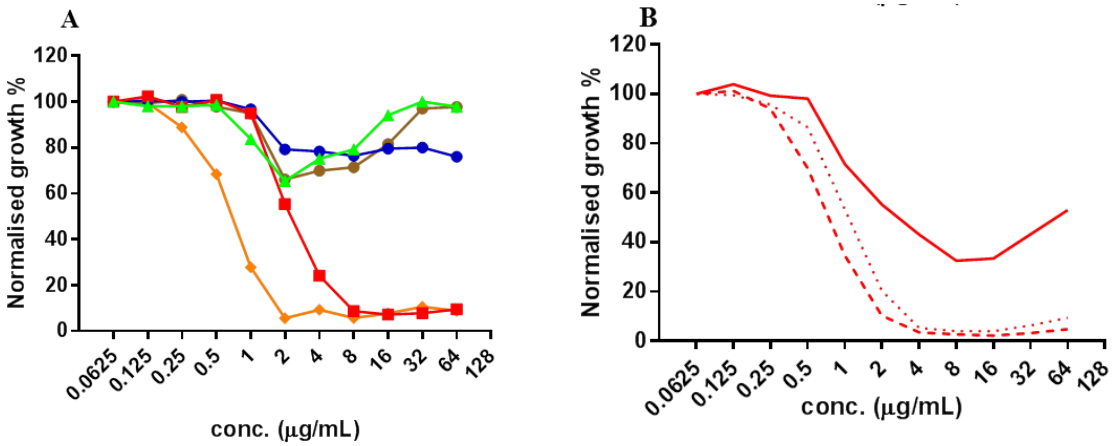

Figure 4. Inhibition of *S. aureus* growth *in vitro*. (A) Compounds, **3** (orange), **4a** (brown), **4b** (blue), **4c** (red), and **4d** (green) were tested against *S. aureus* strain ATCC 49775. (B) Compound **4c** was tested for antibacterial susceptibility against *S. aureus* RN4220 in the presence and absence of overexpressed *Sa*BPL. *S. aureus* RN4220 harbouring pCN51-BPL (solid line), pCN51 (dashed line) or no vector (dotted line) are shown.

Antibacterial activity was not a result of increased inhibitory activity in compound 4c

To determine if the observed improved whole cell activity of **4c** was due to increased binding activity against the BPL target, *in vitro* binding and enzyme assays were performed (**Table 1**). The bimolecular association and dissociation constants were investigated for **4a-d** through Surface Plasmon Resonance (SPR) binding assays using *Sa*BPL immobilized onto a sensor chip. [16, 27-28] All four compounds displayed rapid association and dissociation rates that were unable to be quantified by the SPR software (Supporting information **Figure S3**). Accordingly, the K_D values were measured using a steady state affinity model. There was no significant difference between the affinity of **4a** (K_D = 8.4 µM) or the halogenated analogues **4b-d** binding to *Sa*BPL (**Table 1**). The indistinguishable and fast dissociation rates observed for all inhibitors rules out increased occupancy of **4c** on the BPL target (a function of slow dissociation kinetics) as a possible mechanism for increased whole cell potency. Next, an *in*

vitro biotinylation assay was employed to measure the inhibition of compounds **4b-d** against recombinant BPLs from *S. aureus* and *Homo sapiens*. The enzymatic incorporation of radiolabeled biotin onto an acceptor protein, the 90 amino acid biotin-acceptor domain from pyruvate carboxylase (*Sa*PC90), was measured in the presence of varying concentrations of inhibitor. Halogenated analogues **4b-d** all had similar activities as the non-halogenated parent against *Sa*BPL, with **4a** being the most potent inhibitor (K_i = 0.23 μM) (**Table 1**). The iodinated (0.41 μM) and the fluorinated (0.42 μM) analogues **4b** and **4c** were the most potent halogenated analogues, whilst the chlorinated analogue **4d** proved to be the weakest compound in the series (K_i = 0.90 μM). All of the compounds tested were inactive against human BPL (K_i > 10 μM) highlighting that the halogenated analogues still maintained the reported selectivity observed with **4a**. This is important as it suggests that the modified triazole is still well accommodated by the *Sa*BPL but not the human homologue. Together the SPR binding and *in vitro* protein biotinylation assays demonstrate that the fluorine of **4c** played no direct role in binding, so the improved whole cell activity of **4c** is not the result of strengthened interactions between inhibitor and BPL target.

Table 1: Binding affinities derived from SPR analysis, inhibition and cytotoxic data for compounds **4a-d**.

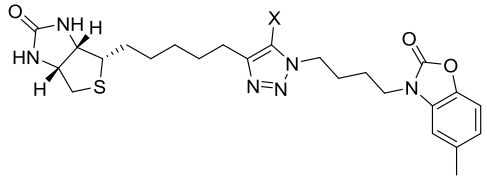

ID	X	K_D *Sa*BPL (μM)	K_i *Sa*BPL (μM)*	K_i *Hs*BPL (μM)	MIC ATCC49775 (μM)	Cytotox HepG2 (μg/mL)
4a	H	8.4 ± 1.0	0.23 ± 0.01	>10	>100	>80
4b	I	3.8 ± 1.5	0.41 ± 0.02	>10	>100	>80
4c	F	7.1 ± 3.4	0.42 ± 0.05	>10	16	>80
4d	Cl	10.1 ± 1.8	0.9 ± 0.11	>10	>100	>80

* Previous enzymology and X-ray crystallography studies have demonstrated that biotin triazole **4a** is a competitive inhibitor against biotin **1**.[12] Therefore, inhibition constants (K_i) were derived from the IC_{50} values using the known K_M for biotin, as previously described.[29]

Finally, a crystal structure of **4c** in complex with *Sa*BPL was determined to define the mechanism of binding (**Figure 5**). The resulting data was compared to the published structures of *Sa*BPL in complex with biotin **1** or biotinyl-5′-AMP **2**, as well as the parent compound **4a** (PDB 3V7S)[12] (**Figure 5A**). Both **4a** and **4c** adopted similar binding modes with the biotinyl and benzoxazolone moieties occupying the biotin and nucleotide pockets, as expected. Importantly for this study, the fluorine of **4c** did not directly contribute any new bonding interactions with *Sa*BPL compared with **4a**. This result was consistent with the *in vitro* assays described above. Previous crystallography studies on *Sa*BPL in complex with **1** and **2** have established that conformational changes accompany ligand binding and these are necessary for inhibitor binding. The same conformational changes were also observed for both **4a** and **4c**. In particular, residues T177-K131 undergo a disordered to ordered transition

when in complex with biotin.[27,30] This feature, known as the biotin-binding loop, encases the active site to prevent ligand dissociation and positions the side chain of W127 in the active site such that it can participate in a π-π stacking interaction with the adenyl group of ATP. Both **4a** and **4c** induced these same disordered-to-ordered conformational changes resulting in ordering of the biotin-binding loop. Hydrogen-bonding between the triazole heterocycle and amino acids in the BBL are apparent in both structures, namely between triazole N2 and the side chain of R125, and triazole N3 with R122 (**Figure 5B-C**). Further interactions were observed between the triazole and side chains of D180 and K187. The main differences between the **4a** and **4c** structures were apparent with the side chain of W127. For *Sa*BPL in complex with **4a**, the indole ring of W127 adopted the same conformation as observed in the co-structure with biotin **1** and a biotinyl-5-AMP **2** that facilitates ATP binding. In the co-complex with **4a**, the conformation of the indole sidechain defines a T-shaped π interaction with the triazole heterocycle. However, for **4c**, the side chain of W127 was tilted, thereby disrupting the protein-triazole interaction. This was offset by a new T-shaped π interaction between W127 and the benzoxazolone group (Supporting information **Figure S1**). The volume and area of the binding pocket of *Sa*BPL were also increased as 5-fluoro triazole **4c** was bound into the binding site of the enzyme. (Supporting information **Table S1**). These data suggest an induced fit model of ligand binding occurs involving the biotin binding loop, and the BPL active site has enough flexibility to accommodate a tri-substituted biotin-triazole inhibitor.

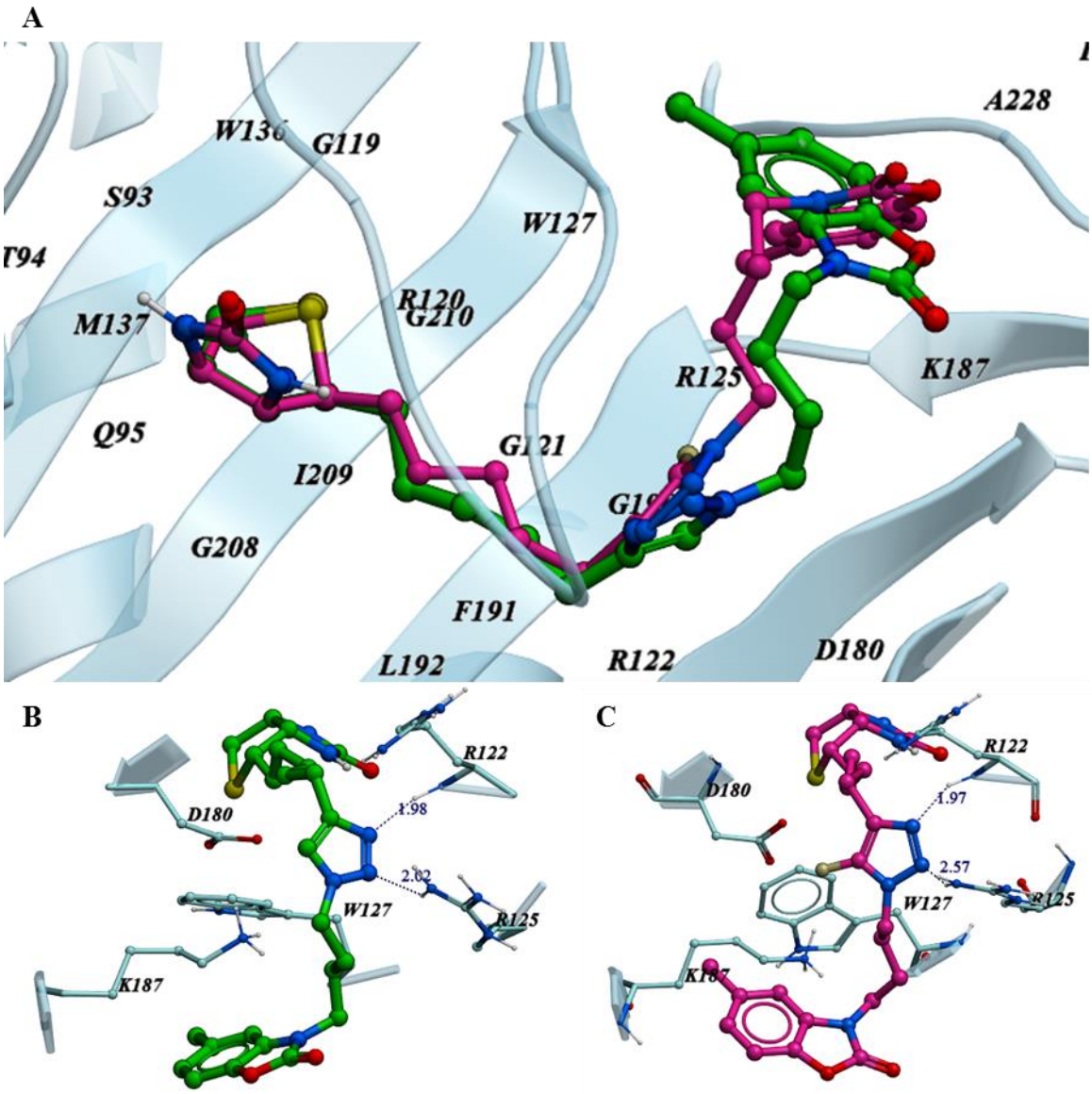

Figure 5. Comparison of co-crystal structures. (A) **4a** (green) and **4c** (magenta) were superimposed to reveal the different binding pose of benzoxazolone ring. (B) Binding Pocket of *Sa*BPL in complex with **4a** (PDB 3V7S). (C) Binding pocket of *Sa*BPL in complex with **4c**. Amino acids that encompass the triazole binding pocket are shown. Dashed lines represent hydrogen bonds.

Series 2: compounds 5a-o, 6a-o, 7a-o (Figure 3B)

A second series was investigated to determine if the improved whole cell activity observed for **4c** could be replicated through halogenation of the smaller benzyl-biotin triazole BPL inhibitors.[13] Substitution of the hydrogen at C5 on the triazole linker with either fluorine or iodine was performed upon the benzyl biotin triazoles **5a-o**[13]. The synthesis of 1-benzyl-5-proto-1,2,3-triazoles **5a-o**,[13] 1-benzyl-5-iodo-1,2,3-triazoles **6a-o**, and 1-benzyl-5-fluoro-1,2,3-triazoles **7a-o** was accomplished as outlined in **Scheme 2-3**. The 5-iodo-1,2,3-triazoles **6a-l** and **6n** were synthesized according to the same procedure described for the synthesis of compound **4b** (**Scheme 2**). However, this method is a two-step reaction requiring the preformation of biotin 1-iodo acetylene **10** and occasionally yields a considerable ratio of 5-proto triazole as a side product. For instance, compound **5l** was isolated as a side product along with compound **6l** after the two-step reaction (**Scheme 3**). The 5-iodo-1,2,3-triazole **6m** was synthesized by reaction of biotin acetylene **8**[12] with 4-trifluoromethylbenzyl azide in the presence of LiI, $Cu(ClO_4)_2$, and TEA in THF (**Scheme 3**). This reaction proceeds by an *in situ* conversion of the alkyne to the iodoalkyne.[31] Synthesis of 5-fluoro-1,2,3-triazoles **7a-n** were carried out using the same conditions as for preparation of **4c** (**Scheme 1**) except the reaction time was reduced from 10 min to 5 min. The 5-iodo-1,2,3-triazoles **6a-n** were separately treated with potassium fluoride in $MeCN/H_2O$ (1:1) mixture and reacted in the microwave for 5 min to give the corresponding 5-fluoro-triazoles **7a-n** in yields of 64-81%. Increased reaction time reduced the observed yields due to decomposition of the starting materials. For example, the yield of **7c** was increased from 33% to 76% as reaction time was decreased from 10 min to 5 min. Carboxylic acids **6o, 7o** were prepared by hydrolysis reaction with LiOH from corresponding methyl ester **6n, 7n** (**Scheme 2**).

Scheme 2. Synthesis of benzyl triazole series

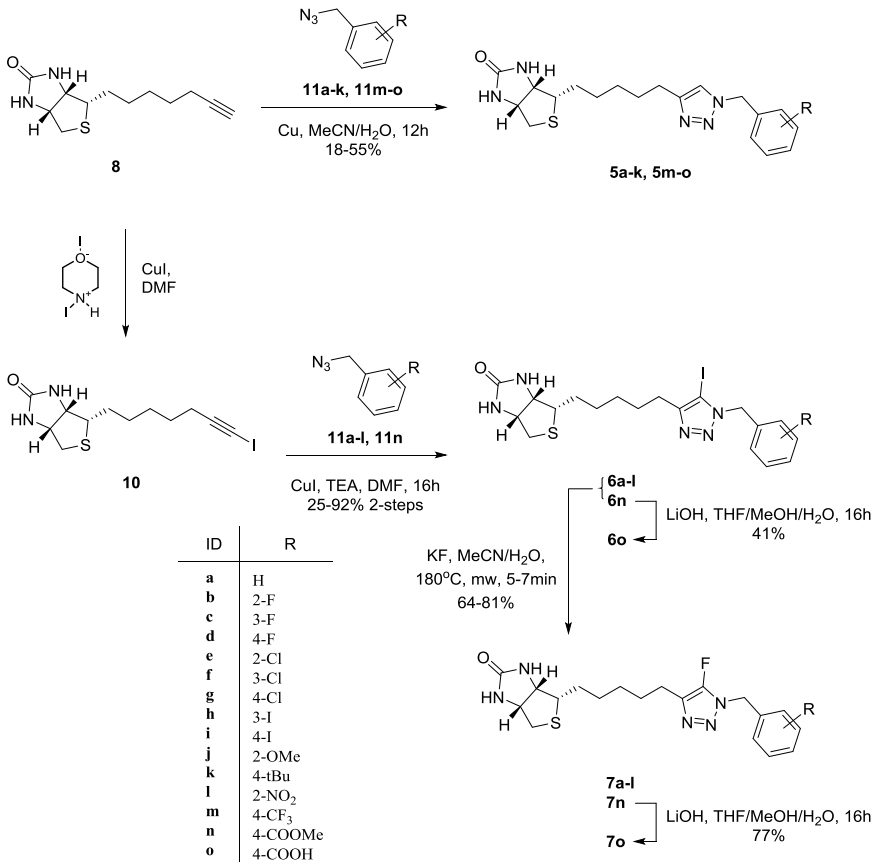

Scheme 3. Synthesis of compounds **5l**, **6l**, **6m** and **7m**.

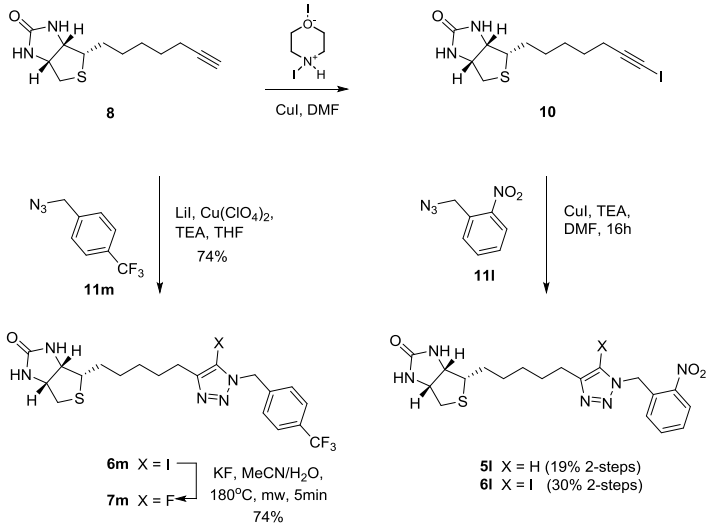

Bioassays of 5a-o, 6a-o, and 7a-o (Figure 6)

To measure the antibacterial and inhibitory potencies of the new analogues, antimicrobial sensitivity assays were performed alongside biochemical assays with derivatives **5a-o, 6a-o, 7a-o**. The anti-bacterial assays performed here employed *S. aureus* RN4220 as our earlier microbiology data revealed this strain to be more sensitive to BPL inhibitors than *S. aureus* ATCC 49775. For example, literature compound **3** was 32-fold more active against RN4220 than ATCC 49775. In this series containing fifteen benzyl substituents, nine iodinated **(6a, b, f-h, j-m)** and six fluorinated compounds **(7a, e, f, h, j, m)** displayed greater whole cell antibacterial bioactivity than their non-halogenated counterparts (**Figure 6A**, **Table 2**). The activity of the compounds was likewise tested in an *in vitro* protein biotinylation assay. A new BPL enzyme assay was employed using a GST tagged biotin domain (GST-*Sa*PC90) as the biotin acceptor protein. Biotinylated protein was captured on white 96-well plates coated with anti-GST antibody and quantitated using Europium-conjugated streptavidin and time resolved fluorescence. This eliminated the need for costly radiolabeled biotin and retains the ability to accurately characterize inhibitory potency with both assays giving comparable K_i values for **3** as a test compound (Supporting information **Table S2**). Concomitant improvements of both *in vitro* inhibition and whole cell bioactivities due to halogenation were observed for five examples in this series, namely **5-7b**, **e**, **h**, **l** and **m,** where the non-halogenated parent compounds were inactive in both the enzyme (K_i > 10 μM) and microbiological assays (MIC > 64 μg/ml) but halogenation greatly improved potency in both cases. For example, iodination of the inactive 4-CF_3 **5m** (K_i > 10 μM, MIC > 64 μg/ml) yielded derivative **6m** (MIC 4 μg/ml), that was one of the most potent of the antibacterials. Similarly, analogues of the 3-I **5h,** iodo-**6h** (K_i 0.38 μM) and fluoro-**7h** (K_i 0.86 μM), were amongst the more potent BPL inhibitors with anti-staphylococci activity (MIC 4 μg/ml) despite a lack of bioactivity for the parent compound. However, like observed with **4a** to **4c,** four examples in this series showed increased whole cell activity without a corresponding decrease in K_i **(5-7f, g, j, k).** This was

highlighted with derivatives of 4-Cl **5g** and 4 t-Bu **5k** where iodination only improved K_i by a modest 2-fold but this translated into a significant improvement in whole cell activity (MIC inactive **5g** *vs* **6g** 16 µg/ml; inactive **5k** *vs* **6k** 8 µg/ml). Likewise, halogenation of 3-Cl **5f** and 2-OMe **5j** did not significantly alter the K_i but greatly improved anti-staphylococci activity over their non-halogenated parents, with iodo **6f** also being one of the most potent antibacterials (MIC 4 µg/ml) in this series. Importantly for this work, no reduced whole cell activity was observed as a result of halogenation. These datum indicated that halogenation of C5 on the triazole linker is a valid approach for improving whole cell antibacterial activity of biotin-triazole BPL inhibitors.

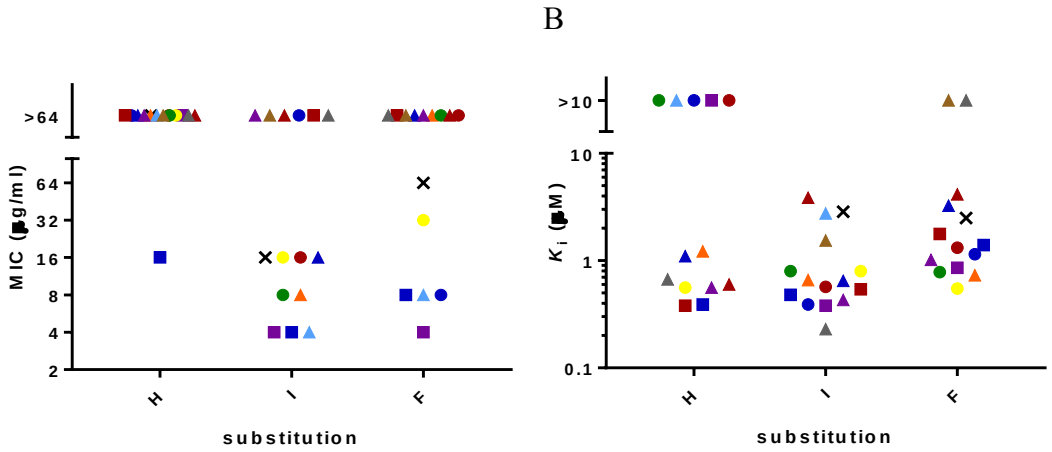

Figure 6. Effect of halogenation at the C5 position on (A) MIC against *S. aureus* RN4220 and (B) K_i against *S. aureus* BPL. × **(H),** ● (2-F), ■ (3-F), ▲ (4-F) ● (2-Cl), ■ (3-Cl) ▲ (4-Cl), ■ (3-I), ▲ (4-I), ● (2-OMe), ▲ (4-tBu), ● (2-NO_2), ▲ (4-CF_3), ▲ (4-COOMe), ▲(4-COOH)

Compound 5c shows alternate binding poses in the *Sa*BPL active site.

The possible modes of binding for the benzyl triazoles in the active site of *Sa*BPL were analyzed using a combination of crystallography and docking studies. To facilitate this, the co-crystal structure of *Sa*BPL in complex with compound **5c**, identified as the most potent unhalogenated BPL inhibitor of the benzyl-biotin-triazoles[13] (Supporting information **Figure S2A**), was determined and served as a template for further docking studies. The crystal data revealed that **5c** induced the same disorder to ordered conformational change in the biotin-binding loop described earlier. However, high B-factors were observed for both main chain and sidechain components of W127- Ser129 indicating high protein flexibility in this region. In addition, the indole ring of the W127 side chain was tilted out of the plane necessary for ATP binding. Well-defined electron densities were observed for the biotinyl and triazole moieties of **5c**, which placed the inhibitor in the biotin-binding pocket as expected. However, the electron density for the appended benzyl group could not be resolved. This observation suggested that the benzyl substitution may adopt more than one binding conformation in the BPL active site. Docking studies were then performed to investigate possible modes of binding for the benzyl group. *In silico* analysis predicted that the benzyl group could occupy one of two adjacent binding pockets; one generated by K187 with BBL residues H126-Ser129, and a second site encompassed by K187, K176, D180 and I321. Further docking analysis with halogenated analogues **6c** and **7c** demonstrated *Sa*BPL could accommodate the substitutions on C5 of the triazole heterocycle, again with two alternative binding poses (Supporting information **Figure S2B-C**). The multiple binding poses adopted by these benzyl triazoles could explain the lack of a clear structure activity relationship from the biochemical and microbiological data.

Table 2. Inhibition and antibacterial data for compounds **5a-o**, **6a-o**, and **7a-o** using *S. aureus* RN4220

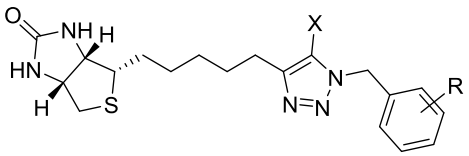

ID	R	X	K_i – *Sa*BPL (μM)	MIC - RN4220 μg/mL (μM)
5a	H	H	N/D	>64 (>172)
6a		I	2.86 ± 0.13	16 (32)
7a		F	2.50 ± 0.13	64 (164)
5b	2-F	H	>10	>64 (>164)
6b		I	0.67 ± 0.09	16 (31)
7b		F	1.32 ± 0.26	> 64 (>157)
5c	3-F	H	0.28 ± 0.02	>64 (>164)
6c		I	0.54 ± 0.08	> 64 (>124)
7c		F	1.77 ± 0.15	> 64 (>157)
5d	4-F	H	0.6 ± 0.1	> 64 (>164)
6d		I	3.86 ± 0.17	> 64 (>124)
7d		F	4.16 ± 0.29	> 64 (>157)
5e	2-Cl	H	>10	>64 9>157)
6e		I	0.39 ± 0.03	> 64 (>120)
7e		F	1.15 ± 0.07	8 (18)
5f	3-Cl	H	0.39 ± 0.04	16 (39)
6f		I	0.48 ± 0.03	4 (7)
7f		F	1.40 ± 0.05	8 (18)
5g	4-Cl	H	1.1 ± 0.07	>64 (>144)
6g		I	0.65 ± 0.06	16 (30)
7g		F	3.26 ± 0.13	> 64 (>150)

5h	3-I	H	>10	>64 (128)
6h		I	0.38 ± 0.01	4 (6)
7h		F	0.86 ± 0.06	4 (7)
5i	4-I	H	0.56 ± 0.06	>64 (>128)
6i		I	0.43 ± 0.07	> 64 (>102)
7i		F	1.02 ± 0.25	> 64 (>124)
5j	2-OMe	H	0.56 ± 0.05	>64 (>159)
6j		I	0.80 ± 0.03	16 (30)
7j		F	0.55 ± 0.04	32 (76)
5k	4-tBu	H	1.22 ± 0.07	>64 (>149)
6k		I	0.66 ± 0.11	8 (14)
7k		F	0.73 ± 0.05	> 64 (>143)
5l	2-NO_2	H	> 10	> 64 (>153)
6l		I	0.80 ± 0.06	8 (14)
7l		F	0.78 ± 0.07	> 64 (>147)
5m	4-CF_3	H	>10	>64 (>145)
6m		I	2.75 ± 0.20	4 (7)
7m		F	N/D	8 (17)
5n	4-COOMe	H	N/D	>64 (>149)
6n		I	1.54 ± 0.08	>64 (>113)
7n		F	>10	>64 (>140)
5o	4-COOH	H	0.67 ± 0.06	>64 (>154)
6o		I	0.23 ± 0.07	>64 (>118)
7o		F	>10	>64 (>148)

Conclusion

The 5-halogenated-1,2,3-triazoles reported here display greater bioactivity against the clinically important bacterial pathogen *S. aureus* than their respective parent compound series. In particular substitution of the hydrogen on C5 of the triazole linker of **4a** with fluorine led to the first example of a biotin triazole inhibitor of *Sa*BPL where an MIC could be quantitated against *S. aureus*. The precise mechanism for the improved whole cell activity observed with the fluorinated derivatives over their non-halogenated parent could be due to several factors. Amongst these are increased permeability across the bacteria membrane, increased resistance to bacterial efflux pumps, increased resistance to metabolic enzymes that degrade the compound, or higher inhibitor occupancy on the BPL target inside the bacterial cell. As the latter is a function of the dissociation rate between the protein target and compound, we employed SPR analysis to probe the kinetics of the biomolecular interaction. The fluorinated analogue exhibited no difference in binding kinetics to its non-halogenated equivalent, so higher occupancy of the target by the halogenated analogue is unlikely. Similarly, it is possible that the addition of a carbon-fluorine bond in the molecule improves upon the metabolic stability inside the bacterial cell, due to the higher energy requirement to hydrolyse a C-F bond compared to its C-H counterpart [32] . However, we suggest this is unlikely to be the causative factor as the triazole heterocycle is already highly resistant to metabolic enzymes[33]. We argue that higher intracellular concentrations of inhibitor as a result of increased uptake and compound accumulation is the most likely mechanism for the observed improvements in whole cell activity.

One mechanism for increased compound uptake would be through increased membrane permeability. In support, fluorination of drugs has been shown to enhance free energy of partitioning and improve passive diffusion across lipid membranes [5]. Future studies will seek to address the mechanisms of biotin-triazole import and efflux in *S. aureus*, as well as other bacterial pathogens. Quantitating cellular uptake of small molecules can be investigated

utilizing technologies sensitive enough to measure intracellular concentrations, such as LC/MS-MS. This has been previously reported for *M. tuberculosis* using BPL inhibitors [34]. This approach would also address compound metabolism in bacteria, confirming the metabolic stability of the biotin triazoles. A recent study probed the physiochemical properties necessary for chemicals to accumulate in Gram-Negative organisms, and defined certain rules that facilitated the conversion of a Gram-positive active compound to one with broad-spectrum activity.[35] The properties that correlated with accumulation were an amphiphilic and rigid structure, with low globularity, and containing a primary amine.[35] Further work is required to determine if the halogenation effect reported here is due to changes in key physiochemical properties. This bears exploring and a broader compound series may serve to address these questions. As the improved whole cell activity appears to be independent of increased inhibitory potency against BPL, halogenation of triazole heterocycles may offer a promising method to improve bioactivity of other compounds utilizing this linker[36-37]. Such a study would offer valuable insight into whether the effect observed here is specific to the biotin-triazole class. As compound entry poses one of the most challenging barriers to antibacterial drug discovery,[2,3,4] a better understanding of the mechanisms of cell entry and efflux in bacteria will drive the development of new antibiotics more than the optimization of affinity for individual targets. Structure activity relationships, as detailed here, comprise an important part of developing such an understanding.

EXPERIMENTAL SECTION

General Materials and Methods.

All reagents were obtained from commercial sources and are of reagent grade or as specified. Solvents were also obtained from commercial sources, except for anhydrous THF and anhydrous DMF that were dried over solvent purifier (PS-Micro, Innovative Technology, USA). Reactions were monitored by TLC using precoated plates (silica gel 60 F254, 250 μm, Merck, Darmstadt, Germany), spots were visualised under ultraviolet light at 254 nm and with either sulphuric acid-vanillin spray, potassium permanganate dip or Hanessian's stain. Column chromatography was performed with silica gel (40-63 μm 60 Å, Davisil, Grace, Germany). HPLC was performed on HP Series 1100 with Phenomenex Gemini C18 5 μM (250 x 4.60 mm) for Analytical. Microwave reactions were performed on a CEM Discovery SP with external IR temperature monitoring. Reactions were stirred for 5 min in a sealed container at ambient temperature, followed by 5 min stirring with increased microwave power until the prescribed temperature was reached. Both power and pressure were kept variable. ^{1}H, ^{13}C, and ^{19}F NMR spectra were recorded on a Varian Inova 500 MHz or a Varian Inova 600 MHz. Chemical shifts are given in ppm (δ) relative to the residue signals, which in the case of DMSO-d_6 were 2.50 ppm for ^{1}H and 39.51 ppm for ^{13}C, $CDCl_3$ were 7.27 ppm for ^{1}H and 77.00 ppm for ^{13}C. High-resolution mass spectra (HRMS) were recorded on an Agilent 6230 time of flight (TOF) liquid chromatography mass spectra (LC/MS) ($\Delta < 5$ ppm).

General Procedure for CuAAC

Copper nano powder (40 mol %) was added to a stirring suspension of biotin acetylene **8**[12] (1.0 equiv) and corresponding azide (1.5 equiv) in CH_3CN:H_2O (2:1) (1 mL per 60 mg of **8**). The reaction was sonicated for 15 min and stirred at room temperature for 17 hours. The reaction mixture was then concentrated under reduced pressure and the residue purified by column chromatography on silica gel. See individual experiments for details.

General Procedure for Synthesis of 5-Iodo-1,2,3-triazoles

To a solution of 1-iodoalkyne **10** (1.0 equiv) and corresponding azide (1.0-1.2 equiv) in dry DMF (1 ml per 10 mg of 1-iodoalkyne) was added CuI (0.05 equiv) and TEA (2.0 equiv) and the mixture was stirred at ambient temperature for 1 day. The mixture was quenched with 10% NH_4OH and extracted with DCM twice. The combined organics were dried over anhydrous sodium sulfate and concentrated under reduced pressure. The resulting residue was purified by column chromatography on silica gel. See individual experiments for details.

General Procedure for Halogen Exchange of 5-Iodo-1,2,3-triazole

To a round-bottomed microwave vial was added 5-iodo-1,2,3-triazole (1.0 equiv) and potassium halide (5.0 equiv). The solids were washed off of the side with acetonitrile (1 ml per 50 mg of triazole) and then de-ionised water (1 ml per 50 mg of triazole). The vial was placed into the microwave reactor set at a pressure of 200 psi and heated at 180 °C for 5-10 min based on ^1H NMR. After the vial was cooled to room temperature, the mixture was diluted with EtOAc and the organic layer was extracted with a Pasture pipette. The resulting aqueous layer was extracted three additional times and the combined organics were dried over anhydrous sodium sulfate and concentrated under reduced pressure. The residue was purified by column chromatography on silica gel. See individual experiments for details.

General Procedure for Synthesis of Benzyl Azides

A solution of the benzyl halide (1 equiv) and sodium azide (1.3 equiv) in DMF (1 mL per 50mg of benzyl halide) was stirred at ambient temperature for 5 hours. The reaction mixture was diluted with ether and wash with water three times. The organic layer was dried over anhydrous sodium sulfate and concentrated under reduced pressure. See individual experiments for details.

General Procedure for Hydrolysis of Ester

To a mixture of ester (1.0 equiv) in THF:MeOH:H_2O (3:1:1) (1 mL per 10 mg of ester) was added LiOH (2.2 equiv) and the mixture was stirred for 17 hours. The resulting mixture was acidified with 1 M HCl to pH = 4. The mixture was diluted with DCM:MeOH (9:1) and washed with 0.5M HCl, water, and brine. The organic layer was dried over anhydrous sodium sulfate and concentrated under reduced pressure. The residue was purified by column chromatography on silica gel. See individual experiments for details.

Recombinant protein production

The cloning and purification of recombinant BPL from *Staphylococcus aureus* and *Homo sapiens* have been previously described.[15,38]

In vitro **biotinylation assays**

^{3}H biotin assay

Quantification of BPL catalyzed ^{3}H-biotin incorporation into the biotin domain substrate was performed as previously described.[12, 16, 39] A reaction mixture was prepared containing 50 mM Tris HCl pH 8.0, 3 mM ATP, 4.94 μM biotin, 0.06 μM ^{3}H-biotin, 5.5 mM $MgCl_2$, 100 mM KCl, 0.1 μM DTT and 10 μM biotin domain of *S. aureus* pyruvate carboxylase. To determine inhibitory activity, BPL activity was measured in the presence of varying concentrations of compound. All compounds were dissolved in DMSO and then diluted into the reaction buffer to give a final concentration of 4% DMSO. BPL reaction was initiated by the addition of enzyme to give final concentrations of 6.25 nM for *Sa*BPL and 140 nM for *Hs*BPL. After 10 minutes at 37 ºC, 90 μL of stopping buffer (110 mM EDTA and 50 mM Tris HCl pH 8.0) was added to terminate the reaction and a 100 μL aliquot of the reaction mixture was added to the wells of 96-well HTS multiscreen plate containing an Immobilon-P® (Merck Millipore) membrane that had been pre-treated with 50 μL of 70% ethanol. 400 μL of MilliQ-H_2O and followed by 200 μL of TBS. Quantitation of protein-bound radiolabelled biotin was determined by liquid scintillation counting. The IC_{50} value of each compound was determined from a dose-response curve by varying the concentration of inhibitor under the same enzyme concentration. The data was analysed with GraphPad prism (version 6) using a non-linear fit of $\log_{10}$ [inhibitor] vs. normalised response. The K_i, the absolute inhibition constant for a compound was determined using Eq 1:[29]

Eq 1:

$$K_i = \frac{IC_{50}}{1 + \frac{[S]}{K_M}}$$

Where [S] is the substrate concentration ([biotin] = 5 μM) and K_M is the affinity of the enzyme for biotin (*S.aureus* BPL = 1 μM, (ref), and *H. sapiens* BPL = 1 μM (ref)).

Europium-streptavidin based enzyme assay

A 96-well assay using Europium labelled streptavidin and time-resolved fluorescence was developed to measure BPL activity. An *in vitro* biotinylation reaction was performed for at least 10 minutes at 37 °C in a 20 µL reaction mix containing 50 mM tris pH 8.0, 3 mM ATP, 5.5 mM $MgCl_2$, 25 µM GST-SaPC90, 0.1 µM DTT, 5 µM biotin and purified BPL (*Sa*BPL 6 nM) .BPL catalysed reactions were stopped with the addition of 80 µL stopping buffer (50 mM Tris pH 8.0, 110 mM EDTA) and 3 x 20 µL aliquots were added to the well of a white lumitrac-600 96-well plate that had been previously coated by overnight incubation at 4 °C with an anti-GST antibody (50 µL per well) at 1:40000 dilution, followed by blocking for 2 hours (200 µL per well) with 1% BSA in TBS at 37 °C and incubated at 37 °C for 1 hour. The plate was then washed 5 times (200 µL per well) with TBS containing 0.1% Tween-20. Europium labelled streptavidin was diluted to 0.1 µg/mL in TBS containing 0.1% Tween-20. The streptavidin probe (50 µL per well) was incubated for 30 minutes at 37 °C followed by washing 5 times in TBS 0.1% Tween-20 followed by another 5 washes in sterile water. Enhancement solution (Perkin Elmer) (50 µL) was added per well and incubated for 10 minutes before reading the plate using time-resolved fluorescence using 340 nm excitation and 612 nm emission filters with a Perkin Elmer® Victor X5 multilabel reader. Data was analysed as described for ^3H biotinylation assay.

Surface Plasmon Resonance

SPR was performed using a Biacore™ S200 instrument (GE healthcare). *S. aureus* BPL was immobilised on a CM5 sensor chip by standard amine coupling chemistry. The carboxymethyl groups on the chip were activated by the addition *N*-ethyl-*N*′-(3-diethylamino-propyl) carbodiimide and *N*-hydroxysuccinimide. BPL (120 μg/mL) in 10 mM sodium acetate buffer (pH 5.8) was coupled onto the surface, and 50 mM Tris pH 8.0 was injected to block any unreacted sites. Typically, 7,000 resonance units of BPL were immobilised on the sensor chip. One channel was left blank which was subtracted from the sample channel to allow analysis methods to distinguish between actual and non-specific binding. Experiments were conducted at 25 ºC with a running buffer containing 10 mM HEPES pH 7.4, 150 mM NaCl, 0.005% surfactant p20 and 5% (v/v) DMSO. For compounds that were poorly water soluble, samples were initially dissolved in DMSO and diluted in running buffer so that the final concentration of DMSO was 5%. To correct for variations in DMSO concentration during the preparation of these compounds, a solvent correction curve was included in the analysis by preparing a series of test solutions between 4.5% and 5.8% DMSO. Binding experiments were performed by injecting the analyte solutions into the instrument across the sensor surface of all flow cells at a flow rate of 30 μL/min with a contact time of 120 seconds followed by a dissociation time of 300 seconds. Zero concentration samples were used as blanks. The time-dependent binding curves of all flow cells were monitored simultaneously. The results of compounds **4a-d** showed fast on and off rates outside the range of kinetic quantification, so K_D values were determined by transforming time-dependent binding curves into an affinity-steady state 1:1 model using Biacore™ S200 evaluation software (GE healthcare).

Antibacterial Activity Evaluation

Antibacterial activity was determined by a microdilution broth method as recommended by the CLSI (Clinical and Laboratory Standards Institute, Document M07-A8, 2009, Wayne, Pa.) using cation-adjusted Mueller-Hinton broth (trek Diagnostics Systems, U.K.). Compounds were dissolved in DMSO. Serial two-fold dilutions of each compound were made using DMSO as the diluent. Trays were inoculated with 5 x 10^4 CFU of each strain in a volume of 100 µL (final concentration of DMSO was 3.2 % (v/v)), and incubated at 35 ºC for 16-20 hours. Growth of the bacterium was quantified by measuring the absorbance at 620 nm.

***Sa*BPL-4c X-ray crystallography methodology**

Crystals used for micoseeding were prepared via the hanging drop method at 4 °C, with 500 µL of reservoir solution (50 mM sodium HEPES pH 7.5, 14% (*w/v*) PEG 3350, 1% (*w/v*) tryptone) and a hanging drop comprised of 2 µL protein solution (5 mg/mL *Sa*BPL-H_6, 1.2 mM BPL199, 6.7% DMSO, 50 mM Tris-HCl pH 7.5, 50 mM NaCl, 1 mM DTT, 5% (*v/v*) glycerol) and 3 µL reservoir solution. To prepare *Sa*BPL-**4c** crystals, 1 mg/mL apo *Sa*BPL-H_6, 790 µM **4c**, 4% (*v/v*) DMSO, 50 mM Tris-HCl pH 7.5, 50 mM NaCl, 1 mM DTT and 5% (*v/v*) glycerol were incubated overnight at 4 °C. The incubation was filtered through a 0.2 µm Nanosep MF centrifugal device (Pall Corp.) and protein was concentrated to 5 mg/mL. Crystals were prepared at 4 °C using the hanging drop vapor diffusion method, with a 500 µL reservoir comprised of 12% (*w/v*) PEG 8000, 0.1 M Tris-HCl pH 7.5 and 10% (*v/v*) glycerol.[12] To prepare the hanging drop, 0.8 µL of reservoir solution was mixed with 0.2 µL microseeds of *Sa*BPL-H_6 in complex with a known inhibitor and 1 µL of protein solution. A single crystal was looped and cryoprotected with reservoir solution containing saturated sucrose, prior to flash freezing with liquid nitrogen. X-ray diffraction data were collected at the Australian Synchrotron's MX2 Micro Crystallography beamline, using an ADSC Quantum 315r Detector. The diffraction data were integrated using XDS[40] and the intensities were merged and scaled using Aimless[41] in the CCP4 program suite[42]. MOLREP[43] was used

to perform molecular replacement, using a single protein chain from PDB 3V7R[12] as a search model. PDB and cif files for **4c** were generated using eLBOW[44] in PHENIX[28]. Refinement was performed in PHENIX[28] and REFMAC[45] and manual model building was undertaken in COOT[46]. Statistics for the data and refinement are reported in Supporting Information **Table S3**.

Assay of cytotoxicity

Mammalian HepG2 cells were suspended in Dulbecco-modified Eagle's medium containing 10% fetal bovine serum, and then seeded in 96-well tissue culture plates at either 5 000, 10 000 or 20 000 cells per well. After 24 hours, cells were treated with varying concentrations of the test compound such that the DMSO concentration was consistent at 2 % (v/v) in all wells. After treatment for 24 or 48 hours, WST-1 cell proliferation reagent (Roche) was added to each well and incubated for 0.5 hours at 37 ºC. The WST-1 assay quantitatively monitors the metabolic activity of cells by measuring the hydrolysis of the WST-1 reagent, the products of which are detectable at absorbance 450 nm.

Docking studies

Docking experiments were performed using ICM software version 3.8-5 (Molsoft L.L.C., San Diego, CA, USA). Proteins for docking were retrieved from RCSB protein data bank: 3V7S[12] and *Sa*BPL-**4c**. Then formal charges were assigned, protonation states of histidines were adjusted, and hydrogens, histidine, glutamine, and aspargine were optimized using the protein preparation procedure implemented in ICM.[47] The original bound ligand and all water molecules were removed from the binding site before docking. The binding site was defined as the cavity delimited by residues with at least one non-hydrogen atom within a 4.0 Å cutoff radius from the ligand **4a** or **4c**. The pocket was represented by 0.5 Å grid maps accounting for hydrogen bonding, hydrophobic, van der Waals, and electrostatic interactions. The molecules were flexibly docked into the rigid binding site and scored based on the ICM scoring function.

Author Contributions

The manuscript was written through contributions of all authors. All authors have given approval to the final version of the manuscript. ‡These authors contributed equally.

ABBREVIATIONS

*Sa*BPL, *Staphylococcus aureus* biotin protein ligase; *Sa*BPL-H_6, *Staphylococcus aureus* biotin protein ligase containing 6 histidine tag; BPL, biotin protein ligase; BBL, biotin binding loop; SPR, surface plasmon resonance, *Sa*PC90, 90 amino acid biotin-acceptor domain from pyruvate carboxylase; $K_{D,}$ equilibrium binding constant; TBS, tris buffered saline; HEPES, 4-(2-hydroxyethyl)-1-piperazineethanesulfonic acid

REFERENCES

1. Butler, M. S.; Blaskovich, M. A.; Cooper, M. A., Antibiotics in the clinical pipeline at the end of 2015. *J Antibiot (Tokyo)* **2016**, 1-22. DOI: 10.1038/ja.2016.72.

2. Payne, D. J.; Gwynn, M. N.; Holmes, D. J.; Pompliano, D. L., Drugs for bad bugs: confronting the challenges of antibacterial discovery. *Nat Rev Drug Discov* **2007,** *6* (1), 29-40. DOI: 10.1038/nrd2201.

3. Tommasi, R.; Brown, D. G.; Walkup, G. K.; Manchester, J. I.; Miller, A. A., ESKAPEing the labyrinth of antibacterial discovery. *Nat Rev Drug Discov* **2015,** *14* (8), 529-42. DOI: 10.1038/nrd4572.

4. Brown, E. D.; Wright, G. D., Antibacterial drug discovery in the resistance era. *Nature* **2016,** *529* (7586), 336-343.

5. Gerebtzoff, G.; Li-Blatter, X.; Fischer, H.; Frentzel, A.; Seelig, A., Halogenation of drugs enhances membrane binding and permeation. *Chembiochem* **2004,** *5* (5), 676-84. DOI: 10.1002/cbic.200400017.

6. Domagala, J. M., Structure-activity and structure-side-effect relationships for the quinolone antibacterials. *J Antimicrob Chemother* **1994,** *33* (4), 685-706.

7. Brighty, K. E.; Gootz, T. D., The chemistry and biological profile of trovafloxacin. *J Antimicrob Chemother* **1997,** *39 Suppl B*, 1-14.

8. Garrison, A. T.; Abouelhassan, Y.; Norwood, V. M. t.; Kallifidas, D.; Bai, F.; Nguyen, M. T.; Rolfe, M.; Burch, G. M.; Jin, S.; Luesch, H.; Huigens, R. W., 3rd, Structure-Activity Relationships of a Diverse Class of Halogenated Phenazines That Targets Persistent, Antibiotic-Tolerant Bacterial Biofilms and Mycobacterium tuberculosis. *J Med Chem* **2016,** *59* (8), 3808-25. DOI: 10.1021/acs.jmedchem.5b02004.

9. Basak, A.; Abouelhassan, Y.; Norwood, V. M. t.; Bai, F.; Nguyen, M. T.; Jin, S.; Huigens, R. W., 3rd, Synthetically Tuning the 2-Position of Halogenated Quinolines: Optimizing Antibacterial and Biofilm Eradication Activities via Alkylation and Reductive Amination Pathways. *Chemistry* **2016,** *22* (27), 9181-9. DOI: 10.1002/chem.201600926.

10. Hagmann, W. K., The many roles for fluorine in medicinal chemistry. *J Med Chem* **2008,** *51* (15), 4359-69. DOI: 10.1021/jm800219f.

11. Purser, S.; Moore, P. R.; Swallow, S.; Gouverneur, V., Fluorine in medicinal chemistry. *Chem Soc Rev* **2008,** *37* (2), 320-30. DOI: 10.1039/b610213c.

12. da Costa, T. P. S.; Tieu, W.; Yap, M. Y.; Pendini, N. R.; Polyak, S. W.; Pedersen, D. S.; Morona, R.; Turnidge, J. D.; Wallace, J. C.; Wilce, M. C. J.; Booker, G. W.; Abell, A. D., Selective inhibition of Biotin Protein Ligase from Staphylococcus aureus. *Journal of Biological Chemistry* **2012,** *287* (21), 17823-17832. DOI: 10.1074/jbc.M112.356576.

13. Feng, J.; Paparella, A. S.; Tieu, W.; Heim, D.; Clark, S.; Hayes, A.; Booker, G. W.; Polyak, S. W.; Abell, A. D., New Series of BPL Inhibitors To Probe the Ribose-Binding Pocket of Staphylococcus aureus Biotin Protein Ligase. *ACS medicinal chemistry letters* **2016,** *7* (12), 1068-1072. DOI: 10.1021/acsmedchemlett.6b00248.

14. Paparella, A. S.; Soares da Costa, T. P.; Yap, M. Y.; Tieu, W.; Wilce, M. C.; Booker, G. W.; Abell, A. D.; Polyak, S. W., Structure guided design of biotin protein ligase inhibitors for antibiotic discovery. *Curr Top Med Chem* **2014,** *14* (1), 4-20.

15. Pendini, N. R.; Polyak, S. W.; Booker, G. W.; Wallace, J. C.; Wilce, M. C., Purification, crystallization and preliminary crystallographic analysis of biotin protein ligase from Staphylococcus aureus. *Acta crystallographica. Section F, Structural biology and crystallization communications* **2008,** *64* (Pt 6), 520-3. DOI: 10.1107/S1744309108012244.

16. Soares da Costa, T. P.; Tieu, W.; Yap, M. Y.; Zvarec, O.; Bell, J. M.; Turnidge, J. D.; Wallace, J. C.; Booker, G. W.; Wilce, M. C.; Abell, A. D.; Polyak, S. W., Biotin analogues with antibacterial activity are potent inhibitors of biotin protein ligase. *ACS medicinal chemistry letters* **2012,** *3* (6), 509-14. DOI: 10.1021/ml300106p.

17. Tieu, W.; da Costa, T. P. S.; Yap, M. Y.; Keeling, K. L.; Wilce, M. C. J.; Wallace, J. C.; Booker, G. W.; Polyak, S. W.; Abell, A. D., Optimising in situ click chemistry: the screening and identification of biotin protein ligase inhibitors. *Chem Sci* **2013,** *4* (9), 3533-3537. DOI: 10.1039/c3sc51127h.

18. Tieu, W.; Jarrad, A. M.; Paparella, A. S.; Keeling, K. A.; Soares da Costa, T. P.; Wallace, J. C.; Booker, G. W.; Polyak, S. W.; Abell, A. D., Heterocyclic acyl-phosphate bioisostere-based inhibitors of Staphylococcus aureus biotin protein ligase. *Bioorg Med Chem Lett* **2014,** *24* (19), 4689-93. DOI: 10.1016/j.bmcl.2014.08.030.

19. Tieu, W.; Polyak, S. W.; Paparella, A. S.; Yap, M. Y.; Soares da Costa, T. P.; Ng, B.; Wang, G.; Lumb, R.; Bell, J. M.; Turnidge, J. D.; Wilce, M. C.; Booker, G. W.; Abell, A. D., Improved Synthesis of Biotinol-5'-AMP: Implications for Antibacterial Discovery. *ACS medicinal chemistry letters* **2015,** *6* (2), 216-20. DOI: 10.1021/ml500475n.

20. Bockman, M. R.; Kalinda, A. S.; Petrelli, R.; De la Mora-Rey, T.; Tiwari, D.; Liu, F.; Dawadi, S.; Nandakumar, M.; Rhee, K. Y.; Schnappinger, D.; Finzel, B. C.; Aldrich, C. C., Targeting Mycobacterium tuberculosis Biotin Protein Ligase (MtBPL) with Nucleoside-Based Bisubstrate Adenylation Inhibitors. *J Med Chem* **2015,** *58* (18), 7349-69. DOI: 10.1021/acs.jmedchem.5b00719.

21. Duckworth, B. P.; Geders, T. W.; Tiwari, D.; Boshoff, H. I.; Sibbald, P. A.; Barry, C. E.; Schnappinger, D.; Finzel, B. C.; Aldrich, C. C., Bisubstrate Adenylation Inhibitors of Biotin Protein Ligase from Mycobacterium tuberculosis. *Chem Biol* **2011,** *18* (11), 1432-1441. DOI: 10.1016/j.chembiol.2011.08.013.

22. Brown, P. H.; Beckett, D., Use of binding enthalpy to drive an allosteric transition. *Biochemistry* **2005,** *44* (8), 3112-21. DOI: 10.1021/bi047792k.

23. Xu, Y.; Beckett, D., Kinetics of biotinyl-5'-adenylate synthesis catalyzed by the Escherichia coli repressor of biotin biosynthesis and the stability of the enzyme-product complex. *Biochemistry* **1994,** *33* (23), 7354-60.

24. Xu, Y.; Beckett, D., Biotinyl-5'-adenylate synthesis catalyzed by Escherichia coli repressor of biotin biosynthesis. *Methods Enzymol* **1997,** *279*, 405-21.

25. Hein, J. E.; Tripp, J. C.; Krasnova, L. B.; Sharpless, K. B.; Fokin, V. V., Copper(I)-catalyzed cycloaddition of organic azides and 1-iodoalkynes. *Angewandte Chemie* **2009,** *48* (43), 8018-21. DOI: 10.1002/anie.200903558.

26. Worrell, B. T.; Hein, J. E.; Fokin, V. V., Halogen Exchange (Halex) Reaction of 5-Iodo-1,2,3-triazoles: Synthesis and Applications of 5-Fluorotriazoles. *Angew Chem Int Edit* **2012,** *51* (47), 11791-11794. DOI: 10.1002/anie.201204979.

27. Soares da Costa, T. P.; Tieu, W.; Yap, M. Y.; Pendini, N. R.; Polyak, S. W.; Sejer Pedersen, D.; Morona, R.; Turnidge, J. D.; Wallace, J. C.; Wilce, M. C.; Booker, G. W.; Abell, A. D., Selective inhibition of biotin protein ligase from Staphylococcus aureus. *J Biol Chem* **2012,** *287* (21), 17823-32. DOI: 10.1074/jbc.M112.356576.

28. Adams, P. D.; Afonine, P. V.; Bunkoczi, G.; Chen, V. B.; Davis, I. W.; Echols, N.; Headd, J. J.; Hung, L. W.; Kapral, G. J.; Grosse-Kunstleve, R. W.; McCoy, A. J.; Moriarty, N. W.; Oeffner, R.; Read, R. J.; Richardson, D. C.; Richardson, J. S.; Terwilliger, T. C.; Zwart, P. H., PHENIX: a comprehensive Python-based system for macromolecular structure solution. *Acta Crystallogr D Biol Crystallogr* **2010,** *66* (Pt 2), 213-21. DOI: 10.1107/S0907444909052925.

29. Cheng, Y.; Prusoff, W. H., Relationship between the inhibition constant (K1) and the concentration of inhibitor which causes 50 per cent inhibition (I50) of an enzymatic reaction. *Biochem Pharmacol* **1973,** *22* (23), 3099-108.

30. Pendini, N. R.; Yap, M. Y.; Polyak, S. W.; Cowieson, N. P.; Abell, A.; Booker, G. W.; Wallace, J. C.; Wilce, J. A.; Wilce, M. C., Structural characterization of Staphylococcus aureus biotin protein ligase and interaction partners: an antibiotic target. *Protein Science* **2013,** *22* (6), 762-773.

31. Barsoum, D. N.; Okashah, N.; Zhang, X.; Zhu, L., Mechanism of Copper(I)-Catalyzed 5-Iodo-1,2,3-triazole Formation from Azide and Terminal Alkyne. *J Org Chem* **2015,** *80* (19), 9542-51. DOI: 10.1021/acs.joc.5b01536.

32. Hernandes, M. Z.; Cavalcanti, S. M.; Moreira, D. R.; de Azevedo Junior, W. F.; Leite, A. C., Halogen atoms in the modern medicinal chemistry: hints for the drug design. *Curr Drug Targets* **2010,** *11* (3), 303-14.

33. Germeroth, A. I.; Hanna, J. R.; Karim, R.; Kundel, F.; Lowther, J.; Neate, P. G.; Blackburn, E. A.; Wear, M. A.; Campopiano, D. J.; Hulme, A. N., Triazole biotin: a tight-binding biotinidase-resistant conjugate. *Org Biomol Chem* **2013,** *11* (44), 7700-4. DOI: 10.1039/c3ob41837e.

34. Bockman, M. R.; Kalinda, A. S.; Petrelli, R.; De la Mora-Rey, T.; Tiwari, D.; Liu, F.; Dawadi, S.; Nandakumar, M.; Rhee, K. Y.; Schnappinger, D.; Finzel, B. C.; Aldrich, C. C., Targeting Mycobacterium tuberculosis Biotin Protein Ligase (MtBPL) with Nucleoside-Based Bisubstrate Adenylation Inhibitors. *J Med Chem* **2015,** *58* (18), 7349-7369. DOI: 10.1021/acs.jmedchem.5b00719.

35. Richter, M. F.; Drown, B. S.; Riley, A. P.; Garcia, A.; Shirai, T.; Svec, R. L.; Hergenrother, P. J., Predictive compound accumulation rules yield a broad-spectrum antibiotic. *Nature* **2017**.

36. Holla, B. S.; Mahalinga, M.; Karthikeyan, M. S.; Poojary, B.; Akberali, P. M.; Kumari, N. S., Synthesis, characterization and antimicrobial activity of some substituted 1, 2, 3-triazoles. *Eur J Med Chem* **2005,** *40* (11), 1173-1178.

37. Aufort, M.; Herscovici, J.; Bouhours, P.; Moreau, N.; Girard, C., Synthesis and antibiotic activity of a small molecules library of 1,2,3-triazole derivatives. *Bioorg Med Chem Lett* **2008,** *18* (3), 1195-8. DOI: 10.1016/j.bmcl.2007.11.111.

38. Mayende, L.; Swift, R. D.; Bailey, L. M.; Soares da Costa, T. P.; Wallace, J. C.; Booker, G. W.; Polyak, S. W., A novel molecular mechanism to explain biotin-unresponsive holocarboxylase synthetase deficiency. *J Mol Med (Berl)* **2012,** *90* (1), 81-8. DOI: 10.1007/s00109-011-0811-x.

39. Chapman-Smith, A.; Morris, T. W.; Wallace, J. C.; Cronan, J. E., Jr., Molecular recognition in a post-translational modification of exceptional specificity. Mutants of the biotinylated domain of acetyl-CoA carboxylase defective in recognition by biotin protein ligase. *J Biol Chem* **1999,** *274* (3), 1449-57.

40. Kabsch, W., Xds. *Acta Crystallogr D Biol Crystallogr* **2010,** *66* (Pt 2), 125-32. DOI: 10.1107/S0907444909047337.

41. Evans, P. R.; Murshudov, G. N., How good are my data and what is the resolution? *Acta Crystallogr D Biol Crystallogr* **2013,** *69* (Pt 7), 1204-14. DOI: 10.1107/S0907444913000061.

42. Collaborative Computational Project, N., The CCP4 suite: programs for protein crystallography. *Acta Crystallogr D Biol Crystallogr* **1994,** *50* (Pt 5), 760-3. DOI: 10.1107/S0907444994003112.

43. Vagin, A.; Teplyakov, A., MOLREP: an Automated Program for Molecular Replacement. *J Appl Crystallogr* **1997,** *30* (6), 1022-1025. DOI: 10.1107/s0021889897006766.

44. Moriarty, N. W.; Grosse-Kunstleve, R. W.; Adams, P. D., electronic Ligand Builder and Optimization Workbench (eLBOW): a tool for ligand coordinate and restraint generation. *Acta Crystallogr D Biol Crystallogr* **2009,** *65* (Pt 10), 1074-80. DOI: 10.1107/S0907444909029436.

45. Murshudov, G. N.; Vagin, A. A.; Dodson, E. J., Refinement of macromolecular structures by the maximum-likelihood method. *Acta Crystallogr D Biol Crystallogr* **1997,** *53* (Pt 3), 240-55. DOI: 10.1107/S0907444996012255.

46. Emsley, P.; Lohkamp, B.; Scott, W. G.; Cowtan, K., Features and development of Coot. *Acta Crystallogr D Biol Crystallogr* **2010,** *66* (Pt 4), 486-501. DOI: 10.1107/S0907444910007493.

47. Neves, M. A.; Totrov, M.; Abagyan, R., Docking and scoring with ICM: the benchmarking results and strategies for improvement. *J Comput Aided Mol Des* **2012,** *26* (6), 675-86. DOI: 10.1007/s10822-012-9547-0.

SUPPORTING INFORMATION

Halogenation of biotin protein ligase inhibitors improve whole cell activity against *Staphylococcus aureus*

Ashleigh S. Paparella, [†‡] *Kwang Jun Lee,* [‡ ‡] *Andrew J. Hayes,* [†‡] *Jiage Feng,* [‡] *David Heim,* [†] *Zikai Feng,* [†] *Danielle Cini,* [§] *Grant W. Booker,* [†] *Matthew C. J. Wilce,* [§] *Steven W. Polyak,* [†] *and Andrew D. Abell* [‡ #]

[‡]Department of Chemistry, University of Adelaide, Adelaide, South Australia 5005, Australia

[†] Department of Molecular and Cellular Biology, University of Adelaide, South Australia 5005, Australia

[§]School of Biomedical Science, Monash University, Victoria 3800, Australia

[#]Centre for Nanoscale BioPhotonics (CNBP), University of Adelaide, Adelaide, South Australia 5005, Australia

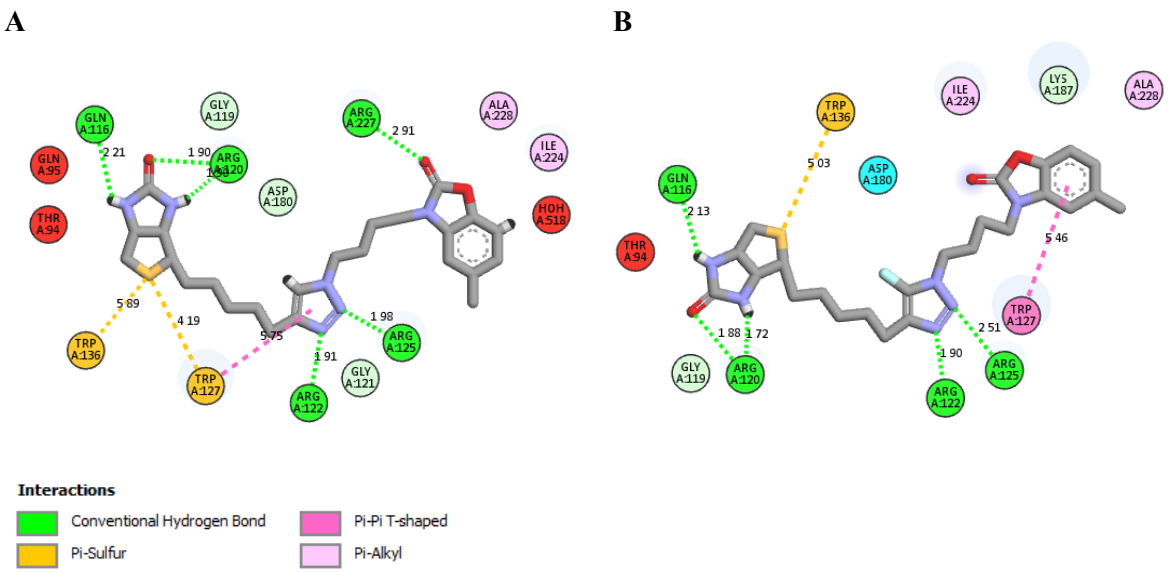

Figure S1. (A) 2D interaction diagram of **4a** and *Sa*BPL. (B) 2D interaction diagram of **4c** and *Sa*BPL. 2D interaction diagrams were viewed using Discovery Studio Visualizer.[1]

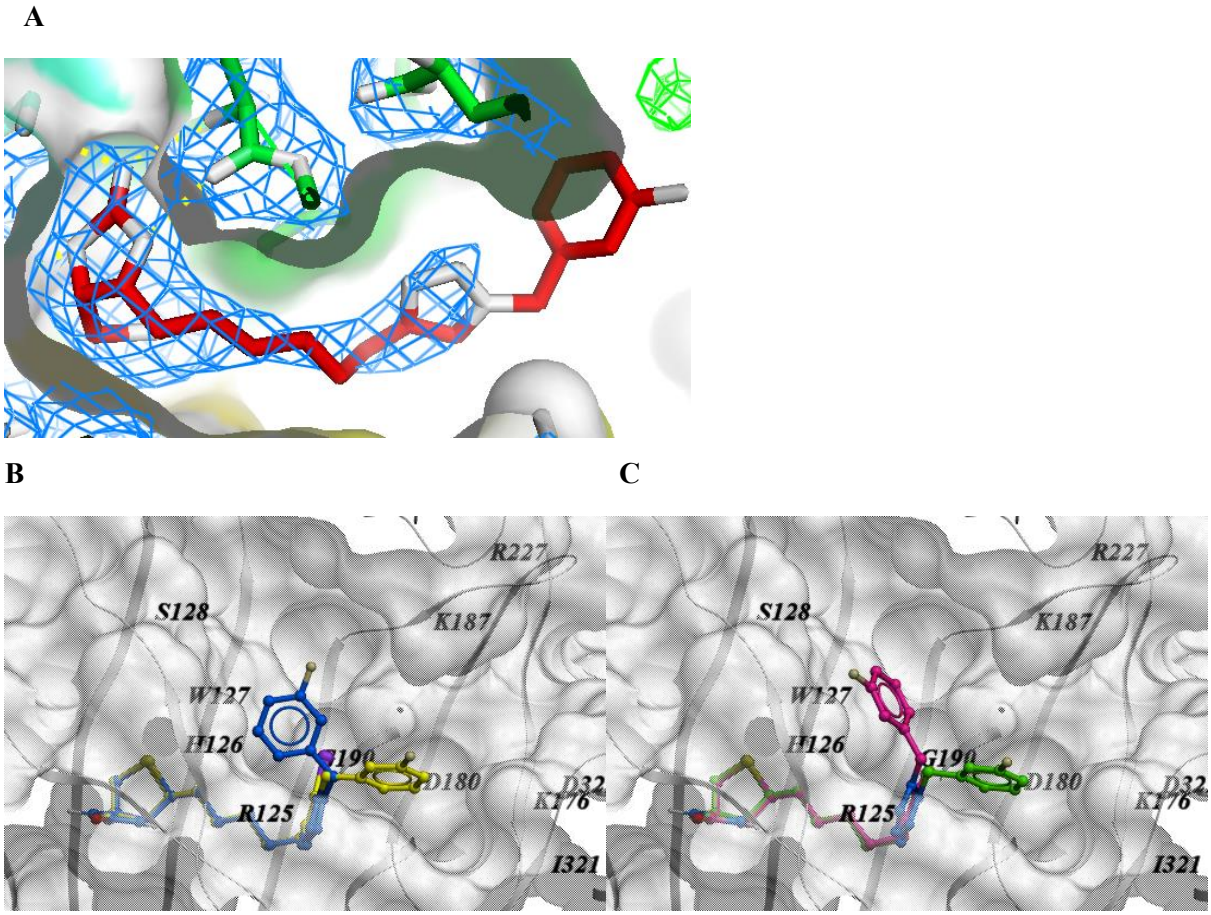

Figure S2. (A) X-ray crystallography of compound **5c** bound to *Sa*BPL revealed density surrounding the biotinyl moiety and triazole ring but lacking for the benzyl ring. (B-C) Docking results of **6c-7c** in the binding pocket**.** (B) The top-scoring conformation (yellow) and the second top-scoring conformation (blue) of **6c**. (C) The top-scoring conformation (magenta) and the second top-scoring conformation (green) of **7c.** The docking studies showed that benzyl ring would be positioned in the ribose binding site or the outer open mouth site.

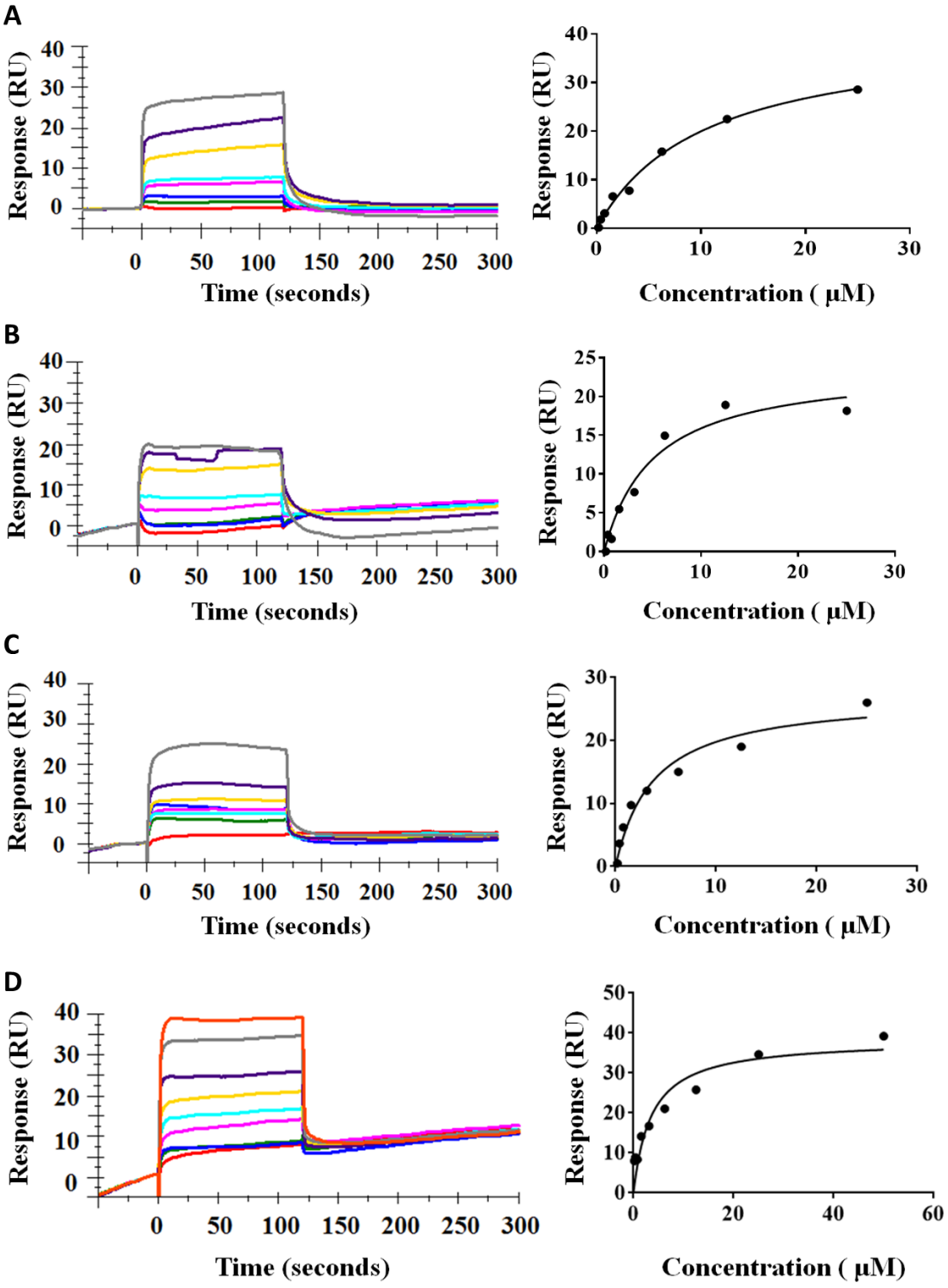

Figure S3. SPR sensograms (left) and concentration vs response plots (right) of compounds **4a-d** binding to *Sa*BPL. (A) SPR sensogram and concentration vs response plot of **4a** binding to *Sa*BPL. (B) SPR sensogram and concentration vs response plot of **4b** binding to *Sa*BPL. (C) SPR sensogram and concentration vs response plot of **4c** binding to *Sa*BPL. (D) SPR sensogram and concentration vs response plot of **4d** binding to *Sa*BPL. Concentrations of compounds **4a-d** used were: 0.2 µM (red), 0.4 µM (green), 0.8 µM (blue), 1.6 µM (magenta), 3.1 µM (cyan), 6.3 µM (yellow), 12.5 µM (purple), 25 µM (grey) and 50 µM (orange).

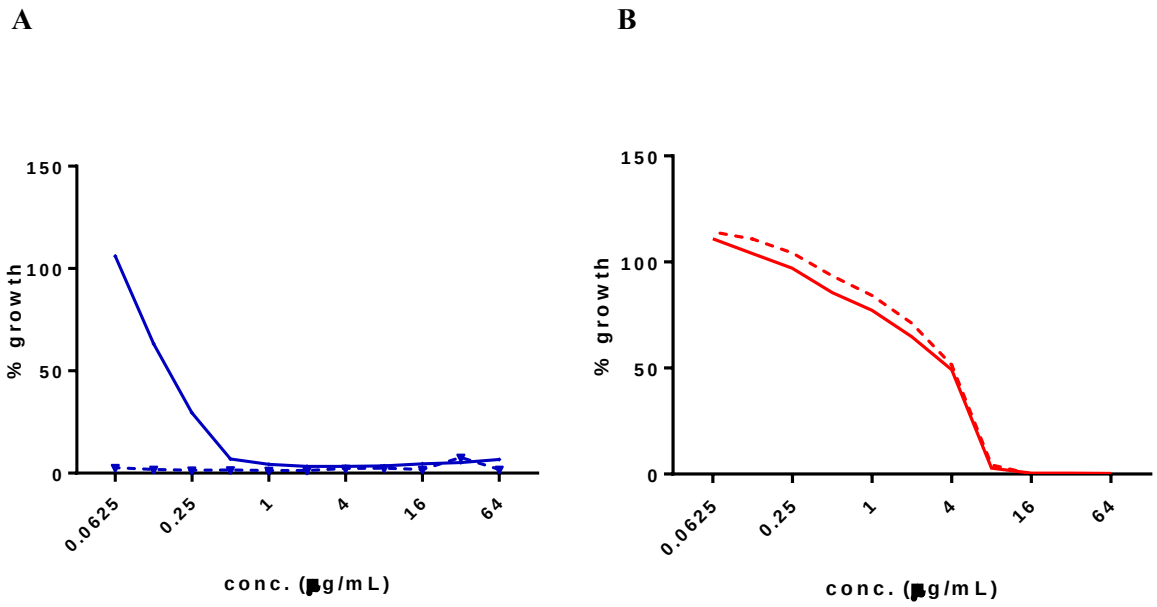

Figure S4. Mechanism of action studies. *S. aureus* RN4220 + pCN51-NcoI control (dashed line) and pCN51-BPL overexpression (solid line) vectors susceptibility to (A) literature BPL inhibitor biotinol-5′-AMP and (B) non BPL targeting antibiotic amoxicillin. Assays were performed in triplicate and normalised to no compound control.

Table S1. Comparison of binding pockets. The volume and area of binding pocket of **4c**-*Sa*BPL was increased in order to accommodate 5-fluoro triazol **4c**. The icmPocketFinder macro was used to measure the properties of the binding site at *Sa*PBL.

ID	Volume (Å^3)	Area(Å^2)	Hydrophobicity	Buriedness
*Sa*BPL-**4a** (PBD 3V7S)	679.9	635.2	0.5932	0.8844
*Sa*BPL-**4c**	800.6	706.9	0.5645	0.8758

Table S2. Comparison of K_i values as determined by enzyme assay with radiolabelled biotin compared to assay utilising GST fusion of SaPC90 for antibody capture and detection with Eu-streptavidin conjugate.

Compound	$K_{i\ radiolabelled\ biotin}$ (μM)	$K_{i\ GST\text{-}fusion}$ (μM)
3	0.016 ± 0.01	0.004 ± 0.001

Table S3. Data collection and Refinement Statistics for *Sa*BPL in complex with inhibitors

Data collection[a]	***Sa*BPL-4c**	***Sa*BPL-5c**
Wavelength (Å)	0.9537	0.9537
Resolution range (Å)	39.67 - 2.397 (2.482 - 2.397)	39.5 - 2.71 (2.807 - 2.71)
Space group	P 42 21 2	P 42 21 2
Unit cell *a*, *b*, *c* (Å)	94.241, 94.241, 131.192	93.6 93.6 130.7 90 90 90
α, *β*, *γ* (°)	90, 90, 90	
Total reflections	84981 (8264)	57903 (5804)
Unique reflections	22814 (2233)	15757 (1587)
Multiplicity	3.7 (3.7)	3.7 (3.7)
Completeness (%)	95.52 (95.26)	95.97 (99.06)
Mean I/sigma(I)	13.86 (1.07)	11.08 (1.94)
Wilson B-factor	57.05	63.68
R-merge	0.06603 (1.2)	0.07975 (0.6741)
R-pim	0.038 (0.79)	0.04545 (0.3941)
CC1/2	0.999 (0.454)	0.996 (0.696)
CC*	1 (0.79)	0.999 (0.906)
R-work (%)	20.77 (37.00)	0.1833 (0.3350)
R-free (%)	25.40 (42.72)	0.2261 (0.3883)
Number of non-hydrogen atoms	2680	2651
macromolecules	2613	2605
ligands	35	27
water	32	19
Protein residues	322	322
RMS(bonds)	0.007	0.008
RMS(angles)	0.94	1.03
Ramachandran favored (%)	98	95.94
Ramachandran allowed (%)	2.7	4.06
Ramachandran outliers (%)	0.3	0
Rotamer outliers (%)	0.0	1.05
Clashscore	8.42	6.35
Average B-factor	66.60	66.02
macromolecules	66.500	65.83
ligands	78.00	90.63
solvent	64.80	75.21

[a]Diffraction data were collected from one crystal
Values given in parentheses are for the high resolution shell

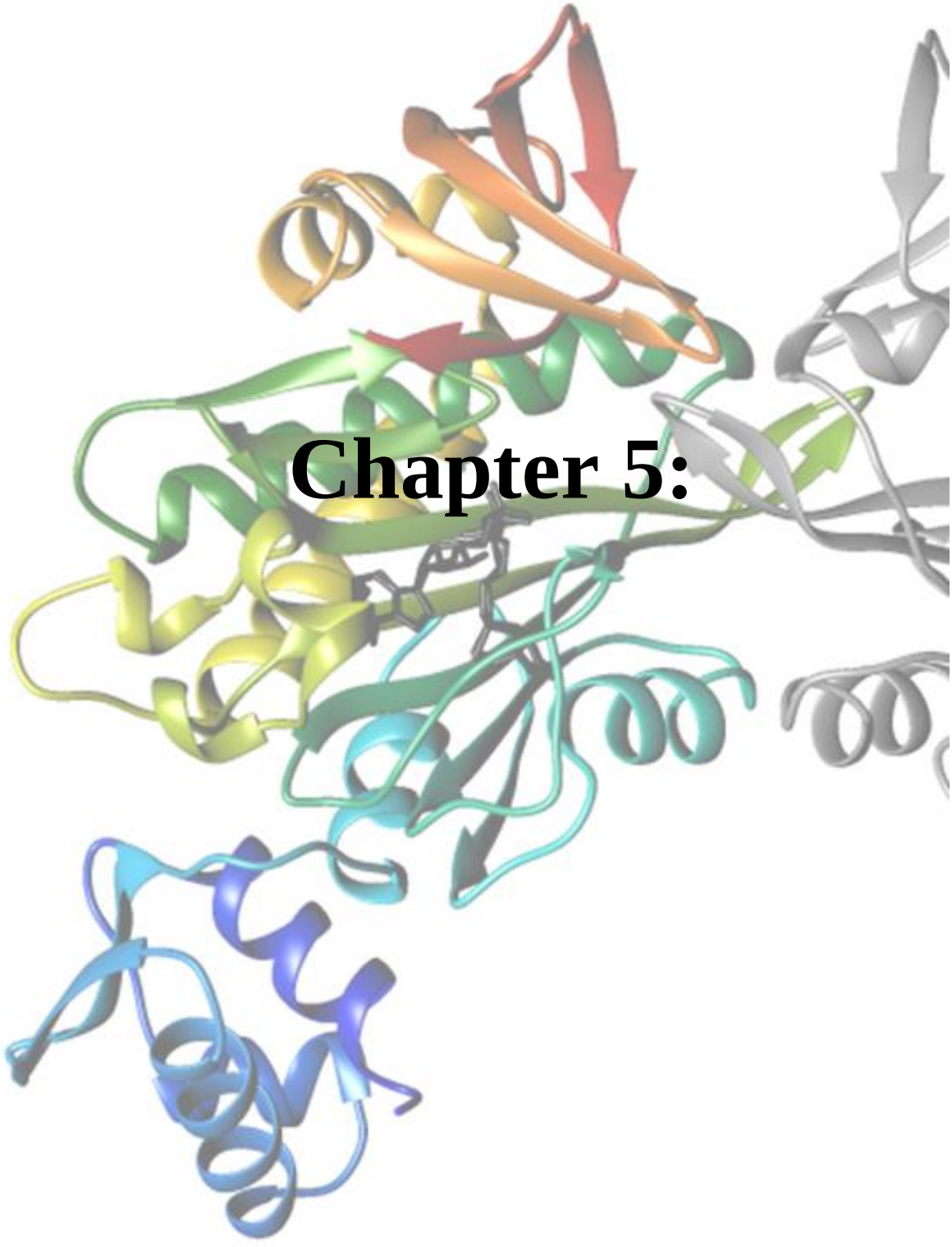

Chapter 5:

Statement of Authorship

Title of Paper	Probing the mechanism of action of BPL inhibitors in *Staphylococcus aureus* using an antibacterial sulfonyl based mimic of biotinyl-5'-AMP.
Publication Status	☐ Published ☐ Accepted for Publication ☐ Submitted for Publication ☑ Unpublished and Unsubmitted work written in manuscript style
Publication Details	Andrew Hayes, Jiulia Satiaputra, Ashleigh Paparella, Louise Sternicki, Jiage Feng, William Tieu, Beatriz Blanco Rodriguez, Danielle Cini, David Heim, Zikai Feng, Jan Bell, Tara Pukala, John Turnidge, Matthew Wilce, Andrew Abell, Grant Booker, Steven Polyak

Principal Author

Name of Principal Author (Candidate)	Andrew Hayes		
Contribution to the Paper	Performed antibacterial susceptibility against ATCC49775 and RN4220, Performed cytotoxicity assays for compound 9 against 2 cell lines, Performed mechanism of action and advanced resistance studies, Expressed, purified and characterised D200E mutant BPL (with Jiulia Satiaputra) Presented advanced manuscript and involved in revising		
Overall percentage (%)	20 %		
Certification:	This paper reports on original research I conducted during the period of my Higher Degree by Research candidature and is not subject to any obligations or contractual agreements with a third party that would constrain its inclusion in this thesis. I am the primary author of this paper.		
Signature		Date	1/08/17

Co-Author Contributions

By signing the Statement of Authorship, each author certifies that:

i. the candidate's stated contribution to the publication is accurate (as detailed above);

ii. permission is granted for the candidate in include the publication in the thesis; and

iii. the sum of all co-author contributions is equal to 100% less the candidate's stated contribution.

Name of Co-Author	Jiulia Satiaputra		
Contribution to the Paper	Performed characterisation of DNA binding aspects of both wild BPL in response to biotin and compound 9. (lacZ assay, EMSA, QRT-PCR). Assisted with DNA binding characterisation of D200E mutant for EMSA and lacZ assays and analysed results. Helped with writing and revising manuscript.		
Signature		Date	22/05/2017

Name of Co-Author	Ashleigh Paparella		
Contribution to the Paper	Expressed and purified *Sa*BPL and *Hs*BPL Performed *in vitro* biotinylation assays against *Sa*BPL and *Hs*BPL		
Signature		Date	3/7/2017

Please cut and paste additional co-author panels here as required.

Name of Co-Author	Louise Sternicki		
Contribution to the Paper	Performed experiments, data analysis and write up of all Mass spectrometry.		
Signature		Date	22/5/17

Name of Co-Author	William Tieu		
Contribution to the Paper	Synthesised compound 9		
Signature		Date	10/7/17

Name of Co-Author	Jiage Feng		
Contribution to the Paper	Synthesised compound 9		
Signature		Date	6/7/2017

Name of Co-Author	Beatriz Blanco Rodriguez		
Contribution to the Paper	Synthesised compound 9 and 11 Scaled up and optimised synthetic route of compound 9 Full data characterisation compound 9.		
Signature		Date	13/07/17

Name of Co-Author	Kwang Jun Lee		
Contribution to the Paper	Synthesised compound 10		
Signature		Date	25/5/17

Name of Co-Author	Danielle Cini,		
Contribution to the Paper	Performed crystallography of compound 9 in complex with *Sa*BPL		
Signature		Date	10/7/17

Name of Co-Author	David Heim,		
Contribution to the Paper	Performed initial antibacterial susceptibility testing of compound 9 and mechanism of action in the presence of excess exogenous biotin and serum fatty acids		
Signature		Date	24/07/2017

Name of Co-Author	Zikai Feng,		
Contribution to the Paper	Performed *in vitro* biotinylation assay of compounds 10 and 11 against *Sa*BPL, performed synergy testing of compound 9, performed spontaneous resistance measurement.		
Signature		Date	11/7/2017

Name of Co-Author	Jan Bell,		
Contribution to the Paper	Tested compound 9 against series of clinical isolates On behalf of Jan Bell		
Signature		Date	1/8/2017

Name of Co-Author	John Turnidge,		
Contribution to the Paper	Tested compound 9 against series of clinical isolates		
Signature		Date	18/7/17

Name of Co-Author	Tara Pukala		
Contribution to the Paper	Supervised mass spectrometry aspects of the project		
Signature		Date	11/7/17

Name of Co-Author	Matthew Wilce,		
Contribution to the Paper	Supervised crystallography aspects of the project		
Signature		Date	10/7/2017

Name of Co-Author	Andrew Abell,		
Contribution to the Paper	Supervised all aspects of medicinal chemistry, revised manuscript		
Signature		Date	25/5/2017

Name of Co-Author	Grant Booker,		
Contribution to the Paper	Supervised all aspects of biology, revised manuscript		
Signature		Date	25/5/2017

Name of Co-Author	Steven Polyak		
Contribution to the Paper	Worked closely with the co-authors to write the manuscript Supervised biological testing		
Signature		Date	25/5/2017

Probing the mechanism of action of BPL inhibitors in *Staphylococcus aureus* using an antibacterial sulfonyl based mimic of biotinyl-5′-AMP.

Hayes, A.J.[1*], Satiaputra, J.[1*], Paparella, A.S.[1], Sternicki, L.M.[1], Rodriguez, B.B.[2], Feng, J., Tieu, W.[2], Cini, D.[3], Heim, D.[1], Feng, Z.[1], Bell, J.M.[4], Pukala, T.L.[2], Turnidge, J.D.[4], Wilce, M.C.J.[3], Abell, A. D.[2], Booker, G.W.[1], Polyak, S.W.[1]

[1] School of Biological Sciences, University of Adelaide, South Australia 5005, Australia
[2] School of Physical Sciences, University of Adelaide, South Australia 5005, Australia
[3] School of Biomedical Science, Monash University, Victoria 3800, Australia
[4] Microbiology and Infectious Diseases Directorate, SA Pathology, Women's and Children's Hospital, South Australia 5006, Australia
*These authors contributed equally to this work

Abstract

Biotin protein ligase (BPL) inhibitors are a novel class of antibacterial agent that can target clinically important pathogens such as drug resistant *Staphylococococcus aureus.* In *S. aureus*, BPL is responsible for catalysing the attachment of biotin onto important metabolic enzymes such as acetyl-CoA carboxylase and pyruvate carboxylase, as well as acting as a transcriptional repressor that regulates the genes involved in biotin homeostasis. Whilst antibacterial BPL inhibitors with *in vitro* antibacterial activity have previously been described, the full effects of these inhibitors on *S. aureus* have never been experimentally explored. Here we report the synthesis of **9**, a new BPL inhibitor that shows potent antibacterial activity (MIC_{90} = 0.5μg/ml) against a panel of clinical *S. aureus* isolates and no associated toxicity against HepG2 or HEK293 cells (EC_{50} >250 μg/ml). Using this compound we further probed the effects of BPL inhibition on *S. aureus*, demonstrating that **9** not only inhibits the catalytic function of BPL but also promotes DNA-binding activity and serves as a co-repressor *in vivo*. Further resistance studies using **9** also led to the discovery of mechanism of resistance using a missense mutation in BPL. This mutation, (D200E) prevented dimerization *in vitro* and reduced repressive capabilities in an *in vivo* β-galactosidase assay. This is the first *in vivo* evidence of a BPL inhibitor acting through transcriptional repression as well as catalytic inhibition and provides insight into the molecular mechanism of antibacterial activity in *S. aureus*.

Introduction

The need for new antimicrobial agents to combat the growing threat of resistance is currently not being met, with only 5 new classes of antibiotics introduced since 2000 [1-3]. Strains that are now resistant to all classes of clinically approved antibiotics have been reported for *Staphylococcus aureus,* Enterococci and *Mycobacterium tuberculosis* [4]. If new antimicrobial agents are not identified, the inability to treat these infections is predicted to result in 10 million deaths every year by 2050 [5]. Unfortunately few new antimicrobial agents are in the drug development pipeline [3], with high risk and low financial reward discouraging investment in this area [1-3, 6]. Despite this, there is a desperate need for new products with novel mechanisms of action that are not subject to existing resistance mechanisms. Therefore new drug targets must be explored. Better understanding of these drug targets and their modes of action *in vivo* are also required to combat resistance. Here we utilise structure guided design to discover a novel antibacterial agent targeting biotin protein ligase (BPL) from *Staphylococcus aureus.* Using this compound we probe the mechanism of action and the potential for resistance.

BPL is an essential protein in *S. aureus* required for enzymatic biotinylation of biotin-dependent enzymes, and repression of certain target genes implicated in biotin homeostasis. This bi-functionality makes BPL a promising new drug target [7]. In *S. aureus* BPL catalyses the attachment of biotin onto two biotin-dependent enzymes, namely, acetyl-CoA carboxylase (ACC) and pyruvate carboxylase (PC). This occurs through two partial reactions. In the first partial reaction BPL binds biotin **(1, Fig 1)** and ATP with ligation of these ligands yielding the reaction intermediate biotinyl-5′-AMP **(2, Fig 1)**. Hydrolysis of biotinyl-5′-AMP then facilitates the attachment of the biotin prosthetic group onto ACC or PC [8] **(figure 1).** These enzymes have important roles in *S. aureus.* ACC catalyses the first committed step in fatty acid synthesis, whilst PC replenishes the TCA cycle with oxaloacetate. Both ACC and BPL have been identified as essential for *in vitro* growth in genetic knockout studies performed on

S. aureus [6, 9-11] and, consequently, been the target of drug discovery programs. The antibacterial efficacy of ACC inhibitors has been demonstrated *in vivo* (reviewed [12, 13]) and BPL inhibitors have shown efficacy *in vitro* [14-19]. PC, whilst dispensable for *in vitro* growth, has been shown to be important in virulence in a mouse model of bacteraemia, [20] with several TCA cycle genes also important for infection in a nematode model [21]. As protein biotinylation is essential for the activity of ACC and PC, inhibition of BPL can impact their respective functions in cell replication and pathogenesis (reviewed [7]).

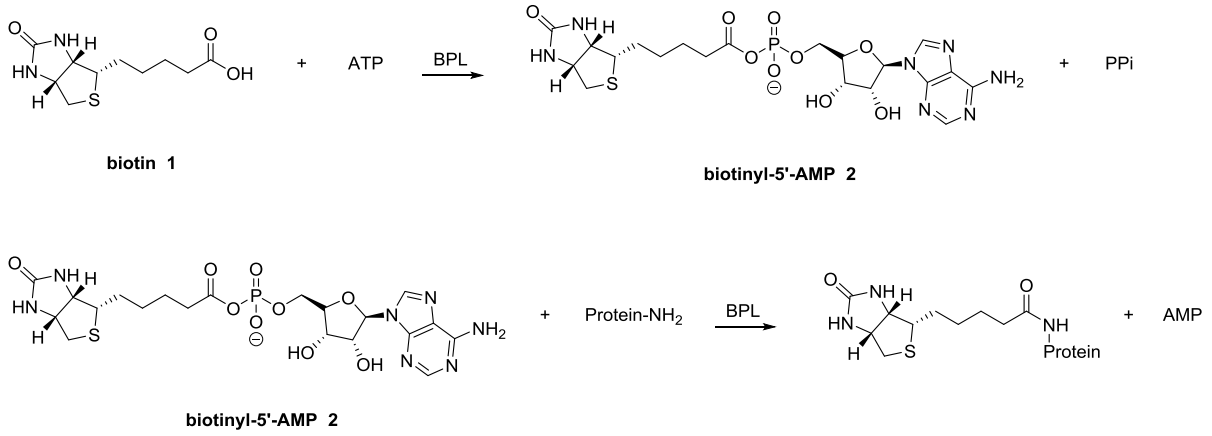

Figure 1. Reaction mechanism of biotin protein ligase. Equation 1, biotin (**1**) interacts with ATP in the binding pockets of BPL to produce and adenylated reaction intermediate, biotinyl-5′-AMP (**2**). Equation 2, biotinyl-5′-AMP interacts with the specific lysine on the biotin domain of biotin dependent enzymes to biotinylate the protein.

In addition to protein biotinylation activity, BPL from *S. aureus* also acts as a transcriptional repressor [19, 22]. *S. aureus* BPL (*Sa*BPL) belongs to structural class II BPLs which contain a helix-turn-helix N-terminal domain responsible for DNA-binding (reviewed [22, 23]). Protein dimerization is believed to be a pre-requisite for DNA binding to the operator sites present in certain target genes [24]. BPL dimerization, and consequent DNA-binding, is induced by the presence of the co-repressor biotinyl-5′-AMP **(2, Fig. 1)** [25, 26][Satiaputra et. al,

unpublished]**.** A series of well-characterized conformational changes that are required to facilitate DNA binding accompany biotinyl-5′-AMP binding. Following biotin binding, residues 118–129 (the biotin binding loop, BBL) undergo a disordered to ordered change that allows ATP binding. The adenosine binding loop (ABL) formed by residues I224 and A228, also undergo structural changes, to accommodate the binding of the adenylate moiety [27]. The protein then undergoes a transition from monomer to dimer. Homo- dimerization involves sidechain interactions between residues R122 and F123, that localize within the biotin binding loop from one subunit, with D200 of the neighbouring subunit [28]. Upon homodimer formation, the two N-terminal DNA binding domains are then optimally positioned for their interaction with DNA [27]. Protein dimerisation can also be induced by chemical analogues of biotinyl-5′-AMP [26, 29]. In *S. aureus*, BPL represses the expression of the biotin biosynthesis operon, the biotin transport protein BioY, as well as a putative fatty acid ligase operon *yhfT-yhfS* [24][Satiaputra et. al, unpublished]. Pharmacologically inducing the repressor state would therefore induce biotin starvation through reduced *de novo* synthesis and import. Hence, as part of the antibacterial mechanism of action, maintenance of homo-dimerization and repressor function is desirable.

Previous attempts at BPL inhibition for antibacterial compounds have been met with varied success. As BPL is a ubiquitous enzyme selective inhibition of BPL from pathogenic bacteria over the human homologue is essential. Initial attempts using mimics of biotin as antibacterial agents were subject to poor selectivity and efficacy due to the highly conserved nature of the biotin binding pocket and relatively low affinity [14]. Subsequent design of BPL inhibitors has focused upon replacement of the labile phosphoanhydride of **2** with more stable bioisosteres. The first of these analogues employed a non-hydrolysable phosphodiester, as in biotinol-5′-AMP **3 (Fig. 2)** [26, 29]. This compound showed promising *in vitro* and whole cell activity against both *S. aureus* (K_i = 18 nM, MIC 1-4μg/ml) and *M. tuberculosis* (K_i = 52 nM, MIC 0.5-2.5μg/ml). [29] However, the human isozyme was similarly inhibited (K_i = 182 nM)

though no associated toxicity was observed against HepG2 cells (CC_{50} > 200μg/ml) [29]. We [14, 17, 18, 29, 30] and others [15, 16, 31] have explored alternative bioisosteres to create more selective antibacterial agents. One promising approach utilised a 1,4-disubstituted 1,2,3-triazole linker (**4, Fig 2)** with inhibitory activity against *Sa*BPL (K_i = 1.17 ± 0.3 μM) and selectivity over the human homologue (K_i > 10 μM) [17]. Removal of the ribose (**5, Fig. 2)** (K_i = 0.66 ± 0.15 μM) and further replacement of the adenine with a benzoxazolone moiety (**6, Fig. 2)** yielded a compound with potent activity (K_i = 90 nM) against *S. aureus* BPL with the required selectivity against the human BPL (K_i > 10 μM) [17]. Whilst the biotin triazole offers a useful pharmacophore for chemical optimisation [17, 18] whole cell antibacterial activity has not been sufficient, with the most potent exemplar producing only 80% inhibition of cell growth at 8μg/ml. Sulfonyl linkers have also been explored to create mimics of **3** targeting the BPL from *E. coli* and *M. tuberculosis*. [15, 16, 32] Noteworthy is Bio-AMS (**8, Fig. 1)**, with potent whole cell efficacy against *M. tuberculosis* including drug resistant isolates (MIC 0.16-0.78 μM). However, this compound shows no activity against *S. aureus.* Here we report that removal of the ribose heterocycle from literature compound **8** improves whole cell activity against *S. aureus.*

3) Biotinol-5′-AMP

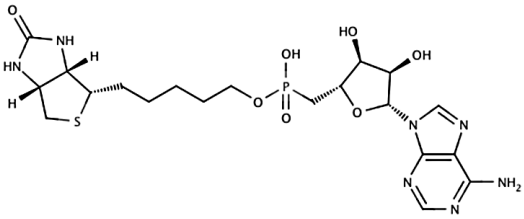

4) Biotin adenosine triazole

K_i = 1.17 µM

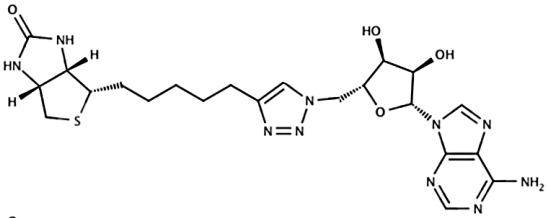

5) Biotin adenine triazole

K_i = 0.66 µM

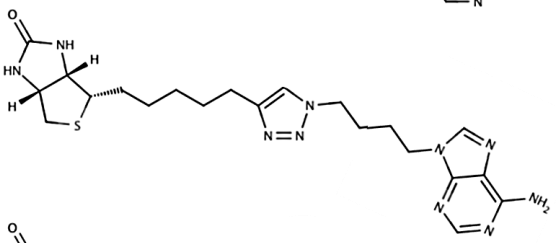

6) Biotin benzoxazolone triazole

K_i = 0.09 µM

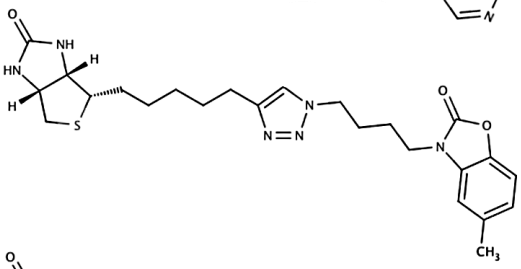

7) Benzyl triazoles

K_i = 0.28 µM

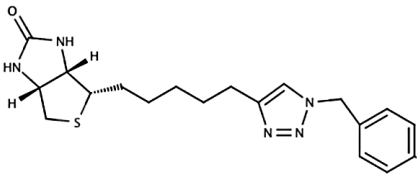

8) Bio-AMS (Duckworth et. al)

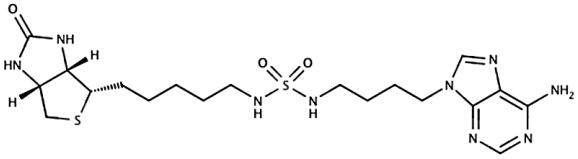

Figure 2: Structure of lead compounds guiding synthesis of inhibitors against *Sa*BirA

(**3**.) derivative of reaction intermediate with non-hydrolysable phosphodiester linker, biotinol-5′-AMP, (**4**.) next generation of inhibitor with increased selectivity containing 1,2,3-triazole linker (**5**.) improved structure of 1,2,3-triazole with removed ribose moiety (**6**.) Modification of the 1,2,3-triazole **4** substituting the adenine moiety for benzaloxazolone. (**7**.) Modification of the 1,2,3-triazole **4** substituting the adenine moiety for benzyl ring. (**8.**) Bio-AMS, containing acylsulfonamide linker and active against *Mt*BPL

Materials and methods

General bacteria culture, molecular biology reagents and protein methods:

All chemicals and reagents were purchased as analytical grade or higher. Unless otherwise stated, all bacterial strains were purchased from the American Tissue Culture Collection. All molecular biology enzymes (DNA polymerase and restriction enzymes) and buffers were supplied by New England Biolabs. Oligonucleotides were purchased from Geneworks Ptd Ltd. BPL protein expression and apo-purification was performed following previously described protocols [33, 34]. Apo-purification was performed by incubating bacterial lysate purified biotin domain-GST fusion from *S. aureus* [35] (*Sa*PC90) at 30°C for 1 hour, as described previously [28]. Protein concentration was determined using Bradford assay. Apo-purified protein was confirmed by nESI-MS and by Western blot analysis as described previously [28]. Detail of apo-purification and apo-protein verification is provided in Supplementary section.

Protein Crystallography: Alignment of X-ray crystal structures was performed using the structural analysis program, UCSF Chimera. Superimposition of *Sa*BPL in complex with either compound **9** (Prof. Matthew Wilce, Monash University, this study) or **2** (PDB ID# 3RIR) was performed using this program. The result of this superimposition is presented in **Figure 3**.

***In vitro* Biotinylation assay:** A 96-well assay using Europium labelled streptavidin and time-resolved fluorescence was used to measure BPL activity. An *in vitro* biotinylation reaction was performed for at least 10 minutes at 37 °C in a 20 µL reaction mix containing 50 mM tris pH 8.0, 3 mM ATP, 5.5 mM $MgCl_2$, 25 µM GST-SaPC90, 0.1 µM DTT, 5 µM biotin and purified BPL (*Sa*BPL 6 nM). BPL catalysed reactions were stopped with the addition of 80 µL stopping buffer (50 mM Tris pH 8.0, 110 mM EDTA) and 3 x 20 µL aliquots were added to the well of a white lumitrac-600 96-well plate that had been previously coated by overnight incubation at 4 °C with an anti-GST antibody (50 µL per well) at 1:40000 dilution, followed

by blocking for 2 hours (200 µL per well) with 1% BSA in TBS at 37 °C and incubated at 37 °C for 1 hour. The plate was then washed 5 times (200 µL per well) with TBS containing 0.1% Tween-20. Europium labelled streptavidin was diluted to 0.1 µg/mL in TBS containing 0.1% Tween-20. The streptavidin probe (50 µL per well) was incubated for 30 minutes at 37 °C followed by washing 5 times in TBS 0.1% Tween-20. Enhancement solution (Perkin Elmer) (50 µL) was added per well and incubated for 10 minutes before reading the plate using time-resolved fluorescence using 340 nm excitation and 612 nm emission filters with a Perkin Elmer® Victor X5 multilabel reader.

Antibacterial susceptibility evaluation: Antibacterial activity was determined by the broth microdilution method as recommended by the CLSI (Clinical and Laboratory Standards Institute, Document M07-A8, 2009, Wayne, Pa.) using cation-adjusted Mueller-Hinton broth (CAMHB) (Trek Diagnostics Systems, U.K.). Compounds were diluted two-fold in CAMHB to a final concentration range of 64 to 0.06 µg/ml in 3.2% DMSO. To prepare the inoculum overnight cultures from a single colony were subcultured 1 in 1000 and grown to mid log phase. Trays were inoculated with 5 x 10^4 CFU and incubated at 37°C for 20-22 hours with shaking. Growth of the culture was quantified by measuring the absorbance at 620 nm using a Thermo Multiskan Ascent plate reader after shaking for 15 seconds to disrupt any sedimentation. Assays were performed in triplicate.

Concentration kill kinetics: An overnight culture of S. aureus ATCC 49775 was prepared and diluted to approximately 2.5× 10^5 CFU/ml in 20 mL CAMHB containing the appropriate concentration of compound **9** (1×,2×,4× MIC [MIC = 0.5 µg/ml]) in a 50 ml falcon tube. Cultures were incubated for 24 hours at 37°C and 100µl samples taken at 0, 1, 2, 4, 8 and 24 hours. Samples were serially diluted and plated with the first countable dilution enumerated to determine CFU/mL.

Cytotoxicity assay: HepG2 or HEK293 cells were seeded in 96-well tissue culture plates at 10^4 cells per well in 100 µl of DMEM+ (10%FCS, 1 mM sodium pyruvate and 2 mM glutamine). After 24 hours growth, cells were treated with varying concentrations of test compound. Dilutions of compound were prepared by two fold serial dilution of compound in DMEM, maintaining a constant DMSO concentration, 2% (v/v) for HepG2 or 0.5% (v/v) for HEK293. After treatment for 48 hours, 10 µl WST-1 cell proliferation reagent (Roche) was added to each well and incubated for 30 minutes at 37°C. The WST-1 assay quantitatively monitors the metabolic activity of cells by measuring the hydrolysis of the WST-1 reagent, the products of which are detectable at absorbance 450 nm on Perkin Elmer plate reader.

Synergy testing: Checkerboard antibacterial susceptibility assay was constructed. In brief compound **9** and a clinically used antibacterial agent were 2 fold serially diluted from 4 to 0.0625 × MIC. The dilutions were arranged perpendicularly so that 64 individual concentrations of antibiotic were present in an 8×8 grid. Antimicrobial susceptibility assays were then performed as per above using *S. aureus* ATCC49775. Synergy was determined by Σ FIC Index < 0.5 as described in [36, 37].

Growth in presence of fatty acids: Antibacterial susceptibility testing was undertaken as above with 0, 10 and 20% FCS added to media to determine any reduction in compound efficacy. Erythromycin was used as a control.

Mechanism of action-increased biotin: Antibacterial susceptibility testing was undertaken as above with 0, 10, 100, 1000 nM of exogenous biotin added to media to determine any reduction in compound efficacy.

Mechanism of action-Overexpression system: Antibacterial activity was determined on *S. aureus* RN4220 containing either pCN51-NcoI (control) or pCN51-BPL (BPL over-expression) vectors [18]. Compounds, dissolved in DMSO, were serially diluted from 64 to 0.06 µg/ml in Mueller Hinton broth (3.2% (v/v) DMSO) supplemented with 10 µg/ml

erythromycin for plasmid selection and 25 nM $CdCl_2$ to induce BPL expression. Log phase cultures of transformed *S. aureus* RN4220 strains, grown in the absence of compound, were diluted 1:1000 into media containing compound. Growth of the cultures at 37°C with shaking was then monitored at OD_{630} every 30 mins for 22 hours using an EL808™ Absorbance Microplate Reader (BioTek Instruments Inc, Winooski, VT, USA). *S. aureus* harbouring pCN51-BPL grown in the absence of compound served as a baseline control. The mechanism of action assays were performed in triplicate.

Quantification of gene expression using QRT-PCR: *S. aureus* NCTC 8325 was grown overnight at 37 °C in biotin-depleted CAMHB. The overnight culture was then used to inoculate 10 mL of biotin-depleted CAMHB which was incubated until mid-log phase was reached. The culture was then treated by adding either biotin (10 nM) or compound **9** (10 nM or 3.9 μM [i.e. 4× MIC]). 500μL of the culture was collected at 0, 15, 30 and 90 minutes post treatment and pelleted. Cell pellets were resuspended in 100 μL of TE buffer containing 1 mg/mL lysozyme and *S. aureus* lysis performed by adding 1 μL of 10 mg/mL of lysostaphin (Sigma Aldrich) followed by incubation at 37°C for 30 minutes. RNA extractions were performed using RNAeasy mini kit (Qiagen), following the manufacturer's instructions. Total RNA was measured using a Nanodrop spectrophotometer (Thermo fisher scientific). 2 μg of total RNA was treated with 20 units of DNAse1 at 37^{o}C for 1 hour using a DNAseI kit (Life technology), followed by inactivation using 2 μL RNase-free EDTA reagent (Sigma Aldrich) at 65°C for 10 minutes. The qRT-PCR reactions were performed using the Superscript® III platinum ® SYBR® 1- step QRT-PCR kit (Life technologies) with 0.2 nM of oligonucleotides. A total of 10 ng of RNA was used as a template in the qRT-PCR reaction and a total of 0.1 ng of RNA was used as a template in 16s rRNA amplification. The reaction and data analysis were performed using the Quantstudio™-Dx real-time PCR instrument and software (Thermofisher). Relative expression was normalized against 16s rRNA and corrected to t = 0. For each experiment, at least 3 independent biological replicates were obtained and each PCR

reaction was performed in triplicates. Statistical two-tailed t-test comparison of each time point against t = 0 was performed using GraphpadPrism (Graphpad Software, Inc., CA, USA)

Electrophoretic Mobility Shift Assay (EMSA): EMSA protocol was adapted from methods previously published in [38]. Briefly, 10 nM double-stranded oligo (containing either *SabioD* or *SabioY* operator sequence) were incubated with varying concentrations of *Sa*BPL in EMSA binding buffer containing 50mM Tris pH 8.0, 50 mM NaCl, 1 mM ATP, 1 mM $MgCl_2$ and 10% (v/v) glycerol. To generate holo-*Sa*BPL, 100 μM biotin was added to the EMSA binding buffer. Binding reactions were performed in a final volume of 10 μL and incubated for 30 minutes at room temperature. For analysis of compound **9**, 100 μM of compound was added to the EMSA buffer. As compound **9** was reconstituted in 100% DMSO, the final DMSO concentration in the binding buffer was 2.5% (v/v). A control reaction was prepared by adding 100μM biotin and 2.5% (v/v) DMSO to the binding reaction. The reaction was run at room temperature, on 4-12% TBE gradient gel in 0.5x TBE buffer (Life technologies) at 100V for 45 minutes, followed by staining with staining solution containing 100mM NaCl, 1x Gel Red (Biotium).

Spontaneous resistance rate: The spontaneous resistance rate of *S. aureus* NCTC 8325 was determined by plating the entirety of a culture with 10^9 CFU onto CAMHB Agar containing 2 μg/mL compound **9** (4× MIC). This was repeated with 9 separate cultures in technical replicate (same starting colony) to control for priming mutations in the initial colony. Plates were checked after 24 hours at 37°C for growth with no detectable colonies observed on any of the plates. As true resistance rate using fluctuation analysis [39-41] requires some colonies a resistance frequency was instead calculated at 4× MIC as $< 10^{-9}$.

Selection of resistant mutants: Mutants were selected by serial passage in 96 well format as previously described [42]. In brief: A 2-fold dilution series of compound **9** was plated across 7 wells. Initial concentrations ranged from 1 μg/ml to 0.016 μg/ml, with the highest

concentration increasing up to 64 μg/ml as the MIC increased. On the first day approximately 10^4 CFU of exponentially growing *S. aureus* 8325 was added to each well. The OD was measured at 620nm for each well and the well with the highest concentration permitting growth (OD_{620} > 0.1 used as threshold) diluted 1000 fold and used to inoculate the next day's assay. This process was repeated for 18 days. From the final day's experiment single isolates were purified by streaking out strains and genomic DNA extracted. The stability of the resistance was also tested by propagating the strains selected for 6 days on MH Agar in the absence of any antibiotic selection. These strains were then retested in the antibacterial susceptibility assay and the BPL gene of each strain sequenced to identify mutations. DNA extraction and sequencing procedure detailed in supplementary section.

Native nESI-MS: Purified apo-*Sa*BPL was buffer exchanged into 200 mM ammonium acetate using Vivaspin 500 MWCO 10,000 spin columns (vivaproducts, MA, USA). Holo-*Sa*BPL samples were prepared by pre-incubating apo-*Sa*BPL with 500 μM biotin, 1 mM ATP and 1 mM $MgCl_2$ prior to buffer exchange. Proteins were diluted to 10 μM in 200 mM ammonium acetate for analysis by nano-electrospray ionization-mass spectrometry (nESI-MS). MS measurements were performed on a Synapt HDMS system (Waters, UK) with the sample introduced by nano-electrospray ionisation in positive ion MS mode from platinum-coated borosilicate capillaries prepared in-house. Instrument parameters were optimized to remove adducts while preserving non-covalent interactions, and were as follows; capillary voltage, 1.5 kV; cone voltage, 60 V; trap collision energy, 20 V; transfer collision energy, 15 V; source temperature, 50°C; backing pressure, 3.95 mbar. Detected molecular weight of protein or protein complex are within 1.5% / 1 MDa of acceptable error mass.

Chromosomal integration and β-galactosidase reporter assay: *Sa*BPL D200E was cloned into the established integration vector and incorporated chromosomally into the λ-attB phage attachment site within the *E. coli* reporter strain containing *β –galactosidase* gene under the

control of either *SabioO* or *SabioY* promoters, (JD26186_*birA*::*CAT_SabioO* and JD26186_*birA*::*CAT_SabioY*, respectively). Chromosomal integration was performed by previously established methods [43]. Detail on the cloning of *Sa*BPL D200E into the integration vector can be found in supplementary section [43]. β-galactosidase assay was performed on an *E. coli* reporter strain containing *Sa*BPL D200E and compared against reporter strains containing *Sa*BPL wild-type and the previously described mutant *Sa*BPL F123G, respectively. [43]. For the assay bacteria were grown overnight in minimal media (0.1% casamino acid , M9 salts, 1 mM $MgSO_4$, 1 μg/mL thiamine, 0.4% glucose) containing 100 nM biotin. The overnight culture was pelleted and washed three times with minimal media containing no biotin and used to inoculate each well of the 96-well growth plate containing minimal media supplemented with 0.5 nM - 500 nM biotin. Cells were grown at 37°C with gentle agitation until the optical density reached OD_{600} = 0.50-0.60, at which point the OD_{600} was recorded, cells were lysed and β-galactosidase activity measured as described previously [43]. The β-galactosidase activity from the no-promoter control strain was subtracted from the activity generated by the strain containing *Sa*BPL. Results were analyzed using Graphpad Prism (Graphpad Software, Inc., CA, USA).

Results

Design and synthesis.

As we have demonstrated that the ribose heterocycle is dispensable for activity, this feature was removed from **8** to form **9**. Biochemical assays revealed the compound retained potent *in vitro* inhibitory activity (K_i = 2.4 ± 0.2 nM) but had vastly improved antibacterial activity against *S. aureus* (MIC = 0.5 μg/ml) over the literature compound **8**. Whole cell activity was also observed with *M. tuberculosis,* albeit with less potency (MIC = 50 μg/ml), but no activity was observed against Gram-negative species. X-ray crystal structure of *Sa*BPL in complex with **9** showed **9** occupies the same binding site as the reaction intermediate **2** (**Figure 3,** PDB 3RIR, **Figure s13**). A key interaction was K187 with the carbonyl of **9**, as removal of this C=O, as in compound **10**, increased the K_i by 700-fold. Likewise, the adenine moiety was preferred over the benzoxazolone group of **6** as this replacement, as in compound **11**, reduced inhibitory activity 940-fold. None of the new compounds showed inhibition against the human enzyme at the highest concentrations tested (K_i >10 μM). This confirmed that the selectivity seen in biotin triazole compounds was also obtainable with the sulfonyl linker. Due to its potent anti-*S.aureus* activity **9** became the lead structure for further biological evaluation.

9. BPL199

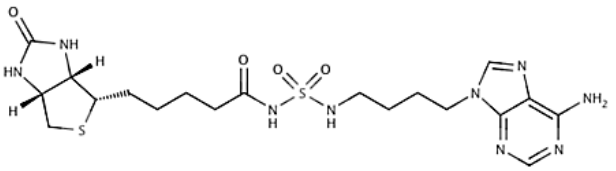

10. ID47P96a

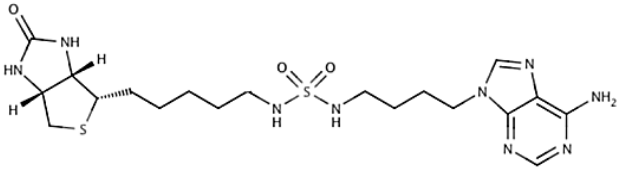

11.BB-R127

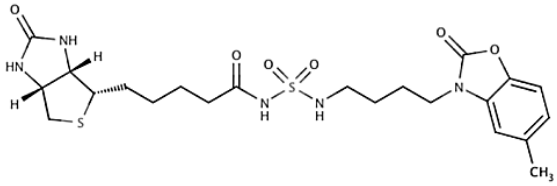

12. WT5087B/ BPL218

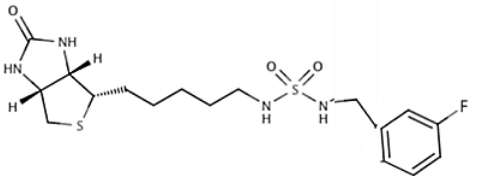

13. BPLWT5001/ BPL198

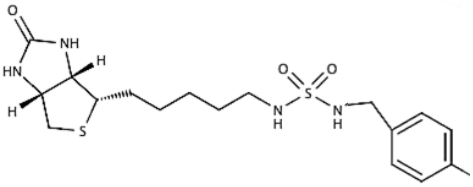

Chemical scheme 1. With compounds (**9**.) a novel derivative of acylsulfonamide **8**, giving rise to a potent *Sa*BirA inhibitor (**10**.) modification of **9** removing the carbonyl (**11.**) modification of **9** utilising a benzoxalone mimic as seen in **5. (12, 13)** modification of the pharmacophore **6** with a sulfonyl linker

a)

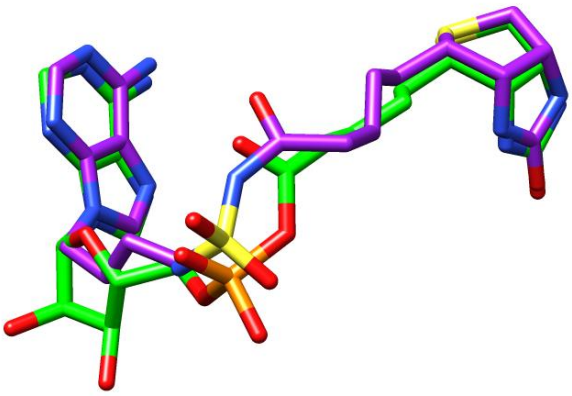

b)

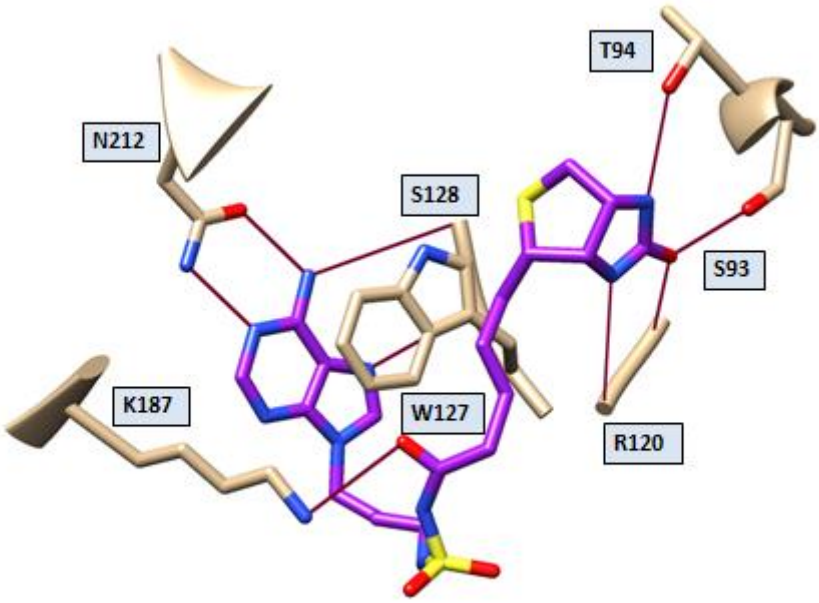

Figure 3: Structural alignment of 9-bound vs. biotinyl-5′-AMP- bound *Sa*BPL (a.) overlay of the binding conformation of biotinyl-5′-AMP (PDB 3RIR) and **9** bound to *Sa*BPL (this study). (b) key residues involved in hydrogen bonding (red lines) and π-π stacking (W127) interactions observed in the **SaBPL:9** complex.

Antistaphylococcal Activity and Therapeutic Index

The antibacterial potency of **9** was assessed against an extended panel of clinical *S. aureus* isolates. Against all multidrug-resistant *S. aureus* strains tested, **9** exhibited MICs ranging from 0.125-0.5 μg/ml (**n=23**, **Table 2**). Cytotoxicity assays were also performed with two human cell lines, namely liver HepG2, and kidney HEK293 cells. Here the growth media contained 10% FCS. No cytotoxicity was observed at the highest concentration tested (250 μg/ml) **(supplementary information figure s1**) representing a greater than 500-fold therapeutic window. To address concerns of serum binding reducing bioactivity in cytotoxicity assays [44, 45], antibacterial activity of **9** was further tested in the presence of foetal calf serum (FCS). No effect on MIC was observed with 10% FCS whilst testing in 20% FCS showed a 2-fold increase in MIC for the erythromycin control and an 8-fold increase in MIC for **9** (MIC = 4 μg/ml) suggesting a slightly reduced efficacy in the presence of higher serum concentrations **(supplementary information figure s4**)**.**

Mechanism of action, antibacterial concentration kinetics and synergy

To demonstrate the mechanism of action of **9** was through BPL inhibition antibacterial susceptibility was determined in the presence and absence of either overexpressed BPL [15], or increased exogenous biotin. Consistent with a mechanism of action through BPL inhibition, overexpression of BPL resulted in an 8-fold increase in MIC of **9** (**supplementary figure s5)** and literature BPL inhibitor **3**. No shift was observed for the β-lactam control antibiotic amoxicillin **(supplementary figure s6).** Additional exogenous biotin also reduced the efficacy of the compound, with dose responsive increases in MIC up to a 64-fold at super-physiological concentrations (1 μM biotin) **(supplementary figure s7).** Kinetics of antibacterial activity was also determined, with viable cell counts measured following 24 hours of treatment with 1, 2 and 4 times MIC. Growth was completely inhibited at these concentrations, however no reduction in cell number was observed, consistent with **9** acting

Table 1: MIC and inhibition data for sulfonyl compounds against *S. aureus*

Compound	K_i SaBPL (μM)	K_i HsBPL (μM)	MIC ATCC49775 (μg/ml)	MIC RN4220 (μg/ml)
9	$2\times10^{-3} \pm 0.2\times10^{-3}$	>10	0.5	0.125
10	2.34 ± 0.19	ND	>64	16
11	1.68 ± 0.17	ND	>64	>64
12	>10	ND	ND	ND
13	>10	ND	ND	ND

Table 2: Biological Activity and Selectivity of **9.**

Species	**Description**	**MIC (μg/ml)**
Active species		
S. aureus (n=22)	Staphylococcus aureus (n=8)	0.25 – 0.5
	Methicillin-resistant *S. aureus* (n=9)	0.25 – 0.5
	Coagulase negative staphylococci (n=7)	0.125 – 0.5
Mycobacterium tuberculosis	H37Rv	50
Inactive species		
Streptococcus pneumoniae (n=6)		>32
Enterococococcus faecalis (n=3)		>128
Enterococococcus faecalis (n=3)		>128
Enterococcus faecium (n=5)		>128
Escherichia coli (n=1)		>128
Cell lines		**EC_{50} (μg/ml)**
HepG2	Liver derived cell line	>250
HEK293	Kidney derived cell line	>250

as a bacteriostatic agent **(supplementary information figure s2).** This bacteriostatic action means **9** requires either host induced killing or combination therapy to clear infection. Consequently synergy with other clinically used antibacterial agents was performed. No antagonism was observed with any combination and synergy was detected for both methicillin and streptomycin with an FIC of less than 0.5 [36, 37]. **(supplementary information, table s2, figure s3).** Having defined the mechanism of antibacterial action and determined the potential for combination therapies further characterisation of **9** was undertaken.

9 induces conformational changes required for DNA binding and functions as an active co-repressor *in vivo*

The structure of **9**-bound *Sa*BPL was compared with that of holo-*Sa*BPL (PDB # 3RIR). Like with the reaction intermediate, biotinyl-5′-AMP (PDB 3RIR), the crystallographic unit for **9** bound *Sa*BPL is a dimer with the two structures in good agreement when superimposed (RMSD = 1.2Å) (**Figure 4)**. This indicates that the binding of **9** to *Sa*BPL initiates the same conformational changes that are required for dimerization, correctly positioning residues F123, R122 and D200 at the dimerization interface. The N-terminal domains are also superimposed suggesting that **9** facilitates DNA binding and, therefore, functions as a co-repressor.

To test the effect of **9** on gene transcription, *S. aureus* NCTC 8325 was grown in biotin depleted media and treated with two concentrations of **9,** either 10 nM or 3.9 μM (i.e. 4x MIC). Cells were harvested at 0, 15, 30 and 90 minutes post treatment and total RNA was prepared to analyse the level of transcript of *bioD* (the first gene in the biotin biosynthesis operon) and *bioY* (biotin transporter gene) using qRT-PCR. Transcriptional repression of *bioD* and *bioY* by 10 nM biotin was used for comparison. In bacteria treated with 10 nM biotin, a 111-fold decrease in *bioD* expression was displayed 15 minutes post-biotin addition and maintained throughout the time course (**Fig. 5a**). Addition of 10 nM of **9** however,

DNA binding structure

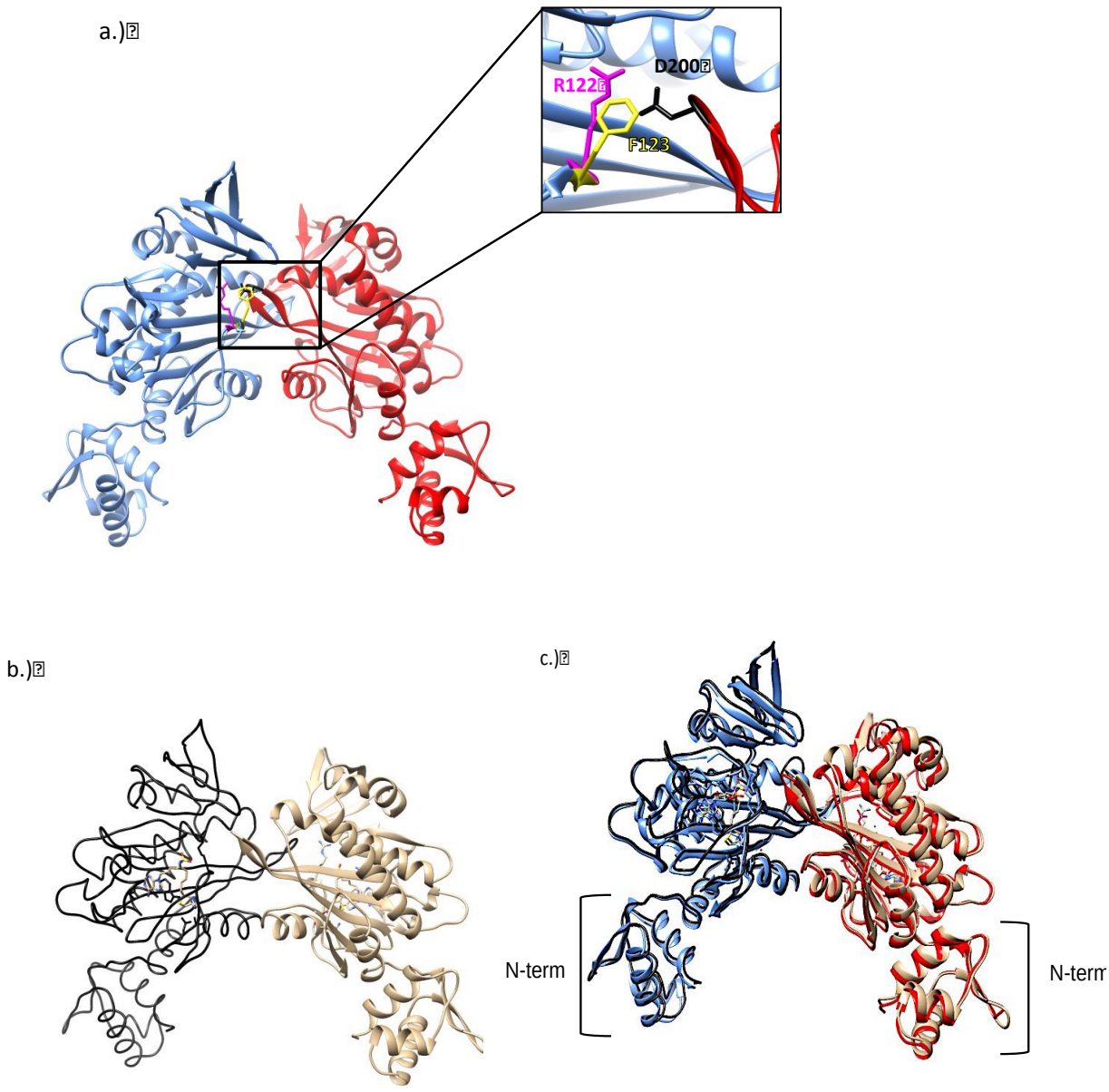

Figure 4: Structural alignment of BPL199-bound vs. biotinyl-5′-AMP- bound *Sa*BirA. (a.) The structure of biotinyl-5′-AMP *Sa*BirA, residues involved in dimerization are shown (boxed diagram). (b.) The structure of BPL199-bound *Sa*BirA. (c.) BPL199-bound *Sa*BirA was aligned with biotinyl-5′-AMP-bound *Sa*BirA. The aligned N-terminal domain is indicated.

resulted in only 14-fold repression of *bioD* expression at 15 minutes post addition ($p \leq 0.0001$, **Fig. 5b**), with this level of repression similarly maintained throughout the time course. Stronger repression of *bioD* was achieved by increasing the dosage of **9** to 3.9 μM (i.e. 4x MIC) with the level of transcripts showing a 52-fold decrease after 15 minutes, with transcript levels dropping further to 32-fold at 30 minutes and 71-fold at 90 minutes compared to time 0 ($p \leq 0.0001$, **Fig. 5c**). The *bioY* transcript exhibited less dramatic repression than *bioD*, with 10 nM biotin addition resulting in only 2-fold repression at 15 minutes ($p < 0.01$), 5–fold at 30 minutes ($p < 0.01$) and 6-fold at 90 minutes ($p < 0.01$) (**Fig. 5d**). Unlike with *bioD*, *S. aureus* treated with 10 nM compound **9** exhibited a similar fold-response, with *bioY* expression reduced by 1.5-fold at 15 minutes ($p < 0.01$), 2-fold at 30 minutes ($p < 0.01$) and 6-fold at 90 minutes ($p \leq 0.0001$, **Fig. 5e**). These results suggest that **9** acts as a functional co-repressor, with repression comparable to that of the natural ligand, biotin. To further probe this, EMSA analysis was performed to determine whether the reduced repression of **9** was due to a reduction in ability to promote DNA-binding *in vitro*. EMSA reactions were prepared by first incubating apo-*Sa*BPL with either; biotin and ATP, to allow the synthesis of biotinyl-5′-AMP (i.e. holo-*Sa*BPL), or compound **9**. The binding data showed that *Sa*BPL:compound **9** exhibits equipotent DNA binding to that of *Sa*BPL:biotinyl-5′-AMP (**Fig. 6**). *Sa*BPL binding to *SabioO* exhibited 100% binding at 156 nM *Sa*BPL for both biotinyl-5′-AMP and compound **9** (**Fig. 6a-b**). The minimal concentration of protein required to produce 100% binding to the *bioY* probe was also 312 nM for both ligands (**Fig. 6c-d**). This *in vitro* analysis supports that **9** induces the same DNA binding activity as biotinyl-5′-AMP and that the differences in response may be due to other factors such as compound uptake.

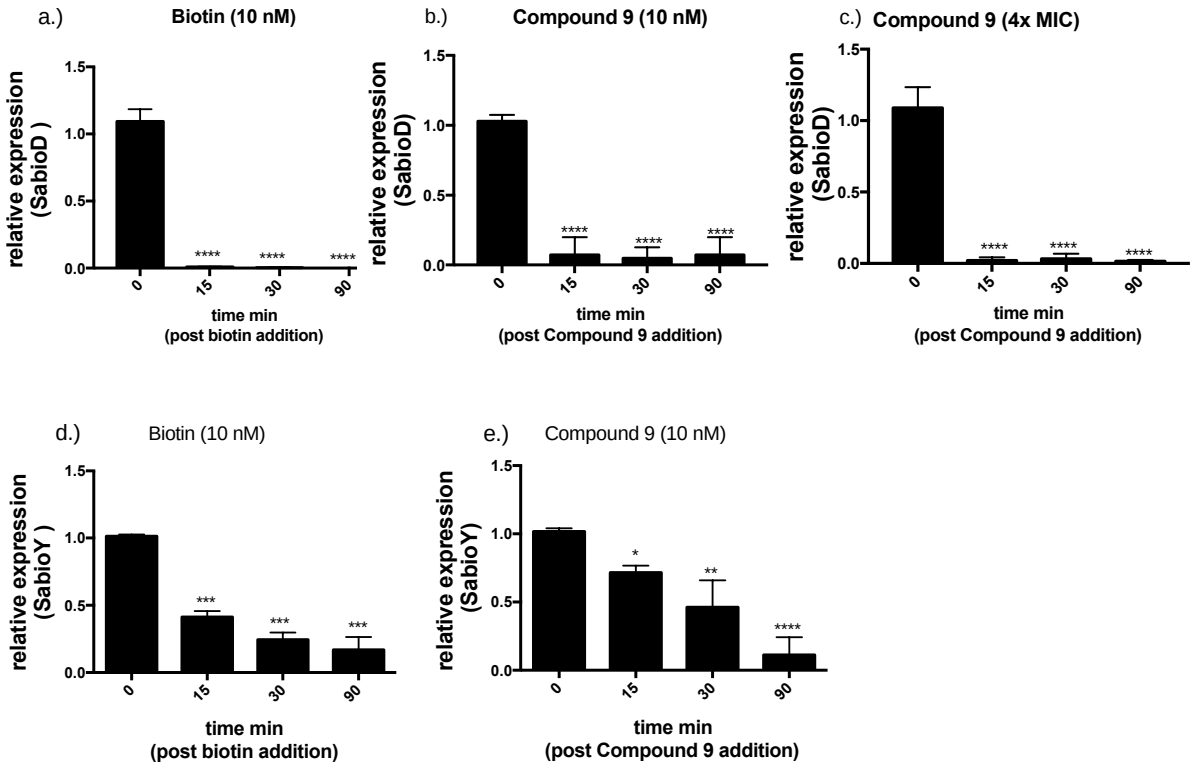

Figure 5: qRT-PCR analysis of biotin vs. 9. *S. aureus* was grown in biotin-depleted Mueller-hinton media until mid-log phase was reached and treated with either 10 nM biotin, 10 nM of **9** or 3.9 μM (i.e. 4x MIC) of **9**. The expression of *SabioD* and *SabioY* was then quantified. The amount of transcripts were normalized against an internal control (16s rRNA) and relative expression for each time point against time = 0 was calculated. The repression of *SabioD* following treatment with a.) 10 nM biotin b.) 10 nM **9** and c.) 4x MIC of **9**, is shown. Repression of *SabioY* in response to treatment with d.) 10 nM biotin and e.) 10 nM of **9** is also shown. Error bars represent S.E.M from independent biological replicates (n=3), * = p <0.05, ** = p <0.01, *** = p >0.001, **** = p <0.0001

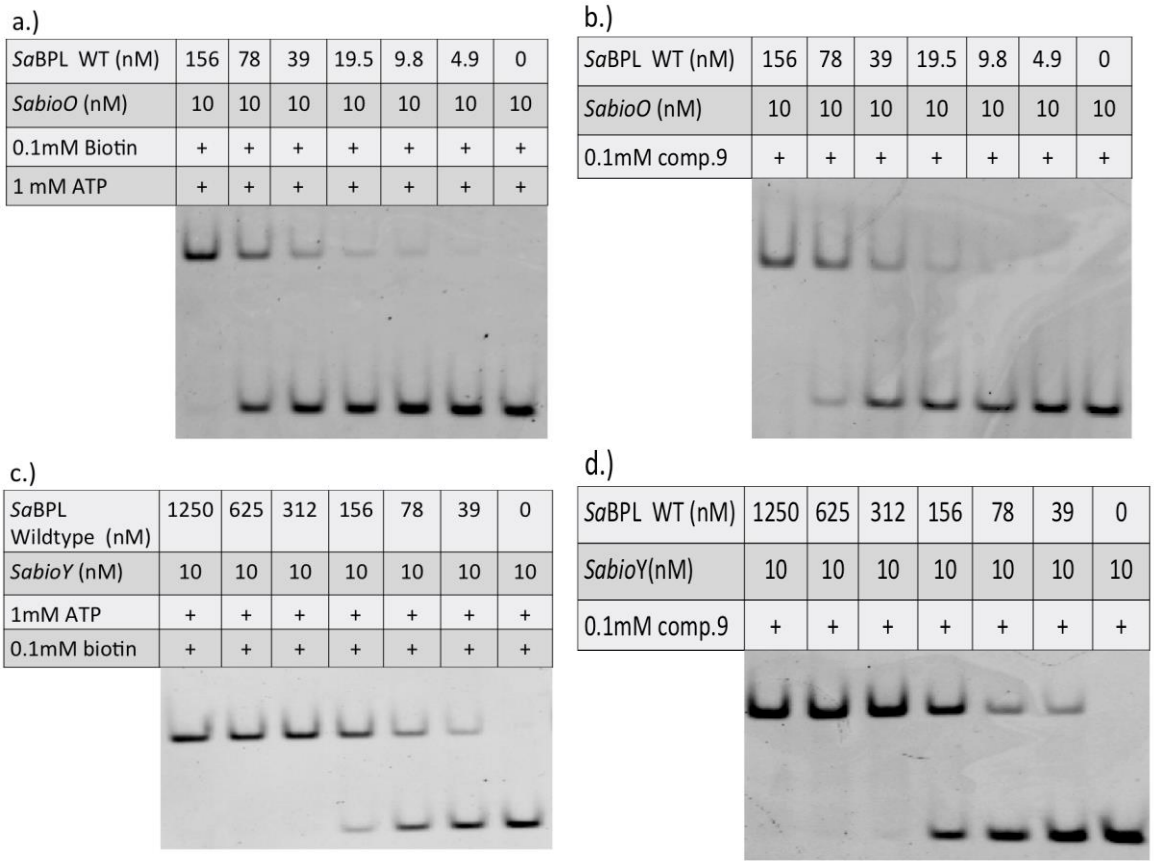

Figure 6: EMSA of biotinyl-5′-AMP vs. 9. (Top) *Sa*BPL binding to *SabioO* probe in EMSA reaction containing a.) biotinyl-5′-AMP and b.) **9**. **(Bottom)** *Sa*BPL binding to *SabioY* probe in EMSA reaction containing c.) biotinyl-5′-AMP and d.) 9. EMSA was performed in standard binding buffer (50 mM Tris pH 8.0, 50 mM NaCl, 1 mM ATP, 1 mM $MgCl_2$ and 10% (v/v) glycerol) using 10 nM of a 44 bp double stranded oligo containing either *SabioO* or *SabioY* operator sequence and wild-type *Sa*BPL at concentrations indicated. Control reactions containing biotinyl-5′-AMP were prepared by adding 0.1mM biotin, 1mM ATP and 2.5% DMSO into the binding buffer, these were compared to reactions containing 0.1 mM of compound 9 (dissolved in 100% DMSO).

Generation of resistant mutants and detection of *Sa*BPL mutation D200E

The capability of *S. aureus* to develop resistance to **9** was tested through use of both spontaneous resistance and serial passage approaches. To facilitate the subsequent analysis of these strains, *S. aureus* NCTC 8325 was utilised due to the availability of a reference genome for comparative sequence analysis. For measuring spontaneous resistance 10^9 cells were plated onto media containing 4× MIC. No spontaneously resistant mutants were observed after 24 hours suggesting a low resistance frequency of less than 10^{-9}. Consequently, generation of resistant strains was achieved by serial passage of seven populations of *S. aureus* NCTC 8325 in sub-inhibitory concentrations of **9** for 18 days **(supplementary figure s8).** After 18 days passage seven individual colonies were isolated and passaged on non-selective media to verify that the mutations were genetically stable. At this point the 7 strains tested had an MIC 4 to 32 fold that of the parent strain ($MIC_{NCTC8325}$ = 0.0625 μg/ml). Strain NCTC8325-B7 exhibited resistance to the highest concentration (MIC = 2 μg/ml) **(table 3)**. Sequencing of the BPL gene from all seven strains was subsequently undertaken to determine any modifications in the BPL target. NCTC8325-B7 was the only isolate which harboured a missense mutation in BPL. This mutation, D200E, maps in the dimerization interface between the two BPL subunits.

Table 3: MIC's of strain NCTC8325 and derivatives against **9** after 18 days serial passage in the presence of suboptimal concentrations to 9. MICs were determined in triplicate. *strain B3 exhibited slow growth making MIC determination difficult. **strain B7 was susceptible to 4μg/ml compound 9 but showed tolerance to 64 μg/ml.

Strain	**MIC (μg/ml)**
NCTC 8325	0.0625
NCTC 8325-B1	1
NCTC 8325-B2	0.5
NCTC 8325-B3	0.125*
NCTC 8325-B4	0.5
NCTC 8325-B5	0.25
NCTC 8325-B6	1
NCTC 8325-B7	2**

Preparation of apo *Sa*BPL D200E and polymorphisms in *Sa*BPL

To test the effect of the *Sa*BPL D200E mutation, the mutation was inserted into the enzyme by mutagenesis and assessed in both *in vitro* and *in vivo* systems. It is worth noting that the enzyme previously used for characterisation of all the inhibitors to date was derived from the methicillin resistant strain *S. aureus* Mu50 which contains 3 polymorphisms between it and the NCTC 8325 enzyme **(see figure s15)**. The D200 residue however is conserved in all strains (**figure s16**). As the Mu50 BPL has more conserved residues compared with other *S. aureus* strains and has previously been characterised both *in vitro* [7, 17, 28] and *in vivo* [Satiaputra et al, unpublished] it was decided to continue using this system for analysis. The recombinant protein was purified in the apo-state for further *in vitro* characterisation with the apo-state of the purified *Sa*BPL D200E verified using native mass spectrometry. This indicated no biotinyl-5′-AMP had co-purified with the recombinant *Sa*BPL. Apo-*Sa*BPL (wild-type) was also purified and verified in the same manner.

***Sa*BPL D200E acts by disruption of dimerization and hence transcriptional repression.**

The effect of the D200E mutation on *Sa*BPL catalytic activity was determined by comparing the D200E mutant to wild type *Sa*BPL in an enzyme assay. The affinity for biotin was modestly altered in the mutant with the K_m for wild type 1.8 ± 0.3 μM, and D200E mutant BPL, 3.8 ± 0.4 μM ($p < 0.05$). However, the inhibitory activity of **9** was not affected with K_i for the wild type 4.8 ± 2.1 nM, and D200E mutant 10.9 ± 3.5 nM not significantly different ($p = 0.18$). The velocity (V_{max}) of the enzymes was also not altered by the mutation. We reasoned due to its location that the mutation may exert its effect on the dimerization of the protein. The dimerisation ability of *Sa*BPL D200E was therefore analysed using native nano-electrospray ionization mass spectrometry. Previous studies have shown the wild type *Sa*BPL is monomeric in solution, but dimerises in the presence of the reaction intermediate [25]. This dimerization is prevented by the presence of a F123G mutation [[28]Satiaputra et. al unpublished]. We similarly observed that the holo-*Sa*BPL dimerises at concentrations as low as 10 μM. The D200E mutation however prevents the formation of the dimer in both the apo and holo state **(table 4, figure s14)** at the highest concentrations tested (≤ 90 μM). This approach provided sufficient resolution to confirm that the reaction intermediate, biotinyl-5′-AMP, is bound in the active site, indicating the lack of dimerization is not due to inability to catalyse the production of the co-repressor.

Table 4: Native ESI-MS analysis of apo and Holo *Sa*BPL D200E and wild-type *Sa*BPL. Summary of molecular weight and protein species detected by ESI-MS for *Sa*BirA D200E and wild-type *Sa*BirA. The predicted and the detected molecular weight (MW) in the absence and presence of biotinyl-5′-AMP (MW =573 Da), as well as the oligomeric state are presented.

***Sa*BirA Sample**	**Measured MW (Da)**	**Complex components**	**Calculated MW (Da)**
Apo-wild type *Sa*BirA 10 µM	37892	Monomer	37892
Holo-wild type *Sa*BirA 10 µM	38470 76925	Monomer, biotinyl-5′-AMP bound Dimer, biotinyl-5′-AMP bound	38466 76931
Apo-*Sa*BirA D200E 1.4 µM	37916	Monomer	37905
Holo-*Sa*BirA D200E 1.4 µM	38488	Monomer, biotinyl-5′-AMP bound	38479
Apo-*Sa*BirA D200E 11.25 µM	37919	Monomer	37905
Holo-*Sa*BirA D200E 11.25 µM	38484	Monomer, biotinyl-5′-AMP bound	38479
Apo-*Sa*BirA D200E 22.5 µM	37912	Monomer	37905
Holo-*Sa*BirA D200E 22.5 µM	38488	Monomer, biotinyl-5′-AMP bound	38479
Apo-*Sa*BirA D200E 45 µM	37915	Monomer	37905
Holo-*Sa*BirA D200E 45 µM	38489	Monomer, biotinyl-5′-AMP bound	38479
Apo-*Sa*BirA D200E 90 µM	37915	Monomer	37905
Holo-*Sa*BirA D200E 90 µM	38486	Monomer, biotinyl-5′-AMP bound	38479

To determine the effect of this inability to dimerise on transcriptional repression apo-purified *Sa*BPL D200E was compared to the wild-type using EMSA and a previously established *in vivo* transcriptional reporter system in *E. coli* [Satiaputra et. al, unpublished]. For the apo protein both wild-type *Sa*BPL and *Sa*BPL D200E showed similar binding in an EMSA, with a minimum concentration required of 20 nM to bind *bioO* and 39 nM-78 nM for binding *bioY* (**Figure 7**). Both apo-*Sa*BPL wild-type and apo-*Sa*BPL D200E also failed to give 100% binding at the given concentrations, as indicated by the appearance of unbound probes. The minimal concentration of wild-type holo-*Sa*BPL required was significantly reduced compared to the apo-state, with 3.12 nM for both *bioO* and *bioY*. This concentration was significantly lower than that of the holo-*Sa*BPL D200E which exhibited binding at concentrations more similar to that of the apo-protein with 10 nM and 19 nM respectively (**Fig. 8**). A difference was also observed in the amount of probe bound, with 100% binding of the holo-*Sa*BPL wild-type to both probes at 50 nM for wild type holo-*Sa*BPL, whilst *Sa*BPL D200E required 156 nM to completely bind *bioO* and failed to generate a complete binding to *bioY* at the highest concentration tested (156 nM, **Fig. 8d**). This result supported that the dimerization capability of the holo-*Sa*BPL D200E, and hence interaction with *SabioY*, was compromised. To determine if this dimerization defect was biologically relevant, an *in vivo* β-galactosidase assay was employed using *E. coli* reporter strain. Previously developed tools for the site specific integration of genetic elements into the *E. coli* genome were used to generate the required *E. coli* strains **(figure s11)** [43], with strains harbouring the wild type *Sa*BPL and another dimerization mutant, *Sa*BPL F123G [28] analysed alongside the *Sa*BPL D200E. The repressor activity of the varied BPLs against *S. aureus bioO* and *bioY* promoters was determined by calculating the concentration of biotin required for 50% reduction of lacZ activity (K_R). The results showed a 3.2 fold difference ($p < 0.05$) in biotin concentration required for repression of the *bioO* reporter between wild type ($K_R = 4.3 \pm 1.9$ nM) and the D200E mutant ($K_R = 13.9 \pm 3.4$ nM), similar to that seen with the F123G ($K_R = 15.3 \pm 3.5$

nM) **(Fig. 7a)**. A larger difference was observed against *bioY* where wild type BPL (K_R = 8.2 ± 0.7 nM) repressed at vastly lower concentrations than the D200E and F123G (K_R >500 nM). For the D200E mutant repression to basal levels was not observed even at 500 nM biotin (**Fig. 7b**). This was consistent with the EMSA analysis which suggested that disruption of dimerization had a greater impact on binding to the *bioY* promoter sequence. These results show that although *Sa*BPL D200E is capable of binding DNA it generates weaker interactions with DNA than the wild-type protein in liganded form. This suggests that *S. aureus* containing the D200E mutation may have elevated rate of *de novo* biotin synthesis and transport.

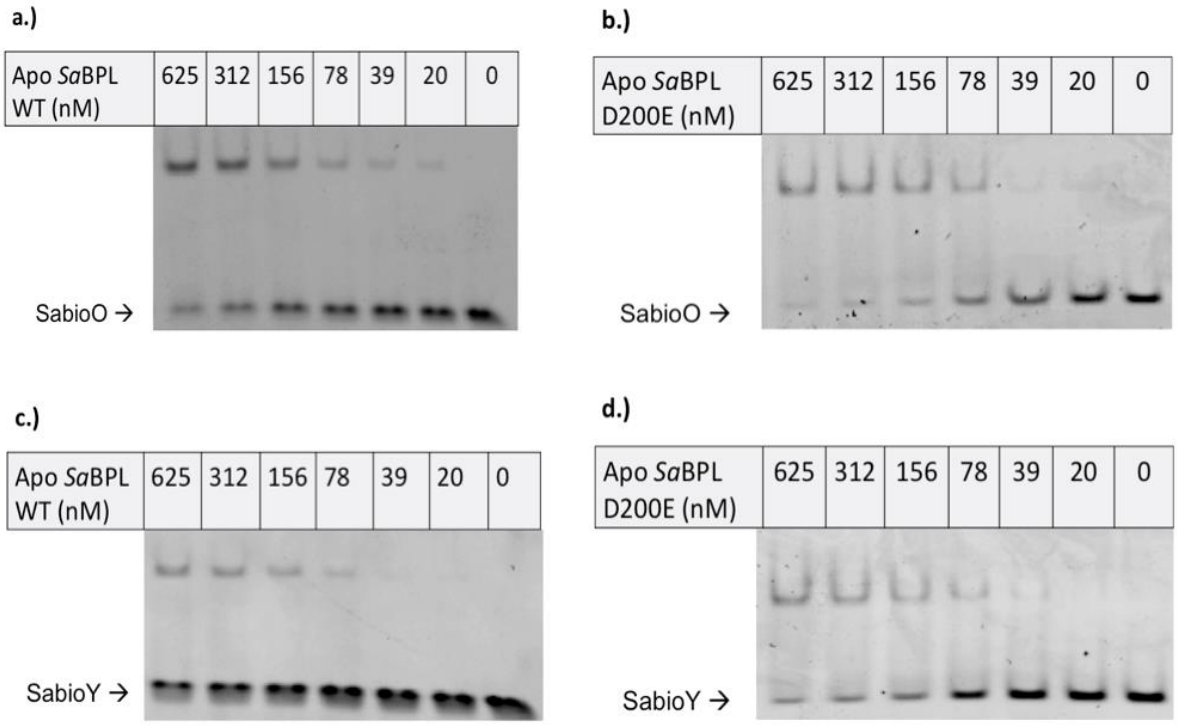

Figure 7: EMSA analysis of apo-*Sa*BPL D200E vs. apo-*Sa*BPL wild-type. a.) *Sa*BPL wild-type binding to *SabioO*, b.) *Sa*BPL D200E binding to *SabioO*, c.) *Sa*BPL wild-type binding to *SabioY* and d.) *Sa*BPL D200E binding to *SabioY*. EMSA was performed in standard binding buffer (50 mM Tris pH 8.0, 50 mM NaCl, 1 mM ATP, 1 mM $MgCl_2$ and 10% (v/v) glycerol) without the addition of biotin. 10 nM of double stranded oligo containing either *SabioO* or *SabioY* operator sequence was used per reaction. Varying concentration of *Sa*BPL was used, as indicated.

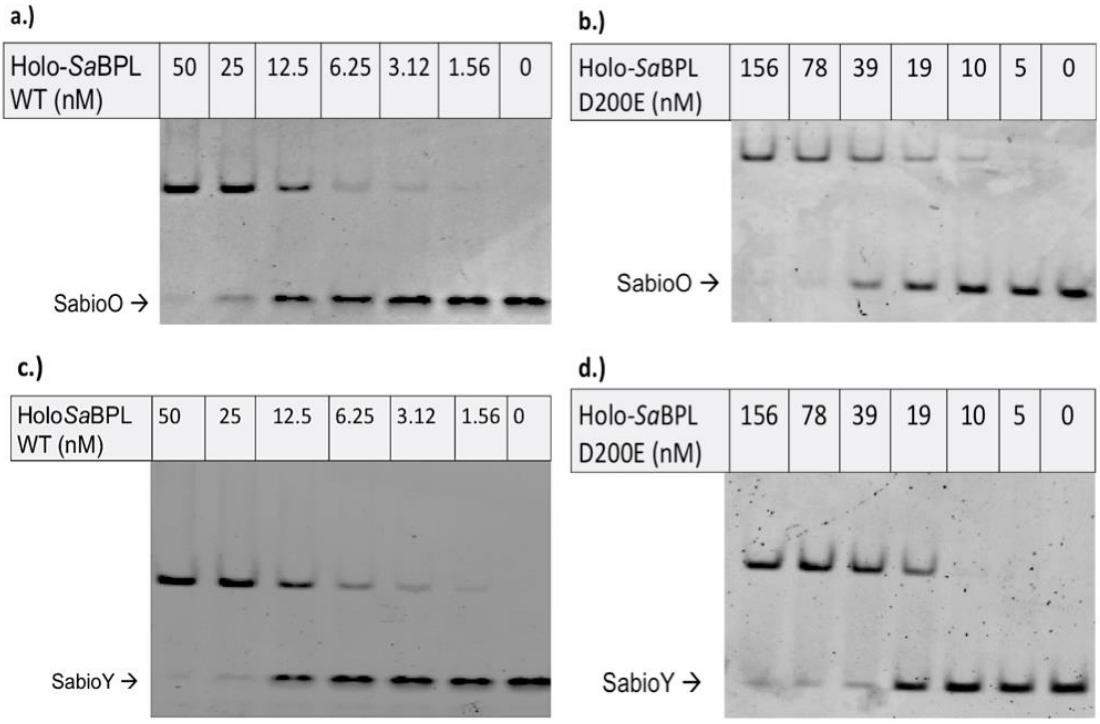

Figure 8: EMSA analysis of Holo wild-type *Sa*BPL compared to Holo-*Sa*BPL D200E . a.) *Sa*BPL wild-type binding to *SabioO*, b.) *Sa*BPL D200E binding to *SabioO*, c.) *Sa*BPL wild-type binding to *SabioY* and d.) *Sa*BPL D200E binding to *SabioY*. EMSA was performed in standard binding buffer (50 mM Tris pH 8.0, 50 mM NaCl, 1 mM ATP, 1 mM $MgCl_2$ and 10% (v/v) glycerol) with the addition of 0.1 mM biotin. 10 nM of double stranded oligo containing either *SabioO* or *SabioY* operator sequence was used per reaction. Varying *Sa*BPL concentration was used, as indicated.

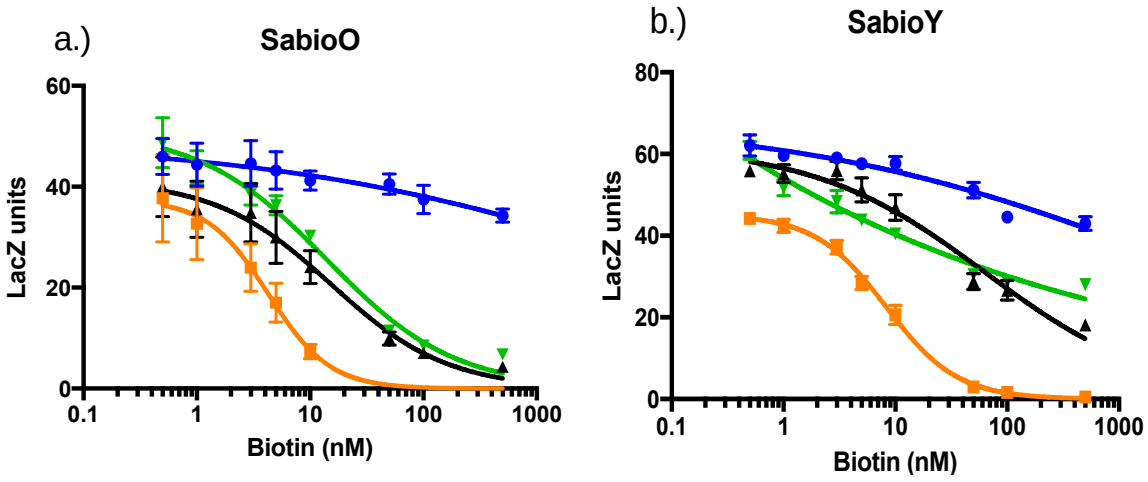

Figure 9: *In vivo* β-galactosidase assay of *Sa*BPL D200E *In vivo* assay was carried out in an *E. coli* reporter strain containing chromosomally integrated repressor and promoter constructs. *LacZ* units were calculated by subtracting the value generated by the control strain containing no integrated promoter construct (*LacZ* unit ≤ 10) from each biotin concentration. β-galactosidase assay showing the repression of (a.) *SabioO* and (b.) *SabioY* by *Sa*BPL D200E (green), *Sa*BPLF123G (black) and *Sa*BirA wild-type *Sa*BPL (yellow). No-repressor control represented in (blue). Error bars represent S.E.M from independent biological replicate (n = 6).

Table 5: Summary of $K_{R\ biotin}$ obtained from *in vivo* β-galactosidase assay. The amount of biotin to reach half-maximum repression (K_R) was calculated from the results generated in **Figure 9,** using Graphpad Prism. Significance of *SabioO* result was determined by two tailed t-test against wild type * $p < 0.05$.

SaBPL	**Promoter**	**Half maximum repression $K_{R\ biotin}$ (nM)**
Wild type	**SabioO**	**4.3 ± 1.9**
F123G	**SabioO**	**15.3 ± 3.5 ***
D200E	**SabioO**	**13.9 ± 3.4 ***
Wild type	**SabioY**	**8.2 ± 0.7**
F123G	**SabioY**	**≥ 500**
D200E	**SabioY**	**≥ 500**

Discussion

The removal of the ribosyl moiety from the literature compound bio-AMS **8** to create **9** vastly improved anti-staphylococcal activity with a ≥ 400 fold decrease in MIC. This improvement in activity was constrained to *S. aureus* species and a concomitant decrease in activity in *M. tuberculosis* was observed. Small changes in this compound structure were also able to drastically reduce activity. This was exemplified by the other sulfonyl compounds which showed limited efficacy in both enzymatic and antimicrobial assays. Unlike the 1,2,3-triazole parent **6** the benzaloxazolone moiety was not well tolerated in the sulfonyl based compound **11** with a greater than 700 fold reduction in K_i. This was unexpected however the crystal structure gives some insight into why it may have occurred. The lack of hydrogen bonding interactions in the adenine binding pocket without the extra interactions mediated by the π-π stacking with the triazole linker could feasibly reduce binding affinity resulting in weaker inhibition. Similarly the lack of inhibitory activity exhibited by **10** is thought to be a result of the removal of the carbonyl H-bonding with K187. These interactions are therefore likely key to binding and future development should attempt to maintain their presence with the sulfonyl linker.

This study also addresses several of the underlying questions around the mechanism of action and resistance to BPL inhibitors. In particular the ability for **9** to act as a co-repressor through facilitating transcriptional repression of both *bioO* and *bioY* suggests this may play a role in the antibacterial activity. Interestingly whilst both biotin and **9** showed similar kinetics in the EMSA and in *S. aureus,* **9** was unable to induce repression in the *in vivo E. coli* system (unpublished observations). Knowing that **9** is capable of repressing these transcripts in *S. aureus* suggests it is incapable of entering the *E. coli* cell. The resistance studies further supported a role of transcriptional repression on antibacterial activity. The D200E mutations role in dimerization and repression is consistent with previous mutagenesis studies in both *S.*

aureus BPL and *E. coli* BPL which indicated that modification of residues involved in the dimerization interface can affect repressor ability. These mutations, F123G [28] and D197Y [46, 47] for *Sa*BPL and *E. coli* BPL respectively, drastically effect transcriptional regulation of their controlled genes (Satiaputra et al., unpublished [46, 47]). In particular the *in vivo* lacZ assay confirmed that this reduction in dimerization led to weaker repression of both *bioO* and *bioY* with the K_R for biotin strikingly high for *bioY* (≥ 500 nM). Considering the predicted intracellular biotin concentration is between 10-100 nM [19, 48], the mutant strain would have to accumulate ≥ 5-fold intracellular biotin concentration, compared to strains with wild-type *Sa*BPL in order to terminate the transcription of biotin transporter protein. It would not be surprising if *bioY* is being expressed constitutively *in vivo*, based on these facts. It is reasonable to conclude that as a result of these increases in both *de novo* synthesis and biotin transport, the cells containing the *Sa*BPL D200E mutation would accumulate more intracellular biotin. This presumably helps outcompete **9**, occupying the active site of *Sa*BPL. Supporting this is the mechanism of action assay, with increasing biotin concentrations reducing compound efficacy. This competitive binding mechanism is not uncommon in resistance development involving vitamin biosynthesis, as suggested by previous studies in antimicrobial resistance [12, 49, 50]. The resistance mechanism is similar to one seen for thiamine synthesis inhibition, where the binding site of the thiamine riboswitch ligand binding site is altered to prevent repression by the mimic pyrithiamine, dysregulating thiamine synthesis as a means of resistance [49]. It is important to note however that this mutation likely does not act in isolation, with stepwise increases in resistance observed in the resistant populations. Whilst the effect of the mutation can be elucidated, without a clearer understanding of the other mutations present, the exact impact of this individual mutation cannot be accurately assessed.

The studies outlined here using **9** have shed some light on the role of DNA binding on antibacterial efficacy of BPL inhibitors. Further development of this series of compounds, maintaining DNA binding and high potency, will hopefully lead to a valid pre-clinical candidate. In particular the synergistic effect seen between 9 and the antibiotics methicillin and streptomycin bodes well for BPL inhibitors clinical use, as does the low spontaneous resistance rate. As well, the single resistance mechanism elucidated here is part of a larger picture, with 6 of 7 strains not demonstrating mutations in the BPL target. Understanding the other mutations correlated with resistance in these strains as well as any additional mutations present in the strain NCTC8325-B7 will help immensely in further understanding the way BPL inhibition affects the cell. Studies to address this are currently underway.

REFERENCES

1. Boucher, H.W., et al., *Bad bugs, no drugs: no ESKAPE! An update from the Infectious Diseases Society of America.* Clin Infect Dis, 2009. **48**(1): p. 1-12.
2. Cooper, M.A. and D. Shlaes, *Fix the antibiotics pipeline.* Nature, 2011. **472**(7341): p. 32-32.
3. Butler, M.S., M.A. Blaskovich, and M.A. Cooper, *Antibiotics in the clinical pipeline at the end of 2015.* J Antibiot, 2016.
4. World Health Organisation, *Antimicrobial resistance: Global report on resistance.* 2014.
5. *Review on Antimicrobial Resistance. Antimicrobial Resistance: Tackling a Crisis for the Health and Wealth of Nations*. 2014.
6. Tommasi, R., et al., *ESKAPEing the labyrinth of antibacterial discovery.* Nat Rev Drug Discov, 2015. **14**(8): p. 529-42.
7. Paparella, A.S., et al., *Structure guided design of biotin protein ligase inhibitors for antibiotic discovery.* Curr Top Med Chem, 2014. **14**(1): p. 4-20.
8. Polyak, S.W., et al., *Biotin Protein Ligase from Saccharomyces cerevisiae THE N-TERMINAL DOMAIN IS REQUIRED FOR COMPLETE ACTIVITY.* J Biol Chem, 1999. **274**(46): p. 32847-32854.
9. Chaudhuri, R.R., et al., *Comprehensive identification of essential Staphylococcus aureus genes using Transposon-Mediated Differential Hybridisation (TMDH).* BMC Genomics, 2009. **10**: p. 291.
10. Forsyth, R.A., et al., *A genome-wide strategy for the identification of essential genes in Staphylococcus aureus.* Mol Microbiol, 2002. **43**(6): p. 1387-400.
11. Payne, D.J., et al., *Drugs for bad bugs: confronting the challenges of antibacterial discovery.* Nat Rev Drug Discov, 2007. **6**(1): p. 29-40.
12. Polyak, S.W., et al., *Structure, function and selective inhibition of bacterial acetyl-coa carboxylase.* Appl Microbiol Biotechnol, 2012. **93**(3): p. 983-92.
13. Yao, J. and C.O. Rock, *Bacterial Fatty Acid Metabolism in Modern Antibiotic Discovery.* Biochimica et Biophysica Acta (BBA)-Molecular and Cell Biology of Lipids, 2016.
14. Soares da Costa, T.P., et al., *Biotin analogues with antibacterial activity are potent inhibitors of biotin protein ligase.* ACS Med Chem Lett, 2012. **3**(6): p. 509-14.
15. Duckworth, B.P., et al., *Bisubstrate adenylation inhibitors of biotin protein ligase from Mycobacterium tuberculosis.* Chem Biol, 2011. **18**(11): p. 1432-41.
16. Shi, C., et al., *Bisubstrate Inhibitors of Biotin Protein Ligase in Mycobacterium tuberculosis Resistant to Cyclonucleoside Formation.* ACS Med Chem Lett, 2013. **4**(12): p. 12131217.
17. Soares da Costa, T.P., et al., *Selective inhibition of Biotin Protein Ligase from Staphylococcus aureus.* J Biol Chem, 2012. **287**(21): p. 17823-17832.
18. Feng, J., et al., *New Series of BPL Inhibitors To Probe the Ribose-Binding Pocket of Staphylococcus aureus Biotin Protein Ligase.* ACS Med Chem Lett, 2016. **7**(12): p. 1068-1072.
19. Beckett, D., *Biotin sensing: universal influence of biotin status on transcription.* Annu Rev Genet, 2007. **41**: p. 443-64.
20. Benton, B.M., et al., *Large-scale identification of genes required for full virulence of Staphylococcus aureus.* J Bacteriol, 2004. **186**(24): p. 8478-89.
21. Bae, T., et al., *Staphylococcus aureus virulence genes identified by bursa aurealis mutagenesis and nematode killing.* Proc Natl Acad Sci U S A, 2004. **101**(33): p. 12312-12317.
22. Satiaputra, J., et al., *Mechanisms of biotin-regulated gene expression in microbes.* Synth Syst Biotechnol, 2016. **1**(1): p. 17-24.

23. Sternicki, L.M., et al., *Mechanisms Governing Precise Protein Biotinylation.* Trends in Biochemical Sciences, 2017.

24. Rodionov, D.A., A.A. Mironov, and M.S. Gelfand, *Conservation of the biotin regulon and the BirA regulatory signal in Eubacteria and Archaea.* Genome research, 2002. **12**(10): p. 1507-1516.

25. Beckett, D., *A conserved regulatory mechanism in bifunctional biotin protein ligases.* Protein Science, 2017.

26. Brown, P.H., et al., *The biotin repressor: modulation of allostery by corepressor analogs.* Journal of molecular biology, 2004. **337**(4): p. 857-869.

27. Pendini, N.R., et al., *Structural characterization of Staphylococcus aureus biotin protein ligase and interaction partners: An antibiotic target.* Protein Sci, 2013. **22**(6): p. 762-773.

28. Soares da Costa, T.P., et al., *Dual roles of F123 in protein homodimerization and inhibitor binding to biotin protein ligase from Staphylococcus aureus.* Mol Microbiol, 2014. **91**(1): p. 110-20.

29. Tieu, W., et al., *Improved Synthesis of Biotinol-5'-AMP: Implications for Antibacterial Discovery.* ACS Med Chem Lett, 2015. **6**(2): p. 216-20.

30. Tieu, W., et al., *Heterocyclic acyl-phosphate bioisostere-based inhibitors of Staphylococcus aureus biotin protein ligase.* Bioorg Med Chem Lett, 2014. **24**(19): p. 4689-93.

31. Park, S.W., et al., *Target-based identification of whole-cell active inhibitors of biotin biosynthesis in Mycobacterium tuberculosis.* Chem Biol, 2015. **22**(1): p. 76-86.

32. Bockman, M.R., et al., *Targeting Mycobacterium tuberculosis Biotin Protein Ligase (MtBPL) with Nucleoside-Based Bisubstrate Adenylation Inhibitors.* J Med Chem, 2015. **58**(18): p. 7349-7369.

33. Brune, I., Gotker, S., Schneider, J., Rodionov, D. A. and Tauch, A., *Negative transcriptional control of biotin metabolism genes by the TetR-type regulator BioQ in biotin-auxotrophic Corynebacterium glutamicum ATCC 13032.* J Biotechnol, 2012. **159**(3): p. 225-34.

34. Pendini, N.R., et al., *Purification, crystallization and preliminary crystallographic analysis of biotin protein ligase from Staphylococcus aureus.* Acta Crystallogr Sect F Struct Biol Cryst Commun, 2008. **64**(Pt 6): p. 520-3.

35. Chapman-Smith, A., et al., *Expression, biotinylation and purification of a biotin-domain peptide from the biotin carboxy carrier protein of Escherichia coli acetyl-CoA carboxylase.* Biochem J, 1994. **302 (Pt 3)**: p. 881-7.

36. Odds, F.C., *Synergy, antagonism, and what the chequerboard puts between them.* J Antimicrob Chemother, 2003. **52**(1): p. 1-1.

37. Garcia, L.S., *Clinical microbiology procedures handbook*. 2010: American Society for Microbiology Press.

38. Hellman, L.M. and M.G. Fried, *Electrophoretic mobility shift assay (EMSA) for detecting protein-nucleic acid interactions.* Nat Protoc, 2007. **2**(8): p. 1849-61.

39. Pope, C.F., et al., *A practical guide to measuring mutation rates in antibiotic resistance.* Antimicrob Agents Chemother, 2008. **52**(4): p. 1209-14.

40. Luria, S.E. and M. Delbrück, *Mutations of bacteria from virus sensitivity to virus resistance.* Genetics, 1943. **28**(6): p. 491.

41. Young, K., *In vitro antibacterial resistance selection and quantitation.* Curr Protoc Pharmacol, 2006. **Chapter 13**: p. Unit13A 6.

42. Friedman, L., J.D. Alder, and J.A. Silverman, *Genetic changes that correlate with reduced susceptibility to daptomycin in Staphylococcus aureus.* Antimicrob Agents Chemother, 2006. **50**(6): p. 2137-45.

43. St-Pierre, F., et al., *One-step cloning and chromosomal integration of DNA.* ACS Synth Biol, 2013. **2**(9): p. 537-41.

44. Gwynn, M.N., et al., *Challenges of antibacterial discovery revisited.* Annals of the New York Academy of Sciences, 2010. **1213**(1): p. 5-19.

45. Zeitlinger, M.A., et al., *Protein binding: do we ever learn?* Antimicrobial agents and chemotherapy, 2011. **55**(7): p. 3067-3074.

46. Wilson, K.P., et al., *Escherichia coli biotin holoenzyme synthetase/bio repressor crystal structure delineates the biotin-and DNA-binding domains.* Proc Natl Acad Sci U S A, 1992. **89**(19): p. 9257-9261.

47. Buoncristiani, M.R., P.K. Howard, and A.J. Otsuka, *DNA-binding and enzymatic domains of the bifunctional biotin operon repressor (BirA) of Escherichia.* Gene, 1986. **44**(2): p. 255-261.

48. Xu, Y. and D. Beckett, *Kinetics of biotinyl-5'-adenylate synthesis catalyzed by the Escherichia coli repressor of biotin biosynthesis and the stability of the enzyme-product complex.* Biochemistry, 1994. **33**(23): p. 7354-60.

49. Blount, K.F. and R.R. Breaker, *Riboswitches as antibacterial drug targets.* Nat Biotechnol, 2006. **24**(12): p. 1558-1564.

50. Pedrolli, D.B., et al., *A highly specialized flavin mononucleotide riboswitch responds differently to similar ligands and confers roseoflavin resistance to Streptomyces davawensis.* Nucleic Acids Res, 2012. **40**(17): p. 8662-73.

Probing the mechanism of action of BPL inhibitors in *Staphylococcus aureus* using an antibacterial sulfonyl based mimic of biotinyl-5'-AMP.

Hayes, A.J.[1*], Satiaputra, J.[1*], Paparella, A.S.[1], Sternicki, L.M.[1], Rodriguez, B.B.[2], Feng, J., Tieu, W.[2], Cini, D.[3], Heim, D.[1], Feng, Z.[1], Bell, J.M.[4], Pukala, T.L.[2], Turnidge, J.D.[4], Wilce, M.C.J.[3], Abell, A. D.[2], Booker, G.W.[1], Polyak, S.W.[1]

[1] School of Biological Sciences, University of Adelaide, South Australia 5005, Australia
[2] School of Physical Sciences, University of Adelaide, South Australia 5005, Australia
[3] School of Biomedical Science, Monash University, Victoria 3800, Australia
[4] Microbiology and Infectious Diseases Directorate, SA Pathology, Women's and Children's Hospital, South Australia 5006, Australia
*These authors contributed equally to this work

Supporting information

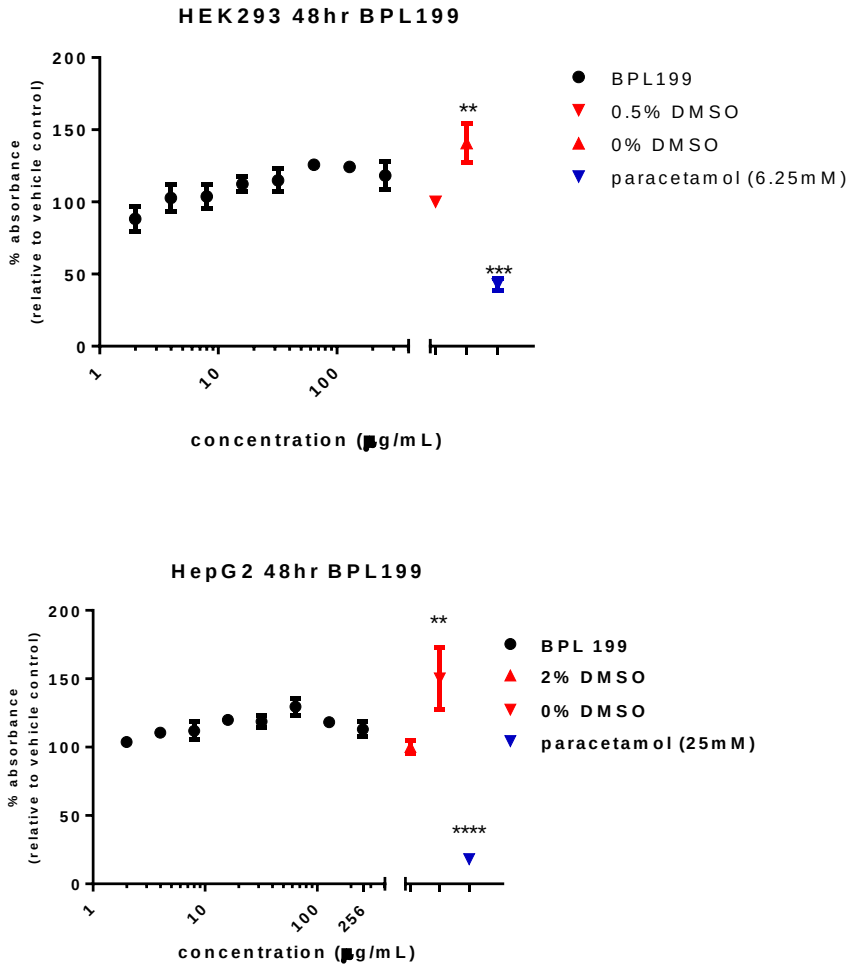

Figure s1: cytotoxicity of BPL199 was tested against both a) HEK293 and b) HepG2cell lines with paracetamol as a positive control. The WST-1 reagent was used to detect metabolic activity after 48 hours treatment. No significant toxicity was observed at any concentration. Paracetamol at 6.25mM and 25mM respectively exhibited >60% reduction of growth ($p<0.001$).

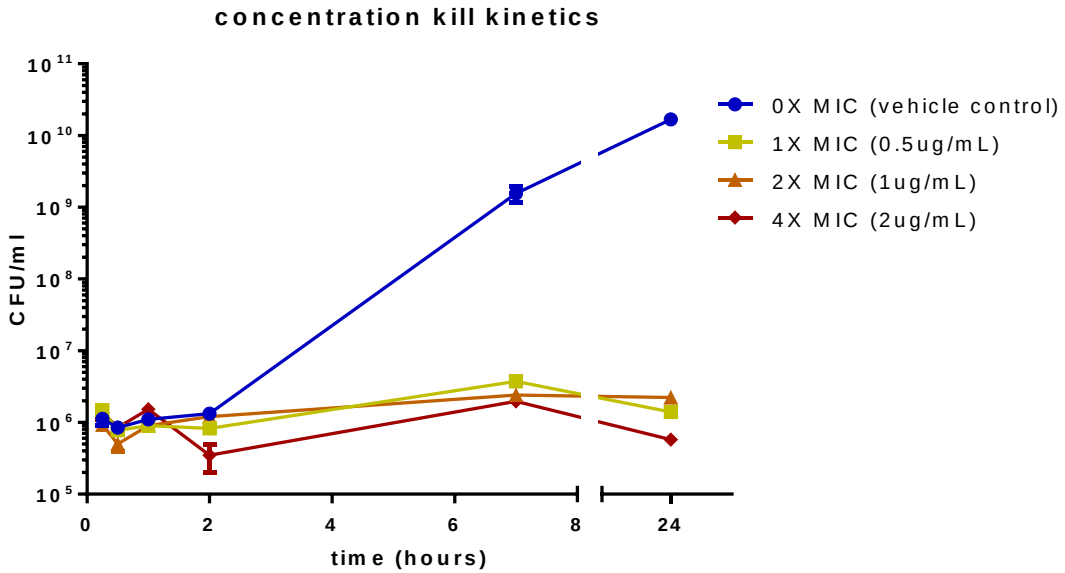

Figure s2: concentration kill kinetics. *S. aureus* ATCC49775 was grown in the presence of no compound (blue), 1× MIC (yellow squares), 2× MIC (orange triangles), 4× MIC (red diamonds) and cell numbers enumerated to determine if killing was observed.

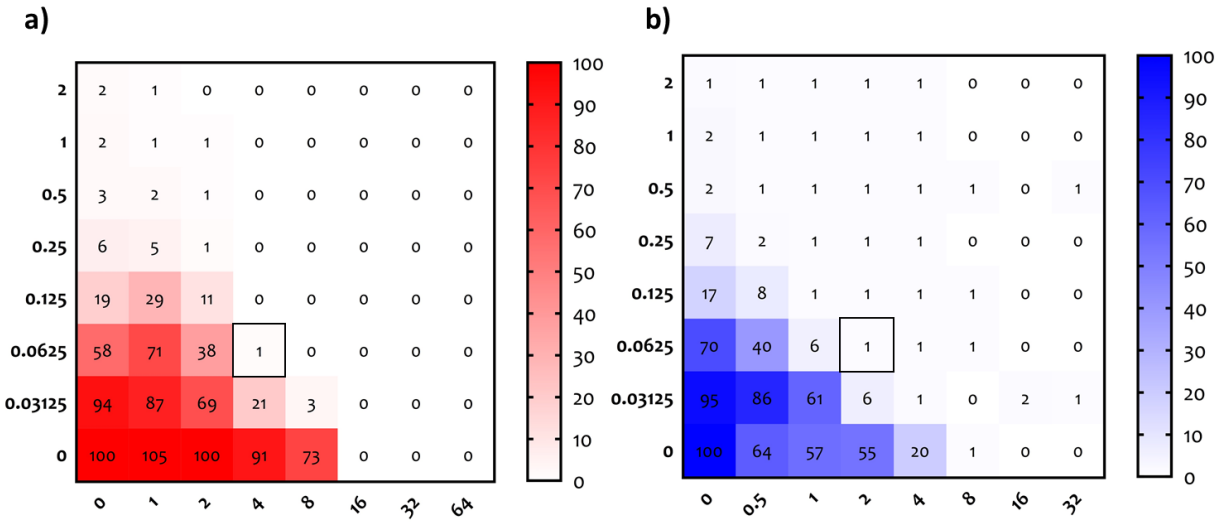

Figure s3: Checkerboard assay results with BPL199 with a) Methicillin and b) streptomycin. Due to variability in the plate reader a consistent value of ≤2% growth in separate plates (n=3) was taken as optical clarity.

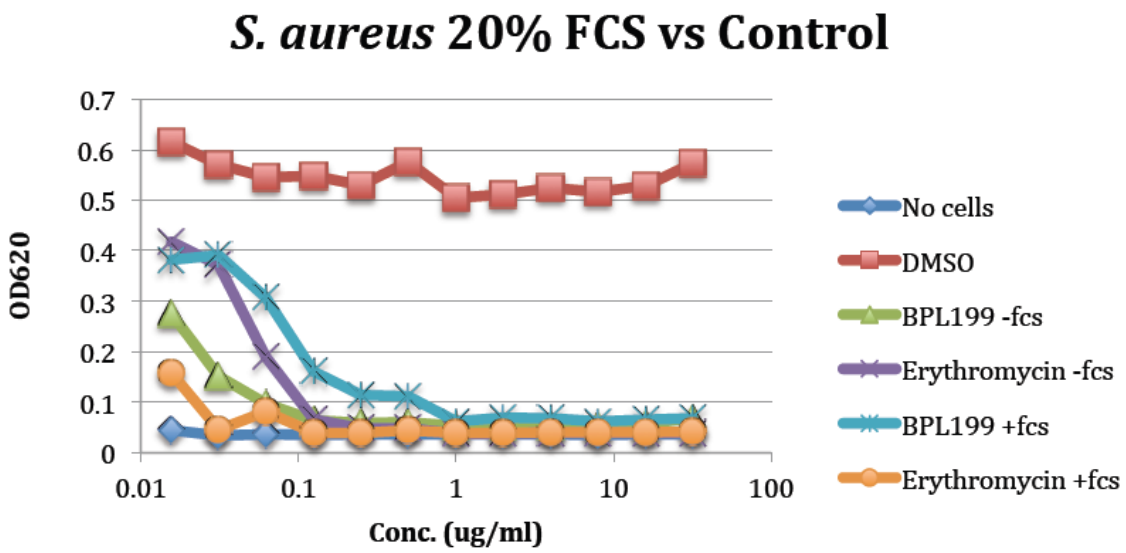

Figure s4: BPL199 antibacterial efficacy in absence of FCS (green triangles), 20% FCS (blue cross) and erythromycin control in absence (purple) and 20% FCS (orange).

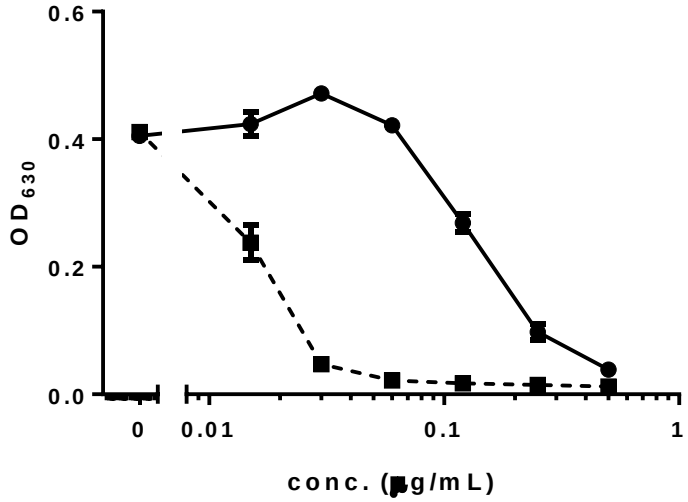

Figure s5: Mechanism of action for *S. aureus* against compound **9.** Susceptibility of *S. aureus* RN4220 containing pCN51-NcoI control (squares) and the PCN51-BPL overexpression (circles) vector.

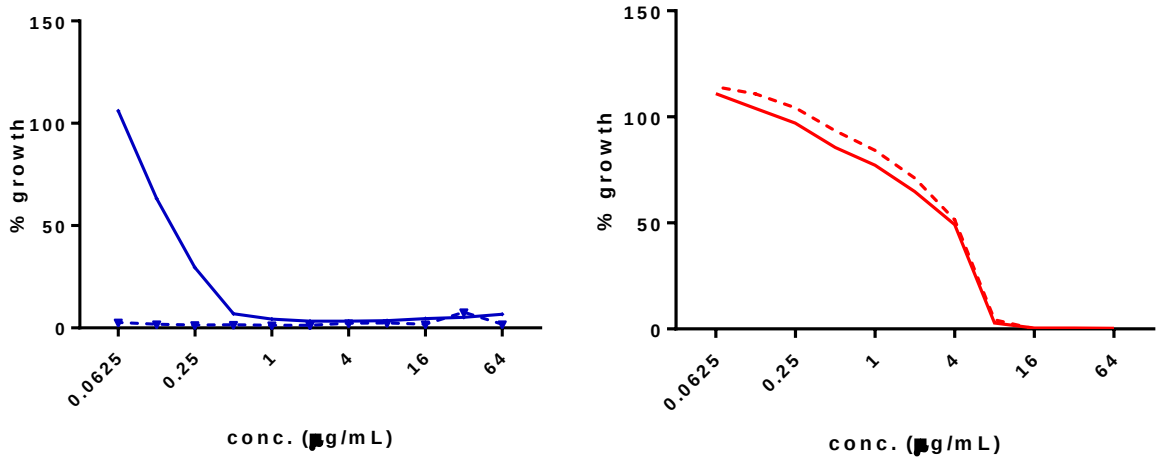

Figure s6: Mechanism of action studies. *S. aureus* RN4220 + pCN51-NcoI control (dashed line) and pCN51-BPL overexpression (solid line) vectors susceptibility to a) literature BPL inhibitor biotinol-5′-AMP and b) non BPL targeting antibiotic amoxicillin. Assays were performed in triplicate and normalised to no compound control.

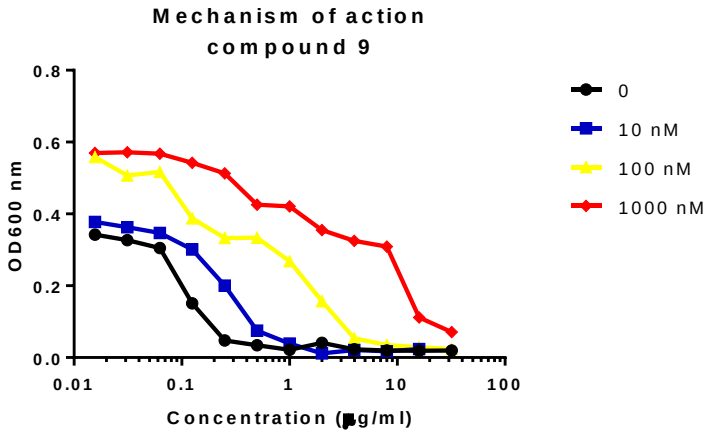

Figure s7: Effect of increased exogenous biotin concentration on antimicrobial effect of **9** against *S. aureus* ATCC 49775. No added biotin (circles), +10nM biotin (squares), +100nM biotin (triangles), +1µM biotin (diamonds).

Advanced resistance studies

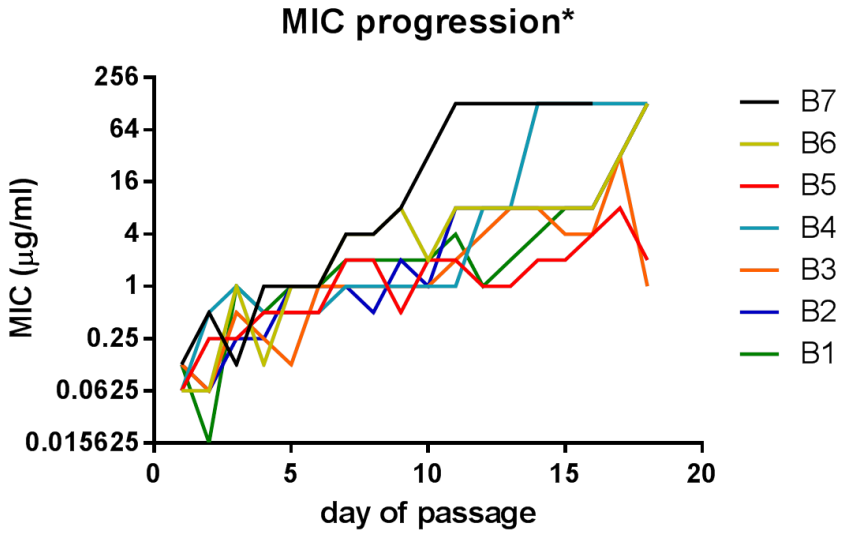

Figure s8: Progression of resistance of a constantly passaged population as determined by the well containing the highest concentration of 9 with an OD reading of >0.1. Due to the nature of the experiment no replicates were obtained. ***several of the populations exhibited susceptibility to lower concentrations of antibiotic (1-4 µg/ml) whilst growing at high (16-64 µg/mL) concentrations, the reason for this paradoxical effect is unknown but similar to that seen in several other antibiotics [1-3]**

Modelling the effect of the mutation

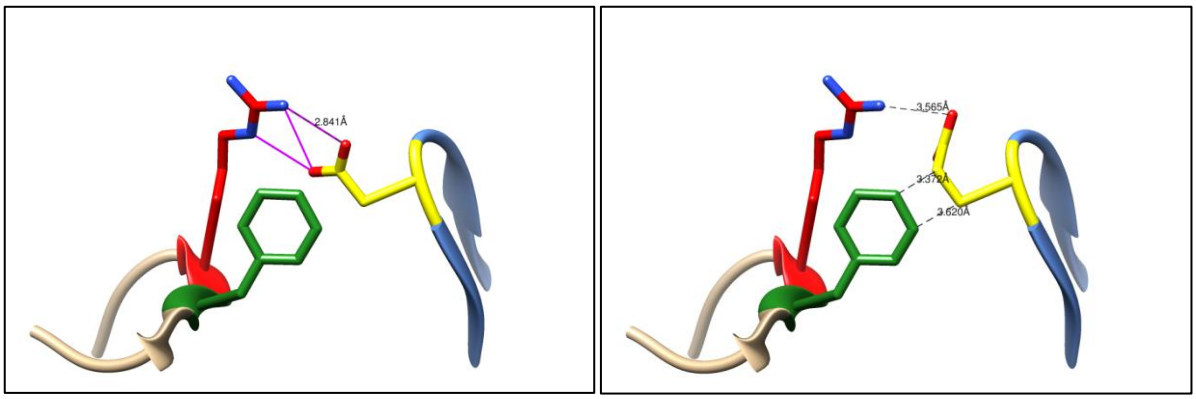

Figure s9: modelling the effect of the D200E mutation on the dimerization interface of SaBPL (Assuming lack of movement in adjacent atoms using UCSF Chimera swapaa tool). Loss of hydrogen bonding between the D200 and R122 of the opposing monomer results as the distance between the relevant residues increases to prevent steric clashes.

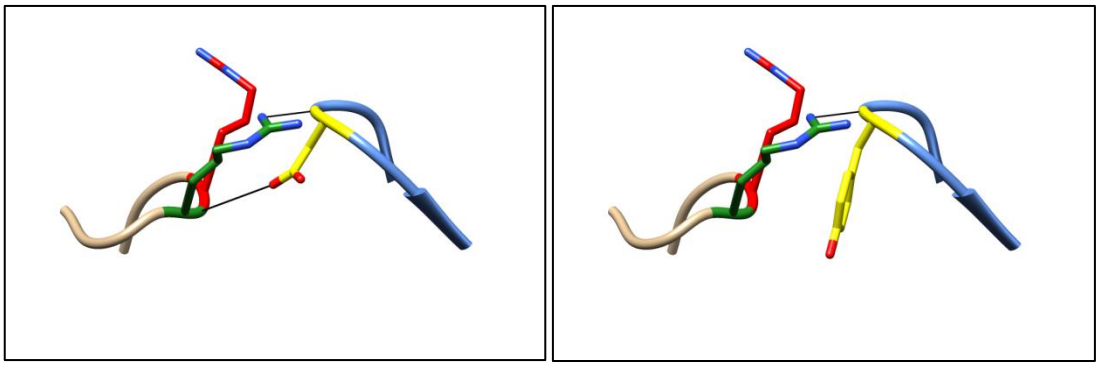

figure s10: modelling the effect of the D197Y mutation on the dimerization interface of EcBPL (Assuming lack of movement in adjacent atoms using UCSF Chimera swapaa tool). Loss of one hydrogen bonding between the D197 and backbone of R119 of the opposing monomer results as the distance between the relevant residues increases to prevent steric clashes.

Supplementary figure verifying no biotinyl co-purified

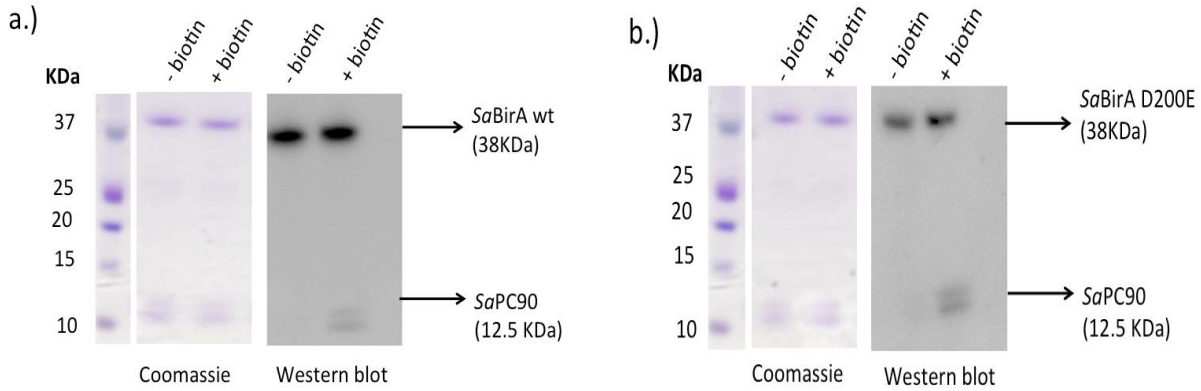

Figure s10: Confirmation of purified apo-*Sa*BirA wild-type and apo *Sa*BirA D200E. Western blot detection using Alexa 488 conjugated streptavidin was used to detect biotinylated *Sa*PC90 domain after incubation with *Sa*BPL in the presence and absence of biotin. The results for (a.) *Sa*BPL wild-type and (b.) *Sa*BPL D200E are shown. A small proportion of biotin might be covalently linked to a non-specific lysine residue within *Sa*BPL during purification, which results in detection of *Sa*BirA in Western blot. Coomassie stained gel was used as a loading control.

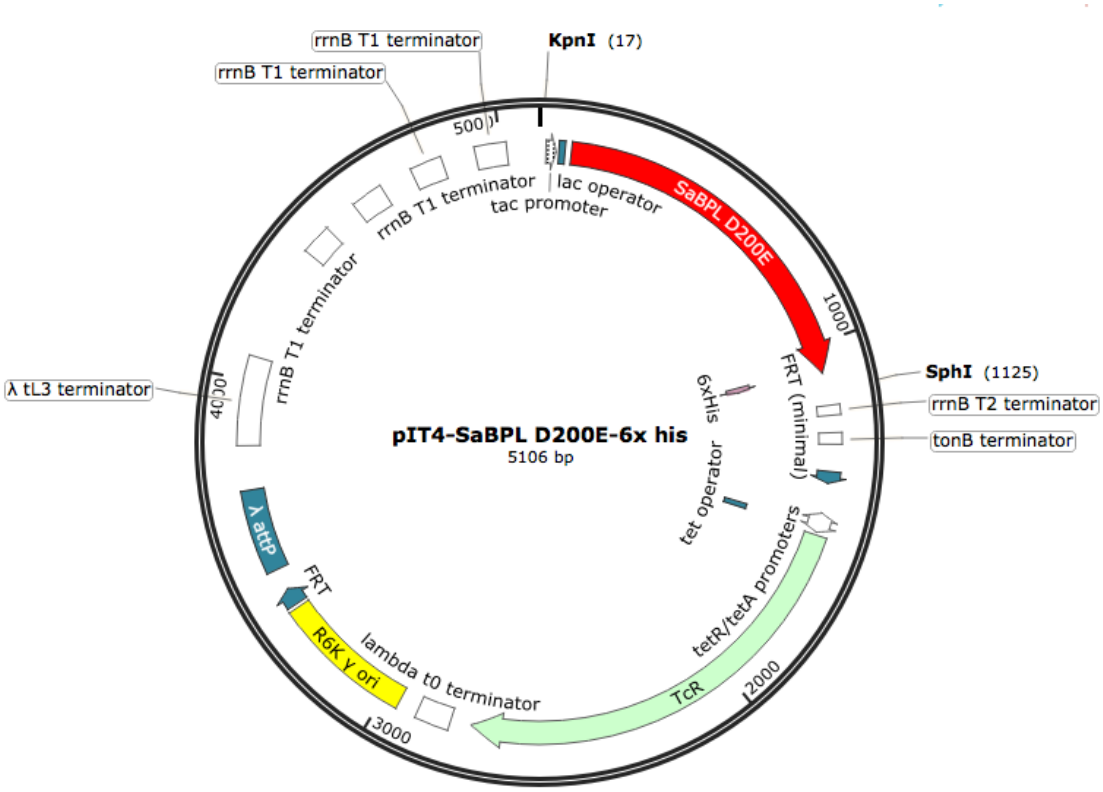

Figure S11: Integration vector containing *Sa*BPL D200E. *Sa*BPL D200E gene fused to a lac promoter was cloned into pIT4_TL_152002 integration vector targeting attB-λ phage attachement site.

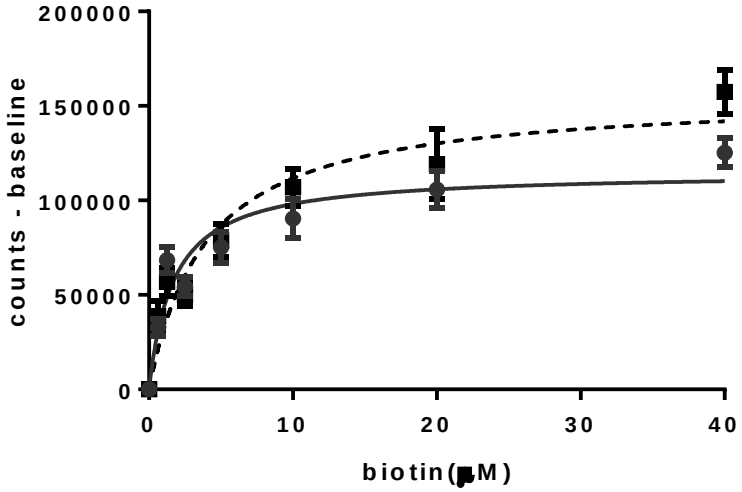

Figure s12: representative dose response for K_m determination enzyme assay with wild type (circles), and D200E (squares) *Sa*BPL in response to increased biotin concentration. Assay was performed in triplicate, error bars represent ± SEM.

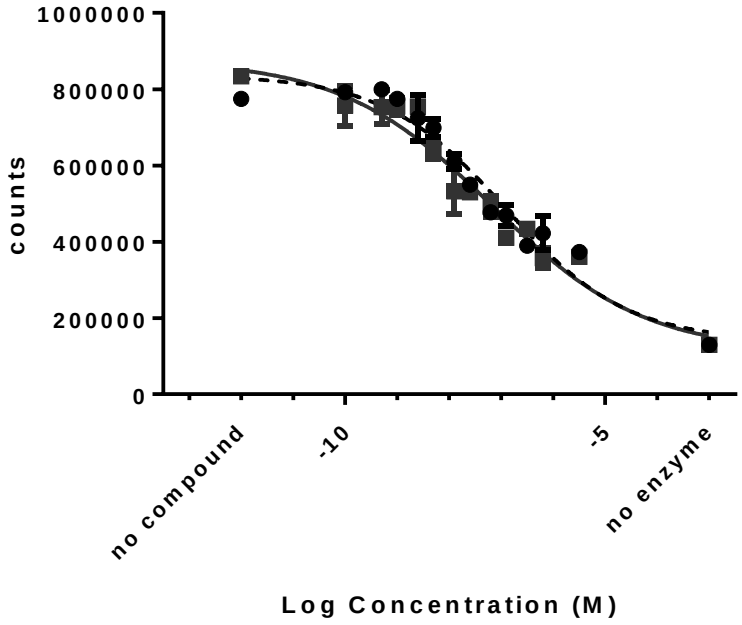

Figure s12: representative dose response for enzyme inhibition assay with wild type (circles), and D200E (squares) BPL in response to increased **9** concentrations.

a)

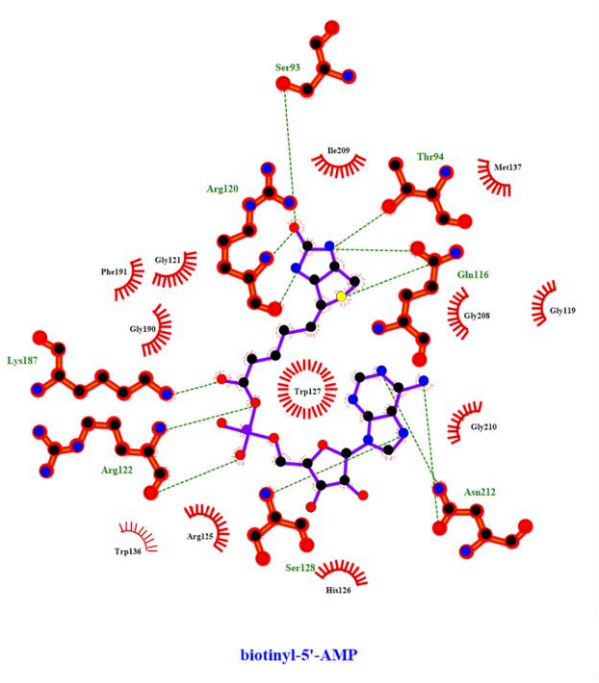

b)

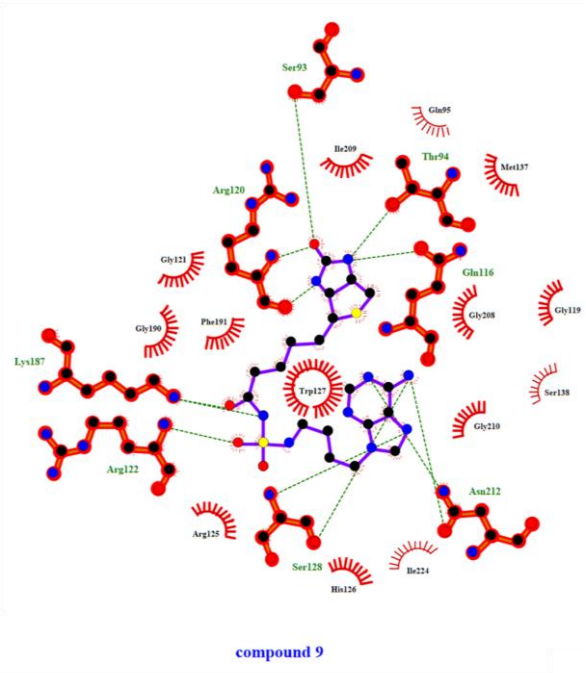

Figure s13: Interactions between a) biotinyl-5′-AMP and b) compound 9 with *Sa*BPL as determined by ligplot+ [4, 5], using their respective crystal structures. (PDB 3RIR, this study). Conserved hydrogen bonding interactions can be observed with all protein residues as well as the key π-pi stacking interaction with W127.

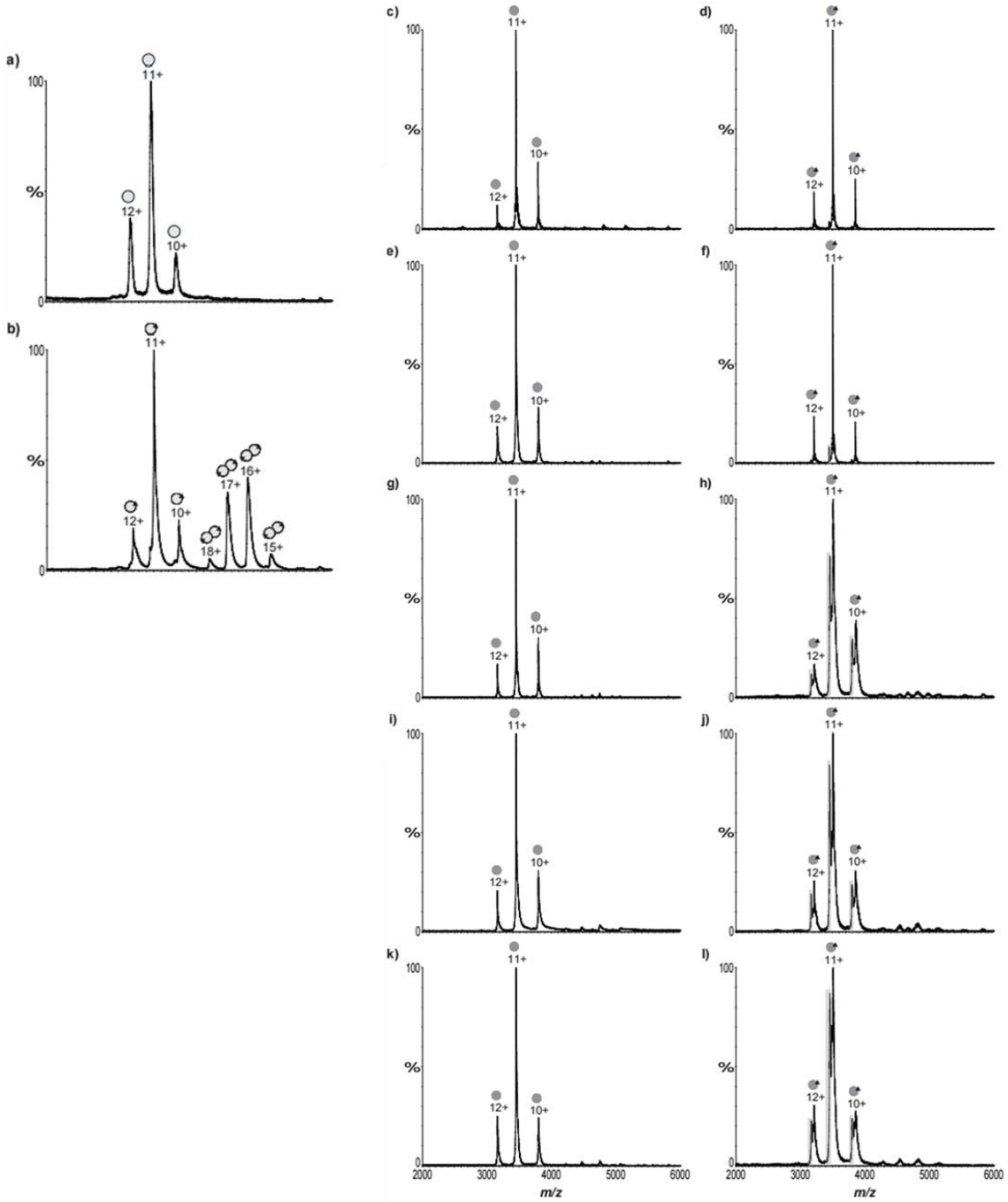

Figure s14. nESI-MS reveals *Sa*BirA D200E is a mutant devoid of dimerization independent of ligand binding. Mass spectra of **(a.)** apo-wild type *Sa*BirA at 10 μM, **(b.)** holo-wild type *Sa*BirA at 10 μM, apo-*Sa*BirA D200E at **(c.)** 1.4 μM, **(e.)** 11.25 μM, **(g.)** 22.5 μM, **(i.)** 45 μM and **(k.)** 90 μM, along with holo-*Sa*BirA D200E at **(d.)** 1.4 μM, **(f.)** 11.25 μM, **(h.)** 22.5 μM, **(j.)** 45 μM and **(l.)** 90 μM are shown. Proteins were purified in their apo states (REF protocol), whilst holo samples were prepared by incubating the apo-purified protein with 500 μM biotin, 1 mM ATP and 1 mM $MgCl_2$ prior to buffer exchange and nESI-MS analysis. Peaks representing the oligomeric state of the proteins are marked with sphere symbols, with outlined light grey circles representing wild type *Sa*BirA and dark grey circles representing *Sa*BirA D200E. Monomeric protein is represented as a single sphere and dimeric by 2 joined spheres. The presence of the biotinyl-5′-AMP ligand is represented by a black triangle. Transparent grey rectangles represent apo species in the holo samples due to the loss of ligand during buffer exchange or ionisation energy.
*Relative error of the detected MW is within the expected range of approximately 1% in 1 MDa.

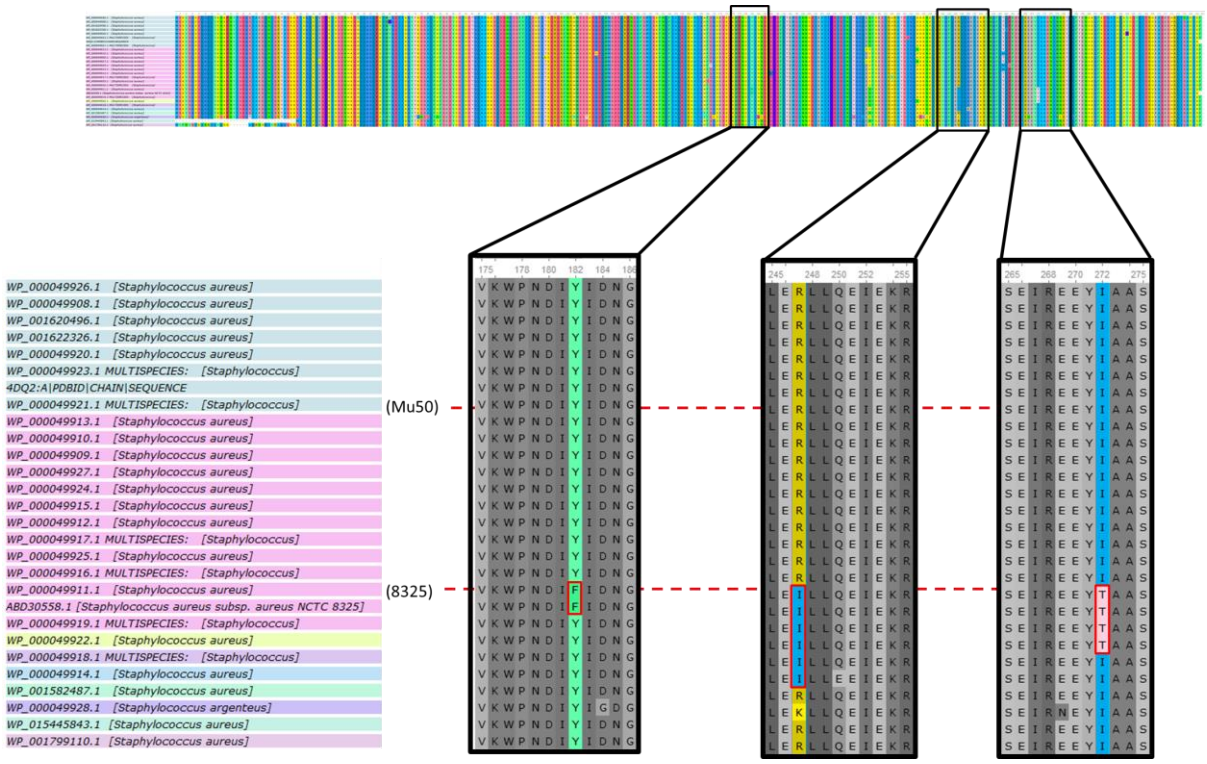

Figure s15: BPL sequences of *S. aureus* were determined as follows: the protein cluster PCLA_885364 containing 71 entries (which encompasses all non-redundant proteins identified as biotin--acetyl-CoA-carboxylase ligase in the Genus Staphylococcus) was further filtered for the clade *Staphylococcus aureus* 19988 to make a list of 26 protein sequences. These sequences were subsequently obtained and compared using UGENE [6] and aligned with clustal omega [7]. The 3 differences that are observed between the strains mu50 (PDB strain), NCTC8325 are highlighted.

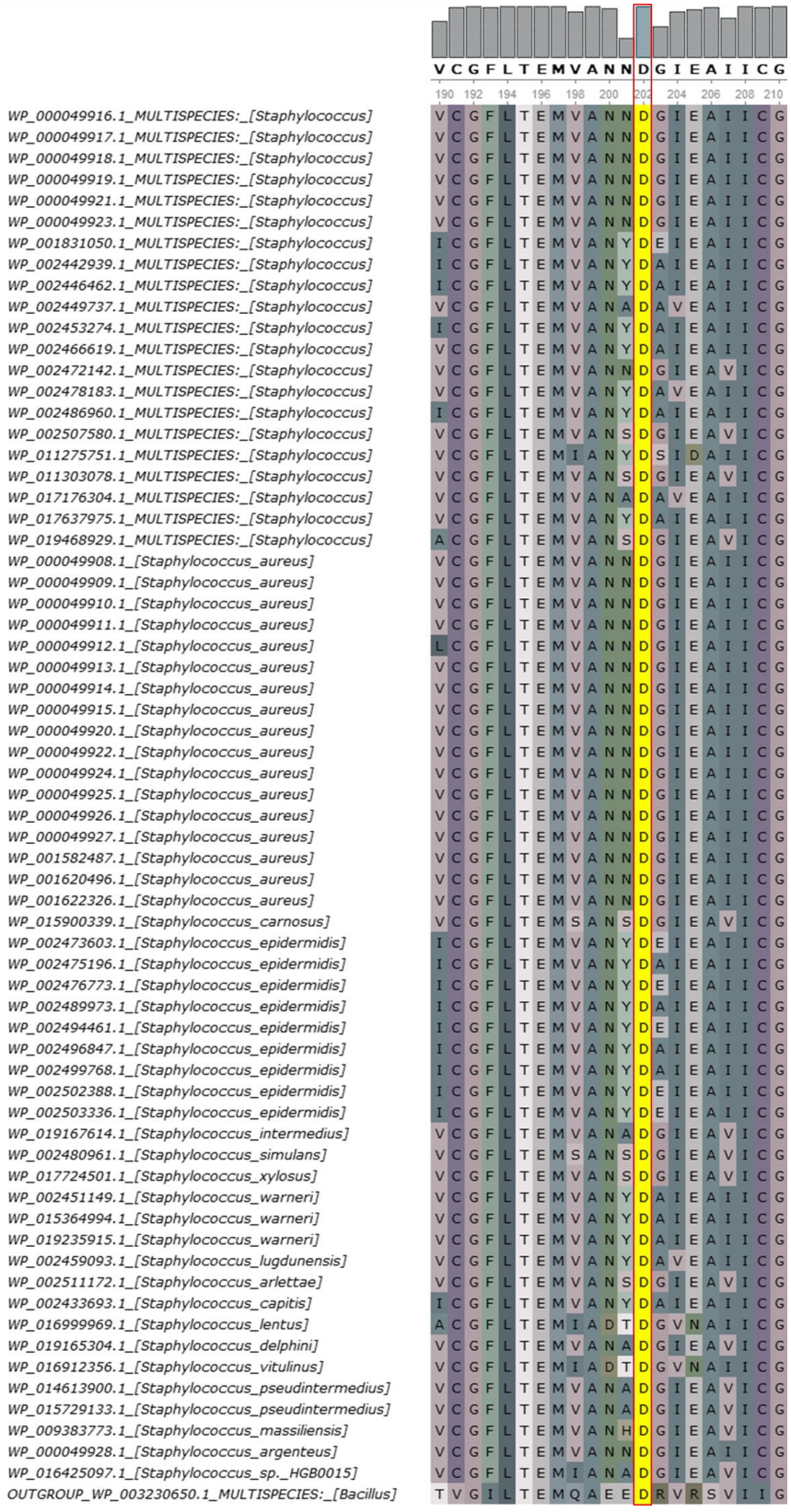

Figure s16: conservation of the D200 residue across the 71 non redundant staphylococcal BPL sequences from the protein cluster PCLA_885364 and outgroup *Bacillu subtillus.* Sequences were aligned with Clustal omega [7] and viewed using UGENE [6]

Tables

Table s1: inhibition of BPL from other clinically relevant species by compound 9

Species BPL	**K_i (nM)**
Acinetobacter calcoaceticus	212 ± 8.3 (n=3)

Table s2: Synergy with clinical antibacterial agents as determined by checkerboard assay (see figure s3)

Antibacterial agent	**Class**	**Mechanism of action**	**∑ FIC index with BPL199**	**Synergy?**
Methicillin	β-lactam	Cell wall synthesis	0.375	Yes
Streptomycin	Aminoglycosides	Protein synthesis	0.375	Yes
Vancomycin	Glycopeptides	Cell wall synthesis	0.625	No
Daptomycin	Lipopeptides	Cell membrane depolarisation; nucleotide and protein synthesis	0.625	No
Erythromycin	Macrolides	Protein synthesis	0.625	No
Chloramphenicol	Chloramphenicols	Protein synthesis	0.5625	No
Tetracycline	Tetracyclines	Protein synthesis	0.5625	No

***Sa*BirA Sample**	**Measured MW (Da)**	**Complex components**	**Calculated MW (Da)**
Apo-wild type *Sa*BirA 10 µM	37892	Monomer	37892
Holo-wild type *Sa*BirA 10 µM	38470 76925	Monomer, biotinyl-5′-AMP bound Dimer, biotinyl-5′-AMP bound	38466 76931
Apo-*Sa*BirA D200E 1.4 µM	37916	Monomer	37905
Holo-*Sa*BirA D200E 1.4 µM	38488	Monomer, biotinyl-5′-AMP bound	38479
Apo-*Sa*BirA D200E 11.25 µM	37919	Monomer	37905
Holo-*Sa*BirA D200E 11.25 µM	38484	Monomer, biotinyl-5′-AMP bound	38479
Apo-*Sa*BirA D200E 22.5 µM	37912	Monomer	37905
Holo-*Sa*BirA D200E 22.5 µM	38488	Monomer, biotinyl-5′-AMP bound	38479
Apo-*Sa*BirA D200E 45 µM	37915	Monomer	37905
Holo-*Sa*BirA D200E 45 µM	38489	Monomer, biotinyl-5′-AMP bound	38479
Apo-*Sa*BirA D200E 90 µM	37915	Monomer	37905
Holo-*Sa*BirA D200E 90 µM	38486	Monomer, biotinyl-5′-AMP bound	38479

Primers used in this study

Primer	**Sequence**	**Function**	**source**
B481	5′ -GGTTGCTAATAATGAAGGTATAGAA GCAATAATATGTGG-3′	D200E mutagenesis	This study
B482	5′ - CCACATATTATTGCTTCTATACCTTCATT ATTAGCAACC -3′	D200E mutagenesis	This study
B200	5′-GGTATAGAAGCAATAATATGT GG-3′	Internal BPL sequencing	
Lambda P1	5'-GGCATCACGGC AATATAC-3'	attp-λ PCR screening primer	(St. Pierre et al, 2013)
Lambda P2	5'-ACTTAACGGCTGACATGG-3'	attp-λ PCR screening primer	(St. Pierre et al, 2013)
Lambda P3	5'-GGGAATTAATTCTTGAAGACG-3'	attp-λ PCR screening primer	(St. Pierre et al, 2013)
Lambda P4	5'-TCTGGTCTGGTAG CAATG-3'	attp-λ PCR screening primer	(St. Pierre et al, 2013)

qPCR oligos

Target gene	Primer name	Primer sequence 5'-3'	Source
S. aureus bioD	qSA2716_F	GCAAGGTGTGGTGATACAGG	(Jiulia's thesis)
	qSA2716_R	ACACGTGGTCATCGAGTTTG	(Jiulia's thesis)
S. aureus 16s rRNA	qSA0002_F	GAACCGCATGGTTCAAAAGT	(Jiulia's thesis)
	qSA0002_R	CGTAGGAGTCTGGACCGTGT	(Jiulia's thesis)

EMSA oligos

Oligo name	Sequence 5'-3'	Description	source
DS-SaBioO oligo 1	CCTTAAATGTAAACTTTTATAATT AATAAGTTTACATTTAAG	Top strand oligo containing *sabioO* wildtype sequence	(Jiulia's thesis)
DS-SaBioO oligo 2	CCTTAAATGTAAACTTATTAATTAT AAAAGTTTACATTTAAGG	Bottom strand oligo containing *sabioO* wildtype sequence	(Jiulia's thesis)
DS-SabioY oligo 1	AACTTATTGTAAACTTTTCATTTCTT AAAGTTTACAATGGTGCT	Top strand oligo containing *sabioY* wildtype sequence	(Jiulia's thesis)
DS-SabioY oligo 2	AGCACCATTGTAAACTTTAAGAAA TGAAAAGTTTACAATAAGTT	Bottom strand oligo containing *sabioY* wildtype sequence	(Jiulia's thesis)

Strains used

Bacterial strains

Strain	***description***	function	source
E. coli DH5α	*sup*EΔ*lac*169 (p80*lac*ZΔM15) *hsdR17* *rec*A1 *end* AA1 *gyr*A96 *thi*-1 *rel*A1	**Plasmid manipulation**	(New England Biolabs, MA, USA)
E. coli BL21-CodonPlus(DE3)-RIPL	*E. coli B F⁻ ompT DhsdS ($rB^{-}mB^{-}$) $dcm^{+}Tet^{R}$ gal λ(DE3) endA Hte [argU proL Cm^{R}] [argU ileY leuW Strep/$Spec^{R}$]*	**Protein expression strain**	(Aglient Technologies, CA, USA).
S. aureus NCTC 8325	Laboratory methicillin sensitive *S. aureus* with reference genome	**parental *S. aureus* to strain B7**	American Tissue Culture Collection
S. aureus NCTC8325-B7	*S. aureus* NCTC8325 after 18 days passage BPL199 (*birA* D200E)	**Strain containing D200E mutation**	(This study)
S. aureus RN4220+PCN51-NcoI	*S. aureus* RN4220 containing control vector for mechanism of action studies	**Overexpression control**	Feng *et al.* (2016)
S. aureus RN4220+PCN51-BPL	*S. aureus* RN4220 containing vector for overexpression of *Sa*BPL for mechanism of action studies	**Overexpression vector**	Feng *et al.* (2016)

LacZ

strain	integrations	description	source
JD26186 *birA::CAT*	*bioC::KanR birA::CAT*	JD28186 strain with N-terminal CAT cassette insertion (knockout)of its endogenous *birA*	(Jiulia's thesis)
JD26186 *birA::CAT-SabioO-SaBPL*	*bioC::KanR birA::CAT (SabioO-lacZ)HK(placUV5-SaBPL)l*	JD26186 birA::CAT strain with SaBioO lacZ reporter chromosomally integrated at HK022 att site, and placUV5-SaBPL(wildtype) cassette chromosomally integrated at lambda att site.	(Jiulia's thesis)
JD26186 *birA::CAT-SabioY-SaBPL*	*bioC::KanR birA::CAT (SabioY-lacZ)HK (placUV5-SaBPL)l*	JD26186 birA::CAT strain with SaBioY-lacZ reporter chromosomally integrated at HK022 att site and placUV5-SaBPL(wildtype) cassette chromosomally integrated at lambda att site.	(Jiulia's thesis)
JD26186 *birA::CAT-SabioO-SaBPL F123G*	*bioC::KanR birA::CAT (SabioO-lacZ)HK (placUV5-SaBPL F123G)l*	JD26186 birA::CAT strain with SaBioO-lacZ reporter chromosomally integrated at HK022 att site, and plac-UV5-SaBPL (F123-monomeric mutant) cassette chromosomally integrated at lambda att site.	(Jiulia's thesis)
JD26186 *birA::CAT-SabioY-SaBPL F123G*	*bioC::KanR birA::CAT (SabioY-lacZ)HK (placUV5-SaBPL F123G)l*	JD26186 birA::CAT strain with SaBioY-lacZ reporter chromosomally integrated at HK022 att site, and plac-UV5-SaBPL (F123-monomeric mutant) cassette chromosomally integrated at lambda att	(Jiulia's thesis)
JD26186 *birA::CAT-SabioO-SaBPL D200E*	*bioC::KanR birA::CAT (SabioO-lacZ)HK (placUV5-SaBPL D200E)l*	JD26186 birA::CAT strain with SaBioO-lacZ reporter chromosomally integrated at HK022 att site, and plac-UV5-SaBPL (D200E) cassette chromosomally integrated at lambda att site.	(Jiulia's thesis)
JD26186 *birA::CAT-SabioY-SaBPL D200E*	*bioC::KanR birA::CAT (SabioY-lacZ)HK (placUV5-SaBPL D200E)l*	JD26186 birA::CAT strain with SaBioY-lacZ reporter chromosomally integrated at HK022 att site, and plac-UV5-SaBPL (D200E) cassette chromosomally integrated at lambda att	(Jiulia's thesis)

Plasmids used

Plasmid	**Description**	**Source**
pGEMT-*Sa*BPL(6xHis)	pGEMT plasmid containing *saBPL* with 6x his-tag	Pendini *et al*, (2008)
pGEMT-*Sa*BPL-D200E-(6xHis)	pGEMT plasmid containing *saBPL* D200E with 6x his-tag	This study
pIT4_TL_152002	Chromosomal integration plasmid (λ-attP, Tc^R, R6Kγ ori, *ccdB*, pUC ori)	St. Pierre, *et a*l (2013)
pIT4_TL_SaBPL (D200E)	plac-UV5 fused with SaBPL (D200E) sequence cloned into pIT4_TL_152002	This study

Supplementary methods:

Chemical synthesis of compound 9.

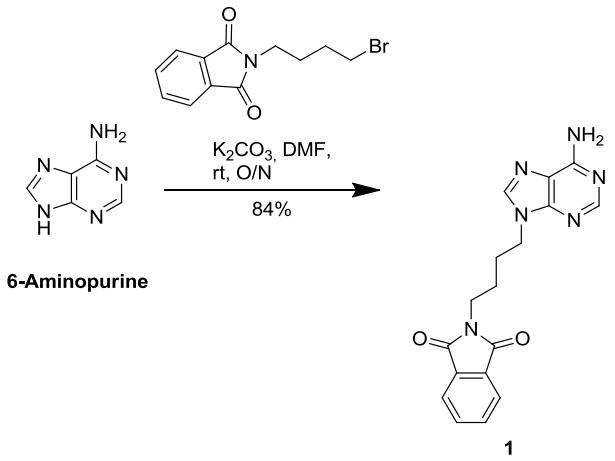

1

Synthesis of 2-(4-(6-amino-9H-purin-9-yl)butyl)isoindoline-1,3-dione

To a suspension of 6-Aminopurine (1.1 G, 8.82 mmol) in *N*,*N*-dimethylformamide (11 mL) was added potassium carbonate (1.8 G 13.23 mmol, 1.5 eq) and N-(4-bromobutyl)phthalamide (2.75 G, 9.7 mmol, 1.1 eq) and the mixture was stirred at 70 °C overnight. The mixture was allowed to cool down to room temperature and partitioned between ethyl acetate and water. The aqueous phase was extracted with ethyl acetate. The organics combined were washed with brine (x2) and water (x1), dried over sodium sulphate anh., filtrated and evaporated under reduced pressure. The solid obtained was triturated from diethyl ether affording the title compound as a pale yellow solid (2.5 G, 84%).

1H NMR (500 MHz, DMSO-*d6*): δ 8.12 (s, 1H, ArH), 8.07 (s, 1H, ArH), 7.84 (m, 4H, ArH), 7.16 (s, 2H, NH_2), 4.17 (t, *J* = 6.7 Hz, 2H, CH_2), 3.61 (t, *J* = 6.7 Hz, 2H, CH_2), 1.83 (dd, *J* = 14.7, 6.9 Hz, 2H, CH_2), 1.56 (dt, *J* = 13.8, 6.9 Hz, 2H, CH_2).
13C NMR (125 MHz, DMSO-*d6*): δ 167.9 (2xCO), 155.9 (C), 152.3 (CH), 149.5 (C), 140.8 (CH), 134.3 (2xC), 131.6 (2xCH), 123.0 (2xCH), 118.7 (C), 42.4 (CH_2), 36.8 (CH_2), 26.7 (CH_2), 25.1 (CH_2) ppm.
MS HRMS (ESI) calcd for $C_{17}H_{16}N_6O_2$ (M^+): 336.1322, found 336.1335.

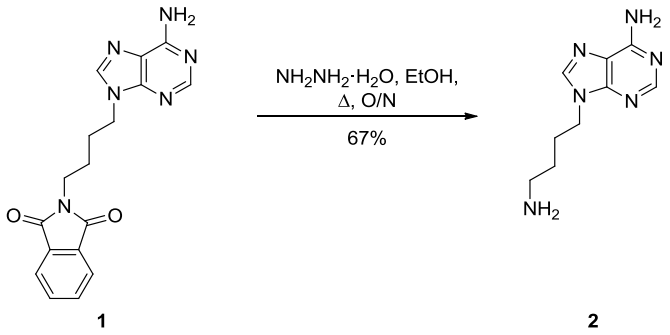

1 **2**

Synthesis of 9-(4-aminobutyl)-9H-purin-6-amine

To a suspension of 2-(4-(6-amino-9H-purin-9-yl)butyl)isoindoline-1,3-dione (2.5 G, 7.43 mmol) in ethanol (125 mL) was added hydrazine hydrate (3.5 mL, 114.45 mmol, 15 eq) and the mixture was stirred at reflux overnight. The mixture was allowed to cooled down to room temperature and concentrated under reduced pressure. A solid was formed which was filtrated and washed with dichloromethane. Trituration from methanol afforded the title compound (1G, 67%) as a colourless solid.

1H NMR (500 MHz, DMSO-*d6*): δ 8.12 (s, 1H, ArH), 8.11 (s, 1H, ArH), 7.14 (s, 2H, NH_2), 4.11 (t, *J* = 7.1 Hz, 2H, CH_2), 3.06 (br s, 2H, NH_2), 2.51 (t, *J* = 6.9 Hz, 2H, CH_2), 1.79 (dd, *J* = 14.9, 7.3 Hz, 2H, CH_2) and 1.28 (dd, *J* = 14.9, 7.3 Hz, 2H, CH_2).
13C NMR (125 MHz, DMSO-*d6*): δ 155.9 (C) 152.3 (CH), 149.5 (C), 140.8 (CH), 118.7 (C), 42.8 (CH_2), 41.0 (CH_2), 30.0 (CH_2) and 26.9 (CH_2) ppm.
MS HRMS (ESI) calcd for $C_9H_{15}N_6$ ($M-H^+$): 207.1313, found 207.1513.

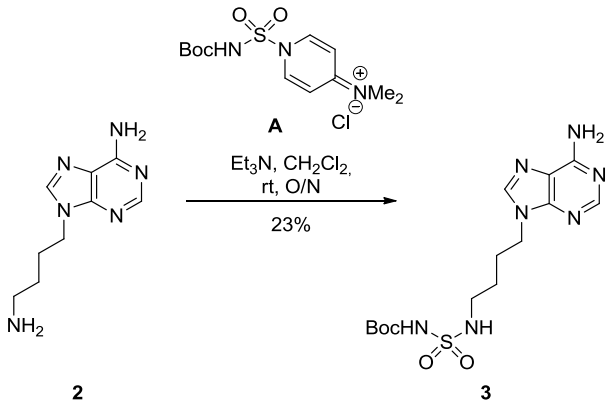

2 **3**

Synthesis of tert-butyl N-(4-(6-amino-9H-purin-9-yl)butyl)sulfamoylcarbamate

A solution of 9-(4-aminobutyl)-9H-purin-6-amine (1.6 G, 7.75 mmol, 1 eq) trietylamine (2.1 mL, 15.5 mmol, 2 eq) and **A** (2.6 G, 7.75 mmol 1 eq) in dichloromethane (15 mL) was stirred at room temperature overnight. The solvent was removed under reduced pressure. Purification by flash chromatography (5% methanol:dichloromethane) afforded the title compound (664 mg, 23%) as a colourless solid.

1H NMR (500 MHz, DMSO-*d6*): δ 10.77 (s, 1H, NH), 8.12 (s, 1H, Ar), 8.11 (s, 1H, ArH), 7.55 (br s, 1H, NH), 7.16 (s, 2H, NH_2), 4.12 (t, *J* = 7.0 Hz, 2H, CH_2), 2.90 (dd, *J* = 13.0, 6.7 Hz, 2H, CH_2), 1.82 (m, 2H, CH_2), 1.41 (m, 2H, CH_2) and 1.38 (s, 9H, *t*Bu) ppm.
13C NMR (125 MHz, DMSO-*d6*): δ 155.9 (CO), 152.3 (C), 150.6 (CH), 149.5 (C), 140.7 (CH), 118.7 (C), 81.0 (C), 42.4 (CH_2), 42.2 (CH_2), 27.7 (3xCH_3), 26.7 (CH_2), and 25.8 (CH_2) ppm.
MS HRMS (ESI) calcd for $C_{14}H_{24}N_7O_4S$ ($M-H^+$): 386.1566, found 386.1989.

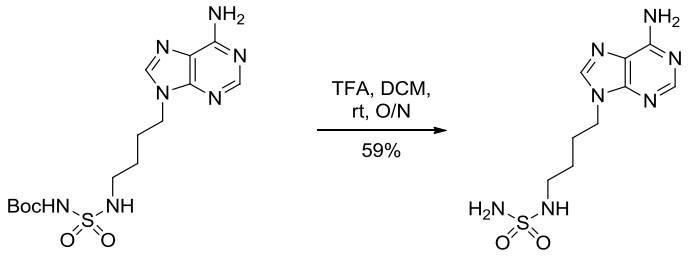

3 4

Synthesis of the sulphonamide precursor

A solution of tert-butyl N-(4-(6-amino-9H-purin-9-yl)butyl)sulfamoylcarbamate (664 mg, 1.72 mmol, 1 eq) in dichloromethane (12 mL) cooled down to 0 °C was treated with trifluoroacetic acid (1.2 mL, 15.7 mmol, 9 eq) and stirred at room temperature. After 2 h trifluoroacetic acid (1.2 mL, 15.7 mmol, 9 eq) was added. After being stirred at room temperature overnight the solvent was removed under reduced pressure. The title compound was obtained as a colourless solid (641 mg, 59%) and was used without further purification.

MS HRMS (ESI) calcd for $C_9H_{15}N_7NaO_2S$ (MNa+): 308.0906, found 308.0883.

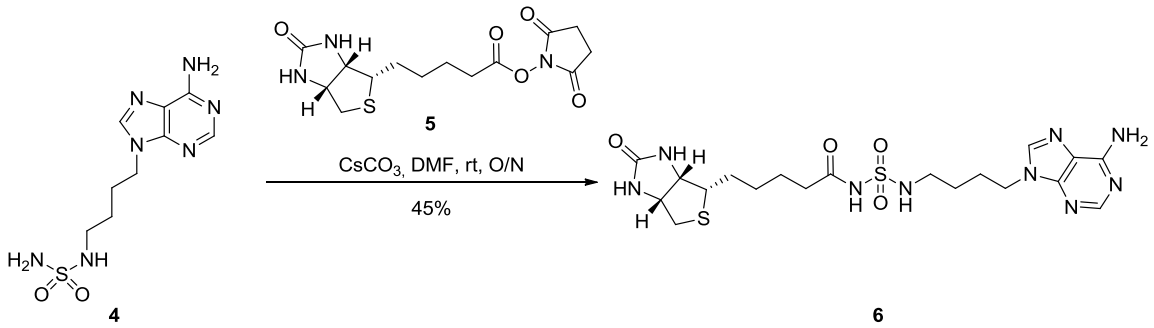

4 6

Synthesis of N-(N-(4-(6-amino-9H-purin-9-yl)butyl)sulfamoyl)-5-((4S)-2-oxohexahydro-1H-thieno[3,4-d]imidazol-4-yl)pentanamide

A suspension of the sulfonamide precursor (641 mg, 2.225 mmol, 1 eq), $CsCO_3$ (520 mg, 2.7 mmol, 1.2 eq) and B (844 mg, 2.4 mmol, 1.1 eq) in DMF (2.8 mL) was stirred at room temperature overnight. The solvent were removed under reduced pressure and the crude was purified by flash chromatography (10-20% MeOH-DCM) affording the title compound (500 mg, 45%) as a colourless solid.

1H NMR (500 MHz, DMSO-*d6*): δ 11.26 (s, 1H, NH), 8.13 (s, 1H, ArH), 8.11 (s, 1H, ArH), 7.59 (t, *J* = 5.7 Hz, 1H, NH), 7.20 (s, 2H, NH_2), 6.50 (s, 1H, NH), 6.38 (s, 1H, NH), 4.30 (dd, *J* = 7.6, 5.2 Hz, 1H, CH), 4.20–4.07 (m, 3H, CH_2+C*H*H), 3.12–3.04 (m, 1H, CH*H*), 2.88 (dd, *J* = 12.9, 6.7 Hz, 2H, CH_2), 2.80 (dd, *J* = 12.4, 5.1 Hz, 1H, C*H*H), 2.57 (d, *J* = 12.4 Hz, 1H, CH*H*), 2.18 (t, *J* = 7.4 Hz, 2H, CH_2), 1.91–1.73 (m, 2H, CH_2), 1.67–1.55 (m, 1H, C*H*H), 1.55–1.36 (m, 5H, CH_2+CH_2+CH*H*) and 1.35–1.21 (m, 2H, CH_2) ppm.

13C NMR (125 MHz, DMSO-*d6*): 171.5 (CO), 162.8 (CO), 155.9 (C), 152.4 (CH), 149.5 (C), 140.8 (CH), 118.7 (C), 61.1 (CH), 59.2 (CH), 55.4 (CH), 48.6 (CH_2), 42.4 (CH_2), 42.2 (CH_2), 35.0 (CH_2), 28.0 (2xCH_2), 26.8 (CH_2), 25.8 (CH_2) and 24.3 (CH_2) ppm.

MS HRMS (ESI) calcd for $C_{19}H_{30}N_9O_4S_2$ (M−H+): 512.1857, found 512.1834.

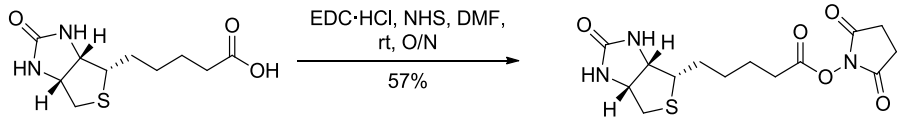

D-biotin **5**

Synthesis of 2,5-dioxopyrrolidin-1-yl 5-((3aS,4S,6aR)-2-oxohexahydro-1H-thieno[3,4-d]imidazol-4-yl)pentanoate

D-Biotin (5.0 G, 20.5 mmol) and N-hydroxysuccinimide (2.3 G, 20.5 mmol, 1.0 eq) were dissolved in hot DMF (150 mL). 1-Ethyl-3-(3-dimethylaminopropyl)carbodiimide hydrochloric salt (4.7 G, 2.4.6 mmol, 1.2 eq) was added, and the solution was stirred overnight at room temperature. The mixture was partitioned between ethyl acetate and water and the aqueous phase was extracted with ethyl acetate (x3). The organics combined were dried over sodium sulphate anh., filtrated and evaporated under reduced pressure. The solid obtained was triturated from diethyl ether affording the title compound (4G, 57%) as a colourless solid.

1H NMR (500 MHz, DMSO-*d6*) δ 6.41 (s, 1H, NH), 6.35 (s, 1H, NH), 4.51–4.20 (m, 1H, C*H*H), 4.20–4.07 (m, 1H, CH*H*), 3.11 (dd, *J* = 12.3, 6.5 Hz, 1H, C*H*H), 2.87–2.78 (m, 5H, CH_2+CH_2+CH*H*), 2.67 (t, *J* = 7.4 Hz, 2H, CH_2), 2.58 (d, *J* = 12.2 Hz, 1H, C*H*H), 1.65 (dt, *J* = 15.2, 7.7 Hz, 3H, CH_2+CH*H*), 1.55–1.46 (m, 1H, C*H*H) and 1.43 (dd, *J* = 12.4, 6.4 Hz, 2H, CH_2) ppm.
13C NMR (125 MHz, DMSO-d6): 170.2 (2xCO), 168.9 (CO), 162.6 (CO), 61.0 (CH), 59.2 (CH), 55.2 (CH), 40.0 (CH_2), 30.0 (CH_2), 27.8 (CH_2), 27.6 (CH_2), 25.43 (2xCH_2), 24.30 and (CH_2) ppm.

Crystallographic data

Table 1. Data collection and refinement statistics (molecular replacement)

	*Sa*BPL + BPL199
Data collection[a]	MX1 Beamline Australian Synchrotron
Space group	*P* 42 21 2
Cell dimensions	
a, *b*, *c* (Å)	92.54, 92.54, 128.98
α, β, γ (°)	90.0, 90.0, 90.0
Resolution (Å)	45.93 - 2.392 (2.478 - 2.392)
R_{sym} or R_{merge}	0.02762 (0.4816)
$I / \sigma I$	15.65 (1.49)
Completeness (%)	99.94 (99.96)
Redundancy	2.0 (2.0)
Refinement	
Resolution (Å)	45.93 - 2.392
No. reflections	22803
R_{work} / R_{free}	0.2069/0.2607 (0.3157/0.3536)
No. non-hydrogen atoms	
Protein	2610
Ligand/ion	34
Water	43
B-factors	
Protein	78.80
Ligand/ion	95.80
Water	58.70
R.m.s. deviations	
Bond lengths (Å)	0.017
Bond angles (°)	1.56

[a]Diffraction data were collected from one crystal for each structure
. *Values in parentheses are for highest-resolution shell.

[AU: Ramachandran statistics should be in Methods section at the end of Refinement subsection.]

[AU: Wavelength of data collection, temperature and beamline should all be in Methods section.]

References

1. Eagle, H. and A. Musselman, *The rate of bactericidal action of penicillin in vitro as a function of its concentration, and its paradoxically reduced activity at high concentrations against certain organisms.* J Exp Med, 1948. **88**(1): p. 99-131.
2. Vanstraelen, K., et al., *The Eagle-like effect of echinocandins: what's in a name?* Expert Rev Anti Infect Ther, 2013. **11**(11): p. 1179-91.
3. Wu, M.L., J. Tan, and T. Dick, *Eagle Effect in Nonreplicating Persister Mycobacteria.* Antimicrob Agents Chemother, 2015. **59**(12): p. 7786-9.
4. Wallace, A.C., R.A. Laskowski, and J.M. Thornton, *LIGPLOT: a program to generate schematic diagrams of protein-ligand interactions.* Protein engineering, 1995. **8**(2): p. 127-134.
5. Laskowski, R.A. and M.B. Swindells, *LigPlot+: multiple ligand–protein interaction diagrams for drug discovery*. 2011, ACS Publications.
6. Okonechnikov, K., et al., *Unipro UGENE: a unified bioinformatics toolkit.* Bioinformatics, 2012. **28**(8): p. 1166-7.
7. Sievers, F., et al., *Fast, scalable generation of high-quality protein multiple sequence alignments using Clustal Omega.* Mol Syst Biol, 2011. **7**(1): p. 539.

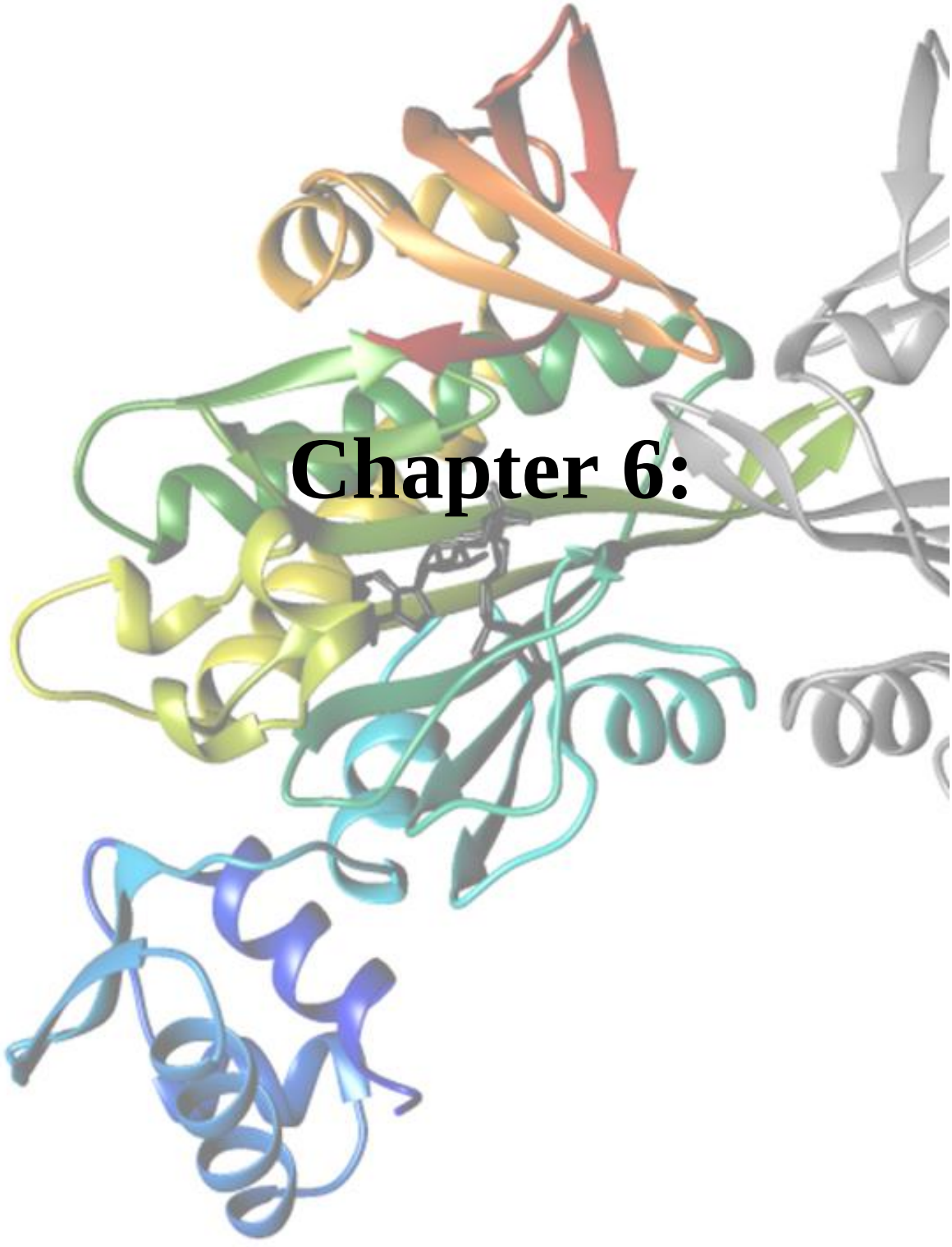

Chapter 6:

Statement of Authorship

Title of Paper	Mutations associated with reduced susceptibility to a novel antibacterial class, Biotin Protein Ligase inhibitors, in *Staphylococcus aureus*
Publication Status	☐ Published ☐ Accepted for Publication ☐ Submitted for Publication ☑ Unpublished and Unsubmitted w ork w ritten in manuscript style
Publication Details	Andrew Hayes, Grant Booker, Steven Polyak

Principal Author

Name of Principal Author (Candidate)	Andrew Hayes,
Contribution to the Paper	Generated resistant strains, prepared genomic DNA, analysed genomic data for mutations, sourced and tested transposon mutant strains, tested strains for antibacterial susceptibility, performed and analysed growth curve data. Analysed results and wrote advanced manuscript
Overall percentage (%)	70
Certification:	This paper reports on original research I conducted during the period of my Higher Degree by Research candidature and is not subject to any obligations or contractual agreements with a third party that would constrain its inclusion in this thesis. I am the primary author of this paper.
Signature	Date 1/08/17

Co-Author Contributions

By signing the Statement of Authorship, each author certifies that:

i. the candidate's stated contribution to the publication is accurate (as detailed above);

ii. permission is granted for the candidate in include the publication in the thesis; and

iii. the sum of all co-author contributions is equal to 100% less the candidate's stated contribution.

Name of Co-Author	Grant Booker,
Contribution to the Paper	Supervised biological aspects of the paper, provided advice and insight into resistance mechanisms, revised manuscript draft
Signature	Date 25/5/2017

Name of Co-Author	Steven Polyak
Contribution to the Paper	Supervised biological aspects of the paper, provided advice and insight into resistance mechanisms. Worked closely with primary author on the construction of the manuscript.
Signature	Date 25/5/2017

Loss of functional pyruvate carboxylase is a major contributor for resistance to antibacterial biotin protein ligase inhibitors in *Staphylococcus aureus*

Andrew Hayes[1], Grant Booker[1], Steven Polyak[1]

[1] School of Biological Sciences, University of Adelaide, South Australia 5005, Australia

Abstract

Biotin protein ligase (BPL) inhibitors are a novel class of antibacterial agent that have *in vitro* efficacy against the clinically important pathogen *Staphylococcus aureus*. In *S. aureus* BPL is a bifunctional protein, acting catalytically to attach biotin to biotin-dependent enzymes, and serving to transcriptionally regulate biotin synthesis and transport genes. Previously we reported the generation of 7 isolates with decreased susceptibility to a potent BPL inhibitor, **BPL199 (compound 9, chapter 5)**. Here we report further investigation of the resistance mechanisms employed in all 7 strains using whole genome sequencing. The most common mutation associated with resistance was a loss of functional pyruvate carboxylase (PC), which occured in 5 of 7 strains. Of the strains without this loss of PC, one contained a missense mutation in the disulphide stress effector *yjbH*. Using transposon disrupted *S. aureus* we demonstrated that deletion of either PC or *yjbH* reduced susceptibility to **BPL199**. Characterisation of cross-resistance with other classes of antibiotics in the 7 original strains was also undertaken. All 7 strains exhibited reduced susceptibility to other BPL inhibitors. The *yjbH* mutant strain also exhibited slight cross-resistance to β-lactam antibiotics, but not any other classes of antibiotics. Together these results suggest 2 distinct mechanisms of resistance to BPL199, one of which is specific to BPL inhibitors.

Introduction

There is a dire need for new antibacterial agents to combat antibiotic resistant infections. *Staphylococcus aureus* is one pathogen that has developed resistance to β-lactam treatments [1], glycopeptide and lipopeptide antibiotics [2], forcing clinicians to consider alternative treatments that often have significant associated toxicities [1, 3, 4]. As a result, discovering new antibacterial agents that are not subject to existing resistance mechanisms is essential for future healthcare. One promising target for a novel antibacterial class is the essential protein, biotin protein ligase (BPL). BPL is both the enzyme responsible for attaching biotin onto biotin-dependent enzymes, as well as a biotin-dependent transcriptional repressor [5]. These bifunctional activities of BPL position the protein as the key regulator of all biotin-mediated events in *S. aureus.* Two biotin-dependent enzymes are present in *S. aureus*, namely acetyl-CoA carboxylase (ACC) and pyruvate carboxylase (PC), which catalyse the first step in fatty acid synthesis and replenish the tricarboxylic acid (TCA) cycle respectively. Without the biotin prosthetic group neither ACC nor PC are capable of performing their important metabolic functions. In *S. aureus* BPL also serves to repress the biotin synthesis (*bioO)*, biotin transport (*bioY)* and a putative fatty acid synthesis (*yhfTS*) operons.[6](satiaputra et al., unpublished). Genome wide knockout studies have demonstrated the essential nature of BPL and ACC in *S. aureus* for growth *in vitro*, [7, 8] and a requirement for PC and the TCA cycle for *in vivo* virulence [9, 10]. BPL inhibition therefore offers a promising approach for antibacterial drug discovery with the ability to inhibit growth and survival both *in vitro* and *in vivo* (reviewed [5]). Small molecule inhibitors that target BPL's enzymatic activity have also been reported with antibacterial activity against *S. aureus* [11-13] as well as *Mycobacterium tuberculosis* [14, 15]. We have also recently published the development and characterisation of a potent antibacterial, **BPL199**, designed as a non-hydrolysable analogue of the BPL reaction intermediate [chapter 5]. Our data showed that **BPL199** functions as both an inhibitor of biotin ligase activity as well as a co-repressor, inducing transcriptional repression with similar potency and kinetics as biotin [chapter 5].

Characterising potential resistance mechanisms early in the antibiotic discovery phase is essential to prevent wasting resources on lead compounds and targets with high resistance rates [16-18]. Compounds that target multiple metabolic pathways generally show lower spontaneous resistance rates than compounds with single targets making them more suitable for mono-therapy [19]. Consistent with this observation, no spontaneous resistant mutants of *S. aureus* NCTC8325 were isolated when grown on media containing **BPL199** at 4× MIC [chapter 5], suggesting multiple mutations were required for high level resistance. Subsequent serial passage in suboptimal concentrations of the antibiotic was undertaken with 7 populations. This allowed for more gradual acquisition of resistance, allowing cells to accumulate the multiple mutations required for growth at 4× the MIC [chapter 5]. The strains isolated from these 7 populations were characterised, with 4 to 32-fold increases in MIC consistent with the low resistance rate observed [chapter 5]. To investigate mutations in the BPL target the gene encoding BPL, *birA*, was sequenced in all 7 isolates. A single strain was identified to harbour a missense mutation, D200E, which is present in the dimerisation interface of BPL. As dimerisation is required for DNA binding, and subsequent transcriptional repression of BPL regulated genes [6, 20], the mutation was hypothesised to play a role in disrupting this process. Biochemical characterisation of the mutant protein confirmed D200E only modestly inhibited the catalytic activity but had a drastic effect upon protein dimerization and, consequently, repressor activity [chapter 5]. We proposed that the resulting increase in expression of the biotin transporter would allow increased scavenging of exogenous biotin to compete against **BPL199**. Whilst the D200E mutant provided one possible resistance mechanism, the lack of BPL mutations in the other strains indicated it was not responsible for resistance in all cases. Here we report whole genome sequencing of the clones from the advanced resistance study to elucidate additional mutations associated with resistance to **BPL199**. This study provides the first insights into possible resistance mechanisms to a novel class of antibiotic.

Materials and methods

Bacterial strains, growth media and antibacterial agents.

Bacterial strains used in this study are listed in table 1. Cation adjusted Mueller Hinton II (Becton, Dickinson and Company, MD, USA) was used to propagate *S. aureus*. **BPL199** was synthesised by Dr Beatriz Bianco-Rodriguez as per the protocol described in [chapter 5]. Other antibacterial agents were obtained from sigma Aldrich.

NCBI BLAST search was used to determine the homologue of genes identified in the WGS in *S. aureus* NCTC 8325 in strain USA300 (JE2). Available strains containing transposon disruption of the genes were then sourced from BEIResources.org. The following reagents were provided by the Network on Antimicrobial Resistance in Staphylococcus aureus (NARSA) for distribution by BEI Resources, NIAID, NIH: *Staphylococcus aureus* subsp. aureus, Strain USA300 (JE2), Transposon Mutants NE754, NE896, NE1022, NE788 and NE792.

Genomic DNA purification and Whole Genome sequencing

Genomic DNA was isolated with the Wizard Genomic DNA purification kit (Promega, Wisconsin, USA) according to the manufacturers' guidelines. Bacteria were treated with 10 μg of lysostaphin (Sigma- Aldrich Inc, MO, USA) and 1mg/ml lysozyme prior to lysis. Quantity of DNA ranged from 15ng/μL-60ng/μL. Genomic DNA from parental strain NCTC 8325 and isolates B1-B7 was submitted to ACRF (Cancer Genomics Facility, Adelaide, South Australia) for library preparation and sequencing. Whole genome sequencing was performed with 150bp paired end reads on Illumina Miseq. Number of sequences for each strain ranged from 434,000-809,000 (between 22 – 40x coverage of genome), 32% GC content

Bioinformatic analysis

The Fastq reads were analysed using the Breseq analysis pipeline software [21]. The parental NCTC 8325 strain that had not undergone antibacterial selection was mapped to the reference genome (NC_007795.1) and the differences were applied to generate a new reference sequence using gdtools. The de-multiplexed reads from isolates B1-B7 were then mapped to this new reference and mutations identified. Greater than 98% of reads from each isolate mapped to the reference genome. Manual inspection of the resulting HTML files was used to determine true positives. Amongst those manually excluded from further analysis was a missense mutation in *rsbU* which is not transcribed in NCTC8325 [22], mislabelling of P626L (as P579L) due to a non-standard start codon and removal of mutations identified in all strains (including the parental NCTC 8325) that did not reach the threshold required for inclusion into the new reference genome.

Antimicrobial susceptibility testing/ cross resistance

Antimicrobial susceptibility assays were performed using a broth microdilution method as recommended by CLSI (Clinical and Laboratory Standards Institute, Document M07-A8, 2009, Wayne, Pa.). Antibacterial compounds were diluted two-fold in Cation adjusted Mueller Hinton Broth (CAMHB) to a final concentration range of 64-0.06µg/ml in 3.2% DMSO. To prepare the inoculum, an overnight culture of *S. aureus* was subcultured 1:1000 into fresh media and grown to mid log phase. 96-well microtitre plates were inoculated with 5 x 10^4 CFU and incubated at 37°C for 20-22 hours with shaking. Growth of the culture was quantified after shaking for 15 seconds to disrupt any sedimentation by measuring the absorbance at 620 nm or 630 nm using either: a Thermo Multiskan Ascent plate reader or Biotek EL808 plate reader respectively. Assays were performed in triplicate.

Kinetics of growth

Growth curves were obtained by subculturing an overnight culture 1:1000 and incubating cells at 37°C to an approximate OD600 of 1 before a further 1:1000 dilution to yield an approximate initial inoculum of 10^5 cells in 100 μL. Cultures were grown in technical duplicate and three independent biological replicates for 24 hours in a 96 well plate at 37°C. Growth of the cultures at 37°C with shaking was then monitored at OD630 every 30 mins for 24 hours using an EL808™ Absorbance Microplate Reader (BioTek Instruments Inc, Winooski, VT, USA). Growth curves were analysed by the method described in [17]. In brief the log of the ODs from OD 0.1-0.3 was plotted against time and log(2)/gradient was determined giving the doubling time.

Results

Distinct resistance mechanisms to BPL199

Whole genome sequencing was employed to characterise the mutations arising in the 7 strains obtained from the advanced resistance studies, [chapter 5] alongside the non-treated NCTC 8325 control **(table 1)**. Sequencing was performed with 150bp paired end reads on the Illumina Miseq platform, with each strain having 434,000-809,000 reads (between 22 – 40x coverage of genome) sufficient for detection of single nucleotide variants (SNV) [23]. The parent NCTC 8325 strain was compared to the reference sequence and the differences observed between the parental strain and reference genome accounted for in a new reference sequence. The resistant strains were then compared to this new parental reference genome. Between 2 to 4 mutations were identified in each strain. Collectively this encompassed 15 nonsynonymous mutations in the coding regions of 11 independent genes. The majority of these were facilitated by SNVs, however, two instances were insertion mediated frame shifts and 5 were the result of a deletion, ranging from three base pairs (i.e. a single a.a. codon) to large scale deletions (194 to 200 bp). Four strains also contained 94 to 139 bp deletions between open reading frames, SAOUHSC_01476 and SAOUHSC_01477, approximately 1kb upstream of the putative operon containing *birA* (ORF SAOUHSC_01473), the gene encoding BPL, which is predicted to span SAOUHSC_01476 to SAOUHSC_01471 [24].

The only gene with non-synonymous mutations in 5 independent strains was *pyc* which encodes the biotin-dependent pyruvate carboxylase. Strains B1, B2, B4, B6 and B7 all contained mutations that led to premature truncation of the PC protein. These strains also exhibited the greatest (8-32 fold) increases in MIC (**Table 1**). Streptavidin blot analysis upon lysates to detect biotinylated protein, confirmed the loss of biotinylated PC in strain B7 (**figure s1**). As previously described strain B7, the most resistant strain, contained an additional mutation in BPL. This was accompanied by a nonsense mutation in the *fmtA* gene, recently characterised as having esterase function removing D-alanine from teichoic acids in

Table 1: Strains used in this study and relevant genetic and phenotypic changes associated with BPL199 resistance. MICs were determined against BPL199. Significance for doubling times was determined by students two tailed t-test. (*p<0.1, **p<0.01, *** p<0.001).

Strain	MIC (µg/ml)	Doubling time (minutes)	Mutations
NCTC 8325	0.06	51.8 ± 2.1	N/A
B1	1	69.2 ± 11.6	*trkA* (+1bp 285/663)(VTAK[95-98]SNC*) *pyc* Δ194bp (2761-2954/3453) SAOUHSC_01981 E20K
B2	0.5	64.5 ± 1.42 *	*pyc* 14bp insertion (1834/3453) Δ94bp intergenic (SAOUHSC_01476 to 01477) presumed silent mutation (no *rsbU*)
B3	0.12	193.6 ± 14.3 ***	*gdpP* H442P *yjbH* Q213-
B4	0.5	53.5 ± 5.5	*pyc* G361* Δ113bp intergenic (SAOUHSC_01476 to 01477)
B5	0.25	68.8 ± 12.1	*greA* Δ111bp SAOUHSC _01504 P15L
B6	1	41.9 ± 0.73 *	p*yc* Δ200bp (917-1116/3453) Δ139bp intergenic (SAOUHSC_01476 to 01477) *rpoβ* P626L SAOUHSC_02984 (*gtfA*-like) R296H
B7	2	67.1 ± 0.90 **	*pyc* Δ200bp (917-1116/3453) Δ139bp intergenic (SAOUHSC_01476 to 01477) *fmtA* K163* *birA* D200E
JE2	0.5	ND	Parent strain, USA300 JE2
NR-47297	4	ND	USA300 JE2 *Δpyc (pyc*::ΦNΣ)
NR-47439	4	ND	USA300 JE2 *ΔyjbH* (*yjbH*::ΦNΣ) SAOUHSC_00938
NR-47565	0.5	ND	USA300 JE2 *ΔfmtA (fmtA*::ΦNΣ)SAOUHSC_00998
NR-47335	0.5	ND	USA300 JE2 *ΔgtfA* (*gtfA*::ΦNΣ) SAOUHSC_02984
NR-47331	1	ND	USA300 JE2 *ΔtrkA (trkA*::ΦNΣ) SAOUHSC_01034

Note. Isolates from B6 and B7 are suspected to be derived from the same intermediate strain, as they contain identical deletions in two separate locations in the genome.

the cell wall [25], and an intergenic deletion between SAOUHSC_01476 and SAOUHSC_01477. Other mutations present in strains containing the PC deletion included the following. Strain B1 contained a frame-shift mutation, leading to premature truncation of the potassium transport protein *trkA* and a missense mutation, E20K, in a putative sensor histidine kinase. Strains B2, B4 and B6 contained deletions in the same intergenic region as B7, and strain B6 contained two additional missense mutations, P626L in the RNA polymerase β-subunit and R296H in a glycosyltransferase-A like gene. It is worth noting that isolates from B6 and B7 are suspected to be derived from the same intermediate strain, as a result of cross contamination, as they contain identical mutations in two separate locations in the genome. Two strains, B3 and B5 exhibited the lowest (2-4 fold) resistance to BPL199 and lacked any mutations in the PC gene. Strain B3 contained two mutations. A missense mutation in the ci-di-AMP phosphodiesterase *gdpP* [26] converted histidine 442 of the presumptive catalytic triad in the DHH domain (**supplementary figure s7**) to a proline. The other was a 3bp deletion which led to the loss of glutamine at position 213 in the disulphide stress effector *yjbH* [27]. Strain B5 contained a 111bp deletion in a gene predicted as a *greA* transcription factor elongation homologue and a missense mutation P15L in a putative bacterial ferredoxin, SAOUHSC_01504.

To determine if there was an *in vitro* fitness cost associated with these mutations, growth curves of the strains were analysed and doubling time calculated as per [17]. All strains had doubling times comparable to the parental strain NCTC8325 (52 minutes) (**figure 1B)** except B3 which exhibited a significant growth defect (doubling time, 193 minutes) preventing it from reaching half the maximum OD of the other strains. These data suggest that *in vitro* resistance to the BPL inhibitor is possible without significant associated fitness costs. The differences in the resistance profiles, growth curves and associated genomic mutations of the strains suggested at least two independent resistance mechanisms in the 7 strains, described further below.

A **B**

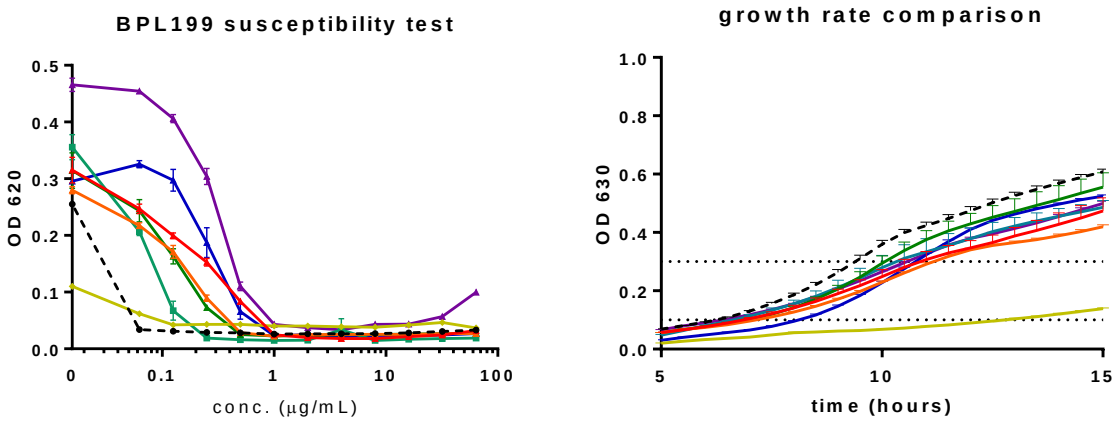

Figure 1: A) Susceptibility of *S. aureus* NCTC8325 derived strains to a BPL inhibitor BPL199 after serial passage in suboptimal concentrations of the antibiotic for 18 days B) Growth of strains in Mueller Hinton media measured half hourly. **Black dashed line, parental NCTC8325; red, B1; orange, B2; yellow, B3; green, B4; light blue, B5; dark blue, B6; purple, B7.** Data are the average readings of three independent experiments. Error = SEM.

Table 2: MICs of parental strain 8325 and the 7 BPL199^{r} mutant strains to BPL inhibitors and β-lactam antibiotics methicillin and amoxicillin. Each MIC was obtained in three independent experiments.

	BPL199	**biotinol-5'-AMP**	**BPL223**	**methicillin**	**amoxicillin**
NCTC-8325	0.06	1	8	2	16
B1	1	>64	64	2	16
B2	0.5	>64	>64	2	16
B3	0.12	>64	16	4-8	32
B4	0.5	>64	>64	2	16
B5	0.25	8-16	8	2	16
B6	1	>64	>64	2	16
B7	4	>64	>64	2	16

BPL199^{r} strains showed general resistance to two other BPL inhibitors.

To test whether antibacterial resistance was general to other antibiotics or specific to **BPL199**, all 7 strains were subjected to antibacterial susceptibility assays against a panel of antibiotics and 2 literature BPL inhibitors. This panel included commercially available antibiotics methicillin, amoxicillin, vancomycin, erythromycin and streptomycin alongside two literature BPL inhibitors biotinol-5′-AMP [28] and BPL223 [chapter 5]. In all but one case the resistance mechanisms appeared specific to the BPL inhibitors with no decrease in susceptibility **(table 2, supplementary figure s2)** to methicillin, amoxicillin, vancomycin, erythromycin or streptomycin (n = 1). The exception to this was strain B3 which exhibited a 2 to 4 fold decrease in susceptibility to the two β-lactams, methicillin and amoxicillin. Conversely, all strains exhibited increased resistance to the two BPL inhibitors. Whereas parent strain NCTC8325 exhibited an MIC of 1 μg/ml against biotinol-5′-AMP all strains are completely resistant to this compound (MIC > 64 μg/ml) except B5 which exhibited an MIC of 8 μg/mL. Wild type NCTC8325 also exhibited an MIC of 8 μg/ml for BPL223, however B2, B4, B6 and B7 again were not susceptible. B1 (MIC = 64 μg/ml) and B3 (MIC = 16 μg/ml) exhibited a modest decrease in susceptibility, and B5 (MIC = 8 μg/ml) showed no change.

Loss of function of PC and YjbH was sufficient for a 4-fold decrease in BPL199 susceptibility.

Of the mutations observed, four were considered likely to induce loss of function of their respective genes due to truncation of the protein (*trkA, pyc*, *fmtA, greA*), whilst two encoded for missense mutations that were likely to drastically effect function (*gdpP, yjbH*). To determine if loss of function in any of these genes was sufficient for resistance, strains containing transposon disruptions in select target genes were obtained from the Nebraska transposon mutant library [29]. As all mutants in the library were generated in *S. aureus* JE2

(CA-MRSA, USA300) this was used as a control strain. Of the 10 discrete genes harbouring mutations identified in B1-B7, 5 transposon disruptions were available (*trkA, pyc, fmtA, gtfA, yjbH*). The strains were initially tested for susceptibility to **BPL199** by monitoring growth for 20 hours in the presence of varying concentrations of **BPL199**. Parental strain JE2 exhibited an MIC of 0.5 μg/ml, consistent with previous reports against clinical isolates [chapter 6]. Only 2 of the 5 transposon disruptions, Δ*pyc* and Δ*yjbH,* led to a decrease in **BPL199** susceptibility similar to that seen in the initial advanced resistance studies with NCTC8325 **(table 3)**. The ability of these strains to grow in the presence of BPL199 was improved over the parent strain at low concentrations of antibiotic, retaining approximately 50% of maximum growth at 0.25 μg/ml, whilst the parental strain had greater than 90% inhibition. However, they were still greatly inhibited by 0.5 μg/mL at 20 hours, with only a slight difference in growth **(figure 2A)**. Further testing carried out over 46 hours showed that whilst the parental strain had no growth post the 20 hour time point at concentrations higher than 0.5 μg/ml, the Δ*pyc* and Δ*yjbH* strains were still growing, increasing to 50% and 25% maximal growth (relative to untreated control) at 46 hours (**Figure 2D)**. At this extended time point the Δ*pyc* strain was able to grow at up to 2 μg/ml (**figure 2E)** and Δ*yjbH* at concentrations up to 4 μg/ml BPL199 (**figure 2E)** , the highest concentration tested. The growth curves of the two strains in the presence of antibiotic also differed markedly at 0.5 μg/ml **(figure 2C)**. The Δ*pyc* strain exhibited a pronounced lag phase before entering a relatively rapid log phase growth. In contrast, the Δ*yjbH* strain showed slower steady growth throughout. The fact the Δ*pyc* strain was able to grow at 4× MIC suggested this mutation alone is sufficient for the 4-fold increase in resistance observed in the NCTC 8325 derived strains containing this mutation. Unlike the Δ*pyc* and Δ*yjbH* disruptions, the Δ*trkA* strain showed 2-fold decrease in susceptibility after 46 hours (MIC = 1μg/ml), whilst the Δ*gtfA* and Δ*fmtA* strains exhibited no improvement in susceptibility. The potential mechanisms for the Δ*pyc* and Δ*yjbH* mutations to have decreased susceptibility are discussed further below.

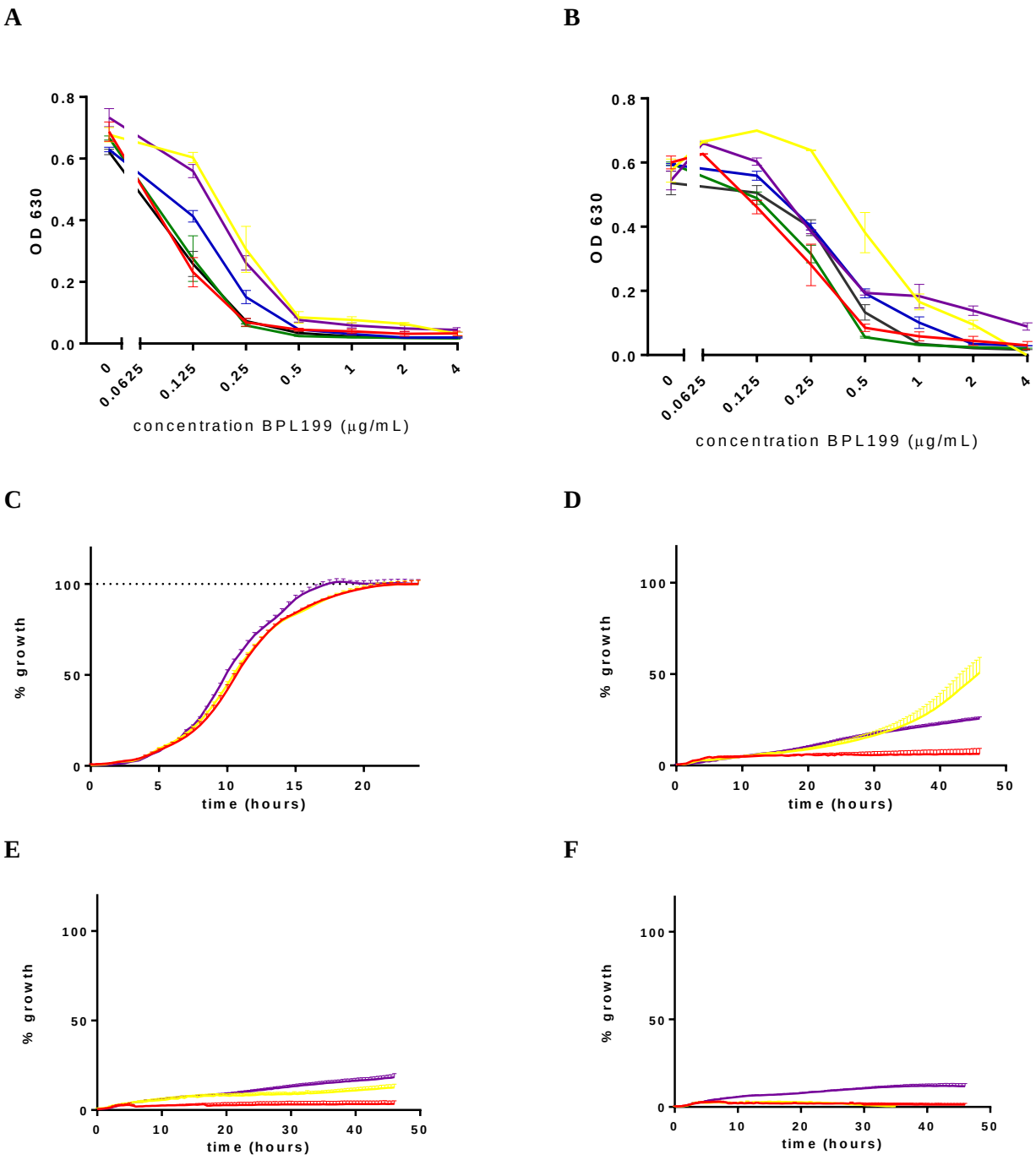

Figure 2: growth of wild type *S. aureus* USA300 (JE2) (red), and transposon mutagenesis strains: Δ*pyc* (yellow), Δ*yjbh* (purple), Δ*fmtA* (grey), Δ*trkA* (blue), Δ*gtfA* (green) after **A)** 20 hours and **B)** 46 hours in the presence of BPL199. **C-E)** growth curves of strains: wild type JE2, Δpyc and Δyjbh after 46 hours in the presence of BPL199 at **C)** untreated control **D)** 0.5 µg/ml, **E)** 2 µg/ml, **F)** 4µg/ml. strains were normalised to plateau of the untreated control (OD 0.75) which was consistent for all strains. Data are the average readings of 3 independent experiments. Error = SEM.

Discussion

It appears that though resistance to some BPL inhibitors can appear both rapidly and completely (biotinol-5′-AMP, BPL223) there is a reduced rate for the antibiotic **BPL199**. This lack of complete resistance occurring in any strain is promising for the future of BPL inhibitors as antimicrobial agents. Coupled with the low spontaneous rate for **BPL199** [chapter 5] it suggests that although resistance may occur it is unlikely to be rapid or pronounced, at least in the NCTC 8325 genetic background. The mutations identified in this study generally have either direct links to biotin metabolism (*pyc*, *birA*) or can be linked to a larger cellular stress response (*gdpP*, *yjbH, trkA*). Whilst the exact mechanism of how these mutations lead to increased BPL inhibitor resistance is unclear, the roles of the respective genes provides a useful basis for identification of resistance mechanisms.

Loss of pyruvate carboxylase was the most common mechanism employed by *S. aureus* to reduce BPL inhibitor susceptibility. A premature truncation of PC was present in 5 of the 7 strains evolved to be resistant to **BPL199**, namely B1, B2, B4, B6 and B7. As the biotinylation domain of PC is contained within the C-terminal region, these truncated PC proteins were unable to be biotinylated and, hence, inactive. The transposon disrupted strain lacking PC (Δ*pyc*) confirmed that PC deletion confers resistance independently of the other mutations in the NCTC8325 genetic background, exhibiting a four-fold decrease in MIC. As a result it is likely a mutation that can increase resistance to BPL inhibitors in any strain. A probable mechanism for this resistance is through increased biotinylation of ACC. Genetic knockout studies have demonstrated ACC, but not PC, is required for growth *in vitro* [7, 8]. Removal of PC from the cell therefore facilitates resistance by removing the only other protein substrate that (normally) competes with ACC for binding to BPL, hence, increasing the chance of ACC being biotinylated. This requires biotin to competitively bind to the BPL over the inhibitor allowing the natural reaction intermediate to form and biotinylation to

occur. Certain BPL inhibitors, including BPL223, used in the cross resistance study, have been found to have fast dissociation kinetics [chapter 5][12], and therefore have low residency on the BPL target. As a result, biotin can also bind more frequently, increasing the efficacy of such a mechanism. Increasing the residency time that inhibitors bind to the BPL target is therefore desirable to reduce the effectiveness of this mechanism. Whilst PC is dispensible for growth *in vitro*, its absence does impact on *S. aureus* virulence and *in vivo* growth. The loss of PC and TCA cycle genes has been shown to reduce virulence in murine and nematode models of infection respectively [9, 10]. The roles of these genes in virulence suggest that the resistance mechanisms identified in this study may require compensatory mutations to alleviate *in vivo* fitness costs. Despite the fact that these compensatory mutations are often not selected for in parallel evolution studies *in vitro* the mutations identified can still occur in clinical settings [30]. This is a result of compensatory mutations being more likely to occur than reversions of beneficial mutations in response to selective pressure.

Two strains in the study (B3, B5) showed increased resistance to BPL inhibitors but maintained functional PC. Strain B3 in particular showed a unique phenotype, displaying markedly reduced growth rate. Cross resistance to two separate β-lactam antibiotics (methicillin and amoxicillin) was also noted in B3, indicating the mutations present in these strains contribute broader resistance to certain cell wall active antibiotics. Intriguingly whilst the strain B3 did show a 2-fold decrease in susceptibility to BPL199, it exhibited a much greater decrease in susceptibility to biotinol-5′-AMP (>64-fold) suggesting that the generalised response is more effective against the less potent inhibitor. The roles of the genes mutated in *S. aureus* B3 (*yjbH* and *gdpP*) and how they convey resistance to other antibiotics gives us insight as to how they may function to reduce susceptibility to BPL199.

YjbH in *S. aureus* and other Gram positive bacteria has a role in the disulphide stress response where it shuttles the transcriptional regulator Spx to the ClpXP protease for degradation [27]. Loss of YjbH function therefore leads to increased Spx levels in the cell [27]. In this study the *yjbH* gene of *S. aureus* was found to have a 3 base pair deletion leading to loss of a glutamine at position 213. As loss of function of *yjbH* in *S. aureus* USA300 (JE2) was sufficient to decrease susceptibility to **BPL199**, the Q213Δ mutation is believed to similarly act by loss or reduction of function. This is consistent with several reports of mutations leading to loss of YjbH function in strains with tolerance to glycopeptide, antimicrobial-peptide and β-lactam antibiotics [31-33]. The Spx regulator acts through controlling the interaction between RNA polymerase and transcriptional regulators, binding to the α-CTD of RNA polymerase. As a result increasing Spx levels effects transcription of certain target genes [34]. In *B. subtilis* these upregulated genes implicated in oxidative stress, whilst downregulated genes are associated with purine and pyrimidine biosynthesis, amino acid synthesis and vitamin synthesis including the biotin biosynthesis operon [35]. In *S. aureus,* proteomic data indicates that stress response genes are similarly regulated, however differences in metabolic gene regulation are apparent. Indeed pyrimidine synthesis regulation by the Spx regulon is reported to be upregulated with increased Spx, the opposite response to *B. subtilis* [34]. We propose that the *yjbH* mutation observed in strain B3 leads to increased intracellular Spx, and subsequent induction of certain stress response genes. However the exact molecular details of this regulation require further investigation.

There is also a large growth defect associated with strain B3. This is likely due to a combination of the *yjbH* and *gdpP* loss of function. Strains in an NCTC8325 derived background lacking *yjbH* have been described as having reduced growth and increased pigmentation [27] which is consistent with the growth defect observed in strain B3. This is not observed in *S. aureus* SA113 [33] and does not appear to be the case for the Δ*yjbH* strain in *S. aureus* JE2 (USA300) **(figure 2B)**, suggesting there are differences in the responses to

this mutation. Strains lacking GdpP and with resulting high c-di-AMP levels also show a small but pronounced growth defect in the *S. aureus* LAC (USA300) background [36] suggesting this mutation may also contribute to B3's slow growth rate. Slow growth like this is often associated with a persister cell type. Many antibiotics work by hijacking active cellular processes of growing bacteria producing a corrupted product [37]. However, persister cells often do not have these cellular processes active due to their slow growth, allowing them to avoid the antibacterial effects [38, 39]. The slow growth and cross-resistance present in strain B3 suggests that this strain may exhibit a persister cell phenotype.

Determining the mutations involved in BPL inhibitor resistance allows us insight on how the antibiotic is affecting the bacteria and resistance mechanisms that may occur in the clinic. The ability for the Δ*pyc* and Δ*yjbH* disruptions to convey resistance in a discrete genomic background suggests the mutations are applicable to multiple genetic backgrounds. However, the lack of effect for the other 3 disruptions (Δ*gtfA*, Δ*trkA*, Δ*fmtA*) indicates *S. aureus* might take different routes to resistance in alternate genetic backgrounds. Testing of the original strains in an infection model would also provide vital information as to the effect of these mutations on virulence and whether the mutations are viable. This would be particularly useful for those strains with genes linked to virulence, such as B1, B2, B4, B6 and B7**,** and those with growth defects, B3. The lack of cross resistance outside of BPL inhibitors is also encouraging as it reduces the chance of current resistance mechanisms being able to address BPL inhibitors. The strain B3 is of particular interest in this respect as it exhibits traits similar to those seen in persister cells, exhibiting slowed growth rate and resistance to multiple antibiotics. Persister cells pose a serious problem for modern healthcare, being able to circumvent many antimicrobial treatments that would typically eradicate an infection (reviewed [38, 40, 41]). This makes understanding of a new potential persister cell phenotype useful in the detection and treatment of these cells.

REFERENCES

1. World Health Organisation, *Antimicrobial resistance: Global report on resistance.* 2014.
2. Gardete, S. and A. Tomasz, *Mechanisms of vancomycin resistance in Staphylococcus aureus.* J Clin Invest, 2014. **124**(7): p. 2836-40.
3. Butler, M.S., et al., *Glycopeptide antibiotics: back to the future.* J Antibiot (Tokyo), 2014. **67**(9): p. 631-44.
4. Boucher, H.W., et al., *Bad bugs, no drugs: no ESKAPE! An update from the Infectious Diseases Society of America.* Clin Infect Dis, 2009. **48**(1): p. 1-12.
5. Paparella, A.S., et al., *Structure guided design of biotin protein ligase inhibitors for antibiotic discovery.* Curr Top Med Chem, 2014. **14**(1): p. 4-20.
6. Rodionov, D.A., A.A. Mironov, and M.S. Gelfand, *Conservation of the biotin regulon and the BirA regulatory signal in Eubacteria and Archaea.* Genome research, 2002. **12**(10): p. 1507-1516.
7. Forsyth, R.A., et al., *A genome-wide strategy for the identification of essential genes in Staphylococcus aureus.* Mol Microbiol, 2002. **43**(6): p. 1387-400.
8. Chaudhuri, R.R., et al., *Comprehensive identification of essential Staphylococcus aureus genes using Transposon-Mediated Differential Hybridisation (TMDH).* BMC Genomics, 2009. **10**: p. 291.
9. Benton, B.M., et al., *Large-scale identification of genes required for full virulence of Staphylococcus aureus.* J Bacteriol, 2004. **186**(24): p. 8478-89.
10. Bae, T., et al., *Staphylococcus aureus virulence genes identified by bursa aurealis mutagenesis and nematode killing.* Proc Natl Acad Sci U S A, 2004. **101**(33): p. 12312-12317.
11. Soares da Costa, T.P., et al., *Biotin analogues with antibacterial activity are potent inhibitors of biotin protein ligase.* ACS Med Chem Lett, 2012. **3**(6): p. 509-14.
12. Soares da Costa, T.P., et al., *Selective inhibition of Biotin Protein Ligase from Staphylococcus aureus.* J Biol Chem, 2012. **287**(21): p. 17823-17832.
13. Feng, J., et al., *New Series of BPL Inhibitors To Probe the Ribose-Binding Pocket of Staphylococcus aureus Biotin Protein Ligase.* ACS Med Chem Lett, 2016. **7**(12): p. 1068-1072.
14. Duckworth, B.P., et al., *Bisubstrate adenylation inhibitors of biotin protein ligase from Mycobacterium tuberculosis.* Chem Biol, 2011. **18**(11): p. 1432-41.
15. Shi, C., et al., *Bisubstrate Inhibitors of Biotin Protein Ligase in Mycobacterium tuberculosis Resistant to Cyclonucleoside Formation.* ACS Med Chem Lett, 2013. **4**(12): p. 12131217.
16. Yao, J. and C.O. Rock, *Bacterial fatty acid metabolism in modern antibiotic discovery.* Biochim Biophys Acta, 2017. **1862**(11): p. 1300-1309.
17. Blake, K.L., C.P. Randall, and A.J. O'Neill, *In vitro studies indicate a high resistance potential for the lantibiotic nisin in Staphylococcus aureus and define a genetic basis for nisin resistance.* Antimicrob Agents Chemother, 2011. **55**(5): p. 2362-8.
18. Gupta, A., et al., *A Polymorphism in leuS Confers Reduced Susceptibility to GSK2251052 in a Clinical Isolate of Staphylococcus aureus.* Antimicrob Agents Chemother, 2016. **60**(5): p. 3219-3221.
19. Silver, L.L., *Challenges of antibacterial discovery.* Clin Microbiol Rev, 2011. **24**(1): p. 71-109.
20. Satiaputra, J., et al., *Mechanisms of biotin-regulated gene expression in microbes.* Synth Syst Biotechnol, 2016. **1**(1): p. 17-24.
21. Deatherage, D.E. and J.E. Barrick, *Identification of mutations in laboratory-evolved microbes from next-generation sequencing data using breseq.* Methods Mol Biol, 2014. **1151**: p. 165-88.
22. Giachino, P., S. Engelmann, and M. Bischoff, *çB Activity Depends on RsbU inStaphylococcus aureus.* J Bacteriol, 2001. **183**(6): p. 1843-1852.
23. Sims, D., et al., *Sequencing depth and coverage: key considerations in genomic analyses.* Nat Rev Genet, 2014. **15**(2): p. 121-132.
24. ten Broeke-Smits, N.J., et al., *Operon structure of Staphylococcus aureus.* Nucleic Acids Res, 2010. **38**(10): p. 3263-74.

25. Rahman, M.M., et al., *The Staphylococcus aureus Methicillin Resistance Factor FmtA Is a d-Amino Esterase That Acts on Teichoic Acids.* mBio, 2016. **7**(1): p. e02070-15.
26. Corrigan, R.M., et al., *c-di-AMP is a new second messenger in Staphylococcus aureus with a role in controlling cell size and envelope stress.* PLoS Pathog, 2011. **7**(9): p. e1002217.
27. Engman, J., et al., *The YjbH adaptor protein enhances proteolysis of the transcriptional regulator Spx in Staphylococcus aureus.* J Bacteriol, 2012. **194**(5): p. 1186-94.
28. Tieu, W., et al., *Improved Synthesis of Biotinol-5'-AMP: Implications for Antibacterial Discovery.* ACS Med Chem Lett, 2015. **6**(2): p. 216-20.
29. Fey, P.D., et al., *A Genetic Resource for Rapid and Comprehensive Phenotype Screening of Nonessential Staphylococcus aureus Genes.* mBio, 2013. **4**(1).
30. Comas, I., et al., *Whole-genome sequencing of rifampicin-resistant Mycobacterium tuberculosis strains identifies compensatory mutations in RNA polymerase genes.* Nat Genet, 2011. **44**(1): p. 106-10.
31. Renzoni, A., et al., *Whole genome sequencing and complete genetic analysis reveals novel pathways to glycopeptide resistance in Staphylococcus aureus.* PLoS One, 2011. **6**(6): p. e21577.
32. Johnston, P.R., A.J. Dobson, and J. Rolff, *Genomic Signatures of Experimental Adaptation to Antimicrobial Peptides in Staphylococcus aureus.* G3 (Bethesda), 2016. **6**(6): p. 1535-9.
33. Göhring, N., et al., *New role of the disulfide stress effector YjbH in β-lactam susceptibility of Staphylococcus aureus.* Antimicrob Agents Chemother, 2011. **55**(12): p. 5452-5458.
34. Pamp, S.J., et al., *Spx is a global effector impacting stress tolerance and biofilm formation in Staphylococcus aureus.* J Bacteriol, 2006. **188**(13): p. 4861-4870.
35. Nakano, S., et al., *Spx-dependent global transcriptional control is induced by thiol-specific oxidative stress in Bacillus subtilis.* Proc Natl Acad Sci U S A, 2003. **100**(23): p. 13603-13608.
36. Corrigan, R.M., et al., *Cross-talk between two nucleotide-signaling pathways in Staphylococcus aureus.* J Biol Chem, 2015. **290**(9): p. 5826-5839.
37. Conlon, B.P., S.E. Rowe, and K. Lewis, *Persister cells in biofilm associated infections*, in *Biofilm-based Healthcare-associated Infections*. 2015, Springer. p. 1-9.
38. Lewis, K., *Multidrug tolerance of biofilms and persister cells*, in *Bacterial Biofilms*. 2008, Springer. p. 107-131.
39. Keren, I., et al., *Persister cells and tolerance to antimicrobials.* FEMS Microbiol Lett, 2004. **230**(1): p. 13-8.
40. Lewis, K., *Persister cells, dormancy and infectious disease.* Nat Rev Microbiol, 2007. **5**(1): p. 48-56.
41. Lewis, K., *Persister cells.* Annu Rev Microbiol, 2010. **64**: p. 357-372.

Loss of functional pyruvate carboxylase is a major contributor for resistance to antibacterial biotin protein ligase inhibitors in *Staphylococcus aureus*

Andrew Hayes[1], Grant Booker[1], Steven Polyak[1]

[1] School of Biological Sciences, University of Adelaide, South Australia 5005, Australia

Supporting information

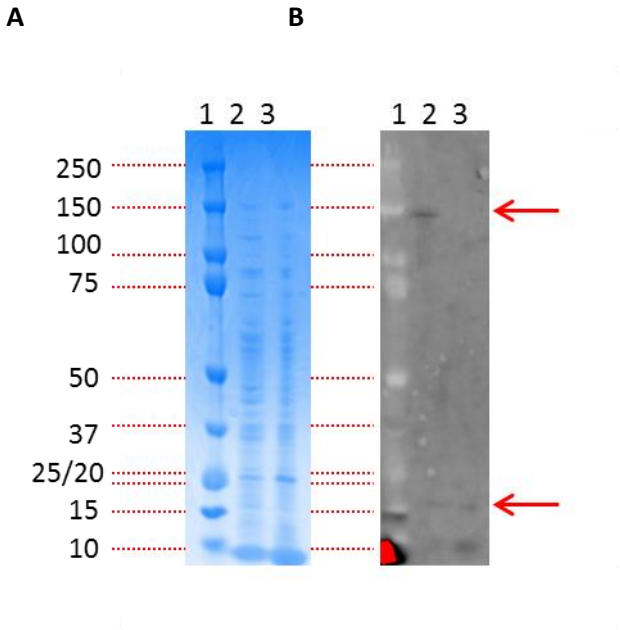

Figure s1: A) Coomassie stained SDS PAGE, and B) Streptavidin blot, of cell lysates from *S. aureus* NCTC 8325 (lane 2), and *S. aureus* B7 (lane 3). A) Both lanes show a dark band between 15 to 20 kDa (biotinylated ACC subunit ≈ 17 kDa) However the band at approximately 130kDa (PC ≈ 130 kDa) in lane 2 is absent in lane 3 indicating loss of biotinylated pyruvate carboxylase.

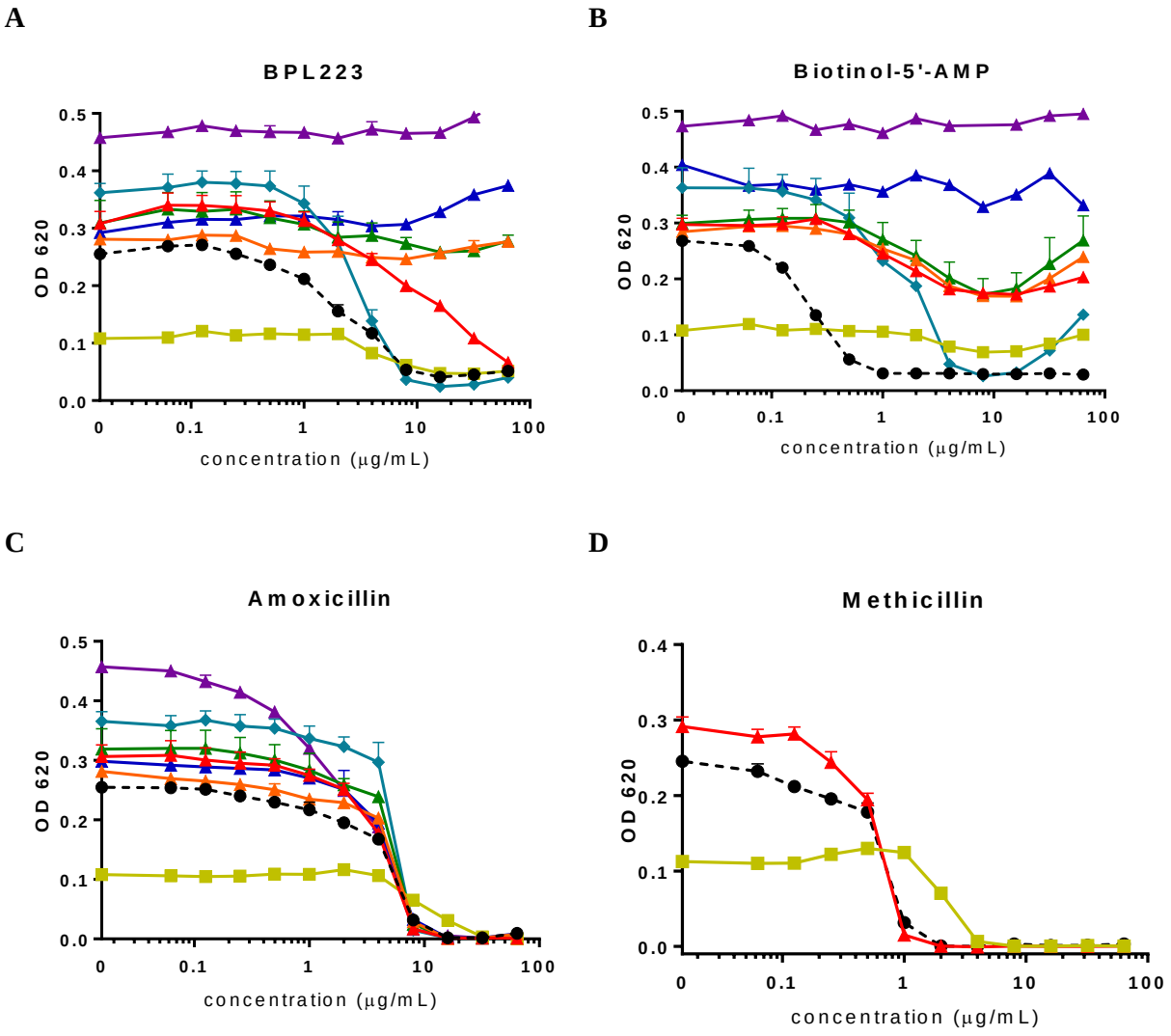

Figure s2: antibacterial susceptibility assays of wild type NCTC8325 and derived strains B1-B7 against BPL inhibitors A) BPL223, B) Biotinol-5′-AMP, and β-lactams, C) Amoxicillin and D) Methicillin. Data is from three independent exp eriments. Error = SEM

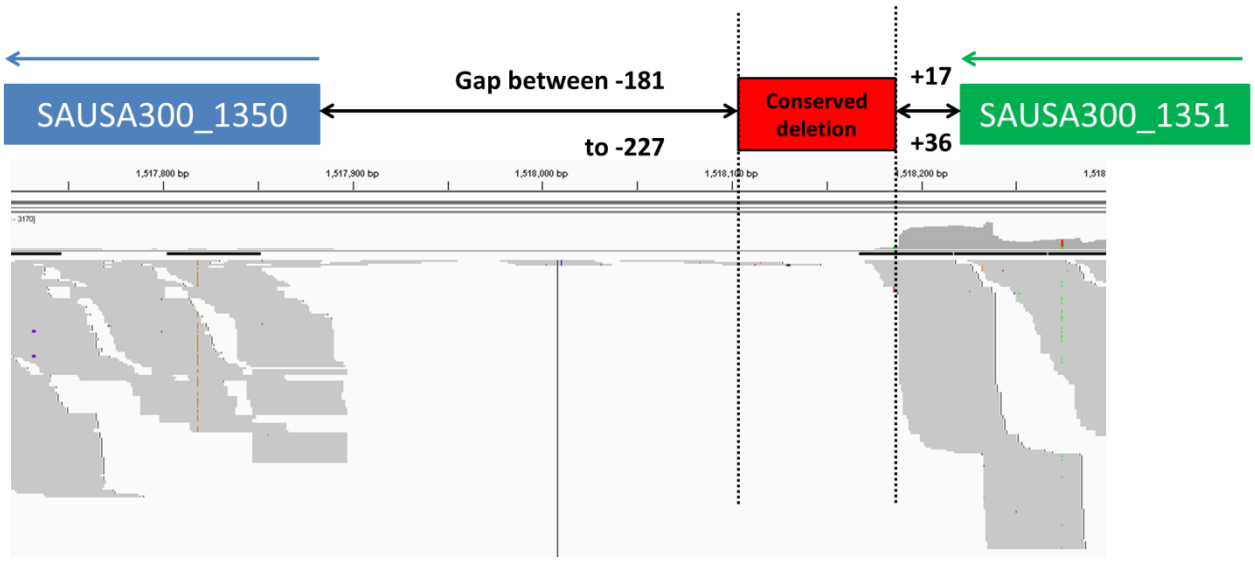

Figure s3: IGV trace of RNAseq reads mapped to the USA300 genome. No significant transcription (≥10 reads mapped) of the intergenic region was detected.

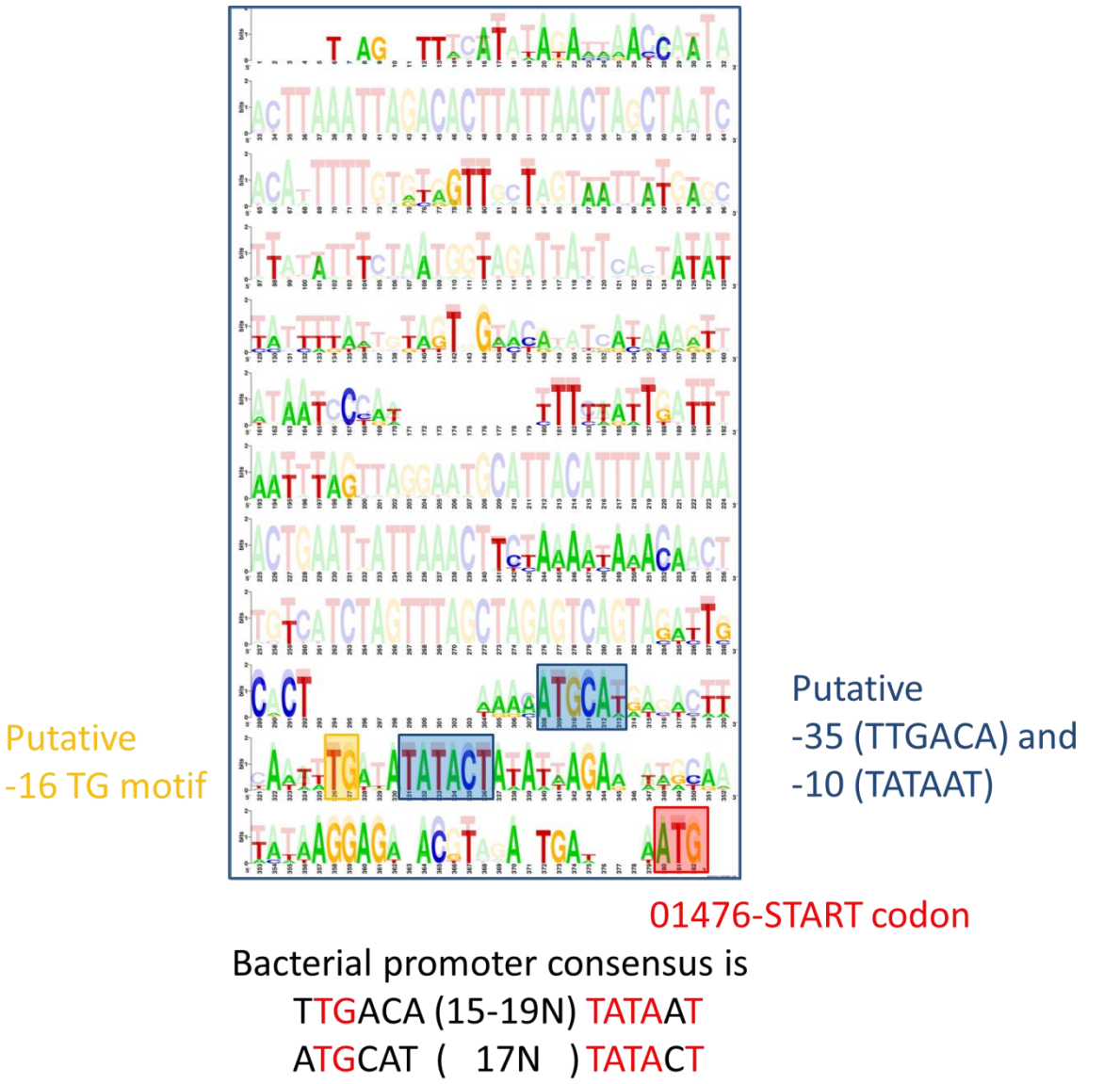

Figure s4 produced as result of sequence alignment of intergenic region between SAOUHSC_01476 and SAOUHSC_01477 in several *Staphylococcus* species (9 *S. aureus* and 4 less closely related, *S. haemolyticus*, *S. epidermidis*, *S. warneri*, *S. carnosus*) using UGENE and muscle aligner. Sequence was then put into logoplot server. Location of sites was chosen to prevent extensive gap regions in the RNA transcript.- Faint = logoplot with sequence from 9 *S. aureus* species

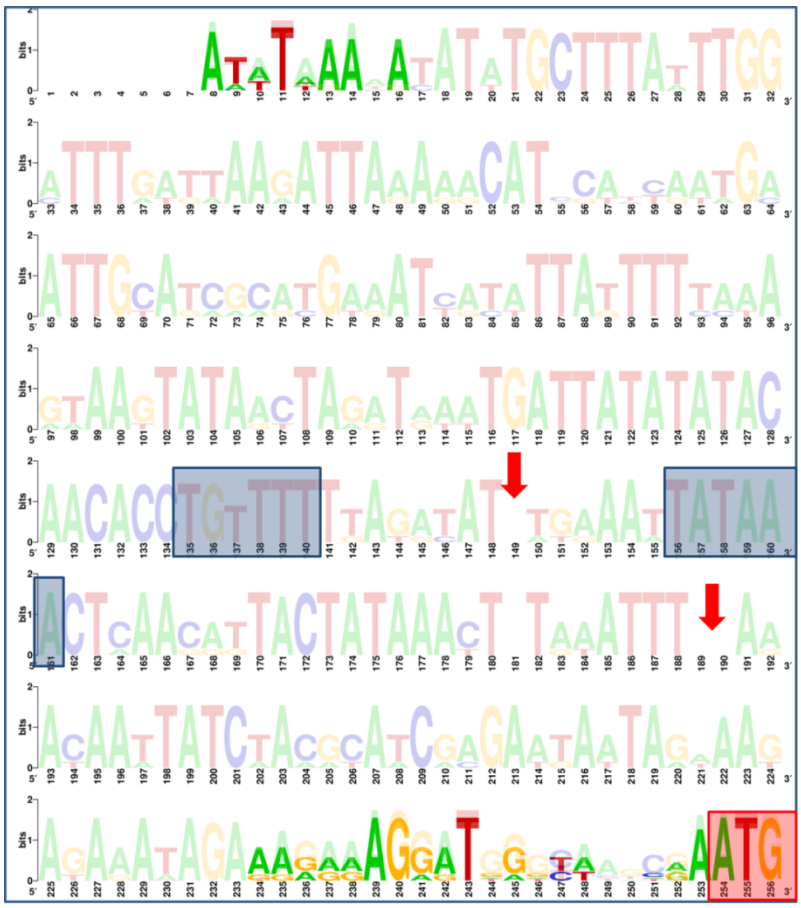

Figure s5 produced as result of sequence alignment of intergenic region between SAOUHSC_01475 and SAOUHSC_01476 in several *Staphylococcus* species (1 *S. aureus* and 4 less closely related *S. haemolyticus*, *S. epidermidis*, *S. warneri*, *S. carnosus*) using UGENE and muscle aligner. Sequence was then put into logoplot server. The untranslated sequence is approximately 20-30bp for non *S. aureus* and 200bp for *S. aureus* (probable insertion). Faint = logoplot with sequence from 6 *S. aureus* species

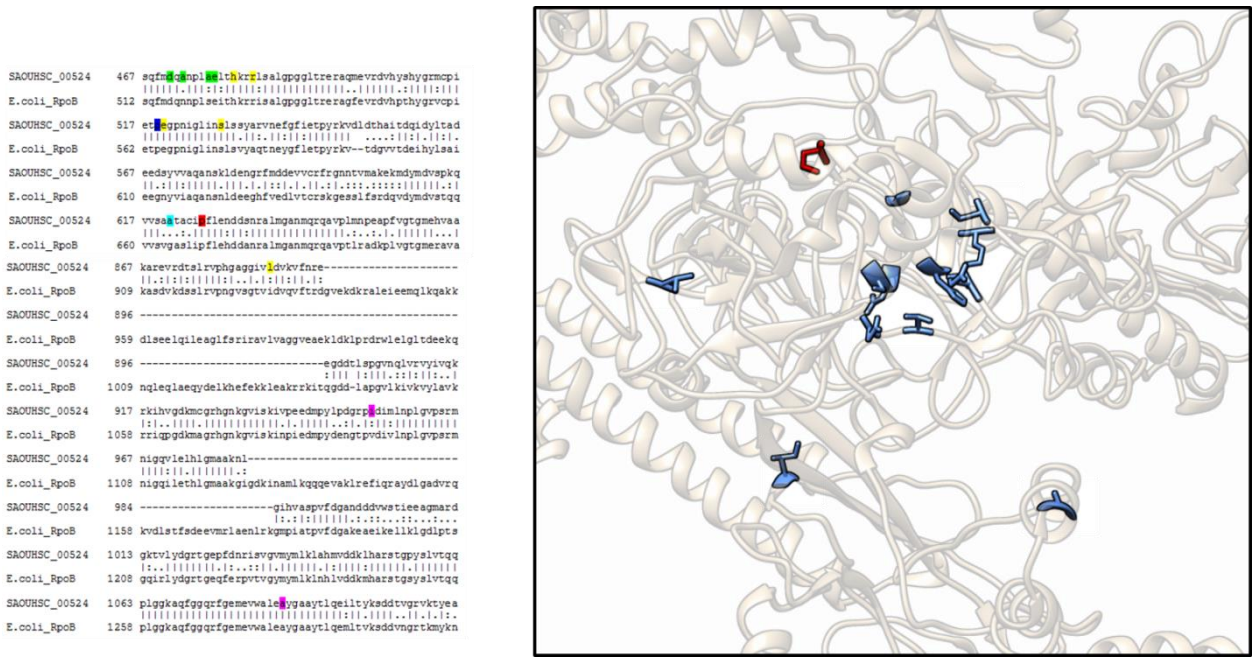

Figure s6 Locations of mutations that have caused decreased susceptibility to vancomycin or daptomycin in *S. aureus* RpoB mapped to the *E. coli* RpoB (red proline is equivalent to P626L in B6).

A **B**

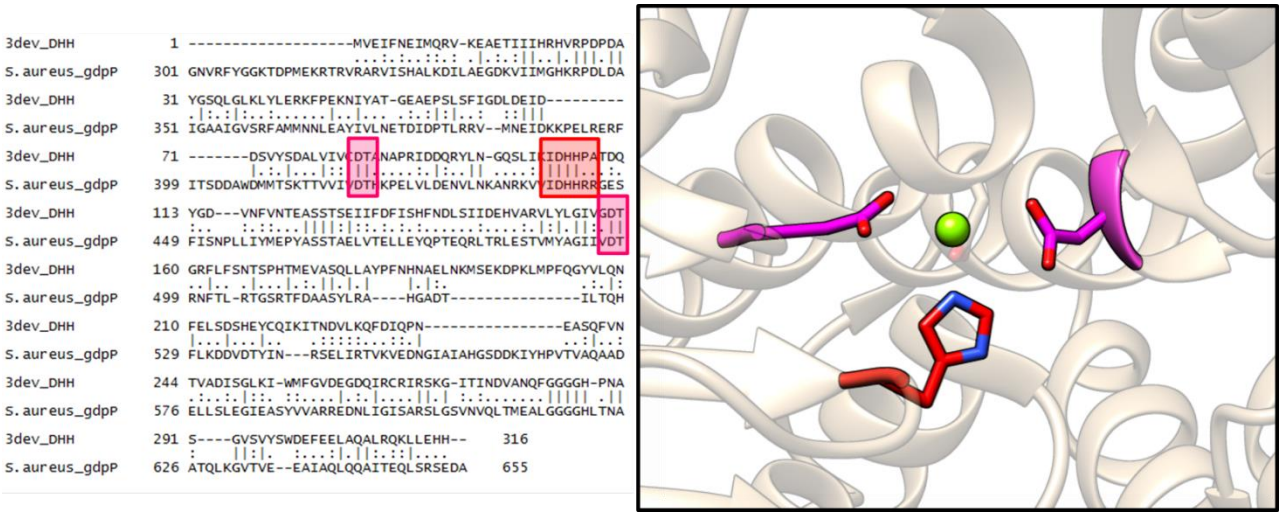

Figure s7: A), sequence alignment between the DHH domain of *S. aureus* GdpP and DHH domain from SH1221 protein from *Staphylococcus haemolyticus* with an available crystal structure (PDB:3DEV). B), the catalytic site identified for the DHH domain crystal structure. The residue In red is the Histidine residue mutated to proline H442P in our strain, the residues in pink correspond to the residues D418 and D497 that when mutated to Alanine have shown loss of phophodiesterase function [1].

Supplementary methods:

Selection of BPL199 resistant mutants. Mutants were selected by serial passage in 96 well format as previously described [chapter 5]. In brief: A 2-fold dilution series of the compound was plated across 7 wells (initially 1 μg/ml to 0.016 μg/ml) with concentration increasing as the MIC increased. On the first day approximately 10^4 CFU of exponentially growing *S. aureus* 8325 was added to each well. The OD was measured at 620nm for each well and the well with the highest concentration permitting growth (OD620 >0.1 used as threshold) diluted 1000 fold and used to inoculate the following day's culture. This process was repeated for 18 days. Single isolates were then purified from a single colony on agar genomic DNA extracted. The stability of the resistance was also tested by propagating the strains selected for 6 days on MHAgar in the absence of any antibiotic selection. These strains were then retested in the antibacterial susceptibility assay.

Mauve alignment and RNAseq analysis

To determine the possible role of an intergenic deletion, the region specified was aligned across several *Staphylococcus* species to determine if it was conserved utilising MAUVE progressive aligner. Further analysis of the region was undertaken by determining if there were any expressed RNA's in the region by mapping the RNAseq datasets (SRX1548042, SRX1548043) from the strain USA300, after 3 and 16 hours growth, to the genome and determining expression profile using Rockhopper [2].

Code used to run whole genome sequencing analysis.

```
# initally mapped every read to the reference genome
# -j 4 refers to using 4 cores to process command
# -r reference sequence follows
# annotated_reference.gb= genbank file downloaded from NCBI + fasta sequence data from NCBI included in Genbank format
# -o output results to mutated_outputall directory
# path to reads ../Fastq/reads${i}-B${i}_S${i} (could have been automated)

path_to//breseq-0.27.1-Linux-x86_64/bin/breseq -j 4 -r ../8325referencegenbanksequenceadded.gb -o mutated_outputall ../Fastq/reads1-B1_S1_L001_R1.fq ../Fastq/reads1-B1_S1_L001_R2.fq ../Fastq/reads2-B2_S2_L001_R1.fq ../Fastq/reads2-B2_S2_L001_R2.fq ../Fastq/reads3-B3_S3_L001_R1.fq ../Fastq/reads3-B3_S3_L001_R2.fq ../Fastq/reads4-B4_S4_L001_R1.fq ../Fastq/reads4-B4_S4_L001_R2.fq ../Fastq/reads5-B5_S5_L001_R1.fq ../Fastq/reads5-B5_S5_L001_R2.fq ../Fastq/reads6-B6_S6_L001_R1.fq ../Fastq/reads6-B6_S6_L001_R2.fq ../Fastq/reads7-B7_S7_L001_R1.fq ../Fastq/reads7-B7_S7_L001_R2.fq ../Fastq/reads8-B8_S8_L001_R1.fq ../Fastq/reads8-B8_S8_L001_R2.fq

# then created new reference based on the mutations predicted in the mutated all results

path_to/breseq-0.27.1-Linux-x86_64/bin/gdtools APPLY –r ../8325referencegenbanksequenceadded.gb -f GFF3 -o mutatedallref.gff3 mutated_outputall/output/output.gd

#the newly created reference sequence was then used to run all of the separate sequencing results (in pairs)

for i in 1 2 3 4 5 6 7 8; do
path_to /breseq-0.27.1-Linux-x86_64/bin/breseq -j 4 -r mutatedallref.gff3 -o mutated_outputall${i} ../Fastq/reads${i}-B${i}_S${i}_L001_R1.fq ../Fastq/reads${i}-B${i}_S${i}_L001_R2.fq
done


#the completed outputs were manually screened for mutations (HTML document) the marginal predictions an unassigned data were also looked at but the differences were conserved, these were in a small enough quantity they could be manually excluded rather than needing to make additions to the mutated reference. They appear to be clustered around 2 regions of repetitive sequence identity making working out junctions or deletions difficulty. as they appear conserve and this region is highly repetitive i have not looked further into them.
```

References.

1. Corrigan, R.M., et al., *c-di-AMP is a new second messenger in Staphylococcus aureus with a role in controlling cell size and envelope stress.* PLoS Pathog, 2011. **7**(9): p. e1002217.
2. McClure, R., et al., *Computational analysis of bacterial RNA-Seq data.* Nucleic Acids Res, 2013. **41**(14): p. e140.

Chapter 7:

Final Discussion & Future Directions

Chemical optimisation of BPL inhibitors as antibacterial agents

Non-hydrolysable BPL reaction intermediate mimics have had success in inhibiting BPLs from a variety of organisms [1-8]. However, whole cell antibacterial activity against *S. aureus* has been difficult to achieve with these compounds [5, 6]. Improving the whole cell antibacterial activity of inhibitors has therefore been a major focus of compound design in this thesis. Using two established literature compound series as a starting point, a biotin-triazole and biotin sulphonamide **(2, 5, figure 1)**, we were able to improve the antibacterial activity against *S. aureus*. These new compound series include the most potent anti-staphylococcal inhibitors to date.

The first series of compounds were the Benzyl biotin-triazoles (chapter 4). Previous to this work the most potent and selective *SaBPL* inhibitor was the biotin-triazole **2**, which despite potent inhibitory activity (K_i 90nM) did not completely inhibit *S. aureus* growth (i.e. only 80% inhibition) [5]. Benzyl biotin triazoles focused on reducing the size of this biotin-triazole pharmacophore, and increasing affinity by appending functional groups to extend into the binding pocket for the ribose of ATP. These benzyl biotin-triazoles had sub-micromolar inhibitory activity, but, like the precursor compounds, lacked the ability to completely inhibit bacterial growth. Halogenation of the benzyl ring, as in **BPL178 (3, figure 1)**, produced the most potent compound (K_i 280nM), however a clear structure activity relationship (SAR) was difficult to define. The co-crystal structure of this compound suggested the benzyl ring could bind in multiple conformations in the ribose pocket, providing a possible molecular explanation for the unusual SAR. Further stabilising one of these conformations, or extending the compound into another binding pocket, may be an avenue to improve potency.

A second attempt to improve whole cell antibacterial activity was through halogenation on the C5 of the triazole ring (chapter 5). Whilst this generally did not improve on inhibition against the BPL, halogenated compounds showed vastly improved antibacterial activity. This included a fluorinated analogue of compound **2**, **(4, figure1)**, able to completely

inhibit growth of the clinical isolate *S. aureus* ATCC 49775 (MIC = 8 μg/ml). The *in vitro* characterisation of this inhibitor:enzyme interaction suggested that the whole cell activity was not due to increased target occupancy or improved inhibition of the BPL. Hence, we argue that increased compound accumulation was likely responsible for the improved antibacterial activity. It remains unclear however if this is due to passive diffusion into the cell, increased affinity to a transport protein, such as the biotin transporter BioY (discussed further below) or an alternate mechanism such as decreased efflux. If halogenation can improve whole cell activity independently of the biotin-triazole pharmacophore, then trisubstitution of other antibacterial di-substituted triazoles [9, 10] may similarly improve activity. Such an approach would inform the generality of this response and potentially offer an avenue to improve whole cell activity for an extended range of compounds.

Despite the improvements made to the triazole pharmacophore, inhibitory potency and antibacterial activity were lacking compared to the pan inhibitor **biotinol-5′-AMP, (1, figure 1)**. As a result, a new pharmacophore was investigated from a bio-active literature molecule against *M. tuberculosis* reported to lack anti-staphylococcal activity (**5, figure 1)** [1]. Here the phosphodiester group of **1** was replaced with an alternative bioisostere, a sulfonyl linker. By removing the ribose moiety, that we previously demonstrated to be dispensable for activity, a new potent inhibitor was identified, **BPL199 (6, figure 1)** (K_i = 2nM). This compound offered promising antibacterial activity (MIC 0.125-0.5 μg/ml) whilst retaining selectivity against the human enzyme and exhibiting no cytotoxicity against two human cell lines (K_i > 10 μM, EC_{50} > 250 μg/ml). To address the clinical potential of **6** the antibacterial spectrum, synergy with other antibacterials and spontaneous resistance rates were all tested. These data demonstrated that the compound was narrow spectrum, exhibited synergy with two commercially available antibacterial agents (Streptomycin and Methicillin) and had a low resistance rate (< 1×10^{-9}). The mechanisms of antibacterial action and resistance were also investigated, discussed further below.

1) Biotinol-5′-AMP

K_i = 0.018 µM, MIC 1-4 µg/ml

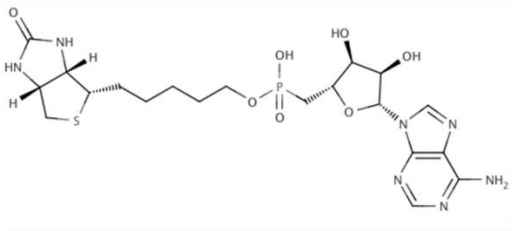

2) BPL068

K_i = 0.09 µM/ 0.23 µM

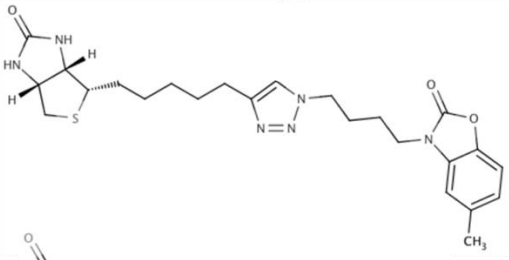

3) BPL178

K_i = 0.28 µM,

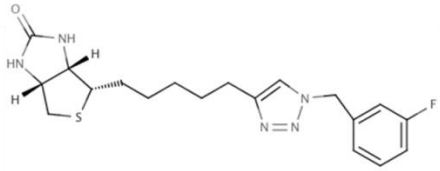

4) BPL 223

K_i = 0.42 µM

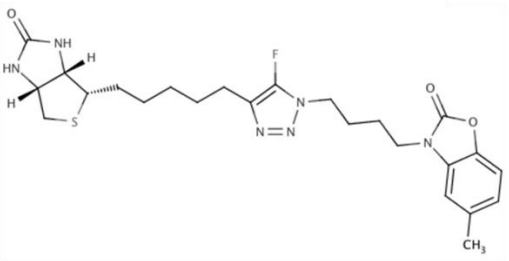

5) Bio-AMS (Duckworth et. al)

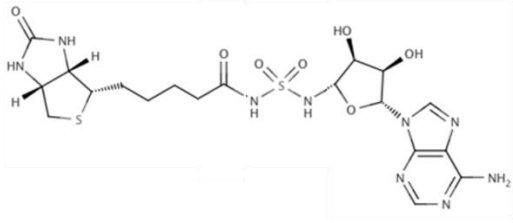

6) BPL199

K_i = 0.004 µM, MIC 0.5 µg/ml

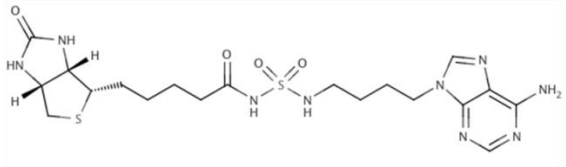

7) BB-R127

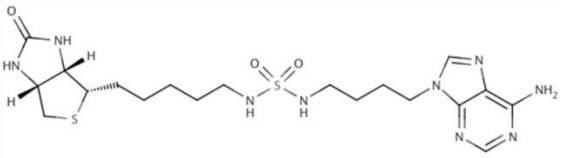

8) ID46P96a

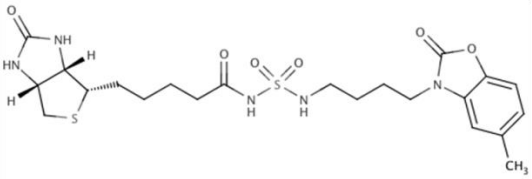

Figure 1: Key compounds created in this study and literature precursors

Mechanism of action

Whilst *in vitro* evidence supported BPL as an antibacterial target [7] no study had demonstrated the mechanism of action of BPL inhibitors in *S. aureus*. In chapters 3-6 we demonstrated that alongside catalytic inhibition of BPL, the transcriptional repression of *Sa*BPL also plays a role in the antibacterial activity of **6**. Transcriptional repression induced by **6** led to a reduction in biotin synthesis and transport genes and, hence, would reduce intracellular biotin concentrations. A mutation, D200E, in the BPL of a *S. aureus* strain resistant to **6** was also identified. This mutation had no significant effect on inhibitor binding but prevented dimerization and the resulting repressor activity of the protein. This further validated transcriptional repression in the antibacterial mechanism of action.

Despite understanding the role of the transcriptional repression capability of **6** in antibacterial activity, the ability of other BPL inhibitors to act as co-repressors has not been thoroughly explored. Work on *E. coli* BPL has shown certain BPL inhibitors can exhibit different co-repressor capabilities, despite similar affinities for enzyme binding and similar structures [1, 11]. It stands to reason that similar differences may occur for inhibitors binding the *S. aureus* BPL. Together with differences in cellular accumulation, differences in co-repressor capability may serve to explain how whole cell activity can be vastly different for compounds with the same inhibitory activity. As there are few co-crystal structures with compounds that lack antibacterial efficacy against *S. aureus* we lack data to determine whether conformational changes that prevent DNA binding activity occur in the BPL when these compounds bind. As well, no high resolution structure of BPL in complex with DNA has yet been obtained. This makes interpreting the effect of any conformational changes challenging. Addressing these gaps in our understanding would hopefully shed light onto whether different conformations could be responsible for the reduced activity of some compounds.

BioY transporter and mechanism of whole cell entry.

As established in chapter 4, and discussed above, inhibitory and antimicrobial activity of BPL inhibitors is not always well correlated. One possible reason for this is the ability of the compounds to accumulate inside the cell. Currently two mechanisms for cell entry of BPL inhibitors are hypothesised, either, by passive transport across the cell membrane or recognition and transport by the biotin transporter BioY. If the latter case occurs then improving affinity for BioY could allow for increased efficacy of inhibitors. Studies performed by Dr. Al Azhar in our laboratory have demonstrated that BPL inhibitors can have different affinities for BioY. In particular the biotin-triazole **2** is able to bind competitively to BioY over fluorescent biotin, whilst biotinol-5′-AMP **1** is not [12]. If cellular uptake is through BioY such differences in affinity for the transporter could play an important role in antimicrobial activity. In an attempt to address whether BioY is required for cellular uptake, and whole cell activity, a strain of *S. aureus* with the *bioY* gene disrupted has been sourced. Preliminary studies using this strain indicate that the compound biotinol-5′-AMP is less effective against a strain lacking the transporter, though activity is not abolished (personal communications). This indicates that whilst the BioY transporter contributes to uptake this is not the only mechanism. Following up on this result with a larger compound series would provide useful insight into the role of the transporter on whole cell activity, potentially guiding further inhibitor design.

Resistance studies methodology

In chapter 6, experiments were performed to address the ability of *S. aureus* to evolve resistance to the BPL inhibitor **6**. This was achieved using evolution by continually subculturing *S. aureus* in suboptimal concentrations of inhibitor, a well-established route for the generation of resistance. Whole genome sequencing revealed several mutations that correlated with resistance, offering insight into potential resistance mechanisms. However, the sequencing analysis was restricted to the genome of a single isolate from each experimentally evolved population, limiting the information available. New technologies are now available that provide the potential for more in depth analysis. One example is the use of systems that allow for more reproducible and controllable growth conditions, such as chemostats that maintain constant media conditions, or morbidostats [13] that modify antibiotic concentration based on density of the culture. Spatial concentration gradients are another technology which offer a unique ability to map the evolution of drug resistance, with an evolutionary trajectory visible as a path to higher concentrations [14, 15]. Furthermore, improved DNA sequencing capability and computation power allow for the use of more isolates and larger datasets for analysis. This enables mapping of genetic fluctuations in populations over time, revealing evolutionary trajectories and dead ends [13, 14, 16-20]. Through this analysis, information about competing mutations, the presence of mutations that become dominant, and loss of lines that are unable to adapt, can all be gleaned [15, 16]. With these technological improvements and decreased sequencing costs, resistance studies will be able to provide valuable new information about resistance in both the laboratory and clinical settings.

One notable deficiency in the literature is a consensus on the number of samples required to gain confidence that mutations observed are representative of a larger population. Commonly 5 isolates are used in recent studies [13, 17, 21] though no rationale behind this number is provided, with personal experience indicating this is likely due to sequencing costs. As generating larger datasets becomes more cost effective, the amount of information that can be extracted from such experiments will also increase. For example population analysis can determine if a particular gene is overrepresented in a study, the rate of mutation is higher than expected, or if mutations are constrained to defined trajectories [20]. This would assist in certain cases, such as those presented in chapter 7, where 5 of 7 strains contained a mutation leading to loss of function of pyruvate carboxylase. Using a mathematical model that assesses the accumulation of mutations in a model system, it should be possible to determine whether a particular gene is statistically over-represented, given a large enough sample size. However, the framework for how to approach such analysis has not yet been established (reviewed [15]). Whilst in no way encompassing a complete model for such an analysis, the criteria presented in Box 1 provides some considerations and assumptions that should be considered.

BOX 1: parameters that may be useful for the generation of a statistical model surrounding the likelihood of mutations occurring in response to selection pressure.

1. **Mutation rate** - (≈4-14× 10^{-11} per bp/generation* ≈ 0.3 per genome/ generation for *S. aureus*) [16, 22, 23]

2. **Estimate of mutational events/ population –** The number of mutational events in a population is a function of the number of doubling events and the mutation rate. As population growth is largely exponential, and the initial population is significantly lower than the final population, the number of generations/day can be represented by $\log_2$ (final population density/day) ≈ number generations/ day.

3. **Genetic drift -** depending on the situation this is either a static rate such as the dilution from one day's passage to the next or a continuous rate of cell removal as is observed in chemostats. For the experiment in chapter 6 each population sampled 1/20,000th of the previous day's overnight culture.

4. **Mutation impact** - The rate of silent mutations in protein coding regions is approximately 20% of total mutations. At least 20% of mutational events in protein coding genes therefore have no effect on protein coding, reducing the impact of mutations [16].

*this may be effected by the presence of mutator strains [16] or increased mutation as a result of reactive oxygen species produced as a result of antibiotic exposure.[24]

Issues facing antibiotics beyond resistance

This study also helps to highlight one emerging issue in addressing antibiotic resistance, that of cells that avoid antibiotic effects without developing genetic resistance. In particular one of the strains identified in the advanced resistance studies (B3) was capable of tolerating high concentrations of antibiotic but grew relatively slowly. This phenotype is commonly associated with so-called 'persister' cells which play a key role in recurrent infections. Persister cells are characterised as dormant phenotypic variants, present as a subpopulation of a bacterial population, which can survive concentrations of bactericidal antibiotics higher than the MIC. These are distinct from resistant populations which contain genetic variation that provide a higher MIC for the whole population [25, 26]. Persisters are often tolerant to a wide range of antimicrobial agents, surviving treatments of high doses of antibiotic in their dormant state before exiting this state and re-instating an infection [27, 28]. This makes them an issue in clinical settings. Persister cells and biofilm formation are also linked with the lack of nutrient availability in a biofilm setting predicted to induce a higher proportion of persister cells, leading to their antibiotic tolerance [29-31]. A corollary of this is that agents designed to target persister cells also serve to eradicate biofilm infections[29].

Studying the mechanism of persister formation is difficult due to their transient nature. However, several studies have attempted to define a concerted mechanism by which persisters occur (reviewed [32]). Of particular interest to the work described in this thesis are the established links between metabolic state and the induction of persisters and biofilms. In particular the TCA cycle, involved in cellular energy production and biosynthesis of certain metabolic products, appears to be required for persister cell and biofilm formation [32, 33] **(figure 2)**. In *E. coli* decreased numbers of persister cells are observed in strains containing deletions of several TCA cycle enzymes, implicating this metabolic pathway in persister formation [33]. Similarly in *S. aureus* the deletion of genes encoding succinate

dehydrogenase, involved in the TCA cycle, led to reduced persister formation [34]. Upregulation of TCA cycle genes are also observed in biofilms [35, 36]. These data suggest that the TCA cycle is important for persister cell and biofilm states in *E. coli* and *S. aureus*. Late last year, a development in the ability to track persister cells in cultures of *S. aureus* identified that persister cells were a sub-population of cells that enter stationary phase prematurely [37]. The cause of this was established to be due to decreased ATP concentration in the cell as artificially reducing ATP levels induced the persister phenotype [37]. Replication of this study in *E. coli* suggests that ATP depletion, a hallmark of nutrient deprived biofilms, may be the common mechanism for persister cell formation [38].

It is as of yet still unclear as to the exact effect PC inhibition has on TCA cycle activity and, through it, ATP levels in the cell. The TCA cycle provides ATP to post-exponentially growing cells [39], suggesting inhibiting this process should increase persister formation. To the contrary, the deletion knock-outs of certain TCA cycle genes reduced the number of persisters in a population, [32-34] suggesting the opposite effect. Understanding exactly how reduction of PC activity affects persister formation is therefore important for understanding if BPL inhibition would combat this state. If BPL inhibitors can reduce persister formation this would allow the development of combination therapies to target these difficult to treat infections. Evidence to support this was provided with **6**, which showed efficacy against an *in vitro* biofilm model of *S. aureus* (personal communications). If this can be verified BPL inhibitors may address a vital niche lacking in current antibacterial agents.

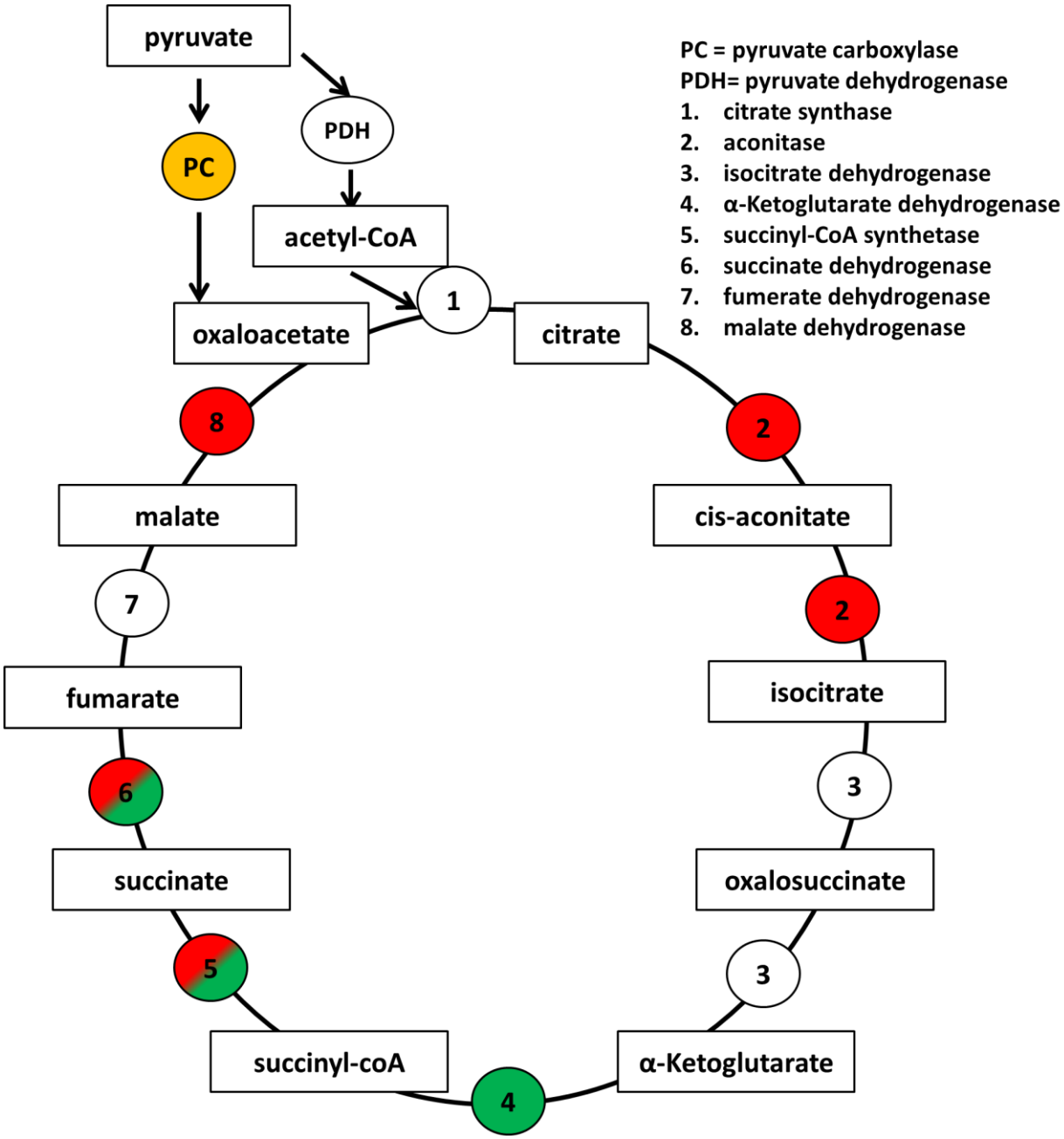

Figure 2: TCA cycle enzymes: aconitase ***acnB***, α-Ketoglutarate dehydrogenase, succinyl-CoA synthetase ***sucB***, succinate dehydrogenase ***sdhA/B/C***, and malate dehydrogenase ***mdh*** are implicated in (red) persister formation in *E. coli* [33] or *S. aureus* [34], or (green) biofilm formation in *S. aureus* [35, 36]. Bolded gene names indicate specific genes tested in knock-out studies [33, 34].

Conclusion

The future of healthcare depends on the discovery of new antibacterial agents alongside new ways to manage antibiotic resistance. The work described in this thesis serves to both improve the antibacterial activity of BPL inhibitors as well as address some of the underlying questions surrounding this compound class. Two independent compound series with improvements on antibacterial activity are described here, an important step in the creation of a pre-clinical candidate. In particular the compound **6** offers the most promising activity described to date against *S. aureus.* With this compound we were also able to probe the mechanism of action of BPL inhibitors, identifying a role for the transcriptional repressor function. The resistance studies using this compound also further enhanced our understanding of how BPL inhibition works, highlighting how resistance may occur. The work presented here also provides vital information for the future development of BPL inhibitors whilst serving to further inform the chemical biology behind the mechanism of action and resistance to this novel compound class.

References

1. Duckworth, B.P., et al., *Bisubstrate adenylation inhibitors of biotin protein ligase from Mycobacterium tuberculosis.* Chem Biol, 2011. **18**(11): p. 1432-41.
2. Park, S.W., et al., *Target-based identification of whole-cell active inhibitors of biotin biosynthesis in Mycobacterium tuberculosis.* Chem Biol, 2015. **22**(1): p. 76-86.
3. Shi, C., et al., *Bisubstrate Inhibitors of Biotin Protein Ligase in Mycobacterium tuberculosis Resistant to Cyclonucleoside Formation.* ACS Med Chem Lett, 2013. **4**(12): p. 12131217.
4. Tieu, W., et al., *Improved Synthesis of Biotinol-5'-AMP: Implications for Antibacterial Discovery.* ACS Med Chem Lett, 2015. **6**(2): p. 216-20.
5. Soares da Costa, T.P., et al., *Selective inhibition of Biotin Protein Ligase from Staphylococcus aureus.* J Biol Chem, 2012. **287**(21): p. 17823-17832.
6. Feng, J., et al., *New Series of BPL Inhibitors To Probe the Ribose-Binding Pocket of Staphylococcus aureus Biotin Protein Ligase.* ACS Med Chem Lett, 2016. **7**(12): p. 1068-1072.
7. Paparella, A.S., et al., *Structure guided design of biotin protein ligase inhibitors for antibiotic discovery.* Curr Top Med Chem, 2014. **14**(1): p. 4-20.
8. Tieu, W., et al., *Heterocyclic acyl-phosphate bioisostere-based inhibitors of Staphylococcus aureus biotin protein ligase.* Bioorg Med Chem Lett, 2014. **24**(19): p. 4689-93.
9. Aufort, M., et al., *Synthesis and antibiotic activity of a small molecules library of 1,2,3-triazole derivatives.* Bioorg Med Chem Lett, 2008. **18**(3): p. 1195-8.
10. Holla, B.S., et al., *Synthesis, characterization and antimicrobial activity of some substituted 1, 2, 3-triazoles.* Eur J Med Chem, 2005. **40**(11): p. 1173-1178.
11. Brown, P.H., et al., *The biotin repressor: modulation of allostery by corepressor analogs.* J Mol Biol, 2004. **337**(4): p. 857-869.
12. Azhar, A., *Structure-function relationships of the biotin transporters from Staphylococcus aureus*. 2015, The University of Adelaide.
13. Toprak, E., et al., *Evolutionary paths to antibiotic resistance under dynamically sustained drug selection.* Nat Genet, 2012. **44**(1): p. 101-5.
14. Baym, M., et al., *Spatiotemporal microbial evolution on antibiotic landscapes.* Science, 2016. **353**(6304): p. 1147-1151.
15. Lukačišinová, M. and T. Bollenbach, *Toward a quantitative understanding of antibiotic resistance evolution.* Curr Opin Biotechnol, 2017. **46**: p. 90-97.
16. Barrick, J.E. and R.E. Lenski. *Genome-wide mutational diversity in an evolving population of Escherichia coli*. in *Cold Spring Harbor symposia on quantitative biology*. 2009. Cold Spring Harbor Laboratory Press.
17. Friedman, L., J.D. Alder, and J.A. Silverman, *Genetic changes that correlate with reduced susceptibility to daptomycin in Staphylococcus aureus.* Antimicrob Agents Chemother, 2006. **50**(6): p. 2137-45.
18. Comas, I., et al., *Whole-genome sequencing of rifampicin-resistant Mycobacterium tuberculosis strains identifies compensatory mutations in RNA polymerase genes.* Nat Genet, 2011. **44**(1): p. 106-10.
19. Toprak, E., et al., *Evolutionary paths to antibiotic resistance under dynamically sustained drug selection.* Nat Genet, 2011. **44**(1): p. 101-5.
20. Dettman, J.R., et al., *Evolutionary insight from whole-genome sequencing of experimentally evolved microbes.* Mol Ecol, 2012. **21**(9): p. 2058-77.
21. Johnston, P.R., A.J. Dobson, and J. Rolff, *Genomic Signatures of Experimental Adaptation to Antimicrobial Peptides in Staphylococcus aureus.* G3 (Bethesda), 2016. **6**(6): p. 1535-9.
22. Drake, J.W., et al., *Rates of spontaneous mutation.* Genetics, 1998. **148**(4): p. 1667-1686.
23. Ochman, H., S. Elwyn, and N.A. Moran, *Calibrating bacterial evolution.* Proc Natl Acad Sci U S A, 1999. **96**(22): p. 12638-12643.
24. Kohanski, M.A., M.A. DePristo, and J.J. Collins, *Sublethal antibiotic treatment leads to multidrug resistance via radical-induced mutagenesis.* Mol Cell, 2010. **37**(3): p. 311-20.

25. Sebastian, J., et al., *De Novo Emergence of Genetically Resistant Mutants of Mycobacterium tuberculosis from the Persistence Phase Cells Formed against Antituberculosis Drugs In Vitro.* Antimicrob Agents Chemother, 2017. **61**(2): p. e01343-16.
26. Levin-Reisman, I., et al., *Antibiotic tolerance facilitates the evolution of resistance.* Science, 2017: p. eaaj2191.
27. Mulcahy, L.R., et al., *Emergence of Pseudomonas aeruginosa strains producing high levels of persister cells in patients with cystic fibrosis.* J Bacteriol, 2010. **192**(23): p. 6191-9.
28. LaFleur, M.D., Q. Qi, and K. Lewis, *Patients with long-term oral carriage harbor high-persister mutants of Candida albicans.* Antimicrob Agents Chemother, 2010. **54**(1): p. 39-44.
29. Conlon, B.P., et al., *Activated ClpP kills persisters and eradicates a chronic biofilm infection.* Nature, 2013. **503**(7476): p. 365-370.
30. Lewis, K., *Riddle of biofilm resistance.* Antimicrob Agents Chemother, 2001. **45**(4): p. 999-1007.
31. Singh, R., et al., *Role of persisters and small-colony variants in antibiotic resistance of planktonic and biofilm-associated Staphylococcus aureus: an in vitro study.* J Med Microbiol, 2009. **58**(8): p. 1067-1073.
32. Harms, A., E. Maisonneuve, and K. Gerdes, *Mechanisms of bacterial persistence during stress and antibiotic exposure.* Science, 2016. **354**(6318): p. aaf4268.
33. Orman, M.A. and M.P. Brynildsen, *Inhibition of stationary phase respiration impairs persister formation in E. coli.* Nat Commun, 2015. **6**.
34. Wang, W., et al., *Transposon Mutagenesis Identifies Novel Genes Associated with Staphylococcus aureus Persister Formation.* Front Microbiol, 2015. **6**: p. 1437.
35. Resch, A., et al., *Differential gene expression profiling of Staphylococcus aureus cultivated under biofilm and planktonic conditions.* Appl Environ Microbiol, 2005. **71**(5): p. 2663-76.
36. Resch, A., et al., *Comparative proteome analysis of Staphylococcus aureus biofilm and planktonic cells and correlation with transcriptome profiling.* Proteomics, 2006. **6**(6): p. 1867-1877.
37. Conlon, B.P., et al., *Persister formation in Staphylococcus aureus is associated with ATP depletion.* Nat Microbiol, 2016. **1**.
38. Shan, Y., et al., *ATP-Dependent Persister Formation in Escherichia coli.* mBio, 2017. **8**(1): p. e02267-16.
39. Somerville, G.A. and R.A. Proctor, *At the crossroads of bacterial metabolism and virulence factor synthesis in Staphylococci.* Microbiol Mol Biol Rev, 2009. **73**(2): p. 233-48.

Appendix 1-assay development

Introduction

It is important to understand the mechanism of action of a drug before embarking on preclinical and clinical testing for both ethical and economic reasons. The ability to understand how a drug works allows for better prediction of potential positive and negative interactions with other treatments, as well as side effects and how resistance may occur. One way to demonstrate mechanism of action is through overexpression of the presumed target. By overexpressing the target enzyme and observing decreased efficacy of the compound it is possible to validate the mechanism of action of an antibacterial agent. Using this method it has been demonstrated that BPL inhibitor Bio-AMS exhibits reduced efficacy in a strain of *Mycobacterium* with increased BPL expression [1]. However, a BPL overexpression system has not been established in *S. aureus*.

For this purpose I constructed a recombinant expression vector and transformed this into *S. aureus* RN4220. By measuring the growth of the bacteria treated with BPL inhibitors in the presence and absence of this overexpression it was possible to either validate or invalidate the hypothesis that the antibacterial activity occurs through BPL inhibition. For an appropriate control, the parental vector lacking the *Sa*BPL coding region was also transformed into *S. aureus*. *S. aureus* has a restriction modification system which poses a high barrier to the transformation of plasmids [2]. As a result a shuttle vector capable of replication and selection in both *E. coli* and *S. aureus* was required. The vector chosen was pCN51 [3] which had several desirable traits: a large copy number origin of replication and ampicillin selection in *E. coli,* small copy number origin of replication and erythromycin selection in *S. aureus* and a cadmium inducible promoter for controlled expression of target proteins. In this appendix I report the construction and validation of the overexpression system for BPL in *S. aureus*. This system was subsequently used to determine the mechanism of antibacterial action of several series of BPL inhibitors in the following chapters.

Methods

Antibacterial susceptibility testing

Antibacterial susceptibility testing was undertaken as per standard protocol (**2.2.1.1)** with relevant antibiotic and inducing agents added as specified.

Cloning and creation of pCN51-SaBPL vector (figure 1)

All vectors were propagated in *E. coli* DH5α unless specified elsewhere.

The pCN51 vector lacked appropriate restriction sites around the multiple cloning site for cloning in the *Sa*BPL-H6 gene from the pGEM-SaBPL-H6 vector. To facilitate cloning of *Sa*BPL from pGEM-SaBPL-H6 to pCN51 an *Nco*I site was inserted by amplifying the existing cadmium cassette using primers B458 (equivalent to 594 described in [3]) and B459 containing *Nco*I site and *Pst*I restriction sites. The resulting PCR product was digested with *Sph*I and *Pst*I and ligated into similarly treated pCN51, yielding pCN51-*Nco*I. The desired plasmid was confirmed by restriction analysis **(figure 2)** and DNA sequencing. The *Sa*BPL over-expression vector was then constructed by ligating the 2kb *Pci*I / *Eco*RI fragment from pGEM-SaBPL-H6 into *Nco*I and *Eco*RI treated pCN51-*Nco*I Restriction analysis and DNA sequencing, using the primers B493 and B200, confirmed the desired vector was obtained **(figure 3)**.

Preparation of competent *S. aureus* RN4220

Competent cells of *S. aureus* strain RN4220 were prepared essentially as described by Monk et al. [2], bolded sections represent deviations from published protocol. Overnight cultures of *S. aureus* RN4220, 10mL, were grown in Mueller Hinton Media (CAMHB) and diluted to OD600 of 0.5 in 50 mL of prewarmed **CAMHB** before being incubated at 37℃ for 30 minutes. The cells were chilled on ice for 10 minutes with subsequent steps performed at 4°C unless specified. Cells were centrifuged at 4000 × g for 10 minutes and the pellets resuspended in equal volume ice cold MilliQ water. This was repeated twice. The washed cells were then resuspended in 5 ml, 2 mL and finally 250 µl of ice cold

10% (w/v) glycerol. Aliquots of 60 µl were added to pre-chilled microcentrifuge tubes. Cells were then allowed to sit for approximately 30 minutes before being incubated for 5 minutes at room temperature and centrifuged at 4000 × g for 1 minute. The resulting cell pellet was resuspended in 50 µl of a 10% glycerol, 400 mM sucrose solution**.**

Transformation of competent cells

Plasmid DNA (4µl at approximately 500 ng/µl) was added to the cells before being transferred to a 2mm electroporation cuvette. The cuvette was pulsed on the micropulser electroporator ™ (Bio-Rad, California, U.S.A.) on the *S. aureus* setting (single pulse at 1.8 kv, with 2.5msec time constant) at room temperature. **Time constants of approximately 1.8 msec were observed.** The cells were immediately recovered in 1mL of prewarmed **CAMHB** containing 500 mM sucrose before incubation for 2 hours at 37 °C. **200 µL of the culture was plated onto CAMHB agar containing 10 µg/mL erythromycin for selection.** Colonies did not appear on the plate until after approximately **36 hours** had passed. Colonies were picked and grown in liquid culture supplemented with 10 µg/ml erythromycin overnight to select for true transformants. Plasmid extraction of pCN51-*Nco*I or pCN51-BPL using the QIAGEN kit with an additional lysostaphin incubation step (**2.2.4.4**) confirmed the cells harboured the desired plasmid.

Cadmium chloride overexpression protocol

An overnight culture of RN4220 + PCN51_*Nco*I and RN4220 + PCN51_*Sa*BPL was prepared with 10 µg/ml erythromycin for the maintenance of the plasmid. The overnight culture was subcultured (10 µl into 5mL) into media with 10 µg/ml erythromycin and 25nM $CdCl_2$. The cultures were incubated for 5 hours before being subcultured 1: 1000 into media containing 50nM $CdCl_2$ to maintain the 25nM $CdCl_2$ after subsequent dilution into the testing plate. An antibacterial susceptibility plate was then prepared as per standard antibacterial susceptibility protocol (**2.2.1.2**) with additional 10 µg/mL erythromycin and 25nM $CdCl_2$, for selection and induction respectively. Plates were incubated with shaking for 22 hours at 37°C and OD630 nM taken every 30 minutes using an EL808™ Absorbance Microplate Reader (BioTek Instruments Inc, Winooski, VT, USA)

Validation

Optimising growth conditions for recombinant expression

To verify that the plasmids or conditions themselves were not having an adverse effect on growth, the growth of strains containing each plasmid was compared. Initial testing of the system using conditions described in [3] of 1-15 μM of $CdCl_2$ led to toxicity, with cells unable to tolerate the $CdCl_2$ over periods of time longer than the 1 hour induction described in the paper. Using a dilution series of $CdCl_2$ the appropriate concentration of $CdCl_2$ was determined to be 25 nM as growth was hindered at higher concentrations counteracting the decreased susceptibility to BPL199 **(figure 3).** This slight reduction in growth appears to be dependent on BPL expression with the parental vector control not inhibited by 100nM $CdCl_2$. To determine if the recombinant system was expressing sufficient *Sa*BPL to observe the effect of over-expression on BPL inhibitor efficacy the literature compound biotinol-5′-AMP was tested. *S. aureus* RN4220 containing the pCN51-BPL vector challenged with biotinol-5′-AMP exhibited a shift in MIC of 16 fold **(figure 4a)** over the parental control, indicating overexpression of *Sa*BPL reduced susceptibility to BPL inhibitors. This effect was specific to BPL inhibitors, as the two strains when challenged with amoxicillin showed no observable difference in MIC or growth **(figure 4b).**

pCN-BPL shuttle vector for overexpression of SaBPL

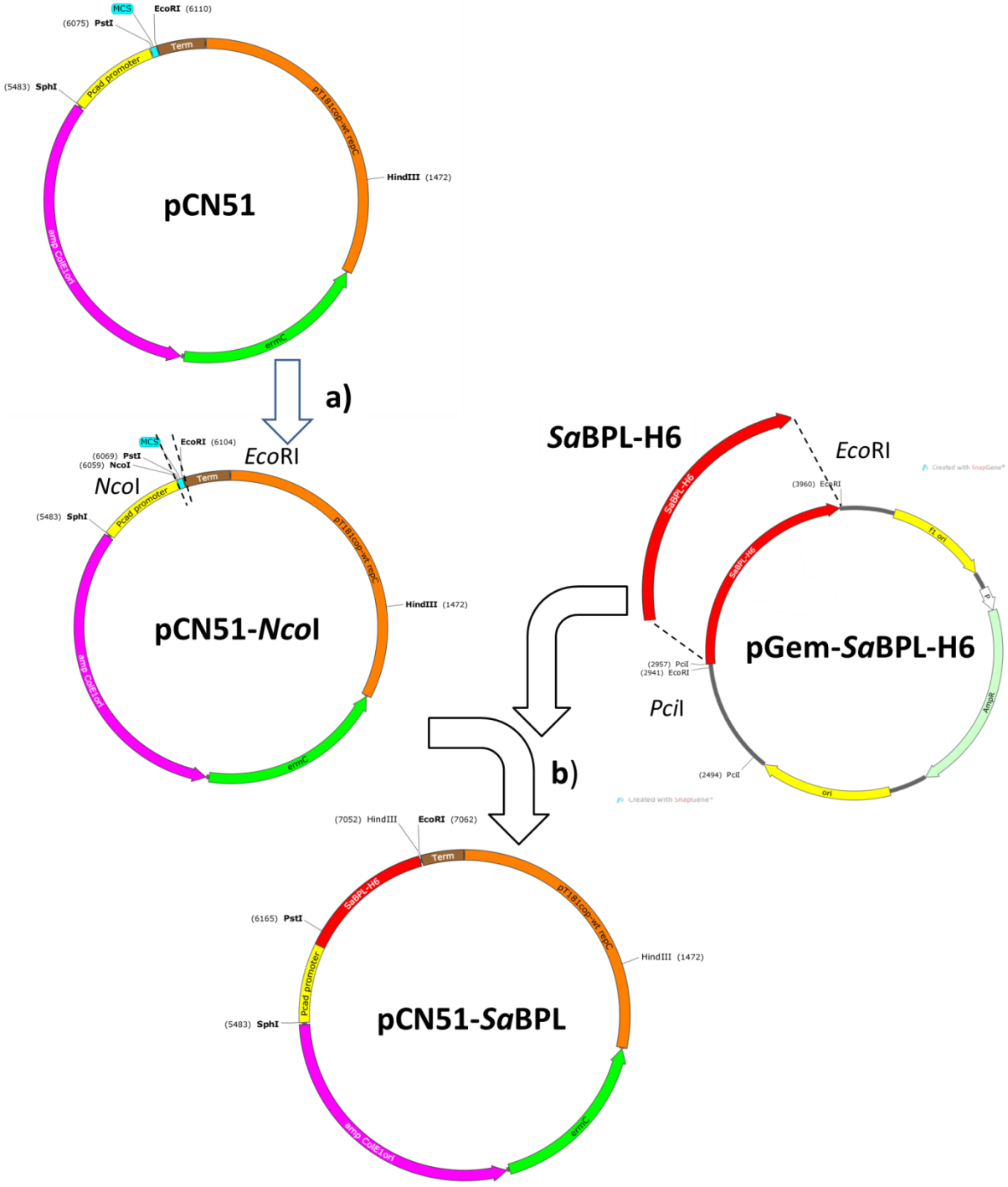

Figure 1: PCN51-SaBPL-H6 plasmid creation diagram. a) PCR was used to insert an *Nco*I restriction site into the MCS of pCN51. PCR product and pCN51 vector were digested with *Sph*I and *Pst*I and ligated to form PCN51-*Nco*I. b) pCN51-*Nco*I and pGem-SaBPL-H6 were digested using *Pst*I/*Nco*I and *Pst*I/*Eco*RI respectively. The 2kb *Sa*BPL-H6 fragment from pGem-SaBPL-H6 was subsequently ligated into the MCS of digested pCN51-*Nco*I to form PCN51-SaBPL.

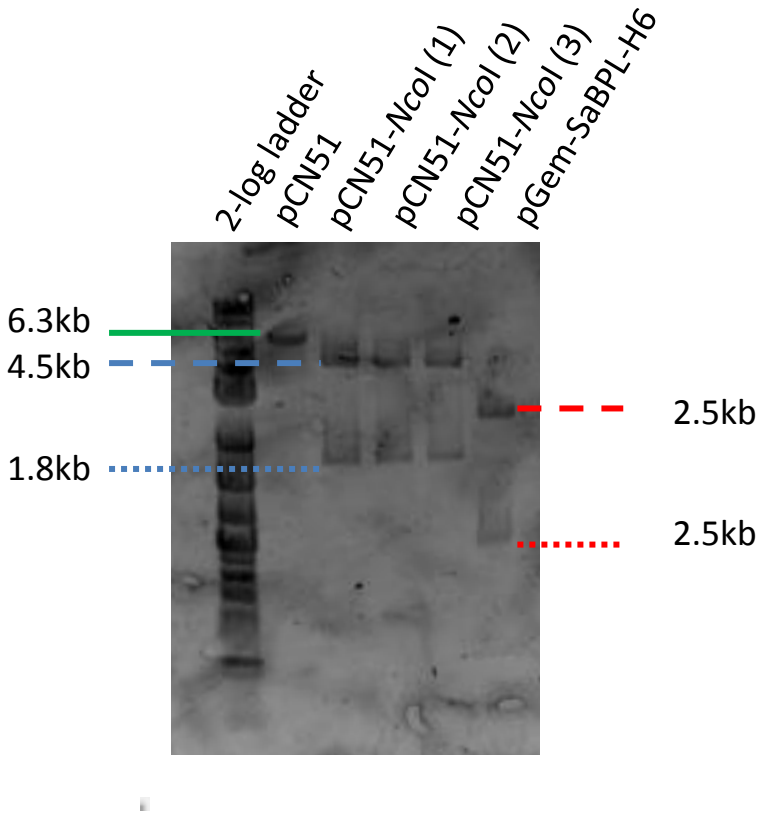

Figure 2: Confirmation of successful integration of *Nco*1 site into pCN51 vector by restriction digest with *Nco*I and HindIII. a) From Left: 1) DNA ladder 2) PCN51 *Nco*I/HindIII, 3-5) pCN51-*Nco*I clones1-3 *Nco*I/HindIII digested, 6) pGEM SaBPL-H6 *Eco*RI/PciI digested.

A)

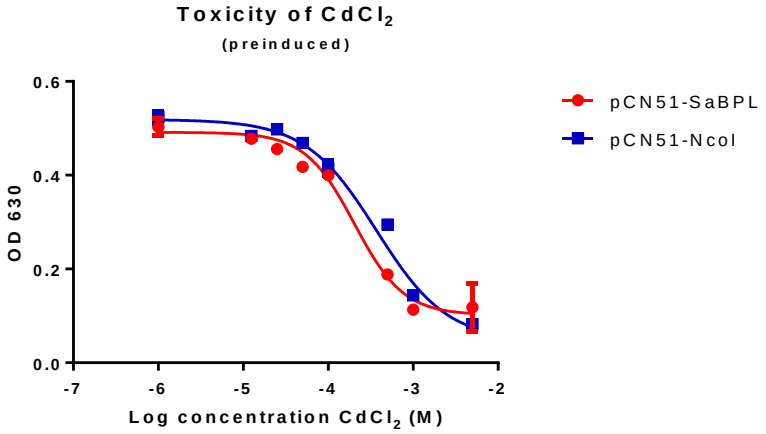

B)

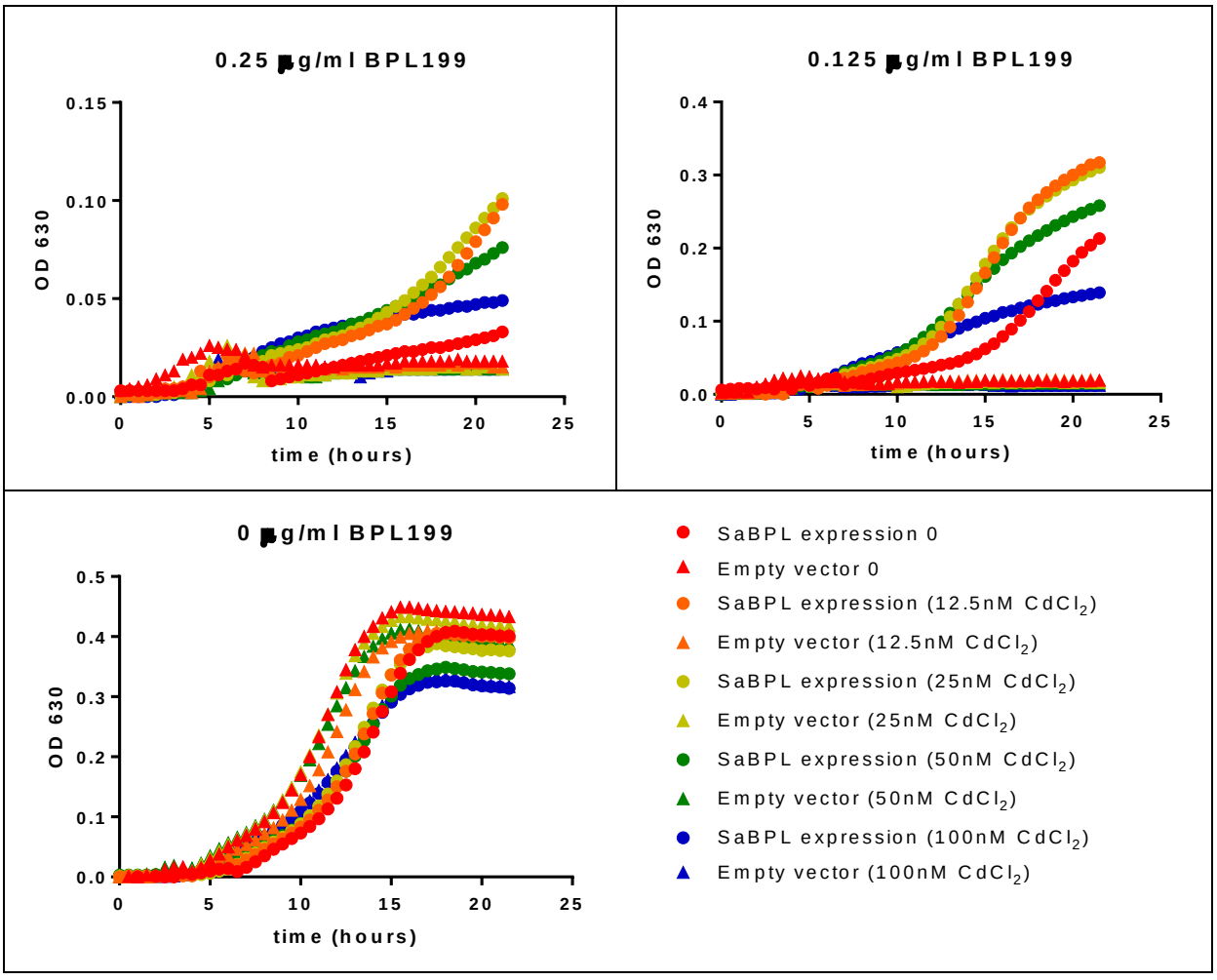

Figure 3: A) dose response of S. aureus RN4220 + PCN51-*Nco*I (blue squares) and +PCN51-BPL (red circles) to $CdCl_2$. B) effect of cadmium chloride at non-toxic concentrations on growth of SaBPL expression vector (circles) and empty PCN51 vector (triangles) in presence of 0.25 and 0.125 µg/ml BPL199 and in absence of compound.

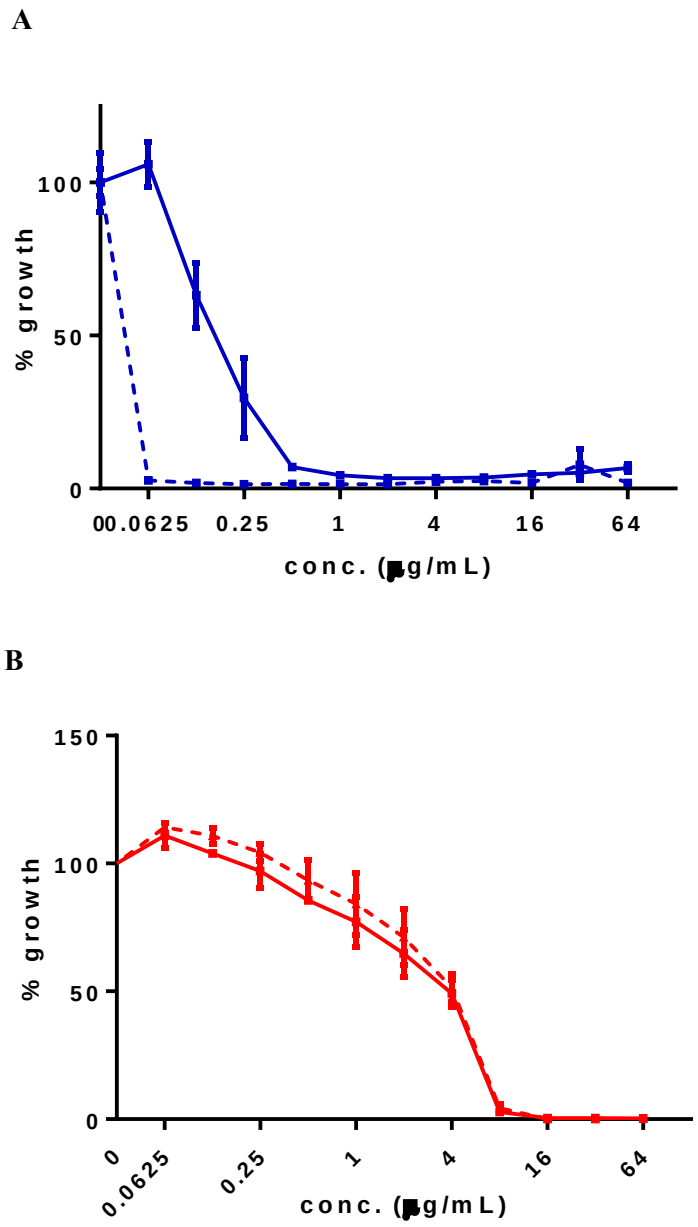

Figure 4: Mechanism of action studies. *S. aureus* RN4220 + pCN51-NcoI control (dashed line) and pCN51-BPL overexpression (solid line) vectors susceptibility to (A) literature BPL inhibitor biotinol-5′-AMP and (B) non BPL targeting antibiotic amoxicillin. Assays were performed in triplicate and normalised to no compound control.

References

1. Duckworth, B.P., et al., *Bisubstrate adenylation inhibitors of biotin protein ligase from Mycobacterium tuberculosis.* Chemistry & biology, 2011. **18**(11): p. 1432-1441.
2. Monk, I.R., et al., *Transforming the untransformable: application of direct transformation to manipulate genetically Staphylococcus aureus and Staphylococcus epidermidis.* MBio, 2012. **3**(2): p. e00277-11.
3. Charpentier, E., et al., *Novel cassette-based shuttle vector system for gram-positive bacteria.* Applied and environmental microbiology, 2004. **70**(10): p. 6076-6085.
4. Grosser, M.R. and A.R. Richardson, *Method for Preparation and Electroporation of S. aureus and S. epidermidis.* The Genetic Manipulation of Staphylococci: Methods and Protocols, 2016: p. 51-57.

Appendix 2-Chapter 6 mutations

Deletion of intergenic region (strains B2, B4, B6, B7)

The second most prevalent mutation, appearing in 4 of the 7 strains isolated, was a deletion in a conserved intergenic region. This mutation was only present in strains also containing the loss of pyruvate carboxylase function, though order of acquisition is unclear. There are several possible explanations for the role of an intergenic deletion. One possible role of the region was transcription of non-coding RNAs. To determine if this was the case an analysis of an available RNAseq dataset in *S. aureus* USA300 at 3 (Accession: SRX1548042) and 16 hours (Accession: SRX1548043) was undertaken using Rockhopper [1] **(Chapter 6, figure s3).** This yielded no detectable transcription. Whilst it is possible that under specific stresses the region is transcribed it was considered unlikely and wasn't further investigated. Another possible explanation is a regulatory region such as a transcription factor binding site. The location of the mutation (approximately 3 kb upstream of BPL gene) suggests a possible link between the deleted region and BPL expression.

Attempts to elucidate the role of the intergenic region were undertaken bioinformatically. If the region contained a binding site for a transcriptional regulator the sequence would need to be conserved. Alignment of several *S. aureus* genomes in the region using MAUVE progressive aligner showed that the deleted region is relatively well conserved **(Chapter 6, figure s4)** in *S. aureus.* However, looking at other Staphylococcal species suggests that the region is unique to the *S. aureus* species. The operon structure of *S. aureus* has yet to be fully characterised so different predictions are required to try and determine co-transcribed genes. The genomic arrangement of the genes suggests the presence of a four gene operon which would be 1000bp downstream of the conserved deleted region. However closely related staphylococcus species, *S epidermidis*, *S. carnosus*, *S. haemolyticus and S. warneri*, have a larger predicted operon containing 5 genes only 200bp downstream of the deleted region. This

larger operon has been disrupted in *S. aureus* by acquisition of a 200bp intergenic region distancing SAOUHSC_01476 from the four genes including *birA* (BPL). Whilst feasible that a new transcription start site and promoter binding region was acquired with this intergenic region it seems possible that the *Sa*BPL operon still includes the SAOUHSC_01476 gene. The larger operon structure is also supported by microarray data linking the regulation of the equivalent of SAOUHSC_01476-01471 in *S. aureus* strain MSSA476 [2] though this has not been validated by other techniques. Based on both this ancestral operon prediction and the microarray data it seems likely that the intergenic deleted region could affect BPL expression in some way. If the deletion removed a DNA recognition motif then it is feasible that it could lead to an increase in BPL and reduced BPL199 susceptibility. This could occur by either removal of a repressor protein or by structural rearrangements that facilitate expression. Previously we have demonstrated that increased BPL expression conveys a level of resistance to BPL199 with an overexpression strain RN4220 [Chapter 5]. This suggests that increased BPL may be a viable resistance method *in vitro*. Further investigation into the effect of the intergenic region in isolation however would be required to make any conclusions as to its role in resistance.

Mutations additional to the PC and intergenic deletions (strains B6, B7)

Strains 6 and 7 each contained two additional mutations [(*gtfA, rpoB*) and (*birA, fmtA*) respectively]. As the PC and intergenic deletions were identical in these two strains it is considered likely that cross contamination of the populations occurred during the experiment as the simplest explanation for such an event is shared evolutionary history [3]. This gives us some insight into the order that the mutations occurred, with the additional mutations almost certainly occurring after the PC and intergenic deletions. Based on comparison with strains B2 and B4, which contained only the PC and intergenic deletions, the additional mutations reduced susceptibility to BPL199 a further 2-fold in B6 and 4-fold in B7. B7 also exhibits an unusual phenotype with increased tolerance at 64μg/ml **(Chapter 6, Figure 1A)**. The

mutations involved in the strains therefore have an additive effect upon resistance either dependent or independent of the previous mutations. The potential roles for each mutation are discussed below.

BPL D200E (strain B7)

The strain B7 had the most pronounced resistance to BPL199 and contained two mutations separate from the commonly shared PC and intergenic deletions. As discussed above one of these mutations one was a missense mutation in BPL (D200E) that altered the reduced repression of biotin biosynthesis (*bioO*) and transport (*bioY*) genes in an *E. coli* lac Z expression system [chapter 5]. It was therefore suggested that resistance to BPL inhibitors was mediated by increasing intracellular biotin. This resistance mechanism was similar to one seen for thiamine synthesis inhibition, where the binding site of the thiamine riboswitch ligand binding site is altered to prevent repression by the mimic pyrithiamine, dysregulating thiamine synthesis as a means of resistance [4]. The presence of the PC loss of function mutation however indicates the potential that D200E is instead a compensatory mutation. The DNA binding function of BPL requires a homo-dimer, the formation of which is thought to be disrupted by un-biotinylated substrate (ACC or PC) either through protein-protein interactions [5] or removal of the co-repressor, biotinyl-5′-AMP [6]. In the strain B7 we have mutations which reduce the amount of un-biotinylated substrate through removal of one of the biotinylated proteins. This could feasibly disrupt the stoichiometry of BPL dimerization leading to increased repression of biotin synthesis and transport genes, the subsequent mutation in BPL serving to mitigate the effects and reduce repression.

***fmtA* (strain B7)**

A premature stop codon present in the penicillin binding protein FmtA was also observed in B7. As the Δ*fmtA* strain in genetic background JE2 showed no decrease in susceptibility to BPL199, any effect granted by this mutation either requires the NCTC 8325 genetic background or prior mutations. FmtA is a putative penicillin binding protein and has been reported to be induced upon treatment with cell wall active antibiotics such as β-lactams as part of the cell wall stress stimulon [7]. Inactivation of the gene has been demonstrated to affect the structure of the peptidoglycan [8] with FmtA recently characterised as having esterase function removing d-ala from wall teichoic acids [9]. Hence, the disruption of FmtA activity may have broad effects on cell surface charge and possibly lead to induction of genes that respond to such changes in cell membrane structure [10].

Additional mutations in strain B6 include a putative Glycosyltransferase *gtfA* and the RNA polymerase β-subunit *rpoB*.

As strain B6 only showed a 2-fold difference in MIC against BPL199 compared to strains B2 and B4, the mutations individually are unlikely to convey resistance to BPL inhibitors. This was supported by the fact that a loss of function mutation in GtfA does not affect the resistance to BPL199 in the transposon disrupted USA300 strain. The *gtfA* gene is proposed to have roles in glycosylation of factors from the secA/Y secretory system. However, there is little evidence on how this may affect resistance. Indeed, the mutation (R296H) converts arginine to histidine, conserving charge suggesting the mutation may not have a large impact on function. Combined this suggests that the mutation in RpoB may be responsible for the shift in MIC observed.

RpoB mutations are capable of widespread transcriptional changes that could facilitate resistance.

Mutations in RpoB have been implicated in resistance to several different antibiotic classes [11, 12] and stress response regulation [13]. In particular, studies have demonstrated that in *S. aureus* mutations in RpoB, evolved in response to Rifampicin treatment, can convey cross resistance to the glycopeptide antibiotics daptomycin and vancomycin [11, 12, 14] **(Chapter 6, figure s6)**. Due to the initial selective pressure these mutations largely occur in the rifampicin binding pocket however there are mutations outside of this pocket, suggesting that the location is not constrained. The ability to effect cell wall active antibiotics that do not interact directly with RNA polymerase sets a precedent for mutations in RpoB to play a role in resistance to cell wall active antibiotics like BPL. Determining the exact method by which this occurs is not possible without extensive studies into *S. aureus* RpoB structure. However, one possible mechanism that could lead to increased resistance to cell wall active antibiotics is through activation of the cell wall stress stimulon. One of the major activators in the cell wall stress response is the transcription factor spx [15] with increased Spx levels implicated in β–lactam and glycopeptide tolerance [16, 17]. There is evidence in the literature of mutations (P519L and R484H) in RpoB conveying a protective effect in strains lacking the Spx transcription factor, indicating that RpoB mutants can induce Spx independent activation of the Spx regulon [13]. Further supporting a role of the Spx regulon in BPL resistance, the strain B3 has a mutation in YjbH (discussed in the main text) which is responsible for degradation of Spx. It is possible that both the YjbH loss of function and RpoB missense mutation serve a similar function, allowing the activation of the Spx regulon by either increased Spx or Spx independent activation.

Strains lacking in PC deletions B3 and B5.

GdpP phosphodiesterase (strain B3)

The other gene mutated in B3 is *gdpP* which encodes a cyclic-di-AMP (c-di-AMP) phosphodiesterase [18]. Relatively newly discovered as a secondary messenger c-di-AMP has roles in controlling potassium transport systems [19, 20] and is upregulated in stationary phase growth, suggesting importance in late stage growth survival [21]. Loss of function in GdpP leads to increased c-di-AMP levels in the cell. The GdpP mutation occurring in strain B3 is a missense mutation, H442P occurring after this truncation. This mutation disrupts one of the presumptive key residues in the DHH domain of the protein, essential for the phosphodiesterase activity of the enzyme (**Chapter 6, figure s7).** Hence, we expect that the mutation observed converting the histidine to a proline would abolish or drastically lessen the phosphodiesterase activity of GdpP and lead to increased intracellular c-di-AMP. Though only directly implicated in osmotic stresses transport, through binding TrkA [19] and regulating the sensor histidine kinase KdpD [19, 20], the exact signalling pathways c-di-AMP interacts with are still being discovered with recent evidence of c-di-AMP influencing the stringent response in *S. aureus* [21] and acting as a ligand for riboswitches in other bacteria [22]. As well loss of GdpP function reduces β-lactam susceptibility in *S. aureus*. Despite this, the mutation present in our strain is unlikely to play a role on the β-lactam susceptibility of the strain as β-lactam susceptibility is restored with a truncated GdpP (370aa) [23]. As further roles of the c-di-AMP messenger are elucidated the effects of its increase on resistance to BPL inhibitors will become clearer.

Strain B1 contains both PC loss of function as well as truncation in potassium transporter TrkA and a missense mutation in a putative sensor histidine kinase.

The strain B1 has a 2-fold decrease in susceptibility to BPL199 compared to strains B2 and B4 that contain only PC loss of function and intergenic deletion. As well as the loss of pyruvate carboxylase function, strain B1 has two additional mutations that could be responsible for this reduction. One, an insertion in the potassium transport gating protein TrkA, leads to a truncation and possibly loss of function. To determine if loss of function of TrkA alone is able to reduce susceptibility to BPL inhibitors the ΔTrkA strain in *S. aureus* JE2 (USA300) was tested. Loss of TrkA led to slightly increased resistance suggesting that the truncation likely induces loss of function. The potassium transporter TrkA is a gating protein for the KtrB membrane bound potassium channel. This gating is regulated by c-di-AMP binding to one of two independent domains in TrkA, the C-terminal (RCK_C) domain [19]. As *gdpP* and *trkA* loss of function mutants have similar phenotypes in response to low potassium conditions, it is thought likely that c-di-AMP binding inactivates channel activity [19]. Therefore, increased c-di-AMP levels in the cell, as expected in strain B3, may have a similar effect to loss of TrkA function. This suggests the mutations in B1 and B3 may both work through reduction of potassium transport. Interestingly, the removal of TrkA has been shown to increase susceptibility to certain antibacterial agents in *S. aureus*, including vancomycin and several cationic antimicrobials including polymixin B [24]. This has been suggested to be mediated by dysregulation of membrane polarisation, increasing uptake of positively charged cationic antimicrobials. As BPL199 is predicted to have a negative charge at physiological pH the same dysregulation may decrease its uptake. Additionally the loss of TrkA reduces competitiveness of *S. aureus* JE2 *in vivo* [24] and in *Streptococcus suis* loss of function of *gdpP* negatively impacts virulence with decreased cell entry in a HepG2 based invasion assay and decreased virulence factor expression [25].

Strain B5 –Slight resistance to Biotinol and BPL199 but not to BPL223

The strain with the least resistance against all of the BPL inhibitors was strain B5 containing two mutations, a deletion in the transcription elongation factor GreA and a missense mutation in the *S. aureus* ferredoxin. Both of these genes have been identified as putative essential genes in *S. aureus* but not *B. subtilis* in a transposon mutagenesis study [26] suggesting that complete loss of function may not be tolerated though it is possible that these are false positives.

The GreA transcription elongation factor in *E. coli* has a diverse set of genes under its control including several TCA cycle components. These genes were found to be upregulated in the absence of GreA suggesting that loss of functional GreA may upregulate the TCA cycle. Ultimately however there is not sufficient information to comment on the potential role of the GreA deletion on resistance to BPL inhibitors in *S. aureus* and studying the effect of the truncation in isolation would be required to determine if it leads to a loss or gain of function. Unfortunately a knockout of GreA is not available through the transposon mutagenesis library though an insertion at nucleotide 386/477 was tolerated in one library screen [27]. This is possibly due to it being essential in at least some conditions used to prepare the library though the fact that a c-terminal transposon insertion was tolerated indicates that this region may be dispensable for the essential function. The other mutation, in the bacterial ferredoxin, is a missense mutation converting a proline to leucine which may have some effect on the overall fold of the protein. Again the ferredoxin is deemed a putative essential gene in *S. aureus* [26] though it is the only member of the ferredoxin cluster not found to be essential in *B. subtilis*. Any effect due to this mutation would require further study and is likely not a direct action.

References

1. McClure, R., et al., *Computational analysis of bacterial RNA-Seq data.* Nucleic Acids Res, 2013. **41**(14): p. e140.
2. ten Broeke-Smits, N.J., et al., *Operon structure of Staphylococcus aureus.* Nucleic Acids Res, 2010. **38**(10): p. 3263-74.
3. Palmer, A.C. and R. Kishony, *Understanding, predicting and manipulating the genotypic evolution of antibiotic resistance.* Nat Rev Genet, 2013. **14**(4): p. 243-8.
4. Blount, K.F. and R.R. Breaker, *Riboswitches as antibacterial drug targets.* Nat Biotechnol, 2006. **24**(12): p. 1558-1564.
5. Weaver, L.H., et al., *Competing protein: protein interactions are proposed to control the biological switch of the E coli biotin repressor.* Protein Sci, 2001. **10**(12): p. 2618-2622.
6. Solbiati, J. and J.E. Cronan, *The switch regulating transcription of the Escherichia coli biotin operon does not require extensive protein-protein interactions.* Chemistry & biology, 2010. **17**(1): p. 11-17.
7. Fan, X., et al., *Diversity of Penicillin-binding Proteins RESISTANCE FACTOR FmtA OF STAPHYLOCOCCUS AUREUS.* J Biol Chem, 2007. **282**(48): p. 35143-35152.
8. Komatsuzawa, H., et al., *Characterization of fmtA, a gene that modulates the expression of methicillin resistance in Staphylococcus aureus.* Antimicrob Agents Chemother, 1999. **43**(9): p. 2121-2125.
9. Rahman, M.M., et al., *The Staphylococcus aureus Methicillin Resistance Factor FmtA Is a d-Amino Esterase That Acts on Teichoic Acids.* mBio, 2016. **7**(1): p. e02070-15.
10. Campbell, J., et al., *An antibiotic that inhibits a late step in wall teichoic acid biosynthesis induces the cell wall stress stimulon in Staphylococcus aureus.* Antimicrob Agents Chemother, 2012. **56**(4): p. 1810-1820.
11. Cui, L., et al., *An RpoB mutation confers dual heteroresistance to daptomycin and vancomycin in Staphylococcus aureus.* Antimicrob Agents Chemother, 2010. **54**(12): p. 5222-5233.
12. Watanabe, Y., et al., *Impact of rpoB mutations on reduced vancomycin susceptibility in Staphylococcus aureus.* J Clin Microbiol, 2011. **49**(7): p. 2680-2684.
13. Villanueva, M., et al., *Rifampin Resistance rpoB Alleles or Multicopy Thioredoxin/Thioredoxin Reductase Suppresses the Lethality of Disruption of the Global Stress Regulator spx in Staphylococcus aureus.* J Bacteriol, 2016. **198**(19): p. 2719-2731.
14. Howden, B.P., et al., *Evolution of multidrug resistance during Staphylococcus aureus infection involves mutation of the essential two component regulator WalKR.* PLoS Pathog, 2011. **7**(11): p. e1002359.
15. Pamp, S.J., et al., *Spx is a global effector impacting stress tolerance and biofilm formation in Staphylococcus aureus.* J Bacteriol, 2006. **188**(13): p. 4861-4870.
16. Jousselin, A., et al., *The Staphylococcus aureus thiol/oxidative stress global regulator Spx controls trfA, a gene implicated in cell wall antibiotic resistance.* Antimicrob Agents Chemother, 2013. **57**(7): p. 3283-3292.

17. Renzoni, A., et al., *Whole genome sequencing and complete genetic analysis reveals novel pathways to glycopeptide resistance in Staphylococcus aureus.* PLoS One, 2011. **6**(6): p. e21577.

18. Corrigan, R.M., et al., *c-di-AMP is a new second messenger in Staphylococcus aureus with a role in controlling cell size and envelope stress.* PLoS Pathog, 2011. **7**(9): p. e1002217.

19. Corrigan, R.M., et al., *Systematic identification of conserved bacterial c-di-AMP receptor proteins.* Proc Natl Acad Sci U S A, 2013. **110**(22): p. 9084-9.

20. Moscoso, J.A., et al., *Binding of c-di-AMP to the Staphylococcus aureus sensor kinase KdpD occurs via the USP domain and down-regulates the expression of the Kdp potassium transporter.* J Bacteriol, 2015: p. JB. 00480-15.

21. Corrigan, R.M., et al., *Cross-talk between two nucleotide-signaling pathways in Staphylococcus aureus.* J Biol Chem, 2015. **290**(9): p. 5826-5839.

22. Nelson, J.W., et al., *Riboswitches in eubacteria sense the second messenger c-di-AMP.* Nat Chem Biol, 2013. **9**(12): p. 834-839.

23. Griffiths, J.M. and A.J. O'Neill, *Loss of function of the gdpP protein leads to joint beta-lactam/glycopeptide tolerance in Staphylococcus aureus.* Antimicrob Agents Chemother, 2012. **56**(1): p. 579-81.

24. Gries, C.M., et al., *The Ktr potassium transport system in Staphylococcus aureus and its role in cell physiology, antimicrobial resistance and pathogenesis.* Mol Microbiol, 2013. **89**(4): p. 760-73.

25. Du, B., et al., *Functional analysis of c-di-AMP phosphodiesterase, GdpP, in Streptococcus suis serotype 2.* Microbiol Res, 2014. **169**(9-10): p. 749-58.

26. Chaudhuri, R.R., et al., *Comprehensive identification of essential Staphylococcus aureus genes using Transposon-Mediated Differential Hybridisation (TMDH).* BMC Genomics, 2009. **10**: p. 291.

27. Bae, T., et al., *Staphylococcus aureus virulence genes identified by bursa aurealis mutagenesis and nematode killing.* Proc Natl Acad Sci U S A, 2004. **101**(33): p. 12312-12317.